Contributions to the Synthesis of Planar and Conformal Arrays

by

Eugene Botha

Submitted in partial fulfillment of the requirements for the degree

Ph.D (Electronic Engineering)

in the

Faculty of Engineering

UNIVERSITY OF PRETORIA

August 2000

Acknowledgements

I would like to thank the following people without whom this thesis would not have been possible:

1. Derek McNamara, who interested me in antennas in general and array syntehsis in particular; and who was my mentor throughout my studies and promotor for the first part of this thesis.
2. Johan Joubert, my promotor for the latter part of my thesis.
3. My wife, Jo-Anne, for her continued support and understanding.
4. My parents for their support and encouragement.
5. Friends and fellow students at Tukkies, Wimpie, Pieter, Martin, Thys, Louis, Marcus, Danie and Maggie for stimulating discussions.

Lastly, our Father in Heaven for providing every opportunity.

Synopsis

Title: Contributions to the Synthesis of Planar and Conformal Arrays
Name: E. Botha
Promotor: Prof. J. Joubert
Department: Electrical, Electronic and Computer Engineering
Degree: Philosophiae Doctor (Electronic Engineering)

The transformation technique, used for the synthesis of centro-symmetrical contoured beams for rectangular planar arrays, is extended to enable the synthesis of planar arrays with arbitrary contoured footprint patterns; planar arrays with non rectangular boundaries and planar arrays with triangular lattices. The transformation based synthesis technique utilises a transformation that divides the problem into two decoupled sub-problems. One sub-problem involves the determination of certain coefficients in order to achieve the required footprint contours, while the other sub-problem consists of a linear array synthesis.

A well ordered, step by step procedure for the synthesis of planar arrays with difference patterns is presented. The method utilises the convolution synthesis method and uses the extended transformation method as one of the steps. The technique in effect provides a structured procedure for spreading out the linear array excitations. The result is near-optimum difference patterns for planar arrays with rectangular or hexagonal lattices. The difference pattern performance in the selected cut is identical to that of the archetypal linear array used, and will thus be optimum if the latter is optimum. In the other pattern cuts the sidelobes are below those of the archetypal linear array, but not unnecessarily low.

Conformal array synthesis is an ill conditioned inverse problem with a multitude of local minima. Due to the non linear nature of conformal array synthesis an effective conformal array synthesis method must have a rapid rate of convergence and some measure of confidence that the result will be close to the optimal solution. The synthesis of arrays of arbitrary geometry and elements was stated as the search for the intersection of properly defined sets. Effective relaxation was implemented in the excitation space as well. A number of possible ways of calculating starting points were investigated, and a novel method to obtain a set of initial values as close to the global minimum as possible is proposed for shaped and contoured beam synthesis. The phase variation in the shaped beam region is slow and may be written as a function of few variables. Genetic algorithm is used to optimise these phase function variables. The importance of practical element patterns in the analysis and synthesis of conformal arrays is also shown.

Abstract

Title: Contributions to the Synthesis of Planar and Conformal Arrays
Name: E. Botha
Promotor: Prof. J. Joubert
Department: Electrical, Electronic and Computer Engineering
Degree: Philosophiae Doctor (Electronic Engineering)

The transformation technique, used for the synthesis of centro-symmetrical contoured beams for rectangular planar arrays, is extended to enable the synthesis of planar arrays with arbitrary contoured footprint patterns, planar arrays with non rectangular boundaries and planar arrays with triangular lattices. The transformation based synthesis technique utilises a transformation that divides the problem into two decoupled sub-problems. One sub-problem involves the determination of certain coefficients in order to achieve the required footprint contours. The other sub-problem consists of a linear array synthesis, for which powerful methods for determining appropriate element excitations, already exist. The final planar array size is linked to the number of contour transformation coefficients and the prototype linear array size. The biggest advantage of the transformation based synthesis technique is its computational efficiency, making it feasible to conduct parametric studies of array performance design tradeoff studies even for very large arrays.

A well ordered, step by step procedure for the synthesis of planar arrays with difference patterns is presented. The method utilises the convolution synthesis method and uses the extended transformation method as one of the steps. The technique in effect provides a structured procedure for spreading out the linear array excitations, thereby eliminating any guesswork that may otherwise be required. The result is near-optimum difference patterns for planar arrays with rectangular or hexagonal lattices. The difference pattern performance in the selected cut is identical to that of the archetypal linear array used, and will thus be optimum if the latter is optimum. In the other pattern cuts the sidelobes are below those of the archetypal linear array, but not unnecessarily low. The synthesis procedure is very rapid for even very large arrays, making it feasible to conduct design trade-off and parametric studies.

Conformal array synthesis is an ill conditioned inverse problem with a multitude of local minima. Due to the non linear nature of conformal array synthesis an effective conformal array synthesis method must have a rapid rate of convergence and some measure of confidence that the result will be close to the optimal solution. The synthesis of arrays of arbitrary geometry and elements can be stated as the search for the intersection of properly defined sets. Proper sets were defined in both the radiation pattern space and excitation space; along with the necessary projector between these sets. Effective relaxation can be implemented in the excitation space as well. A number of possible ways of calculating starting points were investigated, and a novel method to obtain a set of initial values as close to the global minimum as possible is proposed for shaped and contoured beam synthesis. The phase variation in the shaped beam region is slow and may be written as a function of few variables. The starting pattern is a summation of component beams, each weighted by the proper value of the shaping function and phase shifted by the proper value of the phase function. Genetic algorithm is used to optimise these phase function variables. The importance of practical element patterns in the analysis and synthesis of conformal arrays is also denomstrated.

Keywords: Antenna theory, Antenna arrays, Antenna synthesis, Array synthesis, Planar arrays, Conformal arrays, Antenna pattern synthesis, Power synthesis, Conformal array synthesis, Planar array synthesis.

Samevatting

Titel: Bydraes tot die sintese van Vlak- en Konforme-samestellings
Naam: E. Botha
Promotor: Prof. J. Joubert
Department: Elektriese, Elektroniese en Rekenaar Ingeniuersewe
Graad: Philosophiae Doctor

Die transformasie tegniek, wat vir die sintese van sentro-simmetriese gekontoerde patrone van reghoekige vlaksamestellings gebruik word, is uitgebrei vir arbitrêre gekontoerde patroon sintese; die sintese van vlaksamestellings met nie reghoekige rande en die sintese van vlaksamestellings met driehoekige roosters. Die transformasie gebaseerde tegniek verdeel die probleem in twee subprobleme. Een subprobleem (kontoer transformasie probleem) behels die berekening van sekere koëffisiente om die verlangde kontoer te omskryf. Die ander subprobleem bestaan uit 'n prototipe liniêresamestelling sintese; waarvoor daar reeds kragtige metodes bestaan om die element aandrywings te bereken. Die grootte van die finale vlaksamestelling is afhanklik van die hoeveelheid kontoer transformasie koëffisiente en die aantal prototipe liniêresamestelling elemente. Die grootste voordeel van die metode is die rekenaar effektiwiteit daarvan, selfs vir groot samestellings. Dus is dit moontlik om parametriese en ontwerpskreteria studies te doen selfs vir baie groot samestellings.

'n Goed ge-ordende stap-vir-stap prosedure vir die sintese van verskil patrone van vlaksamestellings is voorgestel. Die metode behels die konvolusie sintese metode so wel as die uitgebreide transformasie gebaseerde tegniek as van die stappe. Die tegniek bied 'n gestruktureerde uitsprei van die samestelling aandrywings. Die prosedure lewer byna-optimum verskilpartone vir vlaksamestelling met reghoekige of heksagonale elementroosters. Die verskilpatroon in die hoofsnit is identies aan die patroon van die prototipe samestelling; en sal dus optimaal wees as die prototipe samestelling patroon optimaal is. Die sylobbe in ander patroon snitte is net so laag, of laer, as die van die prototipe samestelling; maar nie onnodig laag nie. Die prosedure is rekenaar effektief, wat parametriese studies vir baie groot samestellings is moontlik maak.

Konforme-samestelling sintese is 'n swak gekondisioneerde inverse probleem met meer as een lokale minimum. As gevolg van die nie-liniariteit van konforme-samestelling sintese moet enige toepaslike sintese metode vinnig konvergeer en 'n mate van vertroue bied dat die resultaat naby aan optimum is. Die sintese van samestellings met 'n arbitrêre geometrie en arbitrêre elemente is beskryf as die soek na die snyding van korrek gedefinieerde stelle. Stelle, met meegaande projektors, is in die aandrywingsvlak en die patroonvlak gedefinieer. 'n Begin punt so naby as moontlik aan die optimum punt is belangrik om konvergensie na die optimale punt se verseker. Die fase van die verveld is stadig variërend in die hooflob gebied, en kan met behulp van net 'n paar veranderlikes beskryf word. Die beginpatroon is die sommering van komponent bundels, elk geweeg met die korrekte waarde van die gespesifiseerde hoofbundel vorm en in fase geskuif met die waarde van 'n fasefunksie. Die fasefunksie veranderlikes word dan geoptimeer met Genetiese Algoritme. Die belangrikheid van praktiese elementpatrone in die analise sowel as sintese van konforme-samestellings is aangetoon.

Sleutelwoorde: Antenneteorie, Antennesamestellings, Antennesintese, Samestellingsintese, Vlaksamestellings, Konformesamestellings, Antennepatroon sinteses, Drywingsintese, Konformesamestelling sintese, Vlaksamestelling sintese.

Contents

List of Figures

List of Tables

Chapter 1

Introduction

1.1 Array Antennas

A source of electromagnetic radiation may take many different forms. It could be a conducting wire, horn radiator, waveguide slot, or one of many other possibilities. The radiation pattern of a single element is fixed for a given frequency of excitation and consists, in general, of a main beam and a number of smaller sidelobes [1:pp.15-19]. In many applications there is a need for improving the performance above that obtainable with a single radiating element. There are, broadly speaking, two methods available for this purpose. One technique uses a properly shaped reflector or lens fed by a radiating element, and the other employs a number of radiating elements correctly arranged in space and interconnected to form an antenna array. Whether the reflector or array option is to be used depends on a multitude of factors related to the particular application and environment in which the antenna will operate.

Up to the present time reflector antennas have dominated the antenna domain, mainly because antenna arrays are more expensive. But as antenna array elements can be mass produced the element cost will decrease [2]. Another factor limiting the use of antenna arrays is large heavy beam-formers. However, recent advances in optical beam-formers promise compact and light beam-forming networks [3, 4, 5]. Despite these disadvantages there is a number of potential advantages in using arrays. Electronic beam scanning is much faster than mechanical scanning, allowing greater flexibility in multiple target tracking. Digital beam-formers [6] allow reconfigurable arrays (that is, the excitation of the elements can be altered when the need for different radiation characteristics arise), that can adapt to future requirements. Arrays may present a more compact configuration since it can be so fabricated that it conforms to it's host's fuselage.

Array antennas can be divided into three main classes according to the geometry in which the elements are arranged. A number of radiating elements positioned in a straight line forms a linear array. A planar array, as the name indicates, is an array with all its radiating elements arranged to lie on a plane. Conformal arrays can have an arbitrary

geometry, with the array elements mounted flush on a host surface [7:p.921].

1.2 The Synthesis Problem

Array antenna development can be divided into three stages: specification, synthesis and realization. These should not be taken as clear-cut divisions, however, as there is a considerable amount of overlap between the last two stages.

Three sets of parameters are accessible for variation in array synthesis with a given kind of element, namely the total number of elements, the spatial distribution of the elements and the relative complex excitation (amplitude as well as phase) of the elements. The synthesis problem involves the determination of these parameters to obtain the desired radiation characteristics. The synthesis problem is in general an ill-conditioned inverse problem as only a relative power level is specified (power synthesis), while the far-field phase is usually not of interest and is in general left unspecified. If some far-field phase distribution is assumed the synthesis problem, (now reduced to field synthesis) is less difficult, but not all of the available degrees of freedom are used. In the power synthesis problem the non-uniqueness of the solution can be used to select the most useful of the family of solutions. Synthesis is usually performed subject to a set of constraints. The latter may limit certain radiation pattern characteristics (eg. sidelobe levels), but may also include constraints on other quantities in an attempt to allow easier practical realisability. This second kind of constraint may include factors such as the sensitivity of the array performance to imperfections, or constraints on the complexity of the feed network. It is in the setting of constraints that engineering judgement must be exercised in the midst of the mathematical techniques.

The final step in the design of an antenna array is the actual establishment of the determined excitations in the form of hardware. The realization of the array includes the selection of the radiating elements to be used, though this would no doubt have been kept in mind during the synthesis stage (eg. the radiation pattern of the array elements may already be needed during synthesis). The realization phase would further involve the determination (theoretically and/or experimentally) of the element radiation characteristics and the coupling between elements, both externally and internally via the feed network. This information is then used to establish the correct excitation determined from the synthesis procedure.

1.3 Goals and Contribution of the Thesis

The objectives for the thesis are:

- A general transformation based synthesis method for contoured footprint patterns for planar arrays (Chaper 3). The synthesis procedure must allow for:

  - Arbitrary contoured footprint patterns.
  - Planar arrays with non rectangular boundaries.
  - Planar arrays with triangular lattices.

- Difference pattern synthesis of planar arrays with rectangular or triangular element lattices (Chaper 4).

- Contributions to general conformal array synthesis using generalised projections (Chaper 5). These contributions are:
  - The formulation of backward operators to enable conformal array synthesis.
  - The use of relaxation to increase the rate of convergence.
  - The proper selection of initial values to avoid local minima.
  - An investigation into the importance of accurate element patterns in the synthesis of conformal arrays.

1.4 Overview of the Thesis

This thesis deals exclusively with array synthesis. The complete electromagnetic evaluation of the array element in the array environment is not considered, existing techniques are used to compute the element patterns.

Essential information on array analysis relevant to this work is presented in Chapter 2. Firstly, definitions of numerous factors used in the literature that would be required to unambiguously specify the performance of antennas, irrespective of the particular type used, are summarised. Secondly, the development of the array synthesis techniques, on which the contents of the present thesis builds, are reviewed. Chapters 3 through 5 contain the principal contributions of the present work to the theory of array synthesis. A more detailed indication of the contents of these chapters is more appropriate after the limitations of existing synthesis techniques have been gauged; this is therefore postponed until the end of the second chapter (Section 2.9). Finally, Chapter 6 completes the thesis by drawing a number of general conclusions.

Chapter 2

Review of Relevant Array Synthesis Techniques

2.1 Introductory Remarks

Several radiating elements can be arranged in space and interconnected to produce a directional radiation pattern. Such a group of antenna elements is referred to as an array antenna, or simply, an array. The radiation pattern of the array is dependent on the radiation pattern of each of the individual antenna elements, the relative excitation of each element and the geometry of the array.

The primary goal of antenna synthesis is to obtain a radiation pattern with specified characteristics. The best way to learn about synthesis is to learn all you can about analysis. The antenna characteristics or performance indices must be unambiguously defined before any synthesis can be attempted. This chapter therefore begins with a discussion of the relevant array analysis techniques, followed by a discussion of various array performance indices. The development of array synthesis techniques relevant to the thesis is then reviewed. Array synthesis started with equi-spaced linear arrays, and this forms the first part of the review. This is followed by an investigation of the continuous line source distributions synthesis methods. Next, the existing synthesis techniques for planar arrays are discussed. The synthesis of any array can be viewed as a numerical optimisation problem, this approach forms the topic of Section 2.8. The chapter concludes with a summary of the synthesis problems which have not been adequately dealt with in the literature and which form the subject of this thesis.

2.2 Array Analysis

Before a synthesis problem can be attempted, means of analysing an array must be available. Such analysis is treated in some detail in references [8, 9, 10, 11, 12, 13] and

a complete treatment is not intended here. Instead, only the most relevant material will be considered, and some concepts expressed in a concise form. In the sections to follow, background is given and statements made without proof.

2.2.1 The Radiation Pattern of an Arbitrary Array

An array consists of a collection of discrete radiating elements mounted on some surface. The discrete distribution of excitations is called the aperture distribution of the array. Each element's radiation pattern is influenced by the the structure on which it is mounted. In many cases the surface, and the location of the elements on the surface, are chosen in such a way that the influence of the structure is kept to a minimum, for example the array is assumed to be mounted on an infinite ground plane. This simplifies the analysis of the element patterns considerably. However, in the most general case of a conformal array, the structure's influence is marked, and the complete structure must be included when the element's radiation pattern is calculated. The element pattern of each element can then be evaluated about its phase reference, using a method like geometrical theory of diffraction (GTD) [14] or method of moments (MoM) [15]. The arbitrary array can be modelled as an array of point source elements located in space. Each of these point source elements is located at the phase reference of the corresponding original element, and has the element pattern of the original element. In this way the effect of the structure is accounted for during the determination of the element patterns prior to application of the synthesis procedure, and then simply used as if they were closed form expressions for the element patterns.

Consider the general array geometry shown in Figure 2.1. It is convenient to use a Cartesian coordinate system for the positions of the array elements, while a spherical coordinate system would be most prudent for the radiation pattern expressions. The n-th element is at position (x_n, y_n, z_n). Using the origin of the coordinate system as a reference point, the contribution of the n-th element to the far-field, in the direction (θ, ϕ), is:

$$f(\theta,\phi) = E_n(\theta,\phi)\, e^{\mathrm{j}k(x_n \sin\theta\cos\phi + y_n \sin\theta\sin\phi + z_n\cos\theta)} \tag{2.1}$$

where k is the free space wavenumber, and $E_n(\theta,\phi)$ represents the co-polarised far-field radiation pattern (or element pattern) associated with the n-th element. The array co-polarised radiation pattern, $F(\theta,\phi)$, is a superposition of the co-polar contribution from each element in the array to the far-field

$$F(\theta,\phi) = \sum_{n=1}^{N} a_n\, E_n(\theta,\phi)\, e^{\mathrm{j}k(x_n \sin\theta\cos\phi + y_n \sin\theta\sin\phi + z_n\cos\theta)} \tag{2.2}$$

The relative complex excitation (amplitude and phase) of the n-th element is denoted by a_n and N is the total number of elements in the array. Similar expressions can be written for the cross-polarised radiation pattern. Since the co-polarised pattern is usually considered, "radiation pattern" in the text refers to the co-polarised radiation pattern.

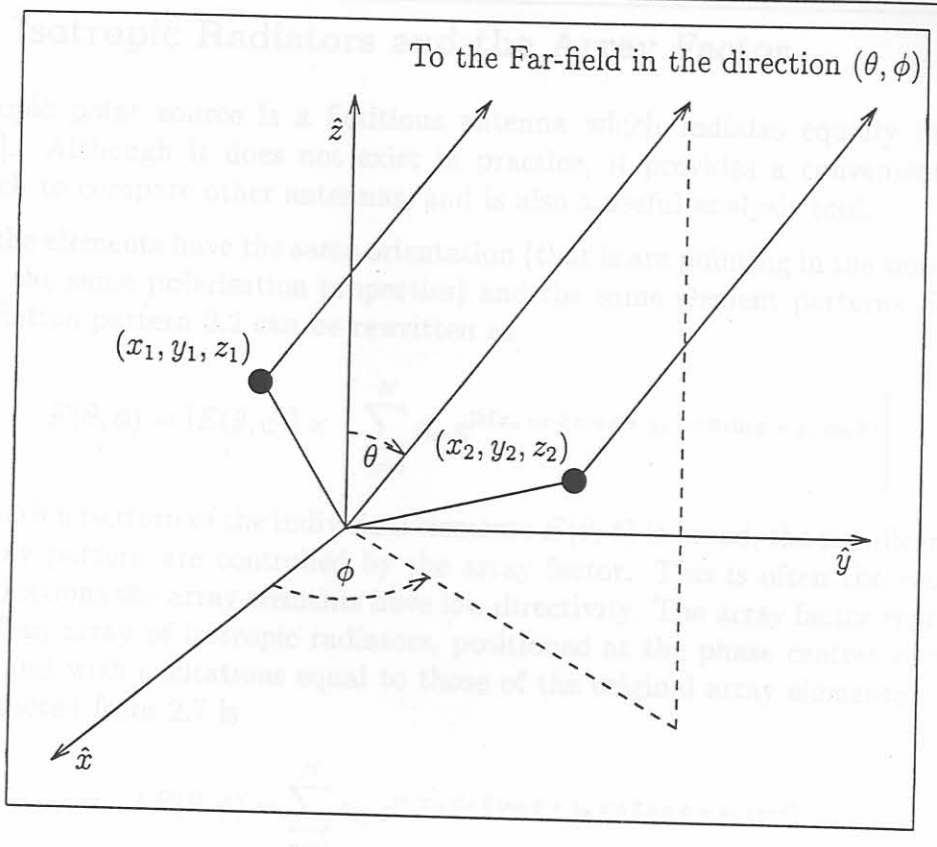

Figure 2.1: Arbitrary array geometry.

If the radiation pattern is evaluated in a number of far-field directions, the radiation pattern can be expressed as a vector

$$\vec{F} = [f_1, f_2, \ldots, f_m, \ldots, f_M]^T \tag{2.3}$$

where f_m is the value of the radiation pattern in the (θ_m, ϕ_m) direction and M is the total number of field points. $[\cdot]^T$ denotes the transpose. The radiation pattern 2.2 in matrix notation then is

$$\vec{F} = \tilde{B}\,\vec{A} \tag{2.4}$$

where $\vec{A}$ is the excitation column vector

$$\vec{A} = [a_1, a_2, \ldots, a_n, \ldots, a_N]^T \tag{2.5}$$

and $\tilde{B}$ is the radiation matrix. The mn-th component of the radiation matrix is the contribution of the n-th element to the far-field in the m-th direction,

$$b_{mn} = E_n(\theta_m, \phi_m)\, e^{\mathrm{j}k(x_n \sin\theta_m \cos\phi_m + y_n \sin\theta_m \sin\phi_m + z_n \cos\theta_m)} \tag{2.6}$$

2.2.2 Isotropic Radiators and the Array Factor

An isotropic point source is a fictitious antenna which radiates equally in all directions [16]. Although it does not exist in practice, it provides a convenient reference with which to compare other antennas, and is also a useful analysis tool.

If all the elements have the same orientation (that is are pointing in the same direction and have the same polarisation properties) and the same element patterns $E(\theta, \phi)$, the array radiation pattern 2.2 can be rewritten as

$$F(\theta, \phi) = [E(\theta, \phi)] \times \left[\sum_{n=1}^{N} a_n \, e^{\mathrm{j}k(x_n \sin\theta\cos\phi + y_n \sin\theta\sin\phi + z_n \cos\theta)} \right] \tag{2.7}$$

If the radiation pattern of the individual elements $E(\theta, \phi)$ is broad, the significant features of the array pattern are controlled by the array factor. This is often the case since in most applications the array elements have low directivity. The array factor represents the pattern of an array of isotropic radiators, positioned at the phase centres of the actual elements, and with excitations equal to those of the original array elements. The array factor extracted from 2.7 is

$$AF(\theta, \phi) = \sum_{n=1}^{N} a_n \, e^{\mathrm{j}k(x_n \sin\theta\cos\phi + y_n \sin\theta\sin\phi + z_n \cos\theta)} \tag{2.8}$$

Expression 2.7 represents the principle of pattern multiplication, which states that the radiation pattern of an array consisting of identical elements is the product of the element pattern of the actual array elements and the array factor.

2.2.3 Linear Array Factor

If all the elements of an array lie along a straight line, they form a linear array. This geometry is not only important in its own right, but is also an essential building block of the majority of planar arrays. The synthesis of such linear arrays is therefore fundamental to all array design. Consider the linear array along the x-axis with uniform inter element spacing d, so that the n-th element is located at position $(nd, 0, 0)$ in a Cartesian system, as shown in Figure 2.2(a).

The array factor is rotationally symmetric about the x-axis, thus it is necessary to determine the array factor in only one plane through the x-axis. If we choose the xz-plane, we can use angle θ as positive for positive x values ($\phi = 0$) and negative for negative values of x ($\phi = \pi$) without loss of generality. Although it would be simpler to select the xy-plane and use ϕ as the angular variable, the choice made will become apparent in Chapter 3

The path difference between two consecutive sources to a distant point in space gives rise to an electrical phase difference. It is thus convenient to define an additional variable,

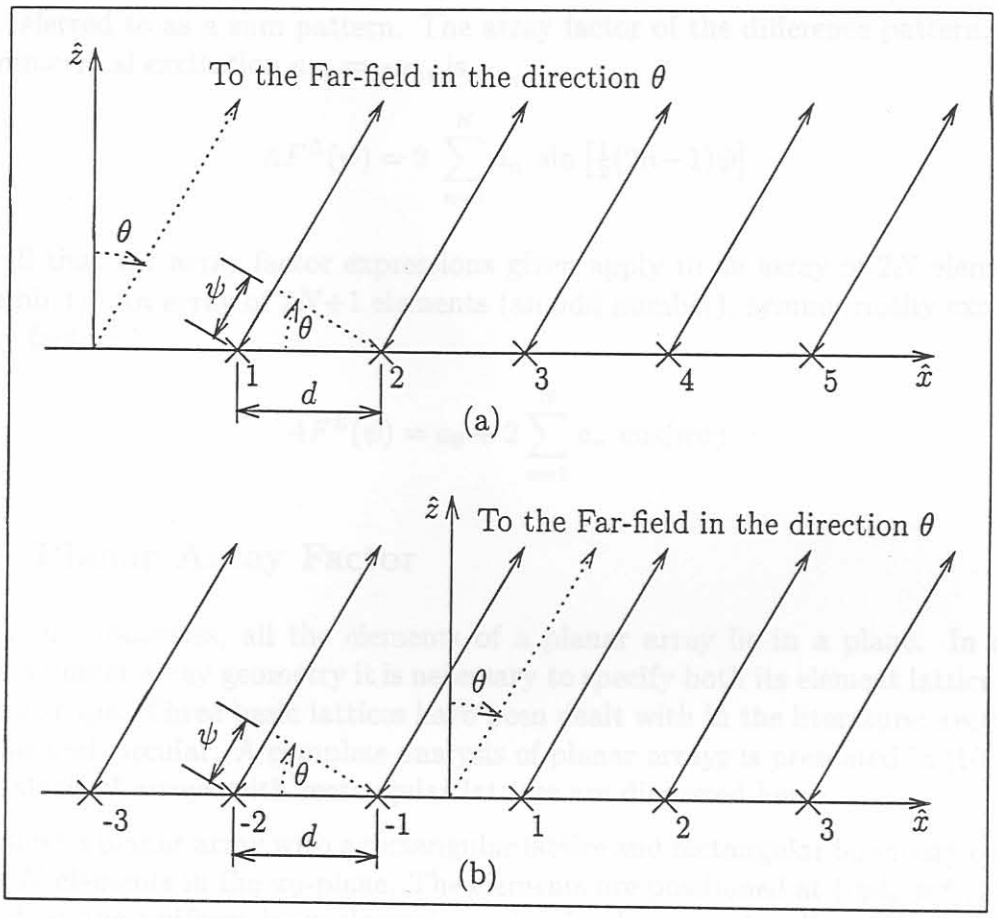

Figure 2.2: Uniformly spaced linear array geometry; (a) general linear array and (b) symetrical even element number linear array.

namely the path length difference,

$$\psi = \mathrm{k}d\sin\theta \tag{2.9}$$

Using this new variable, the linear array factor is expressed as

$$AF(\psi) = \sum_{n=1}^{N} a_n \, e^{\mathrm{j}n\psi} \tag{2.10}$$

Consider the $2N$ element uniformly spaced linear array geometry in Figure 2.2(b), with the element numbering scheme and array phase reference as indicated. The distributions for which $|a_{-n}| = |a_n|$ are of particular importance; with symmetrical excitation $a_{-n} = a_n$ the array factor becomes,

$$AF^{\Sigma}(\psi) = 2\sum_{n=1}^{N} a_n \, \cos\left[\tfrac{1}{2}(2n-1)\psi\right] \tag{2.11}$$

This is referred to as a sum pattern. The array factor of the difference pattern, with an anti-symmetrical excitation $a_{-n} = -a_n$, is

$$AF^{\Delta}(\psi) = 2 \sum_{n=1}^{N} a_n \sin\left[\tfrac{1}{2}(2n-1)\psi\right] \tag{2.12}$$

Recall that the array factor expressions given apply to an array of $2N$ elements (an even number). An array of $2N+1$ elements (an odd number), symmetrically excited, has an array factor:

$$AF^{\Sigma}(\psi) = a_0 + 2 \sum_{n=1}^{N} a_n \cos(n\psi) \tag{2.13}$$

2.2.4 Planar Array Factor

As the name indicates, all the elements of a planar array lie in a plane. In order to describe a planar array geometry it is necessary to specify both its element lattice and the boundary shape. Three basic lattices have been dealt with in the literature: rectangular, triangular and circular. A complete analysis of planar arrays is presented in [10, 17, 18]. Only analysis of arrays with rectangular lattices are discussed here.

Consider a planar array with a rectangular lattice and rectangular boundary consisting of M by N elements in the xy-plane. The elements are positioned at $(md_x, nd_y, 0)$, where d_x and d_y is the uniform inter element spacing in the x- and y-directions respectively. Using the substitution

$$\begin{aligned} u &= \mathrm{k} d_x \sin\theta \cos\phi \\ v &= \mathrm{k} d_y \sin\theta \sin\phi \end{aligned} \tag{2.14}$$

the planar array factor can be written as

$$AF(u,v) = \sum_{m=1}^{M} \sum_{n=1}^{N} a_{mn} \, e^{\mathrm{j}\mathrm{k}(mu+nv)} \tag{2.15}$$

with a_{mn} the normalised complex excitation of the mn-th element.

A planar array of $2M+1$ by $2N+1$ elements in the xy-plane, with a rectangular lattice and rectangular boundary is shown in Figure 2.3. If these elements are excited with quadrantal symmetry, $a_{mn} = a_{-mn} = a_{-m-n} = a_{m-n}$ a sum pattern results. Note that $(-m-n)$ represents a quantity with two subscripts, namely "$-m$" and "$-n$", and not a single subscript quantity with subscript "$-m-n$"; and so on. The planar array factor becomes,

$$AF(u,v) = 4 \sum_{m=0}^{M} \sum_{n=0}^{N} \zeta_m \zeta_n a_{mn} \cos(mu)\cos(nv) \tag{2.16}$$

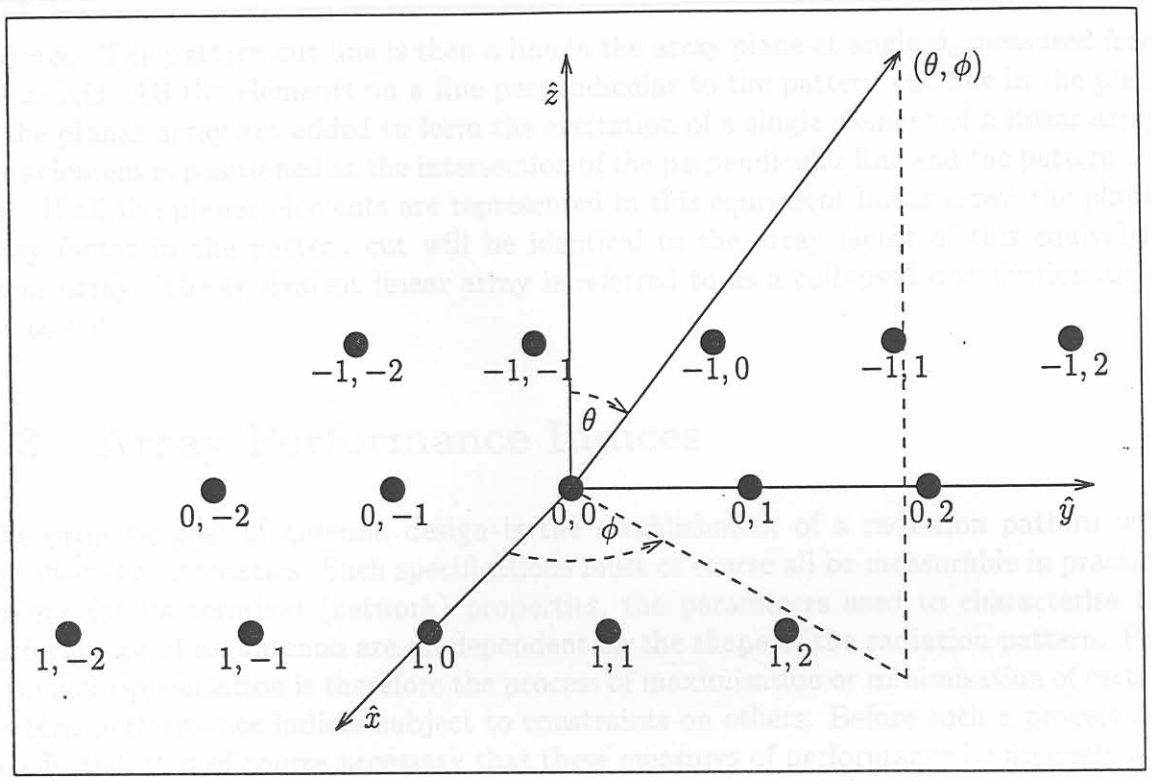

Figure 2.3: Uniformly spaced rectangular planar array geometry.

with

$$\zeta_i = \begin{cases} \frac{1}{2} & \text{for } i=0, \\ 1 & \text{for } i \geq 1. \end{cases} \tag{2.17}$$

The array factor expression of a planar array consisting of $2M$ by $2N$, with a similar numbering scheme and quadrantally symmetric excitation, is

$$AF(u,v) = 4 \sum_{m=1}^{M} \sum_{n=1}^{N} a_{mn} \cos\left[\tfrac{1}{2}(2m-1)u\right] \cos\left[\tfrac{1}{2}(2n-1)v\right] \tag{2.18}$$

If the radiation pattern of a planar array is required along one of its principal planes, say $\phi = 90°$, the excitations of each row (all the elements with the same y position coordinate) of the planar array can be represented by a single element with an excitation equal to the sum of all the elements of that row. A linear array along the y-axis is then obtained; we refer to this linear array as the collapsed distribution along the y-axis. Similarly, if the excitations of the elements of each column (elements with the same x position) are added ($\phi=0°$ principal plane), a collapsed distribution along the x-axis is obtained [19].

The above comment can be generalised to any planar array geometry as well as any pattern cut. Let us assume the planar array is in the xy-plane and the pattern cut angle

is $\phi = \phi_c$. The pattern cut line is then a line in the array plane at angle ϕ_c measured from the x-axis. All the elements on a line perpendicular to the pattern cut line in the plane of the planar array are added to form the excitation of a single element of a linear array. This element is positioned at the intersection of the perpendicular line and the pattern cut line. If all the planar elements are represented in this equivalent linear array, the planar array factor in the pattern cut will be identical to the array factor of this equivalent linear array. The equivalent linear array is referred to as a collapsed distribution along the ϕ_c-cut.

2.3 Array Performance Indices

The primary goal of antenna design is the establishment of a radiation pattern with specified characteristics. Such specifications must of course all be measurable in practice. Except for its terminal (network) properties, the parameters used to characterise the performance of an antenna are all dependent on the shape of the radiation pattern. Performance optimisation is therefore the process of maximisation or minimisation of certain pattern performance indices subject to constraints on others. Before such a process can be effected, it is of course necessary that these measures of performance be precisely and unambiguously defined. This will be done here, using the *IEEE* standards definitions of terms for antennas [20]. Though all of the performance specifications considered are applicable to antennas in general, the terminology here is specifically directed toward arrays.

2.3.1 Nomenclature and Radiation Pattern Characteristics

A radiation pattern is generally divided into two regions, the main lobe region (the maximum radiation is in this region) and the sidelobe region consisting of a number of smaller sidelobes. A number of specifications relating to the radiation pattern (or array factor) are illustrated in Figure 2.4. The radiation pattern properties are dependent on the shape of the pattern, not the absolute levels, thus the pattern is usually normalised to its maximum value and plotted in decibels (dB). This practice will be followed in this thesis. The following characteristics can be defined:

- The sidelobe level (SLL) is the level of the highest sidelobe with respect to the pattern maximum. The sidelobe ratio (SLR) is the reciprocal of the sidelobe level. Therefore the sidelobe level, in decibels, will be a negative number and the sidelobe ratio positive.
- The root-mean-square sidelobe level (RMS-SLL) is the root of the average value of the relative power of the normalised pattern of an antenna taken over a specified angular region, which excludes the main beam.

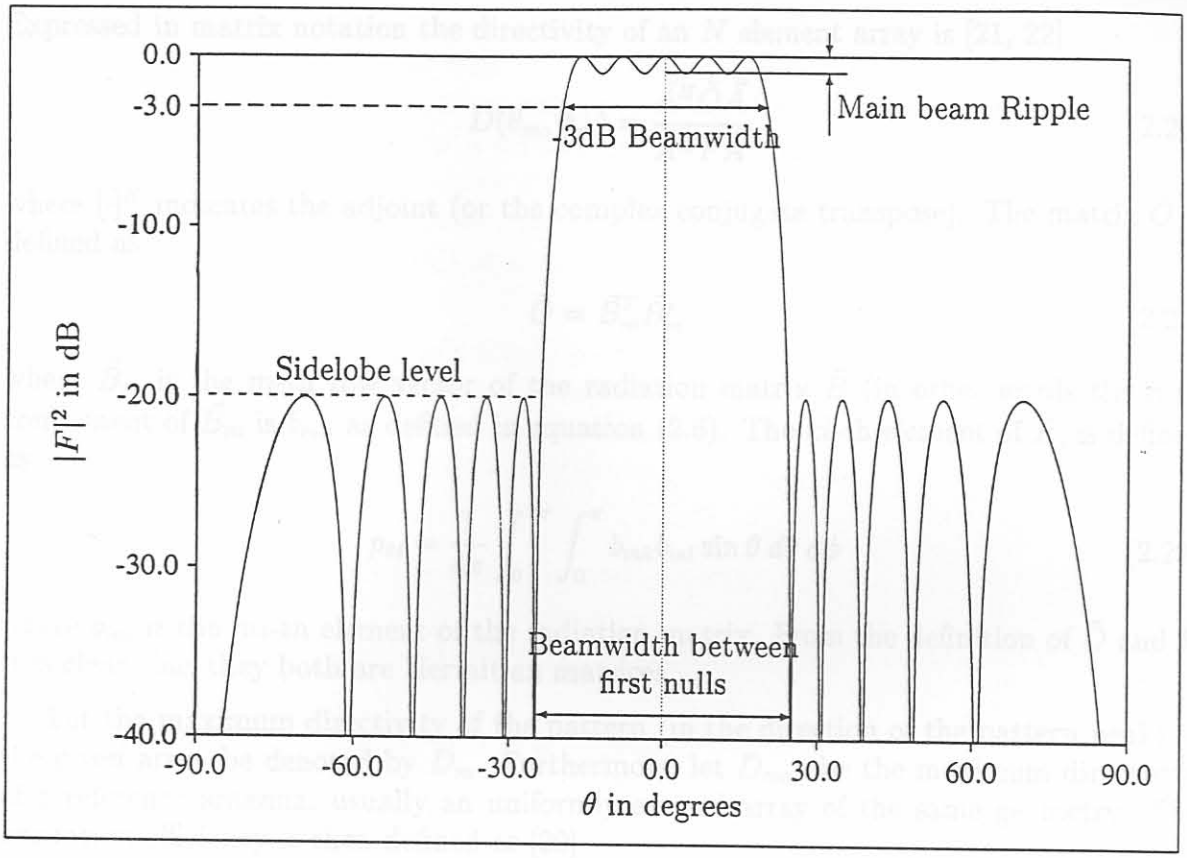

Figure 2.4: Radiation pattern characteristics.

- The beamwidth of the main beam is the angular difference between two selected points on the radiation pattern. Two commonly used beamwidths are the -3dB (or half power) beamwidth and the beamwidth between first nulls.
- In the shaped beam case, the mainbeam ripple is defined as the maximum peak-to-peak deviation of the radiation pattern from the ideal behaviour in the shaped beam region.

2.3.2 Directivity, Gain and Efficiency

The directivity $D(\theta_m, \phi_m)$ in a direction (θ_m, ϕ_m) is defined as the ratio of the radiation intensity from the antenna in that direction, to the average radiation intensity in all directions [20].

$$D(\theta_m, \phi_m) = \frac{4\pi \left|F(\theta_m, \phi_m)\right|^2}{\int_0^{2\pi} \int_0^{\pi} \left|F(\theta, \phi)\right|^2 \sin\theta \, d\theta \, d\phi} \tag{2.19}$$

Expressed in matrix notation the directivity of an N element array is [21, 22]

$$D(\theta_m, \phi_m) = \frac{\vec{A}^H \tilde{O} \vec{A}}{\vec{A}^H \tilde{P} \vec{A}} \tag{2.20}$$

where $[\cdot]^H$ indicates the adjoint (or the complex conjugate transpose). The matrix $\tilde{O}$ is defined as

$$\tilde{O} = \vec{B}_m^T \vec{B}_m^* \tag{2.21}$$

where $\vec{B}_m$ is the m-th row vector of the radiation matrix $\tilde{B}$ (in other words the n-th component of $\vec{B}_m$ is b_{mn} as defined in equation (2.6). The kl-th element of $\tilde{P}$, is defined as

$$p_{kl} = \frac{1}{4\pi} \int_0^{2\pi} \int_0^{\pi} b_{mk} b_{ml} \sin\theta \, d\theta \, d\phi \tag{2.22}$$

where b_{mi} is the mi-th element of the radiation matrix. From the definition of $\tilde{O}$ and $\tilde{P}$ it is clear that they both are Hermitian matrices

Let the maximum directivity of the pattern (in the direction of the pattern peak) of the given array be denoted by D_m. Furthermore, let D_{max} be the maximum directivity of a reference antenna, usually an uniformly excited array of the same geometry. The excitation efficiency is then defined as [20]

$$\eta_e = \frac{D_m}{D_{max}} \tag{2.23}$$

The gain, or absolute gain, of an antenna is the ratio of the radiation intensity, in a given direction, to the radiation intensity that would be obtained if the power accepted by the antenna were radiated isotropically. Gain does not include losses due to impedance and polarisation mismatches [20]. Gain does include conductor and dielectric losses. Directivity is a measure of the directional properties of an antenna and depends only on the radiation pattern of the antenna, while gain takes the radiation efficiency into account. The radiation or conversion efficiency of an antenna is therefore

$$\eta_r = \frac{G_m}{D_m} \tag{2.24}$$

If a single value of directivity or gain is given, the maximum value is implied.

2.3.3 Shaped Beam and Contoured Beam Patterns

There can be no general method of specifying shaped beam (or contoured beams) patterns since each is shaped in its own general way. It is perhaps best to name some typical shaped beam patterns which might be desired by systems designers and to suggest the reasons why this might be so.

The most common shaped beam pattern is probably the cosecant-squared elevation beam. The antenna pattern has a $\csc^2\theta$ beam shape in the vertical principal plane and a pencil beam in the horizontal principal plane. This beam shape is used in airport beacons and ground mapping radars. At a certain ground distance away from the beacon, the actual distance to the aircraft varies with the altitude of the aircraft. This beam shape radiates more electromagnetic power at a higher elevation angle to compensate for the difference in actual distance to the aircraft, resulting in a round trip signal that is θ independent.

Flat-top patterns with various footprint contour shapes, for example a bean shaped footprint for hemispheric coverage or a footprint in the shape of man-made boundaries (say the USA), are widely used in satellite applications where a certain area must be illuminated by an electromagnetic field of uniform strength.

2.3.4 Dynamic Range and Smoothness

Dynamic range is defined as the ratio of the maximum excitation magnitude to minimum excitation magnitude,

$$R = \frac{|a_{max}|}{|a_{min}|} \tag{2.25}$$

An excitation with a large dynamic range will be difficult the realize due to difficulties in building power dividers with large power division ratios in the feed network.

Excitations in close proximity with large difference in magnitude and/or phase are very difficult to implement due to the mutual coupling between the array elements. No explicit definition of the smoothness of an array excitation has been found in the literature. A measure of the smoothness of an array may by defined as the maximum element-to-element ratio variation

$$S_m = \left[\frac{|a_n|}{|a_{n\pm1}|}\right]_{max}. \tag{2.26}$$

To alleviate mutual coupling effects, the smoothness must be as close to unity as possible. This definition is used in most publications [23], but some publications [24] define the smoothness as the maximum Euclidean distance between any two adjacent array element excitations

$$S_m = |a_n - a_{n\pm1}|_{max}. \tag{2.27}$$

With this definition the smoothness must be as small as possible to minimize mutual coupling effects.

2.3.5 Sensitivity

In an engineering problem an important question is that concerning the sensitivity of a particular synthesised array excitation. Since the practical realization of the aperture

distribution is never exact, it is important to ascertain how such imperfections will affect the array factor. Tolerance sensitivity is a measure of the effect imperfections in the aperture distribution will have on the radiation pattern array factor [25:p.744]. A small tolerance sensitivity is always desirable. The tolerance sensitivity S is defined as the ratio of variance of the radiation pattern peak produced by the aperture errors,

$$S = \frac{\vec{A}^T \vec{A}^*}{\vec{A}^T \tilde{B} \vec{A}^*} \tag{2.28}$$

where $[\cdot]^*$ denotes the complex conjugate, and with the excitation vector $\vec{A}$ and the radiation matrix $\tilde{B}$ as defined in Section 2.2.1 .

2.3.6 Visible Space and Grating Lobes

Examination of equation (2.10) reveals that the linear array factor is periodic in the variable ψ. In the linear array case visible space is the part of the infinite periodic function that corresponds to a variation in the directional angle θ from $-90°$ to $90°$. Invisible space is all the values of ψ outside the visible space. As the inter element spacing increases, more of the periodic array factor will be mapped into visible space. If the spacing is large enough the radiation from the elements will add constructively at more than one θ angle. This additional main lobe is called a grating lobe. All array geometries have this phenomenon.

In most cases the grating lobes are unwanted. Close scrutiny of equation (2.19) shows that grating lobes adversely affect the directivity. The directional patterns of the array elements may suppress grating lobes. Larger inter element spacing allows for larger elements which will be more directive and will suppress the grating lobes to a greater extent. Grating lobes can be suppressed in conformal arrays by adjusting the element excitation of the element (if any) pointing in the direction of the grating lobe.

Visible space for planar arrays in the xy-plane is $0° \leq \theta \leq 90°$ and $-180° \leq \phi \leq 180°$. For conformal arrays visible space is $0° \leq \theta \leq 180°$ and $-180° \leq \phi \leq 180°$.

2.4 Classification of Array Synthesis Techniques

The antenna array synthesis problem can be succinctly stated as that of finding the excitations which will produce a radiation pattern with certain performance indices maximised subject to specified constraints on the pattern and possibly even the excitations themselves. Such constraints cannot be completely arbitrary and must be consistent with the basic physical properties of the array.

Array synthesis is, from a mathematical point of view, a problem of optimisation theory, and many engineers apply this approach. It can on the other hand in certain cases also be approached from the point of view of approximation theory. Early work

was based almost entirely on the latter type of consideration, and research in this area continues. Optimisation and approximation theory are disciplines which are of course inextricably linked.

Work on the synthesis of antenna arrays may be divided in a number of ways. For instance, one could classify synthesis techniques according to the geometries being considered. Alternatively, synthesis methods could be separated into those which deal with continuous sources (from which array excitations are obtained by some form of sampling) or discrete elements directly (for which the array element excitations can be obtained in a direct manner without the need for any further approximation, sampling or perturbation procedures). Synthesis techniques could also be grouped in terms of whether they are applicable to single lobe high directivity or shaped beam patterns. We could also classify methods according to whether they are analytical in character or rely on some numerical optimisation procedure.

Lastly, whether the radiated field pattern or the radiated power pattern are of interest in the synthesis problem can also be used as a basis for classification. Field synthesis (where the phase of the radiated fields are fixed) is less complicated as there exist a unique answer to the problem. In practical arrays the phase of the far-field is usually set by the way the arrays is implemented, for example any centre-fed symmetrical array will always have a linear far-field phase. With a correctly chosen optimisation technique convergence is guaranteed.

In power pattern synthesis only the power, or square of the radiated fields, are of interest. The phase distribution of the array pattern is important and may be arbitrary. Thus the power pattern synthesis problem, in general terms, is an ill-conditioned inverse problem with no unique solution. Although this gives a large set of possible solutions, allowing for a solution that makes engineering sense (more effective array or one easier to realise), it makes the synthesis problem much more difficult. Engineering judgement is also necessary to set constraints that will give the optimum result, not only from a synthesis viewpoint, but also from the point of view of the physical realisation of the synthesised distribution.

Most of the work on array synthesis methods described in the literature deals with the linear array problem. These methods are often incorporated in some way to synthesise planar arrays. However, this does not always provide the best results, and more recently attempts have been made to devise approaches which tackle the planar array problem more effectively. Their use often assumes a knowledge of the standard linear array methods. Relatively little has been published on conformal synthesis.

2.5 Direct Synthesis of Equi-spaced Linear Arrays

Consider a linear array of $N+1$ elements, positioned along the x-axis (starting at $x=0$). By the introduction of the substitution $w = e^{j\psi}$ the linear array factor (2.10) can be

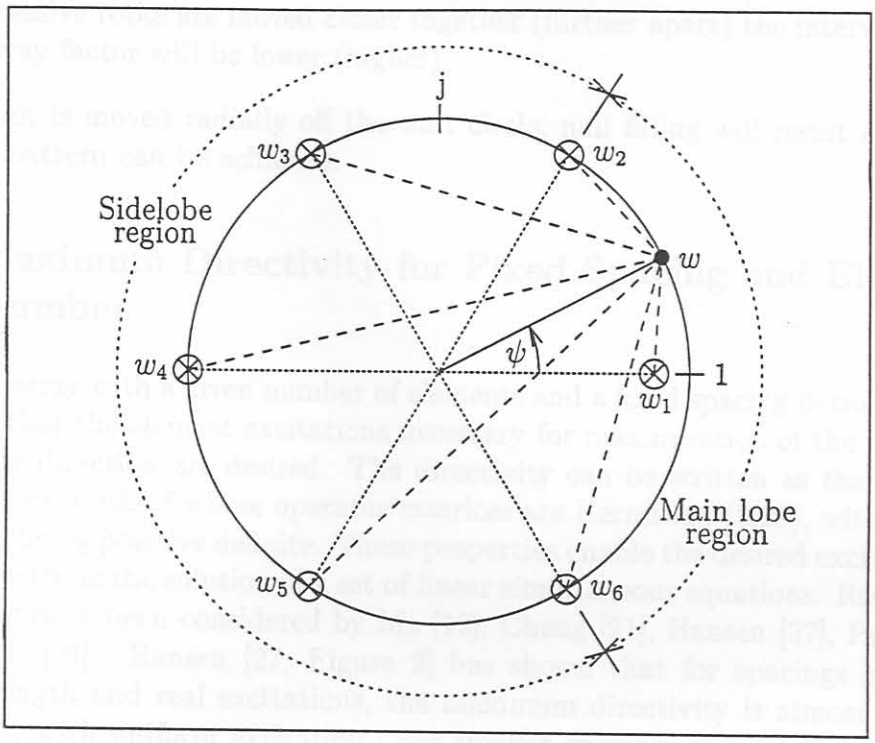

Figure 2.5: Schelkunoff unit circle representation of an eight element linear array

written in the form of a polynomial of degree N, with N distinct roots w_n as

$$AF(w) = \sum_{n=0}^{N} a_n \, w^n = \prod_{n=1}^{N} (w - w_n) \tag{2.29}$$

Schelkunoff [26] introduced the useful concept of constructing a unit circle in the complex w plane. Since ψ is real, the absolute value of $w = e^{j\psi}$ is always unity. Plotted in the complex plane, w (but not w_n) is always on the circumference of the unit circle as depicted in Figure 2.5. For a half wavelength inter element space $d = \frac{\lambda}{2}$, the range of ψ is 2π radians, and so w describes a complete circle as θ varies from $0°$ to $180°$. If the spacing is greater than half wavelength the range of ψ is greater than 2π radians, and the range of w will overlap itself. For $d = \lambda$ spacing w will circumvent the unit circle twice and grating lobes appear (the second pass through the main lobe region is a grating lobe.

Each root w_n is described by its angular position as well as its radial distance off the unit circle. The array factor is the product of the distances between each of the roots and the angular position of w. The array factor is thus completely controlled by the placement of the roots w_n. The synthesis of any desired pattern can be viewed as a problem of finding the proper positions of the roots; in fact many of the successful synthesis methods rely on some zero placement scheme. Three obvious features can be noted, viz:

- if the roots are placed on the unit circle, a pattern with deep nulls will result

- if successive roots are moved closer together (further apart) the intervening lobe of the array factor will be lower (higher)
- if a root is moved radially off the unit circle, null filling will result and a shaped beam pattern can be achieved.

2.5.1 Maximum Directivity for Fixed Spacing and Element Number

Consider an array with a given number of elements and a fixed spacing between elements, and assume that the element excitations necessary for maximisation of the directivity in the broadside direction are desired. The directivity can be written as the ratio of two quadratic forms, both of whose operator matrices are Hermitian (2.20), with that in the denominator being positive definite. These properties enable the desired excitations to be obtained directly as the solution of a set of linear simultaneous equations. Results of such computations have been considered by Ma [12], Cheng [21], Hansen [27], Pritchard [28] and Lo et al. [29]. Hansen [27, Figure 2] has shown that for spacings greater than a half wavelength and real excitations, the maximum directivity is almost identical to that obtained with uniform excitation. For smaller spacings the maximum directivity obtainable is greater than that of a uniform array; this phenomenon is called super directivity. However, the excitations required for super directivity have large oscillatory variations in amplitude and phase from one element to another [25:p.761], and are always associated with an enormously large tolerance sensitivity. For this reason fabrication difficulties are usually prohibitive and super directivity is avoided in most instances. Experimentally it is difficult to produce an array with a directivity much in excess of that produced by a uniformly excited array. In general the sidelobes of a uniformly excited array will be too high for practical use; hence the synthesis techniques to be described immediately below.

2.5.2 Dolph-Chebyshev Synthesis

Rather than maximise the directivity of the array, consider the problem of minimisation of beamwidth; the two approaches are not necessarily equivalent. beamwidth minimisation subject to a constraint on the sidelobe ratio is the classical array synthesis problem solved by C. L. Dolph in his monumental 1946 paper [30]. The underlying argument behind Dolph's approach has been put concisely by Hansen [27]:

> "A symmetrically tapered (amplitude) distribution over the array or aperture is associated with a pattern having lower sidelobes than those of the uniform (amplitude) array. Lowering the sidelobes broadens the beamwidth and lowers the excitation efficiency. ... Some improvement in both beamwidth and efficiency is obtained by raising the farther out sidelobes. Intuitively one might expect equal level sidelobes to be optimum for a given sidelobe level."

In order to synthesise such a pattern for broadside arrays with inter element spacing greater than or equal to a half wavelength, Dolph made use of the Chebyshev polynomials. Expressions for computing the required excitations can be derived from these polynomials. Such formulas have been derived by Barbiere [31], Stegen [32, 33], van der Maas [34] and Bresler [35].

Dolph [30] was able to prove that the array so synthesised is optimum in the sense that for the specified sidelobe ratio and element number, the beamwidth (between first nulls) is the narrowest possible. Alternatively, for a specified first null beamwidth, the sidelobe level is the lowest obtainable from the given array geometry. This means that it is impossible to find another set of excitation coefficients yielding better performance, in both beamwidth and sidelobe ratio, for the given element number and uniform spacing d. It represents a closed form solution to the optimisation problem of first null beamwidth minimisation subject to sidelobe constraints.

The Dolph-Chebyshev theory is indispensable and serves as a firm foundation for sum pattern synthesis. It provides a means of understanding array principles and indicates upper bounds on the performance that can be achieved under certain circumstances. However, it does have a number of drawbacks with regard to its use as a practical distribution. There is a tendency of equal sidelobe level distributions such as the Dolph-Chebyshev to have large excitation peaks at the array ends (a non-monotonic distribution) for certain element number/sidelobe ratio combinations. For a given number of elements there will be a certain sidelobe ratio for which the distribution of excitations is "just" monotonic. If the number of elements is increased but this same sidelobe ratio is desired, the required distribution will be non-monotonic. Increasing the sidelobe ratio (lower sidelobes) will once more allow a monotonic distribution.

The peaks in the distribution at the array ends (called edge brightening) are not only disadvantagious in that they are difficult to implement and make an array more susceptible to edge effects, but they are also indicative of an increase in the tolerance sensitivity [25].

Optimum beamwidth arrays do not necessarily provide optimum directivity, especially if the array is large [36:p.91]. To see this, one can consider a Dolph-Chebyshev array with a fixed sidelobe ratio. Let the array size increase (increase the number of elements while keeping the spacing fixed), at each stage keeping the sidelobe ratio constant and normalising the radiation pattern. This is permissible because the directivity to be found at each stage is only dependent on the angular distribution of the radiation and not on any absolute levels. It is then observed that the denominator of the directivity expression is dominated by the power in the sidelobes after a certain array size is reached, and remains roughly constant thereafter. This is called directivity compression [36:p.91]. Thus it is found that the Dolph-Chebyshev distribution has a directivity limit [33] because of its constant sidelobe level property. For a given array size and maximum sidelobe level it may not be optimum from a directivity point of view. To remove this limitation a taper must be incorporated into the far out sidelobes.

2.5.3 Villeneuve Distributions

As recently as 1986 Hansen [25:p.698] could correctly state that there were "no discrete distributions that yield a highly efficient tapered sidelobe pattern" directly and that in designing most arrays a continuous distribution had to be sampled in some manner. For the narrow beam, low sidelobe pattern, this is no longer the case as a result of an ingenious approach devised by Villeneuve [37]. The method utilises the important principle of synthesising aperture distributions by correct positioning of the space factor zeros. The Villeneuve distribution is the discrete equivalent of the highly desirable Taylor $\bar{n}$ distribution of continuous line sources (to be discussed in Section 2.6.2). The array element excitations can be obtained in a direct manner with the Villeneuve approach.

The application of the Villeneuve procedure consists of the following: Select an array of a specified number of elements with the maximum sidelobe level specified. The first step consists of determining the space factor zeros for a Dolph-Chebyshev distribution with the same sidelobe level. Next determine the zeroes of a uniformly excited array of the same number of elements (the array factor of which will have a tapered sidelobe envelope). Then alter the zeroes of the Chebyshev array so that all except the first $\bar{n}-1$ zeroes now coincide with those of the uniform array. In addition, multiply each of the first $\bar{n}-1$ Chebyshev zeros by a dilation factor σ [25:p.722]. Use these final zeroes of the perturbed Chebyshev array to determine the final element excitations. Villeneuve [37] has devised efficient ways of doing this. These excitations are those of a discrete "Taylor-like" distribution (the latter is discussed in Section 2.6.2), with the close-in sidelobes close to the design maximum specified, and the further out ones decreasing at the rate $\frac{1}{u}$ (where $u = \frac{Nd}{\lambda}\sin\theta$) in amplitude as their position becomes more remote from the main beam. As with the continuous Taylor distribution, $\bar{n}$ is a design variable. A comparison of the excitation efficiencies of the Villeneuve (discrete) and Taylor (continuous) distributions has been published by Hansen [38]. The above technique is now generally referred to as the Villeneuve $\bar{n}$ distribution [38].

Finally, a generalised Villeneuve $\bar{n}$ distribution has been developed by McNamara [39] which can be used to directly synthesise discrete array distributions for high efficiency sum patterns of arbitrary sidelobe level and envelope taper. The Dolph-Chebyshev distribution serves as a "parent" space factor. The correct perturbation of the zeros of this "parent" space factor serves to incorporate the sidelobe behaviour desired, while at the same time keeping the excitation efficiency and beamwidths as close to their optimum values as is possible under the required sidelobe ratio and envelope taper conditions. The level of the first sidelobe is set by the parent Dolph-Chebyshev distribution, the envelope taper rate controlled by a parameter ν, and the point at which the required taper proper begins determined by the transition index $\bar{n}$. The excitations are obtained from the perturbed space factor zeros by solving a set of simultaneous linear equations. The synthesis procedure is rapid and consequently design trade off studies are feasible. The proper choice of the values of $\bar{n}$ and ν for a particular application will depend on the relative importance of the peak sidelobe level compared to that of the farther out sidelobes, the root-mean-square sidelobe ratio desired [40],, and their effect on the excitation efficiency.

2.5.4 Difference Pattern Synthesis

A difference pattern has a null at bore sight with two main lobes of equal height, but 180° phase difference, on each side of the bore sight null, as well as some sidelobes. A difference pattern is obtained by an anti-symmetrical (or out of phase) excitation. For a difference pattern to be optimum in the Dolph-Chebyshev sense it must have the narrowest possible difference lobes and the largest bore sight slope for a specified sidelobe level. Price and Hyneman [41] listed the properties of the polynomial which will provide the optimum difference excitations. McNamara [42] identified the Zolotarev polynomials as the appropriate set of polynomials. The Zolotarev polynomial distribution [42, 43, 44] or its modification [45, 46] can be used for the synthesis of linear arrays with optimum difference pattern performance. The Zolotarev distribution is the difference pattern counterpart for the Dolph-Chebyshev sum pattern, while the modified Zolotarev distribution is the difference analogy of the generalised Villeneuve $\bar{n}$ distribution.

The maximisation of directivity and the maximisation of normalised bore sight slope for difference arrays (without sidelobe constraints) do not result in the same excitation. Difference patterns with maximum directivity and maximum normalised bore sight slope have been discussed in references [47] and [48] respectively. Simultaneous sum and difference pattern synthesis employing quadratic programming is described in reference [49].

2.5.5 Synthesis of Linear Arrays with Shaped Beams

The array factor can be divided into two regions, the shaped beam region and the sidelobe region. The shaping function represents the ideal behaviour of the array factor in the shaped beam region.

The array factor summation (2.10) is very similar to a Fourier series of the same order as the number of elements in the array. The Fourier series synthesis method [9:p.531] equate the Fourier series coefficients, calculated from the desired pattern, to the element excitations. Due to the limited extent (harmonics) of the Fourier series, the resulting array factor exhibits very large ripple in the shaped region with high sidelobes in the sidelobe region.

An alternate particularly convenient way to synthesise a shaped radiation pattern is to sample the ideal pattern at various points. The Woodward-Lawson [50, 9:p.526] technique is the most popular of these methods. The technique relies on the fact that any realizable pattern, of an N-element array, can be analysed as the weighted summation of a set of N orthogonal beams, each having a basic $\frac{\sin(Nx)}{\sin(x)}$ shape. The maximum of each of the $\frac{\sin(Nx)}{\sin(x)}$-shaped beams coincides with a zero in all the other beams. Woodward's synthesis technique samples the ideal pattern at increments of $\frac{2\pi}{N}$. The synthesised array is thus the superposition of array factors from N uniform amplitude, linear progressive phase excitations with the phase increment of each excitation such that the array factor peak is placed at the sampling point. Although the array factor is equal to the ideal pattern at the sample points, it exhibits large ripples in the shaped region and high

uncontrollable sidelobes in the sidelobe region.

An objection to the Woodward method is that it only uses data form N points, whereas there are $2N-2$ degrees of freedom ($N-1$ relative amplitudes and phases) available. Woodward's method makes inefficient use of the zeroes on the Schelkunoff unit circle, placing them in radial pairs. Milne published a method [51] that effectively takes $2N-1$ sample points, spaced at intervals of $\frac{2\pi}{(2N-1)}$, to determine a realizable array factor. The method essentially is a convolution of a "scanning function" (usually a Dolph-Chebychev pattern) and the shaping function.

By a trial-and-error adjustment of the angular positions of the roots of the factorised array factor, on the Schelkunoff unit circle, Elliott [52] obtained any sidelobe topography. Later, Elliott and Stern [53] introduced the concept of null filling to produce shaped beam patterns. This is achieved by moving the roots in the shaped beam region radially from the Schelkunoff unit circle. Orchard et al. [54] presented an iterative method by which the angular and radial positions of all the roots are simultaneously adjusted so that the amplitude of each ripple in the shaped region and the height of each sidelobe in the non-shaped region are individually controlled.

The method was extended by Kim and Elliott [55] to produce pure real distributions for symmetric patterns, such as flat-top patterns. The pure real distributions are obtained by placing the roots in the shaped beam region in conjugate pairs. By pairing the roots in the shaped beam region, both roots at the same angular position but one root inside and the other outside the unit circle, a centre-fed symmetric distribution can be obtained [56]. Ares et al. [57] extended the technique to allow the synthesis of patterns with prescribed nulls.

2.6 Analytical Synthesis of Continuous Line Source Distributions

Although arrays of discrete radiating elements are being dealt with in this work, no review of synthesis techniques would be complete without reference to similar work on the synthesis of continuous line source distributions. Line source synthesis is important in the array context for several reasons. Firstly, some general principles are equally applicable to arrays. Secondly, continuous distributions can be sampled for use with discrete arrays. Furthermore, the direct discrete array synthesis methods have generally developed "under the guidance" of the theory on continuous distributions.

Bouwkamp and de Bruyn [58] showed that with a continuous line source of fixed length it is possible (in theory) to achieve any desired directivity. Although this implies that there is no limit to the directivity, any directivity increase above that obtained from the aperture when it is uniformly excited is accompanied by a sharp increase in the net reactive power required at the source to produce it [18:p.3], and thus a large tolerance sensitivity. Practical considerations therefore makes it unacceptable, as in the case of

the unconstrained maximisation of the directivity of the discrete array discussed earlier (in Section 2.5.1). To be realizable physically, some constraint has to be placed on the proportion of reactive to radiative power, or equivalently on the quality factor [36:pp.3-4].

It is customary, when dealing with continuous line-source distributions, to use the variable $u = \frac{L \sin\theta}{\lambda}$, where L is the length of the source and λ is free-space wavelength. This practice will be followed in the discussions to follow.

2.6.1 Maximisation of Directivity Subject to a Sidelobe Level Constraint

The next question regarding continuous distributions is that of determining a distribution which provides the narrowest beamwidth for a given sidelobe level, and vice versa. This was answered by Taylor [59], who used the Dolph-Chebyshev theory as starting point. Using an asymptotic relationship for the Chebyshev polynomials given by van der Maas [34], Taylor derived the continuous equivalent of the Dolph-Chebyshev distribution. This distribution produces a pattern where all the sidelobes are of an equal level, and is optimum in the sense that it provides the narrowest beamwidth for a given sidelobe ratio of any non-super directive distribution. Taylor called this the "ideal" line source distribution. "Ideal" because of the fact that it is not realizable, having a singularity at each end.

2.6.2 Maximisation of Directivity Subject to a Tapered Sidelobe Level Constraint

A solution to the problem of singularities at the ends of the distribution was also devised by Taylor [59]. He recognised that the synthesis problem is one of correctly positioning the zeros of the space factor. Taylor observed that close-in zeros should maintain their spacings to keep the close-in sidelobes suitably low and the beamwidth narrow, but that at the same time the further out sidelobes should decay as $\frac{1}{u}$ [36:p.55, 25:p.720]. Such sidelobe decay is found in the space factor of a uniform line-source distribution. Taylor stretched the u scale by a dilation factor σ slightly greater than unity (so that the close-in zero locations are not shifted much) and chosen such that at some point a shifted zero is made to coincide with an integer $\bar{n}$. From this transition point, the zeros of the ideal line-source are replaced by those of the uniform line-source. In this pattern the first few sidelobes (the number is determined by the position of the transition point selected) are roughly equal, with a $\frac{1}{u}$-sidelobe decay thereafter. The corresponding aperture distribution is then found as a Fourier series obtained from the above mentioned information on the zeros [8:p.58]. The final result is a distribution (referred to as the Taylor $\bar{n}$ distribution) which, for a given sidelobe ratio, gives both a narrower beamwidth and higher directivity than any comparable continuous line-source distribution. Information relating the sidelobe ratio, dilation factor and $\bar{n}$ values have been given by Hansen [8:p.57]. Also given are expressions for the aperture distribution itself [8:p.58]. Too large a value

for $\bar{n}$ (exactly how large depends on the specified sidelobe ratio) implies that the ideal line-source distribution is "being approached too closely." The aperture distribution then becomes non-monotonic with peaks at the aperture ends (although the singularities of the ideal source do not occur), and an accompanying increase in excitation tolerances. The Taylor $\bar{n}$ distribution was generalised by Rhodes [18:pp.129-137] to a distribution dependent on the transition variable $\bar{n}$, and an additional variable, which controls the taper rate of the sidelobe envelope for a selected transition zero. The "ideal" line-source and Taylor $\bar{n}$ distribution approaches just described are special cases of this generalised distribution.

A third continuous distribution due to Taylor is his one-parameter line-source distribution [8:p.58]. The Taylor $\bar{n}$ distribution essentially selects a design between the "ideal" and one-parameter cases. However, for the same first sidelobe ratio, the Taylor $\bar{n}$ distribution has a higher excitation efficiency (and hence directivity), and is therefore used more often. The reason for this is that the $\bar{n}$ distribution tends to flatten out at the ends of the line source while the one-parameter case does not. The Taylor one-parameter distribution was generalised by Bickmore and Spellmire, whose work has been reported in and [25:pp.731-733], into a two-parameter continuous line-source distribution. One of the parameters selects the starting sidelobe ratio, while the other selects the rate of decay of the sidelobes. These two parameters are completely independent. As expected, the Taylor one-parameter distribution can be shown to be a special case of the Bickmore-Spellmire distribution.

2.6.3 General Pattern Synthesis

The need for sidelobe suppression may vary as a function of direction. Elliott proposed an iterative perturbation method that gives control over each sidelobe [10:pp.162-172, 60]. The Taylor distribution is used as a starting point. If the perturbations are small the expression for the new pattern can be truncated. This truncation results in a set of deterministic linear equations. The perturbed root positions are then computed by matrix inversion. If the required pattern differs too much from the starting Taylor pattern an interim desired pattern can be postulated to ensure convergence.

Ares [61] adapted the general method of Orchard et al. [54] for discrete linear arrays to synthesise continuous line sources. As with linear arrays synthesis the roots can be moved radially from the unit circle to produce filled-in nulls in the shaped region. The method allows the synthesis of shaped beams with any arbitrary sidelobe topography.

2.6.4 Continuous Difference Distributions

An analogous synthesis problem exists for difference patterns: find the line source distribution that will produce an antisymmetric difference pattern with two main beams surrounded by sidelobes of a specified maximum height. The problem was addressed by Bayliss [62]; an ideal space factor was not found from which to determine the null

positions, but Bayliss undertook a numerical parametric study to find formulas for the root placement.

The perturbation used to obtain an arbitrary sidelobe level topography from a Taylor pattern can also be used to synthesise a difference pattern with arbitrary controlled sidelobe levels [63, 10:pp.185-187].

2.6.5 Discrete Versus Continuous Line Source Synthesis

It is clear from the previous section that the theory of continuous aperture line source distributions for sum patterns is extensive and well developed. If these are to be used with arrays of discrete elements, some form of discretization process must be performed. The earliest discretization methods simply sampled the continuous distributions at the element locations. Unless the arrays are extremely large (that is, larger than most practical arrays) a badly degraded pattern may be obtained [64, 65].

An alternative technique was proposed by Winter [66]. The initial array element excitations are determined by sampling the continuous distribution and then iteratively adjusting these using Newton-Raphson minimisation of an error expression comprised of the sum of the squares of the differences between calculated (discrete) and specified (continuous) levels for a selected number of sidelobes. He reported successful discretization of arrays with very low sidelobe levels [67].

Elliott [10:pp.172-180, 64] devised a more sophisticated yet direct alternative method. This method matches zeros. Instead of sampling the continuous aperture distribution, one requires that the pattern zeros of the continuous case also occur in the starting pattern of the discrete case. If the resulting pattern does not meet the design goal, a linear perturbation of the zero positions is iteratively applied to the discrete distribution in order to bring the final pattern within specification.

2.7 Techniques for Planar Array Synthesis

There is considerable interest in the problem of designing satellite-borne antennas that will beam electromagnetic waves of uniform strength onto a specified portion of the earth's surface while causing negligible radiation to reach the remainder of the earth's surface. In order to best utilise the limited spacecraft transmitter power and reduce possible interference problems with other coverage areas, the ideal antenna would have uniform gain over the coverage region and no radiation elsewhere. Such shaped beams are said to have a *contoured footprint* [19]. The fact that a real antenna is of finite size, along with several other practical limitations, means that there will be some sidelobe radiation outside the defined irregularly shaped coverage region.

The most commonly utilised method of generating contoured beams has been that of an array of feed horns illuminating an offset paraboloidal reflector [68, 69]. Each feed

generates a component beam, and these are properly weighted through a beam-forming network to obtain the desired contoured beam. Alternatively, a shaped offset reflector fed by a single feed [70] is also capable of producing fixed contoured beam coverage.

A disadvantage of the component beam approach is the fairly high ripple within the footprint if a rather large number of beams are not used [19], and the relatively poor control of the sidelobe level outside the coverage area. Also, observing that the size, mass and complexity (especially of the feed arrays) of satellite antennas have grown significantly with each new system, Bornemann, Balling and English [71] have argued in favour of eliminating the reflector and using a direct radiating array. Such an approach would seem particularly advantageous for reconfigurable antennas [72], although this is now also possible if reflector antennas are used [70].

The previous sections provide a relatively complete summary of direct methods that can be used to synthesise linear arrays providing high directivity, low sidelobe patterns. Regarding their relation to planar array synthesis, Elliott [10:p.196] notes that: "Under certain circumstances, much of what was developed there (for linear arrays) can be carried over to apply to planar arrays. However, practical considerations will at times require the use of design techniques that are peculiar to planar arrays.". Two-dimensional polynomial roots are not just simple points as in the one-dimensional case, but they can also be contours. One root contour may even cross another. Due to the lack of a general two-dimensional factorisation theorem one dimensional (linear array) root-placement techniques can not in general be extended to the two-dimensional (planar array) case. Synthesis methods for direct radiating planar arrays with fully contoured beams [73, 74, 75, 76] use some form of non-linear numerical optimisation procedure. Albeit successful in some cases, such techniques do not always have guaranteed convergence [77], and are furthermore time consuming and expensive. The method described in [78, 79, 80] represents initial attempts at overcoming these difficulties by utilising root placement based techniques, known to work well in linear array synthesis, for obtaining continuous distributions with elliptical contours. These distributions are subsequently iteratively sampled to obtain the excitations of the actual discrete array. Applying root placement directly to the discrete planar array does not produce satisfactory patterns, but the excitations thus obtained serve well as an initial guess for numerical optimisation techniques [77].

In order to describe a planar array geometry it is necessary to specify both its element lattice and the boundary shape, as mentioned earlier. Again, only those synthesis techniques applicable to the rectangular lattice case are of interest here. In the remainder of this section we will briefly list those methods for planar arrays that can be classed as "analytical", in that no form of iteration, perturbation or numerical optimisation is needed (although a considerable amount of computation may still be required) once the set of specifications for the final pattern has been set. Numerical synthesis methods form the subject of Section 2.8.

2.7.1 Separable Distributions

For rectangular arrays, if the boundary shape is square or rectangular, and if the aperture distribution is separable, the pattern is the product of the patterns of two spatially orthogonal linear arrays (collapsed distributions), and all the methods mentioned for linear arrays in earlier sections can be extended readily. However, separable distributions suffer from some directivity limitations [10:p.211] which are highly undesirable in practice. The separable distribution over achieves in most of the sidelobe region (i. e. gives sidelobe levels far lower than necessary). This reduction is bought at the price of beam broadening, with its concomitant lowering in directivity. These limitations can only be overcome by the use of ϕ-symmetric patterns.

2.7.2 Direct Synthesis of Discrete Arrays

The Dolph-Chebyshev technique has not been extended to general planar arrays. However, Tseng and Cheng [81] have shown how it can be done for a planar array with a rectangular lattice and a rectangular boundary shape, and with an equal number of elements in each principal direction (the $\hat{x}$- and $\hat{y}$-directions). They used the Baklanov transformation (written in terms of the u and v as defined in this chapter) $w = w_0 \cos(\frac{1}{2}u)\cos(\frac{1}{2}v)$ [82] to convert the Chebyshev polynomial, a function of one variable w, to a polynomial of two variables u and v. The resulting Tseng-Cheng distribution is non-separable and gives a Dolph-Chebyshev pattern in every ϕ-cut.

Goto [83] first expressed a symmetrical linear array factor in polynomial form, with the polynomial variable $w = \cos(\frac{1}{2}\psi)$. This allows the synthesis of planar arrays with patterns other than Dolph-Chebyshev patterns. He then used a transformation similar to the Baklanov transformation to synthesise planar arrays with hexagonal lattice; $w = \cos(u)\cos(v)$. Goto extended the technique to planar array with not only a hexagonal lattice but also a hexagonal boundary [84]. To achieve a hexagonal planar array the transformation is $w = \alpha + \beta\cos(\psi) = \frac{1}{2}\cos(u)[\cos(u) + \cos(v)]$. This transformation results in planar arrays with near rotationally symmetric patterns.

The restriction of equal numbers of elements along each array axis of the Tseng-Cheng distribution can be lifted, as shown by Kim and Elliott [85], by using a generalisation of the Baklanov transformation, $w = \cos^p(\frac{1}{2}u)\cos^q(\frac{1}{2}v)$. The ratio of "rows" versus "columns" of the array is fixed by the selection of p and q. They also showed that null-filling is feasible, achieving elliptical footprint contours. A transformation similar to that of Goto [84] was proposed by Kim [86] to synthesise hexagonal arrays to produce almost rotationally symmetric patterns.

Richie and Kritikos [77] applied a root placement technique, known to work well with linear arrays, directly to the discrete planar array. Roots in a two dimensional pattern can be points, lines or more complex contours making root placement difficult. The resulting pattern does not meet all the design criteria, such as sidelobe level and ripple specifications, but the excitation may used as a starting values for numerical optimisation

techniques.

2.7.3 The Convolution Synthesis Method

Realizing the array factor of an array with uniform spacing has the form of a discrete Fourier transform, Laxpati [87] proposed the use of discrete convolution of small arrays to obtain the excitation of a planar array. The planar array factor is the product of the array factors of a number of small arrays. Each of these small array factors has its own prescribed null locus; as a result of the multiplication the planar array factor contains all these null loci [88, 89]. The convolution method can be used to synthesise an array with arbitrary prescribed pattern nulls and almost any boundary shape [90]. Since no closed form relation exists between the null loci and the lobe peaks the placement of loci for the synthesis of more general patterns must be done interactively. This would be very time consuming even for relatively small arrays.

Laxpati [90] synthesised a 36-element diamond by the convolution of 5 four-element rhombiod arrays. The convolution of the diamond shaped array with a six-element linear array (along the x-axis) was then used to obtain a five-ring hexagonal array. Using a larger linear array it is possible to obtain an array with a hexagonal lattice and a stretched hexagonal boundary. The use of differently shaped arrays as building blocks result in differently shaped root loci. For instance a four-element rhombiod array factor has near circular shaped inner contours while all the root loci of a linear array factor are lines perpendicular to its axis. In places in the pattern where root loci are closely spaced the sidelobe will be very low and vice versa. Since the root positions are controled only on one principal axis high sidelobe do appear in the examples in his paper.

The method was extended to synthesis symmetrical square and hexagonal arrays where the sidelobe typography, rather than the null loci, is described [91]. This extension requires the small arrays to have the same geometry. The convolution method is computationally simple and can be used to synthesise very large arrays.

2.7.4 The Transformation Based Synthesis Technique

The transformation technique utilises a transformation, first used to design digital filters [92], that divides the planar array synthesis problem into two decoupled sub-problems [93, 94]. In the antenna array context, one sub-problem consists of a linear array synthesis, for which powerful methods of determining appropriate element excitations exist. The other involves the determination of certain coefficients of the transform in order to achieve the required footprint contours. The number of coefficients which need to be used depends on the complexity of the desired contour, but is very small in comparison to the number of planar array elements. The size required for this prototype linear array depends on the number of transformation coefficients used and the planar array size. Recursive formulas then determine the final planar array excitations from the information forthcoming from the above two sub-problem solutions. Thus the method is computa-

tionally efficient, making trade-off studies feasible even for large arrays. Simple formulas for the calculation of the transformation coefficients for circular and elliptical contours are given in [95, 94]. However, only patterns with quadrantal or centro symmetry can be synthesised using the transformation method up to the stage to which it was developed in [95, 94]. Extensions to the transformation to allow arbitrary contours, as well as non-rectangular boundaries and lattices, form the subject of Chapter 3 of this thesis and a detailed mathematical treatment of the transformation based synthesis method is given there.

2.7.5 Direct Synthesis of Continuous Planar Source Distributions

Taylor [96] extended his continuous line-source analysis to the case of a planar aperture with circular boundary shape with a ϕ-symmetric aperture distribution. A one-parameter circular distribution has been described by Hansen [97, 98] using the procedure adopted by Taylor for the one-parameter line source distribution mentioned earlier in Section 2.6.2. Although similar to the Taylor distribution, the Hansen one-parameter distribution is "slightly less efficient, but the required distribution is smoother and more robust" [25:p.855].

Various extensions to Taylor's method have been proposed [99, 100, 101]. The most significant contribution was made by Elliott and Stern [79], who succeeded in combining Taylor's method with the linear array synthesis method proposed by Orchard, Elliott and Stern [54]. This development permits the synthesis of rotationally symmetric shaped beam patterns with individually controllable ring sidelobes for continuous planar apertures with circular boundaries. Recently Ares, Monero and Elliot [80] extended this combined Taylor method by linearly stretching the distribution to obtain a arbitrarily shaped contoured footprint. A circular flat-top pattern is first synthesised, then the aperture in every ϕ-cut is stretched inversely proportional to the flat-top beamwidth in that ϕ-cut to obtain the desired footprint pattern.

2.7.6 The Sampling of Continuous Planar Distributions

If the continuous distributions described in Section 2.7.5 are to be used with arrays of discrete elements, some form of discretization must be performed. As indicated for the linear array situation in Section 2.6.5, the naive direct sampling of the continuous distribution may lead to noticeable pattern degradation unless the array is very large. Unfortunately, the rather convenient improved sampling ideas for linear arrays, discussed in Section 2.6.5, do not carry over to planar arrays, reasons for which are given by Elliott [10:pp.243-249]. Less direct approaches (albeit using the continuous distributions as starting points) are required to iteratively alter the sampled distribution in order to improve the array pattern performance, and these are better classified as numerical synthesis procedures to be discussed as part of Section 2.8 which follows immediately.

2.8 Numerical Synthesis of Arrays

Numerical techniques which neither take advantage of the peculiar properties of the array factor nor information available from the analytical solution to related synthesis problems, or both, are usually slow to converge and inefficient. Therefore, although it is always possible to formulate the array synthesis problem very precisely as a nonlinear optimisation problem with nonlinear constraints, such general optimisation approaches prove to be undesirable in practice. More "customised" methods which exploit known characteristics and insight into the array synthesis problem are preferred. Some of the more general methods can be used for conformal array synthesis.

In order to summarise the numerical array synthesis methods it will be convenient to divide these into two groups:

- those that can be considered perturbation methods which begin with results obtained from one of the synthesis procedures discussed in earlier sections
- those that make use of minimisation/maximisation (optimisation algorithms) of some array performance index subject to a set of constraints.

2.8.1 Synthesis of Planar Arrays with Contoured Beam Patterns

All the planar synthesis techniques mentioned in Section 2.7 can be used to synthesise the direct radiating array. Bornemann [71] uses a method similar to Woodward's, applied to a planar array, to achieve various complex beam shapes and contours. Guy [102] proposed an interactive iterative synthesis method which uses far-field pattern only. He has reported successful designs of shaped beam and contoured beam antennas for planar as well as conformal arrays. A sampled continuous distribution is used by Elliott [78] and Ares [80] as starting point for numerical optimisation, as discussed in Section 2.8.3

2.8.2 Use of Collapsed Distributions

The concept of a collapsed distribution was mentioned in Section 2.2.4. A planar array synthesis method which uses linear array synthesis on the two orthogonal collapsed distributions of a given planar array, and then spreads out the collapsed distributions using the conjugate gradient technique or the iterative method of Section 2.8.3, has been described by Elliott [19]. The method is applicable to both sum and difference patterns and can yield non-separable final distributions. It has the advantage of beginning with the use of established linear array techniques. In spite of the claims that such a method is a sort of panacea to all planar array synthesis problems, this is not always the case, as evidenced by attempts at further improvements by Autrey [65] and Elliott and Stern [79].

2.8.3 Iterative Perturbation Methods

In Section 2.7.5 the direct synthesis of continuous planar source distributions was mentioned. It was indicated there that the relatively straightforward altered sampling approaches applicable to linear arrays do not carry over to the planar array case. The minimum source density is required for discretization is determined by the behaviour of the radiation pattern outside the visible region [103].

To improve the pattern characteristics of the sampled distribution an iterative sampling scheme was proposed by Stutzman and Coffey [104]. Elliott [10:pp.243-249] has described an iterative procedure which tries to improve on the conventionally sampled continuous planar distribution, the final set of non-separable excitations being distinctly different from the starting ones. Application of this iterative technique to the sampling of continuous planar distributions is also described [10:pp.256-261, 78].

Fletcher-Powell minimisation was successfully used by Ares [80] to minimise a cost function comprising the sum of the squares of the differences between the actual pattern and the required pattern [80], for contoured beam arrays.

2.8.4 Array Synthesis as an Intersection of Sets

The use of the method of projections for the synthesis of antenna arrays has grown out of the development of techniques in the field of image processing, in particular image restoration. Details of the method are described by Levi and Stark [105]. Prasad [106] applied an early version of the method (called the method of alternating orthogonal projections) to the array synthesis problem. Limitations on the type of constraints that could be used led to improvements resulting in the method of successive projections. This has been applied to arrays by Poulton [107, 108]. The generalised projection technique has been used as the basis for a synthesis method [109, 110, 111] which allows constraints not only on the sidelobe levels but also on the excitations (eg. dynamic range, smoothness of the distribution), something that is most advantageous when having to deal with mutual coupling effects. The method searches for the intersection of two sets by iteratively projecting back and forth between the sets. The technique uses the fast Fourier transform and the inverse fast Fourier transform as a projector pair. The method has recently been extended to circular arc conformal array synthesis by using singular value decomposition as a back projector [112]. Even more recently Bucci et al. [113] achieved success in the synthesis of general conformal arrays by using a self-scaled version of the Broyden-Fletcher-Golfarb-Shanno method [114] one of the projectors used in the search for the intersection of the sets.

Array synthesis (with the emphasis on conformal arrays) as the intersection of sets is further investigated in Chapter 5 of this thesis. A complete overview and the progression of these methods are given there.

2.8.5 Constrainted Minimisation/Maximisation (Optimisation)

Constrainted optimisation techniques differ in :

- the way in which the array problem is formulated as an optimisation problem (e.g. the choice of performance indices to be minimised or maximised)
- the type of constraints which are applied (e.g. limited Q, maximum sidelobe levels allowed)
- the particular optimisation algorithm used (e.g. linear programming, quadratic programming, use of ratios of Hermitian quadratic forms, general nonlinear function maximisation/minimisation).

Hansen summarised general methods of this nature [25:pp.743-748]; as indicated earlier the use of such general methods are not always practical. Detailed overviews of optimisation methods have also been given by Cheng [21], Lo et al. [29] and Sanzgiri and Butler [115]. Wilson [116] applied a linear approximation procedure to derive the arrays excitations of rectangular planar arrays with sum or difference patterns. Quadratic programming was proposed by Einarsson [117] for those cases where the directivity must be maximised subject to a set of sidelobe constraints; the technique maximises the directivity by minimising an associated quadratic form. By writing the sidelobe constraints as a linear set, Einarsson [117] was able to formulate the optimisation problem as a quadratic programming one. By the optimisation, using the method of steepest descent, of a piecewise differentiable objective function DeFord and Gandhi [118] synthesised linear and planar arrays.

The method of simulated annealing, used for computing the properties of systems of interacting molecules, was applied to the synthesis of antenna arrays by Farhat and Bai [119]. Simulated annealing is used to optimise the energy (or cost function) of a system by slowly lowering the "temperature" (control variable) of the system until the system "freezes"; in a manner similar to the annealing of a structurally pure crystal. Due to a probabilistic selection rule the process can get out of a local minimum and proceed to the global minimum. However, the choices for the initial temperature and the probabilistic factor are crucial for speed and success of convergence. Recently good results ware obtained using simulated annealing for the synthesis of circular arc and cylindrical arrays [120, 121].

2.9 Array Synthesis Techniques Developed in this Thesis

The conventional array synthesis methods have been reviewed in the previous sections. Three inadequacies have been identified: firstly, the transformation synthesis technique

can be used to synthesise only centro symmetric contours, secondly no difference pattern synthesis method exists for planar arrays and thirdly no effective conformal array synthesis method exists. Due to the non linear nature of conformal array synthesis an effective conformal array synthesis method must have a rapid rate of convergence and a measure of confidence that the result will be close to the optimal solution.

The transformation based synthesis method can be used for the synthesis of rectangular planar arrays with quadrantal or centro symmetrical footprint patterns. In Chapter 3 of this thesis the transformation technique will be extended to allow for the synthesis of:

- arbitrary contoured footprint patterns;
- planar arrays with non rectangular boundaries and
- planar arrays with triangular lattices.

Application of the newly developed and extended transformation based synthesis technique is examined by the use of a number of specific examples.

The principal contribution made in Chapter 4 is the presentation of a well ordered, step by step method for the synthesis of planar arrays with difference patterns. The method uses as one of the steps the extended transformation method developed in Chapter 3, and also utilises the convolution synthesis method. The result is a near-optimum difference pattern for planar arrays.

Due to the nature of conformal arrays no simplification can be made to ease the synthesis problem. Currently no effective synthesis technique exists to produce discrete conformal arrays. Chapter 5 considers the development of a such a conformal array synthesis technique, and explores ways to increase the rate of convergence. Any numerical optimisation is prone to fall into local minima. To avoid local minima a starting point close to the global minimum is needed. A novel selection of the starting point is proposed and investigated. This synthesis method is very flexible, allowing the synthesis of both co- and cross polarisation radiation patterns of arrays with an arbitrary geometry; with constraints on the radiation pattern as well as the excitations.

Finally, Chapter 6 completes the thesis by drawing a number of general conclusions.

Chapter 3

Extensions to the Transformation Based Planar Array Synthesis Technique

3.1 Introductory Remarks

The transformation based synthesis technique [95, 94] mentioned earlier in Section 2.7.4 differs from other approaches in several respects. It utilises a transformation that has been used in the design of two-dimensional digital filters [122]. This transformation divides the problem into two decoupled sub-problems. In the antenna array context the one sub-problem involves the determination of certain coefficients of the transformation in order to achieve the required footprint contours. The number of coefficients needed depends on the complexity of the desired contour, but is very small in comparison to the number of planar array elements. The other sub-problem consists of a linear array shaped beam synthesis, for which there already exist powerful methods for determining appropriate element excitations. The size required for this linear array (which will be called the *prototype linear array*) depends on the number of transformation coefficients used and the planar array size. Simple recursion formulas then determine the final planar array excitations from the information forthcoming from the above two sub-problem solutions. As a result the method is computationally efficient, and thus trade-off studies are feasible even for very large arrays.

This technique as first applied by the author [95, 94] was applicable to arrays with quadrantal and centro (about the centre) symmetry only. In this chapter of the present thesis the transformation based technique will be extended to apply to the general, arbitrarily contoured beam synthesis problem.

Planar arrays can be categorised into three groups; firstly arrays with an odd number of elements along both principal planes, secondly arrays with an even number of elements along both principal planes and lastly arrays with an even number of elements along one

principal plane and an odd number of elements along the other pricipal plane. The first two groups will be referred to as the odd case and the even case, respectively. As the formulation differs slightly for each case, Section 3.2 deals with the odd case and Section 3.3 with the even case. The formulation for the last group of planar arrays is simply a combination of the odd and even case formulations and will not be treated. Details of the original transformation based technique, as developed in [95, 94], will be discussed in the first part of each of these sections. The latter part of each of the two sections discusses the extensions to the technique to enable the synthesis of planar arrays with arbitrary footprint contour patterns. A planar array with a rectangular lattice and rectangular boundary is assumed throughout these two sections. In order not to smother the simplicity of the technique under the associated notationally complex algorithmic details, the latter have all been relegated to Appendix A, which is simply referred to at appropriate stages in the text.

The contour approximation, or the problem of determining the transformation coefficients, will be addressed in Section 3.4.

Section 3.5 deals with the application of the method to synthesise planar arrays with non-rectangular boundaries and/or lattices not available in the original formulation [95, 94]. This is achieved by the appropriate selection of the transformation coefficients.

The method is epitomised by a complete, detailed representative example in Section 3.6. The required footprint contour is the shape of the African continent.

In Section 3.7 the transformation based synthesis method is compared to similar existing synthesis methods.

The chapter ends with some conclusions.

3.2 The Transformation Based Synthesis Technique: The Odd Case

Consider a planar array with a rectangular lattice. The inter-element spacings, d_x and d_y, need not be equal. Only planar arrays consisting of $2M+1$ by $2N+1$ elements, that is an odd number of elements in both principal planes (and an odd total number of elements as well) are examined in this section. In addition, the array is assumed to have a rectangular boundary, no elements having been removed from the lattice in order to alter the boundary shape.

3.2.1 Background on Quadrantally Symmetric Contours

In this section we consider quadrantally symmetric contoured footprint patterns, where the planar array factor is symmetrical about both the u- and v-axes. Such contour patterns are generated by planar arrays with quadrantally symmetric excitations. This

section repeats the work reported in [95], which was also published in [94], as background material which facilitates the discussion of the extended transformation method for the odd case in Section 3.2.2

Consider a rectangular planar array in the xy-plane. Using the substitutions

$$\begin{aligned} u &= \mathrm{k}d_x \sin\theta\ \cos\phi \\ v &= \mathrm{k}d_y \sin\theta\ \sin\phi \end{aligned} \tag{3.1}$$

given in (2.14), with θ and ϕ the direction of the far-field observation point, the $2M+1$ by $2N+1$ element quadrantally symmetric planar array space factor is given in (2.16) as

$$F(u,v) = \sum_{m=0}^{M}\sum_{n=0}^{N} \zeta_m \zeta_n a_{mn} \cos(mu)\cos(nv) \tag{3.2}$$

with a_{mn} the normalised excitation of the $mn-$th element and ζ_i as defined in equation (2.17). The constant "4" before the summation may be omitted as the space factor is usually normalised to its maximum.

Next, consider a $2Q+1$ element, uniformly spaced linear array with symmetrical excitation. As indicated in Section 3.1 this will be referred to as the *prototype linear array.* Assume the prototype linear array is positioned along the x-axis, with inter-element spacing d. The observation angle θ_p is measured from the direction broadside to the prototype linear array. The range of θ_p is from -90° to 90° , as mentioned in Section 2.3.6. The path length difference is defined as

$$\psi_p = \mathrm{k}d \sin\theta_p \tag{3.3}$$

From (2.13), the prototype linear array factor in terms of ψ_p is then

$$F_p(\psi_p) = \sum_{q=0}^{Q} \zeta_q\, a_q\, \cos(q\psi_p) \tag{3.4}$$

in which a_q is the q-th normalised element excitation. Use of the relations [123, p. 17]

$$\cos^{2q} x = \frac{1}{2^{2q}} + \frac{1}{2^{2q-1}} \sum_{i=1}^{q} \binom{2q}{q-i} \cos(2ix) \tag{3.5a}$$

$$\cos^{2q-1} x = \frac{1}{2^{2q-2}} \sum_{i=1}^{q} \binom{2q-1}{q-i} \cos\left[(2i-1)x\right] \tag{3.5b}$$

enables us to write the prototype linear array factor (3.4) in a polynomial form

$$F_p(\psi_p) = \sum_{q=0}^{Q} b_q\, \cos^q \psi_p \tag{3.6}$$

The original McClellan transform [122] is a transformation of a one-dimensional FIR filter into a two-dimensional FIR filter by means of the substitution of variables. In the array context the transformation "converts" the prototype linear array factor (a function of one variable) into a planar array factor (a function of two variables) by means of the substitution of variables

$$\cos(\psi_p) = H(u,v) = \sum_{i=0}^{I}\sum_{j=0}^{J} t_{ij}\ \cos(iu)\cos(jv) \tag{3.7}$$

in which t_{ij} are real coefficients. This function, $H(u,v)$, will be called the *transformation function*. We assume here that the transformation is normalised in the sense that $|H(u,v)| \leq 1$. The scaling of the transformation function will be discussed in more detail Section 3.4.3.

Substitution of the transformation function (3.7) into the prototype linear array factor (3.6) converts the prototype linear array factor $F_p(\psi_p)$ into the following function of two variables, (u and v):

$$F_p(u,v) = \sum_{q=0}^{Q} b_q \left[\sum_{i=0}^{I}\sum_{j=0}^{J} t_{ij}\ \cos(iu)\cos(jv)\right]^q \tag{3.8}$$

Application of the relations in (3.5) a second time allows this two-variable function (3.8) to be re-written in the same form as the planar array factor

$$F_p(u,v) = \sum_{m=0}^{M}\sum_{n=0}^{N} c_{mn}\ \cos(mu)\cos(nv) \tag{3.9}$$

with $M = QI$ and $N = QJ$. Comparison of (3.9) with the planar array factor (3.2) shows that the planar array element excitation is

$$a_{mn} = \frac{c_{mn}}{\zeta_m \zeta_n} \tag{3.10}$$

Recursive formulas, given in Section A.1.1 of Appendix A are used to compute b_q in (3.6) from the prototype linear array excitations a_q. Section A.1.2 of Appendix A is devoted to the recursive formulas necessary to compute the coefficients c_{mn} of (3.9). Although writing these formulas in a mathematically elegant fashion is difficult, the recursive formulas are ideally suited for computation.

On those contours where the transformation function is constant $H(u,v) = constant$, the planar array $F(u,v)$ must be constant. These contours are controlled only by the transformation coefficients t_{ij}. The value associated with a particular contour depends only on the excitation coefficients of the prototype linear array and is equal to $F_p(\psi_p)$ with $\psi_p = \arccos[H(u,v)]$. The synthesis problem has thus been reduced to two smaller and more easily solvable problems; the synthesis of a linear array and the selection of a set of

transformation parameters. As the transformation function is quadrantally symmetrical, the planar array factor (as well as the excitation) will also be quadrantally symmetrical.

The desired accuracy for, or amount of detail in the shape of, the desired contours will determine the values of I and J required; that is, the number of contour transformation coefficients required. The use of contour transformations with larger values of I and J will increase the size of the final planar array. The size $(2Q+1)$ of the prototype linear array used is dependent on the width of the main beam and amount of coverage area gain ripple allowable. The size of the final planar array is $2M+1$ by $2N+1$, with $M=QI$ and $N=QJ$. It may be interesting to note that if the prototype linear array has a pure real distribution then the planar array distribution will also be pure real.

3.2.2 Extension to Arbitrarily Shaped Contours

Details of the extension of the transformation based synthesis technique to enable the design of antenna arrays with arbitrarily shaped contoured footprint patterns are discussed in this section. If the desired contour has no symmetry, the resultant excitations will also have no symmetry.

As $\cos u$ and $\cos v$ are even functions in u and v respectively, the transformation function (3.7) is quadrantally symmetrical. Thus the resultant planar array factor will also exhibit quadrantal symmetry. In order to synthesise arbitrarily shaped contours, the transformation function must include both even and odd terms. The transformation for arbitrarily shaped contours is therefore

$$\cos(\psi_p) = H(u,v) = \sum_{i=0}^{I}\sum_{j=0}^{J} t_{ij}^{cc}\cos(iu)\cos(jv) + t_{ij}^{ss}\sin(iu)\sin(jv) + t_{ij}^{cs}\cos(iu)\sin(jv) + t_{ij}^{sc}\sin(iu)\cos(jv) \tag{3.11}$$

in which t_{ij}^{cc}, t_{ij}^{ss}, t_{ij}^{cs} and t_{ij}^{sc} are real coefficients. Inspection of equation (3.11) reveals that the transformation function has the same form as a Fourier series. From the theory of Fourier analysis we know that the transformation function (3.11) can be used to approximate any real function.

Substitution of the general transformation function (3.11) into the prototype linear array factor (3.6) and use of the relations [123, p. 17]

$$\begin{aligned} \cos A\cos B &= \tfrac{1}{2}[\cos(A-B)+\cos(A+B)] \\ \sin A\cos B &= \tfrac{1}{2}[\sin(A-B)+\sin(A+B)] \\ \sin A\sin B &= \tfrac{1}{2}[\sin(A-B)+\sin(A+B)] \end{aligned} \tag{3.12}$$

allow the prototype linear array factor $F_p(\psi_p)$ to be written as

$$F_p(u,v) = \sum_{m=0}^{M}\sum_{n=0}^{N}\zeta_m\zeta_n\,[c_{mn}^{cc}\cos(mu)\cos(nv) + c_{mn}^{ss}\sin(mu)\sin(nv) + c_{mn}^{cs}\cos(mu)\sin(nv) + c_{mn}^{sc}\sin(mu)\cos(nv)] \tag{3.13}$$

with $M=QI$ and $N=QJ$. Let us now consider the array factor of a planar array which has no special symmetry in its excitation. Using the element numbering scheme described in Section 2.2.4 of Chapter 2 for the quadrantally symmetric factor, expression (2.15) can be written as

$$\begin{aligned} F(u,v) = \sum_{m=0}^{M}\sum_{n=0}^{N} \zeta_m\zeta_n \{ & (+a_{mn} + a_{m-n} + a_{-mn} + a_{-m-n})\cos(mu)\cos(nv) + \\ & (-a_{mn} + a_{m-n} + a_{-mn} - a_{-m-n})\sin(mu)\sin(nv) + \\ & \mathrm{j}(+a_{mn} - a_{m-n} + a_{-mn} - a_{-m-n})\cos(mu)\sin(nv) + \\ & \mathrm{j}(+a_{mn} + a_{m-n} - a_{-mn} - a_{-m-n})\sin(mu)\cos(nv)\} \end{aligned} \tag{3.14}$$

Comparison of (3.13) with the planar array factor (3.14) yields the final array excitation

$$\begin{aligned} a_{mn} &= \tfrac{1}{4\zeta_m\zeta_n}[c_{mn}^{cc} - c_{mn}^{ss} - \mathrm{j}(c_{mn}^{cs} + c_{mn}^{sc})] \\ a_{m-n} &= \tfrac{1}{4\zeta_m\zeta_n}[c_{mn}^{cc} + c_{mn}^{ss} + \mathrm{j}(c_{mn}^{cs} - c_{mn}^{sc})] \\ a_{-mn} &= \tfrac{1}{4\zeta_m\zeta_n}[c_{mn}^{cc} + c_{mn}^{ss} - \mathrm{j}(c_{mn}^{cs} - c_{mn}^{sc})] \\ a_{-m-n} &= \tfrac{1}{4\zeta_m\zeta_n}[c_{mn}^{cc} - c_{mn}^{ss} + \mathrm{j}(c_{mn}^{cs} + c_{mn}^{sc})] \end{aligned} \tag{3.15}$$

and the final array size as $M=QI$ and $N=QJ$.

Recursive formulas for computing c_{mn}^{cc}, c_{mn}^{ss}, c_{mn}^{cs} and c_{mn}^{sc} are given in Section A.1.3 of Appendix A.

Again, as stated in Section 3.2.1, on those contours defined by $H(u,v) = \textit{constant}$, the planar array must be constant and equal to $F_p(\psi_p)$, with $\psi_p = \arccos[H(u,v)]$. These contours are controlled only by the transformation parameters t_{ij}^{cc}, t_{ij}^{ss}, t_{ij}^{cs} and t_{ij}^{sc}, and the value associated with the particular contour depends only on the prototype linear array excitation. In this way the synthesis problem is reduced to two smaller and easily solvable problems; the synthesis of a linear array and the selection of a set of transformation parameters.

The selection of the transformation parameters can be viewed as finding the coefficients of a two-dimensional Fourier series representation of the contour shape. Thus, the narrower the beamwidth and/or the more detailed the contour, the more transformation parameters are needed. The increase in the number of transformation coefficients will cause a proportional increase in the final array size. The problem of determining the appropriate values for the transformation coefficients is discussed in Section 3.4

Illustrative Example #1

To illustrate the transformation based synthesis technique for arbitrary contours, let us consider the synthesis of a contoured pattern in the shape of a skewed tear drop. The synthesis process can be divided into a number of steps:

i, j	t_{ij}^{cc}	t_{ij}^{ss}	t_{ij}^{cs}	t_{ij}^{sc}
0, 0	-0.117050	0	0	0
0, 1	0.257781	0	-0.171854	0
1, 0	0.515561	0	0	0.257781
1, 1	0.343707	-0.343707	0.171854	-0.257781

Table 3.1: Illustrative Example #1: Transformation coefficients.

1. Determine the number of transformation coefficients.
2. Determine the number of prototype linear array elements.
3. Prototype linear array synthesis.
4. Determine the transformation coefficients.
5. Compute planar array excitations

These steps are not completely isolated. The contour complexity obtainable is linked to the number of transformation coefficients. The beamwidth, main beam ripple and sidelobe level depend on the number of prototype linear array elements. The number of transformation coefficients (I and J) and the number of prototype linear array elements (Q) in turn determine the size of the planar array ($M=IQ$ and $N=JQ$).

Let us consider an example of the synthesis of a square array with a main beam footprint contour in the shape of a skewed tear drop. The peak-to-peak ripple desired in the main beam is 1dB while the sidelobe level is set at -20dB. The inter-element spacing is chosen as $d_x=d_y=0.662\lambda$. The step by step synthesis of this example is:

1. The desired tear-drop shaped contour can be achieved with 9 transformation coefficients, that is $I=J=1$.
2. The prototype linear array consists of 21 elements, that is $Q=10$. The first two steps determine the total number of element in the planar array.
3. The method of Orchard, Elliot and Stern [54] was used to synthesise the prototype linear array, with two of the roots placed off the unit circle. The peak-to-peak ripple in the main beam region is 1dB and the sidelobe level is set at -20dB. The inter-element spacing used in this step is $d=\frac{1}{2}\lambda$. This step determines the value of θ_p.
4. The inter-element spacing of the planar array is accounted for in this step, $d_x=d_y=0.662\lambda$. The strictly controlled contour is at $H(u,v)=\cos(\pi\sin\theta_p)$. The values of the transformation coefficients are listed in Table 3.1

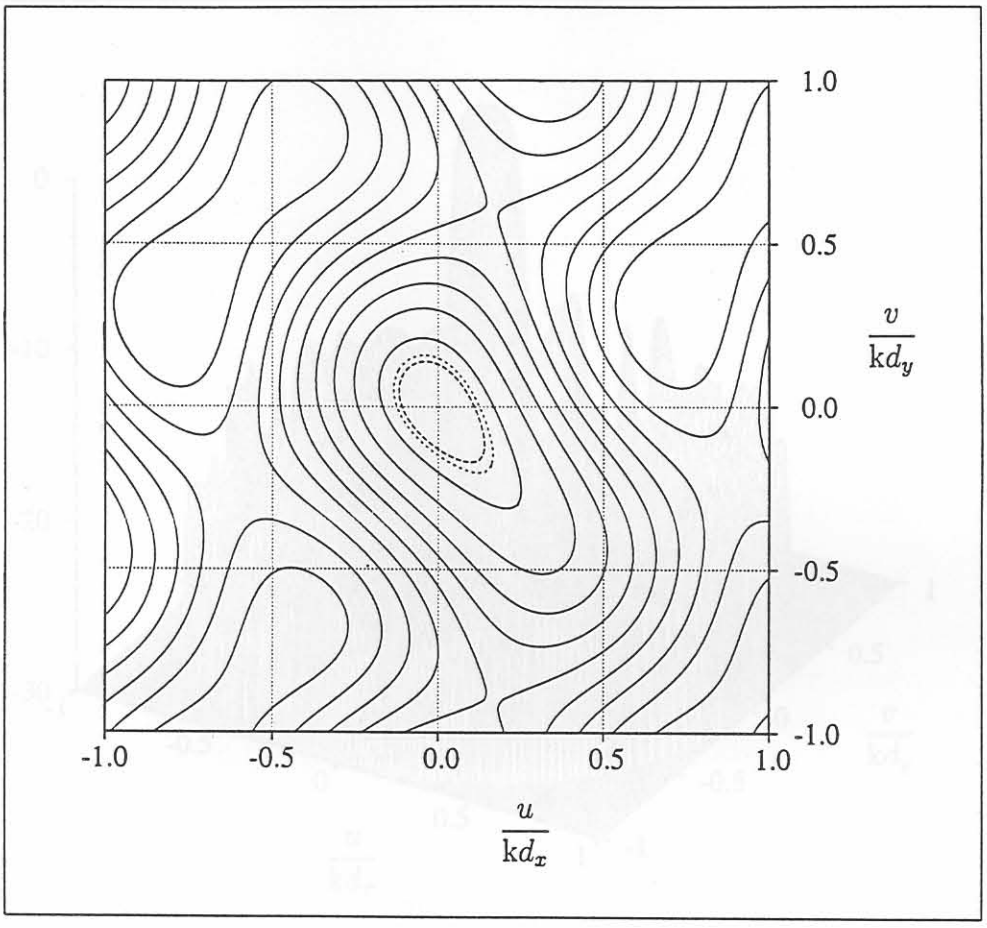

Figure 3.1: Illustrative Example #1: A contour plot of the transformation function. The dashed line represents the -1dB contour and the dotted line the -3dB contour.

5. The planar array elements were computed using the algorithm in Section A.1.3 in Appendix A. This gives the distribution of a planar array with a total of 441 elements, since $M=N=10$ (hence a 21 by 21 square array).

A contour plot of the transformation function is shown in Figure 3.1. The dashed line (in the centre of the graph) represents the -1dB contour at $H(u,v)=0.913$ ($\theta_p=7.7°$) and the dotted line the -3dB contour at $H(u,v)=0.887$ ($\theta_p=8.8°$). The planar array factor of the resulting array is depicted in Figure 3.2.

3.3 The Transformation Based Synthesis Technique: The Even Case

The class of planar arrays regarded in this section consists of an even number of elements in both principal planes, $2M$ and $2N$ elements respectively, and is referred to as the even case. A planar array with a rectangular lattice and boundary is assumed.

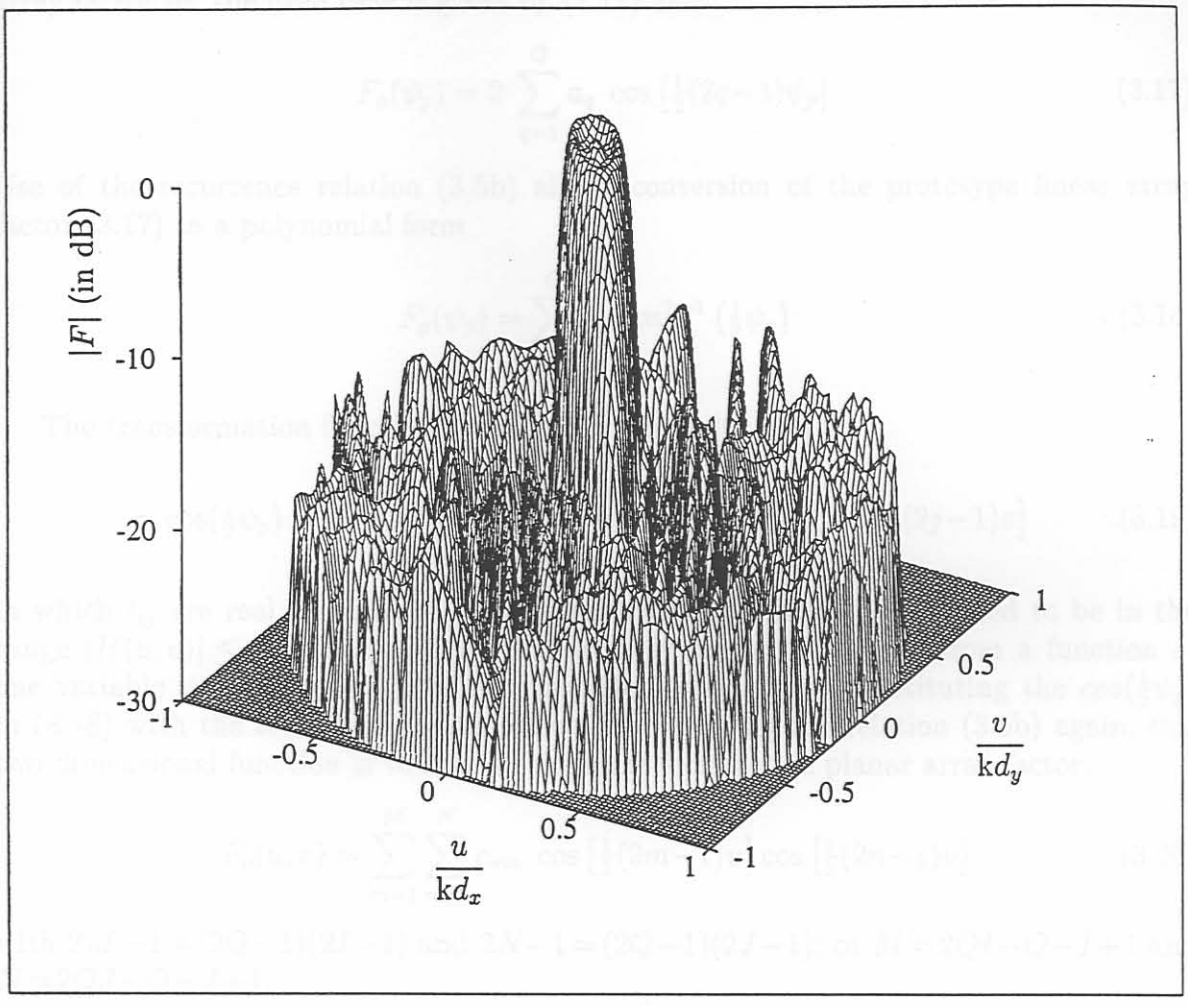

Figure 3.2: Illustrative Example #1: Surface plot of the planar array factor.

3.3.1 Background On Quadrantally Symmetrical Contours

This section deals with quadrantally symmetrical contoured footprint patterns. The information was already published in [95, 94], but is repeated here as background material for the extension described in Section 3.3.2

Consider a rectangular planar array with $2M$ by $2N$ elements excited in phase. The planar space factor is given by (2.18) as

$$F(u,v) = \sum_{m=1}^{M}\sum_{n=1}^{N} a_{mn} \cos\left[\tfrac{1}{2}(2m-1)u\right] \cos\left[\tfrac{1}{2}(2n-1)v\right] \tag{3.16}$$

with a_{mn} the normalised excitation of the mn-th element. The prototype linear array is a $2Q$ element, symmetrically excited, uniformly spaced linear array. The prototype linear

array factor for the even case is given by (2.11) as

$$F_p(\psi_p) = 2\sum_{q=1}^{Q} a_q \cos\left[\tfrac{1}{2}(2q-1)\psi_p\right] \tag{3.17}$$

Use of the recurrence relation (3.5b) allows conversion of the prototype linear array factor (3.17) to a polynomial form

$$F_p(\psi_p) = \sum_{q=1}^{Q} b_q \cos^{2q-1}\left(\tfrac{1}{2}\psi_p\right) \tag{3.18}$$

The transformation function for the even case is [95, 94]

$$\cos(\tfrac{1}{2}\psi_p) = H(u,v) = \sum_{i=1}^{I}\sum_{j=1}^{J} t_{ij} \cos\left[\tfrac{1}{2}(2i-1)u\right]\cos\left[\tfrac{1}{2}(2j-1)v\right] \tag{3.19}$$

in which t_{ij} are real coefficients. The transformation function is assumed to be in the range $|H(u,v)| \leq 1$. The prototype linear array factor is mapped from a function of one variable ψ_p to a function of two variables u and v, by substituting the $cos(\frac{1}{2}\psi_p)$ in (3.18) with the transformation function. By applying the relation (3.5b) again, this two dimensional function is written in the same form as the planar array factor,

$$F_p(u,v) = \sum_{m=1}^{M}\sum_{n=1}^{N} c_{mn} \cos\left[\tfrac{1}{2}(2m-1)u\right]\cos\left[\tfrac{1}{2}(2n-1)v\right] \tag{3.20}$$

with $2M-1=(2Q-1)(2I-1)$ and $2N-1=(2Q-1)(2J-1)$; or $M=2QI-Q-I+1$ and $N=2QJ-Q-J+1$.

The element excitation which is obtained by comparing the planar array factor (3.16) with this function (3.20) is simply

$$a_{mn} = c_{mn} \tag{3.21}$$

The total number of elements in the principal planes of the planar array are $2M = (2Q-1)(2I-1)+1$ and $2N=(2Q-1)(2J-1)+1$. For an $I=J=1$ transformation only one variable is available to control the contour shape, thus only near circular contours can be achieved. As I and J increase, the total number of planar elements, $2M$ and $2N$ increase by $2I-1$ and $2J-1$ respectively. This increase is more rapid than in the case of a planar array with an odd number of elements in both principal planes (as described in Section 3.2.1). The even case suffers another limitation; in order to do a linear scaling of the transformation function a t_{00}-coefficient is needed. Since this coefficient is not available, an additional constraint on the possible values of the transformation function must be included during the determination of the transformation parameters. This will be discussed in Section 3.4.2.

The formula needed to calculate b_q is provided in Section A.2.1 of AppendixA, and the algorithm needed to compute c_{mn} is supplied in Section A.2.2 of Appendix A.

3.3.2 Extension To Arbitrarily Shaped Contours

The extension of the technique for an odd number of elements in both principal planes, to arbitrary contours is very similar to that of Section 3.2.2; thus only the most relevant equations will be given. The transformation function for arbitrarily shaped contours is

$$\begin{aligned} H(u,v) = \sum_{i=1}^{I}\sum_{j=1}^{J} & t_{ij}^{cc}\cos\left[\tfrac{1}{2}(2i-1)u\right]\cos\left[\tfrac{1}{2}(2j-1)v\right] + \\ & t_{ij}^{ss}\sin\left[\tfrac{1}{2}(2i-1)u\right]\sin\left[\tfrac{1}{2}(2j-1)v\right] + \\ & t_{ij}^{cs}\cos\left[\tfrac{1}{2}(2i-1)u\right]\sin\left[\tfrac{1}{2}(2j-1)v\right] + \\ & t_{ij}^{sc}\sin\left[\tfrac{1}{2}(2i-1)u\right]\cos\left[\tfrac{1}{2}(2j-1)v\right] \end{aligned} \tag{3.22}$$

in which t_{ij}^{cc}, t_{ij}^{ss}, t_{ij}^{cs} and t_{ij}^{sc} are real coefficients. The transformation function must be in the range $|H(u,v)| \leq 1$. Normalisation of the transformation function is discussed in Section 3.4.3

Substitution of the general transformation function (3.22) into the prototype linear array factor (3.18), and use of the relations in (3.12), allows the prototype linear array factor $F_p(\psi_p)$ to be written as

$$\begin{aligned} F_p(u,v) = \sum_{m=1}^{M}\sum_{n=1}^{N}\zeta_m\zeta_n & c_{mn}^{cc}\cos\left[\tfrac{1}{2}(2m-1)u\right]\cos\left[\tfrac{1}{2}(2n-1)v\right] + \\ & c_{mn}^{ss}\sin\left[\tfrac{1}{2}(2m-1)u\right]\sin\left[\tfrac{1}{2}(2n-1)v\right] + \\ & c_{mn}^{cs}\cos\left[\tfrac{1}{2}(2m-1)u\right]\sin\left[\tfrac{1}{2}(2n-1)v\right] + \\ & c_{mn}^{sc}\sin\left[\tfrac{1}{2}(2m-1)u\right]\cos\left[\tfrac{1}{2}(2n-1)v\right] \end{aligned} \tag{3.23}$$

with $2M-1=(2Q-1)(2I-1)$ and $2N-1=(2Q-1)(2J-1)$; or $M=2QI-Q-I+1$ and $N=2QJ-Q-J+1$. Now consider the array factor of a planar array which has no special symmetry in its excitation. Using the numbering scheme described in Section 2.2.4 of Chapter 2 for the quadrantally symmetric array factor, expression (2.15) can be written as

$$\begin{aligned} F(u,v) = \sum_{m=1}^{M}\sum_{n=1}^{N} & \{(+a_{mn}+a_{m-n}+a_{-mn}+a_{-m-n})\cos(\tfrac{1}{2}(2m-1)u)\cos(\tfrac{1}{2}(2n-1)v) + \\ & (-a_{mn}+a_{m-n}+a_{-mn}-a_{-m-n})\sin(\tfrac{1}{2}(2m-1)u)\sin(\tfrac{1}{2}(2n-1)v) + \\ & \mathrm{j}(+a_{mn}-a_{m-n}+a_{-mn}-a_{-m-n})\cos(\tfrac{1}{2}(2m-1)u)\sin(\tfrac{1}{2}(2n-1)v) + \\ & \mathrm{j}(+a_{mn}+a_{m-n}-a_{-mn}-a_{-m-n})\sin(\tfrac{1}{2}(2m-1)u)\cos(\tfrac{1}{2}(2n-1)v)\} \end{aligned} \tag{3.24}$$

By equating (3.23) and (3.24) planar array excitations are

$$\begin{aligned} a_{mn} &= \tfrac{1}{4}\left[c_{mn}^{cc} - c_{mn}^{ss} - \mathrm{j}(c_{mn}^{cs} + c_{mn}^{sc})\right] \\ a_{m-n} &= \tfrac{1}{4}\left[c_{mn}^{cc} + c_{mn}^{ss} + \mathrm{j}(c_{mn}^{cs} - c_{mn}^{sc})\right] \\ a_{-mn} &= \tfrac{1}{4}\left[c_{mn}^{cc} + c_{mn}^{ss} - \mathrm{j}(c_{mn}^{cs} - c_{mn}^{sc})\right] \\ a_{-m-n} &= \tfrac{1}{4}\left[c_{mn}^{cc} - c_{mn}^{ss} + \mathrm{j}(c_{mn}^{cs} + c_{mn}^{sc})\right] \end{aligned} \tag{3.25}$$

The final planar array size is $2M-1=(2Q-1)(2I-1)$ by $2N-1=(2Q-1)(2J-1)$. The extension of the transformation based method to arbitrarily shaped contours suffers the same limitations as the quadrantally symmetrical contours; a rapid increase in the number of elements as the number of transformation coefficients increase and linear scaling is not possible. Recursive formulas for computing c_{mn}^{cc}, c_{mn}^{ss}, c_{mn}^{cs} and c_{mn}^{sc} are given in Section A.2.3 of Appendix A.

Illustrative Example #2

Let us consider an example of the synthesis of a rectangular array with a half circle shaped main beam footprint contour. The footprint contour must be symmetrical about the x-axes. The peak-to-peak ripple desired in the main beam is 1dB while the sidelobe level is set at -20dB. The inter-element spacing is chosen as $d_x = d_y = 0.662\lambda$. The step by step synthesis of this example is:

1. Since the desired contour must be symmetrical about the x-axis, $t_{ij}^{ss} = t_{ij}^{cs} = 0$. In order to obtain a good excitation efficiency the ratio of the number of elements along the major axes of the array must be the inverse of the ratio of beamwidths along the principal cuts. From the desired contour shape (and assuming the centre of the half circle will be in the $\theta = 0°$ direction) the ratio of beamwidths along the principal cuts is about 1:1.73. The contour shape is obtainable with $I=3$ and $J=2$; for these values the number of elements along the x-axis would be approximately 5/3 times the number of elements along the y-axis.

2. A prototype linear array of 12 elements was used, that is $Q=6$. The number of transformation coefficients (from the previous step) and the number of prototype linear set the number of planar array elements, $M=28$ and $N=17$

3. The method of Orchard, Elliot and Stern [54] was used to synthesise the prototype linear array, with four roots placed off the unit circle. The peak-to-peak ripple in the main beam region is 1dB and the sidelobe level is set at -20dB. An inter-element spacing of $d=\frac{1}{2}\lambda$ was used in this step.

4. The strictly controlled contour is at $H(u,v) = \cos(\pi \sin\theta_p) = 0.786$. The inter-element spacing is $d_x = d_y = 0.662\lambda$. The values of the transformation coefficients shown in Table 3.2.

i	t_{i1}^{cc}	t_{i1}^{ss}	t_{i1}^{cs}	t_{i1}^{sc}	t_{i2}^{cc}	t_{i2}^{ss}	t_{i2}^{cs}	t_{i2}^{sc}
1	0.430000	0	0	-0.100000	-0.100000	0	0	-0.100000
2	0.250000	0	0	0.100000	0.233891	0	0	-0.150000
3	0.080000	0	0	0.210000	0.080000	0	0	0.000000

Table 3.2: Illustrative Example #2: Transformation coefficients.

5. The final planar array excitations were computed using the algorithm in Section A.2.3 in Appendix A. This gives a total of 1904 elements (a 56 by 34 rectangular array) in the planar array.

Figure 3.3 displays a contour plot of the transformation function. The dashed line (in the centre of the graph) represents the -1dB contour and the dotted line the -3dB contour. In Figure 3.4 a surface plot of the planar array factor is shown.

3.4 The Transformation Function Sub-Problem

This section is devoted to the problem of choosing the transformation parameters to produce iso-contours of the transformation $H(u,v) = constant$ in the uv-plane that have some desired shape. The contours of transformation $H(u,v)$ are controlled by the transformation coefficients t_{ij}^{cc}, t_{ij}^{ss}, t_{ij}^{cs} and t_{ij}^{sc} only. In contoured beam synthesis it will usually be sufficient to firmly control (by the appropriate selection of the transformation coefficients) the shape of a single contour, typically the half-power (-3dB) contour or the first null contour.

Section 3.4.1 deals with transformation grating lobes, a phenomenon unique to the transformation based synthesis technique. The problem of determining the transformation coefficients, or the contour approximation problem, is formulated in Section 3.4.2. To ensure that the transformation function is within certain bounds, it may need to be scaled. A linear scaling technique, only applicable to the odd case, is discussed in Section 3.4.3. If the number of transformation coefficients is small the coefficients of the transformation may be obtained by using some form of approximation. The approximation approach is addressed in Section 3.4.4. The transformation coefficients can also be obtained by using a constrained optimisation technique as described in Section 3.4.5. Alternatively, Section 3.4.6 demonstrates how the transformation function can be viewed as a small planar array, with a pure real array factor and excitation. The problem of selecting the correct values is then a planar array field synthesis problem.

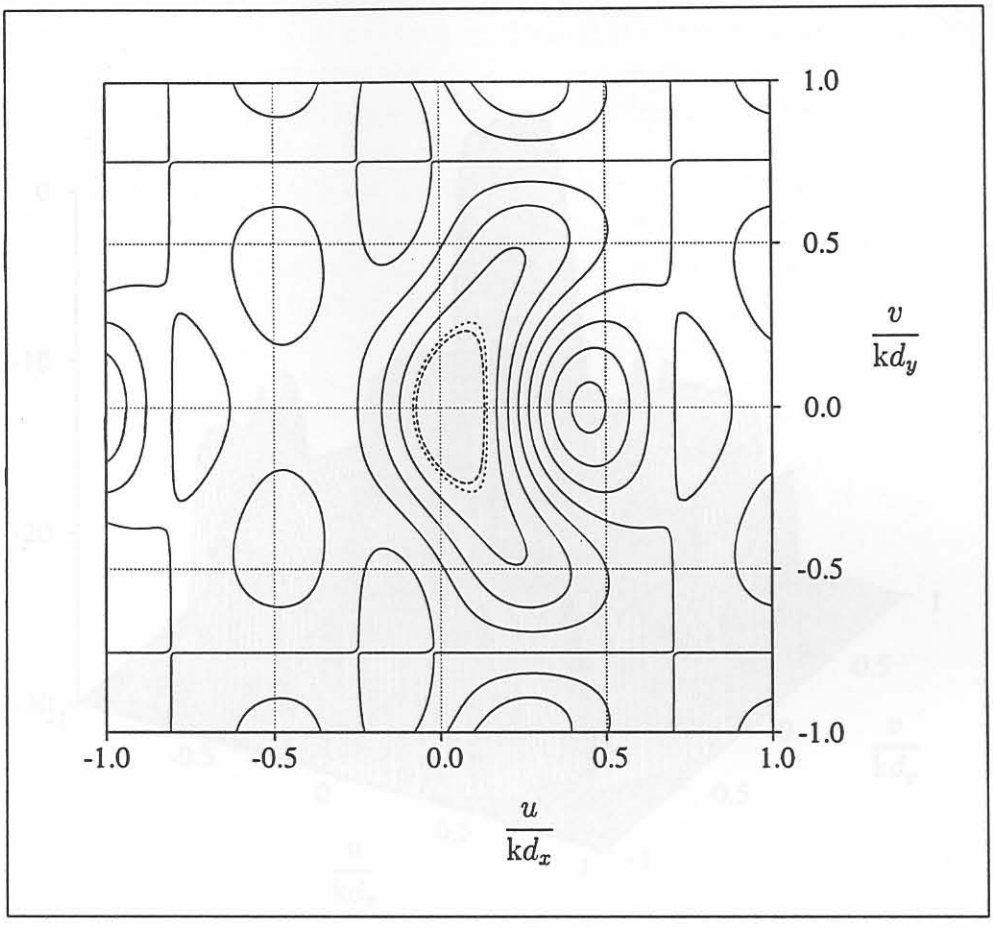

Figure 3.3: Illustrative Example #2: A contour plot of the transformation function. The dashed line represents the -1dB contour and the dotted line the -3dB contour

3.4.1 Transformation Grating Lobes

At this stage it is worthwhile to discuss the relationship between angle θ_p of the prototype linear array factor, and θ for any constant ϕ-cut of the planar array factor. These are of course related via the transformation function $H(u, v)$. In what follows we only consider the odd case; all the comments and conclusions hold for both the odd and even case. Figure 3.5 shows a plot of this relationship in, for example, the $\phi = 0°$ plane for four different transformations. Suffice it to say that two of these are $I = 1$ transformations and the other two $I = 2$ transformations, all having different values for their coefficients t_{ij} (note that the value of J is irrelevant as only the $\phi = 0°$ cut is of interest). Details of the t_{ij} values themselves are unimportant for the purposes of the point being made here. Note then that for both the $I = 1$ transformations, as θ (the "physical" angle) of the planar array moves from 0° out to 90° , we monotonically sweep through values of θ_p, and we will not move through the main beam of the prototype linear array (located around $\theta_p = 0°$) more than once. However, for the $I = 2$ transformations, we see that once the "physical" angle θ moves beyond a certain value the value of θ_p begins to decrease once more, and

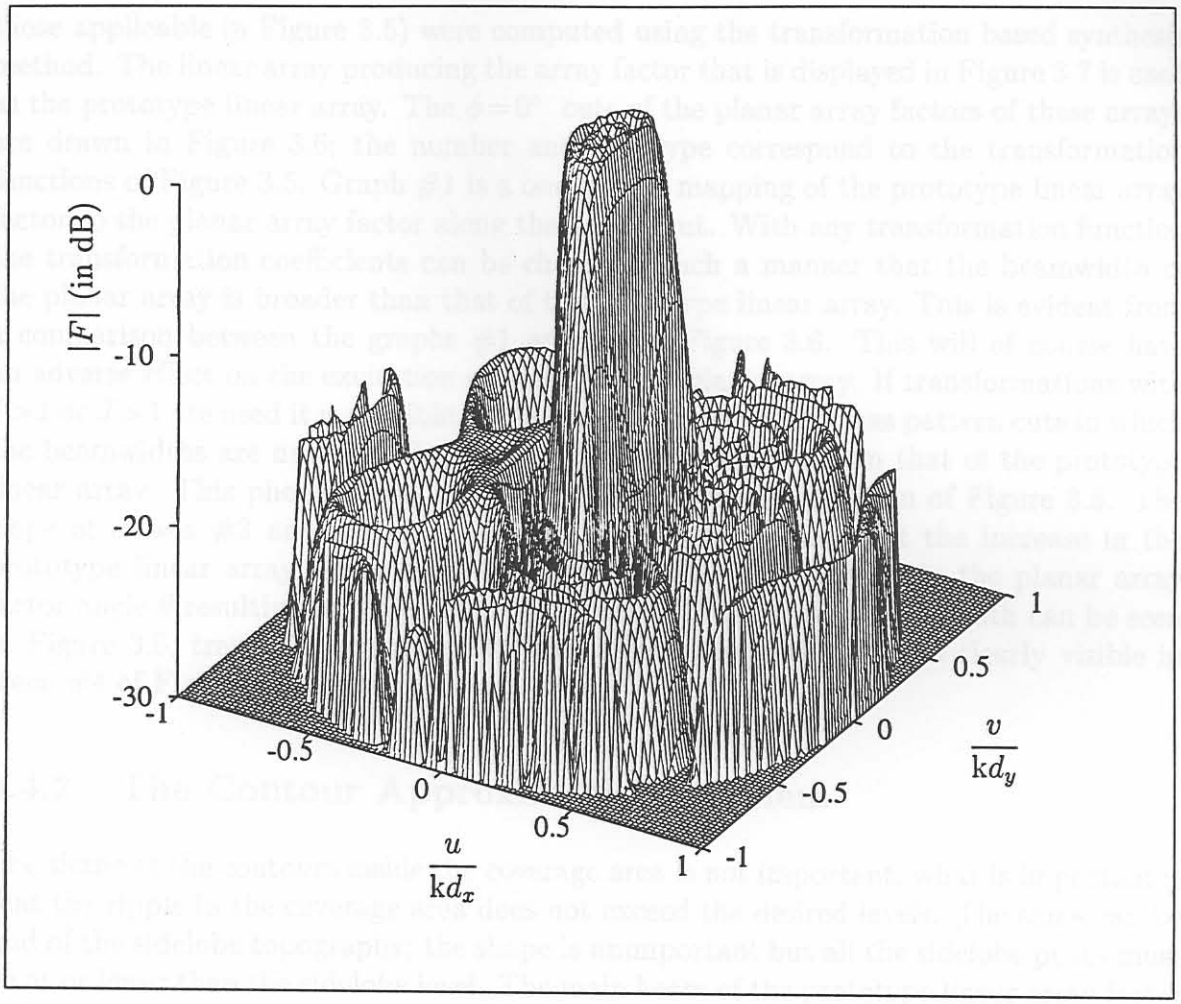

Figure 3.4: Illustrative Example #2: Surface plot of the planar array factor.

may move back into the main beam region of the prototype linear array, thus causing some of the sidelobes of the planar array outside the coverage area to be higher than the sidelobes designed in the prototype linear array. These might be called *transformation grating lobes.* The situation might be such that the $I=2$ transformation marked #3 in Figure 3.5 might be free of transformation grating lobes while #4 might not be (since at $\theta=90°$ the θ_p values of the two transformations differ by 18° , which may determine whether the prototype linear array main beam has been "entered" a second time or not). With contour transformations in which $I>1$ or $J>1$ one must thus ensure that such transformation grating lobes do not arise. These grating lobes are easily located, and can be avoided by imposing additional constraints, equations (3.27) and (3.28), on the transformation function. If the transformation grating lobe persists, it implies that a too narrow beamwidth is being attempted. More transformation coefficients or a prototype linear array with a narrower beamwidth must then be used to get rid of the transformation grating lobe.

Planar array excitations for the above-mentioned transformation coefficients (that is,

those applicable in Figure 3.5) were computed using the transformation based synthesis method. The linear array producing the array factor that is displayed in Figure 3.7 is used as the prototype linear array. The $\phi=0°$ cuts of the planar array factors of these arrays are drawn in Figure 3.6; the number and line type correspond to the transformation functions of Figure 3.5. Graph #1 is a one-on-one mapping of the prototype linear array factor to the planar array factor along the $\phi=0°$ cut. With any transformation function the transformation coefficients can be chosen in such a manner that the beamwidth of the planar array is broader than that of the prototype linear array. This is evident from a comparison between the graphs #1 and #2 in Figure 3.6. This will of course have an adverse effect on the excitation efficiency of the planar array. If transformations with $I>1$ or $J>1$ are used it is possible to obtain a planar array that has pattern cuts in which the beamwidths are narrower (in terms of the view-angle θ) from that of the prototype linear array. This phenomenon can be observed from consideration of Figure 3.5. The slope of curves #3 and #4 are greater than 45° ; indicating that the increase in the prototype linear array factor angle θ_p is greater than the increase in the planar array factor angle θ resulting in a narrower beamwidth. The narrower beamwidth can be seen in Figure 3.6, trace #3 and #4. The transformation grating lobe is clearly visible in trace #4 of Figure 3.6.

3.4.2 The Contour Approximation Problem

The shape of the contours inside the coverage area is not important, what is important is that the ripple in the coverage area does not exceed the desired levels. The same can be said of the sidelobe topography; the shape is unimportant but all the sidelobe peaks must be at or lower than the sidelobe level. The main beam of the prototype linear array factor will be mapped into the coverage area planar array factor. Thus, the prototype linear array factor must, in general, have a main beam with a specified maximum ripple and beamwidth, and sidelobes lower than the required sidelobe level. The transition region is the roll-off region between the main beam region and the sidelobe region. Figure 3.7 displays a typical prototype linear array factor. The end of the main beam region is denoted by α; this is the pattern angle where the prototype linear array factor main beam falls below the ripple specification. The quantity β is the pattern angle where the main beam has fallen to the sidelobe level.

Assume that we want to firmly control the contour $u=f_u(\theta,\phi)$ and $v=f_v(\theta,\phi)$, and that this firmly controlled contour must map to the point $\psi=\psi_0$ (usually the -3dB point).

$$\begin{aligned} \text{Odd case:} \quad & \cos(\psi_0) = H[f_u(\theta,\phi), f_v(\theta,\phi)] \\ \text{Even case:} \quad & \cos(\tfrac{1}{2}\psi_0) = H[f_u(\theta,\phi), f_v(\theta,\phi)] \end{aligned} \tag{3.26}$$

In some methods of determining the transformation function coefficients this will be the only consideration, no additional constraints are enforced; scaling may be necessary for the coefficients obtained with such methods. However, additional constraints may be imposed, which means some optimisation method must be used to calculate the transfor-

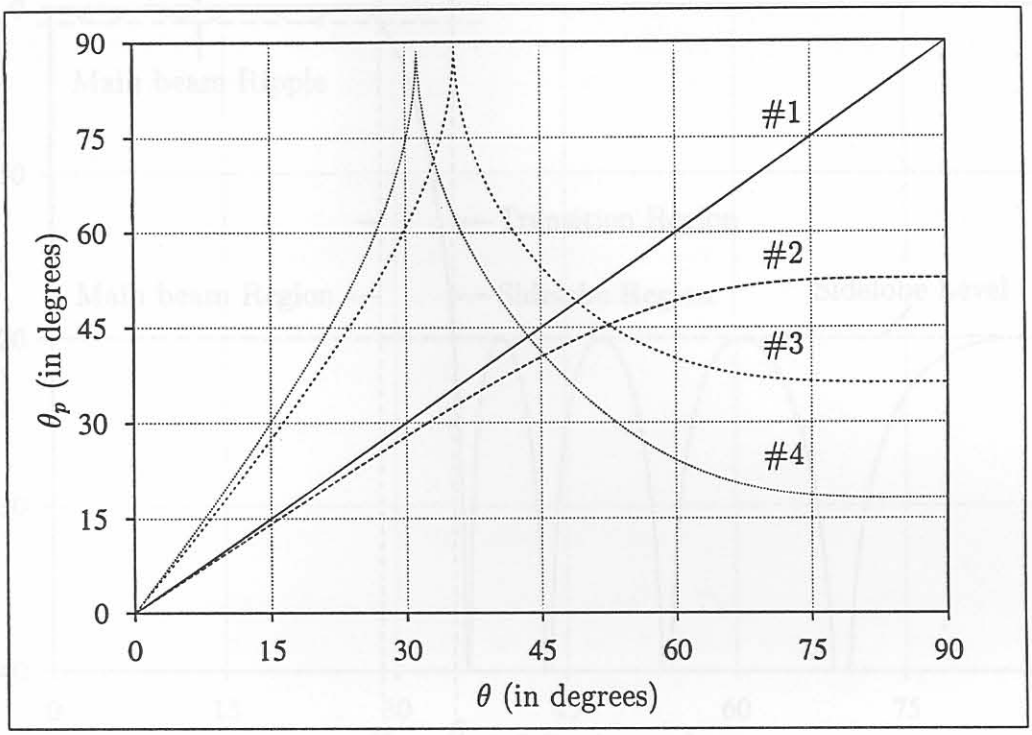

Figure 3.5: Transformation grating lobes: θ_p versus θ.

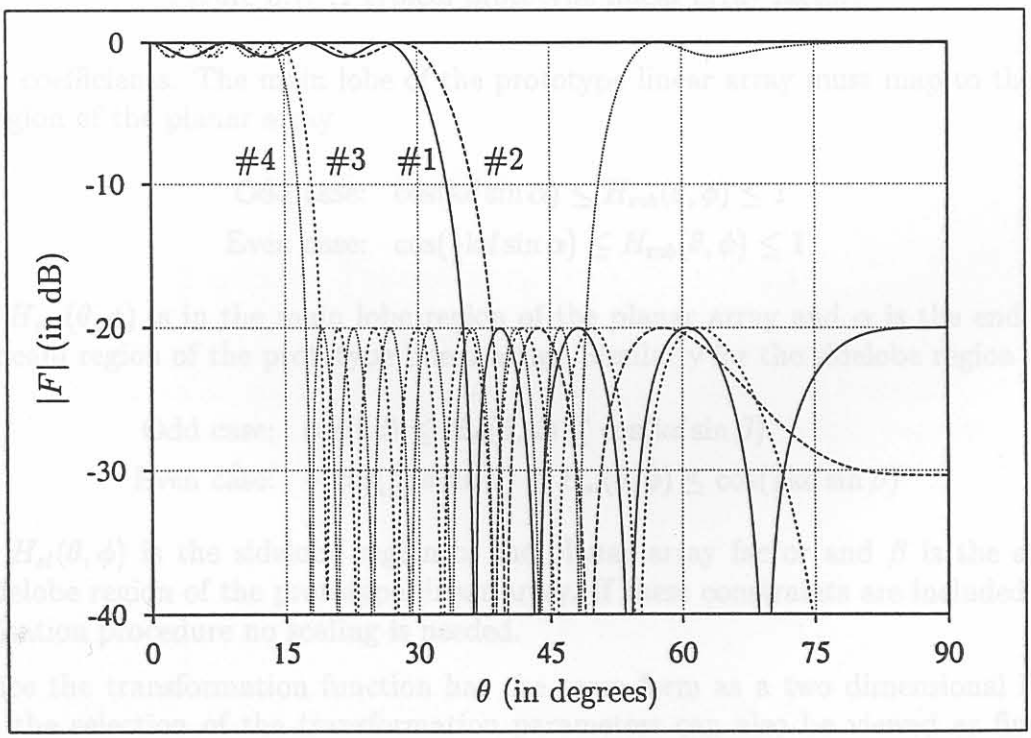

Figure 3.6: Transformation grating lobes: Planar array factors, ϕ=0° cuts only.

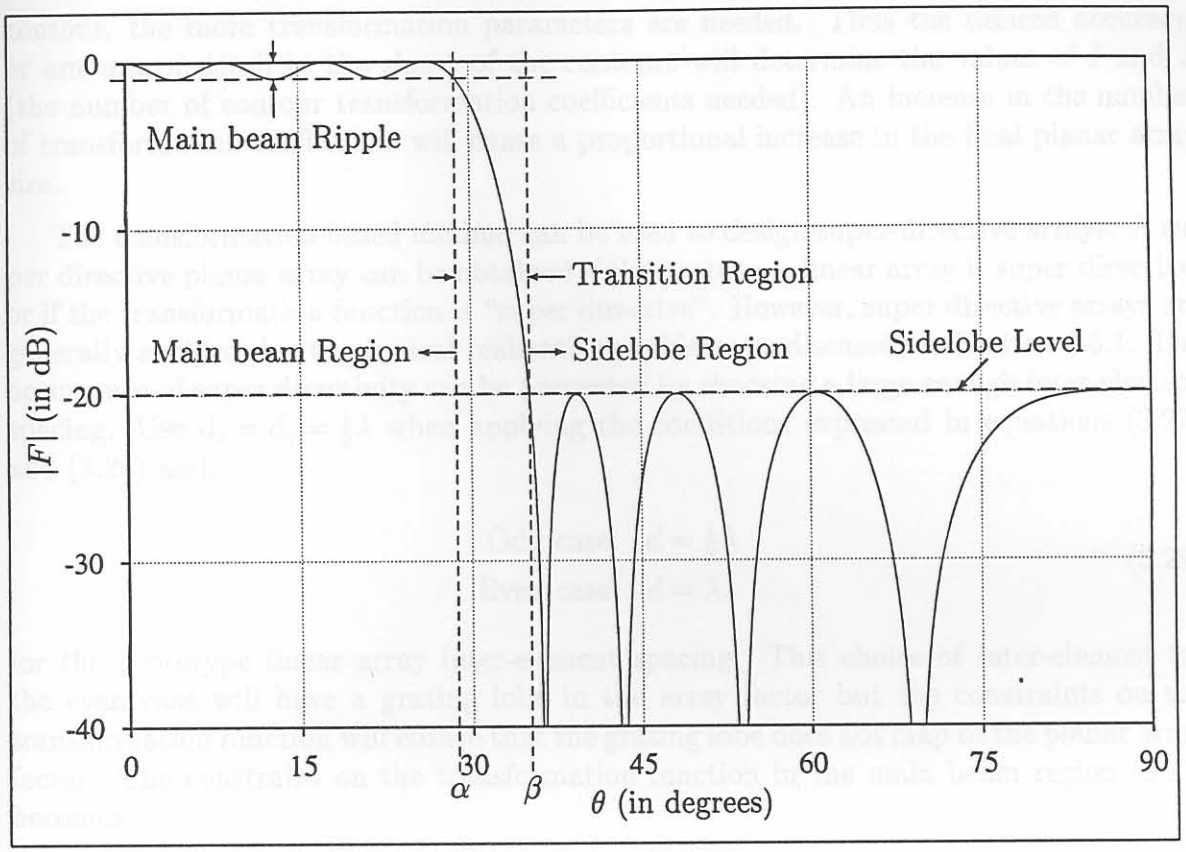

Figure 3.7: A typical prototype linear array factor.

mation coefficients. The main lobe of the prototype linear array must map to the main lobe region of the planar array

$$\begin{aligned} \text{Odd case:} \quad & \cos(\mathrm{k}d\sin\alpha) \leq H_{mb}(\theta,\phi) \leq 1 \\ \text{Even case:} \quad & \cos(\tfrac{1}{2}\mathrm{k}d\sin\alpha) \leq H_{mb}(\theta,\phi) \leq 1 \end{aligned} \tag{3.27}$$

where $H_{mb}(\theta,\phi)$ is in the main lobe region of the planar array and α is the end of the main beam region of the prototype linear array. Similarly for the sidelobe region

$$\begin{aligned} \text{Odd case:} \quad & \cos(\mathrm{k}d) \leq H_{sl}(\theta,\phi) \leq \cos(\mathrm{k}d\sin\beta) \\ \text{Even case:} \quad & -\cos(\tfrac{1}{2}\mathrm{k}d\sin\beta) \leq H_{sl}(\theta,\phi) \leq \cos(\tfrac{1}{2}\mathrm{k}d\sin\beta) \end{aligned} \tag{3.28}$$

where $H_{sl}(\theta,\phi)$ is the sidelobe region of the planar array factor and β is the start of the sidelobe region of the prototype linear array. If these constraints are included in the optimisation procedure no scaling is needed.

Since the transformation function has the same form as a two dimensional Fourier series, the selection of the transformation parameters can also be viewed as finding a two-dimensional Fourier transformation of the strictly specified contour. From Fourier analysis it then follows that the narrower the beamwidth, and the more detailed the

contour, the more transformation parameters are needed. Thus the desired accuracy, or amount of detail in the shape of the contours will determine the values of I and J (the number of contour transformation coefficients needed). An increase in the number of transformation coefficients will cause a proportional increase in the final planar array size.

The transformation based method can be used to design super-directive arrays. A super directive planar array can be obtained if the prototype linear array is super directive, or if the transformation function is "super directive". However, super directive arrays are generally avoided due to physical realization problems as discussed in Section 2.5.1. The occurrence of super directivity can be prevented by choosing a large enough inter-element spacing. Use $d_x = d_y = \frac{1}{2}\lambda$ when applying the conditions expressed in equations (3.27) and (3.28) and;

$$\begin{aligned} \text{Odd case:} \quad & d = \tfrac{1}{2}\lambda \\ \text{Even case:} \quad & d = \lambda. \end{aligned} \tag{3.29}$$

for the prototype linear array inter-element spacing. This choice of inter-element for the even case will have a grating lobe in the array factor but the constraints on the transformation function will ensure that the grating lobe does not map to the planar array factor. The constraint on the transformation function in the main beam region (3.27) becomes

$$\cos(\pi \sin\alpha) \leq H_{mb}(\theta, \phi) \leq 1 \tag{3.30}$$

for both the odd and even case; and the constraint in the sidelobe region (3.28) becomes

$$\begin{aligned} \text{Odd case:} \quad & -1 \leq H_{sl}(\theta, \phi) \leq \cos(\pi \sin\beta) \\ \text{Even case:} \quad & -\cos(\pi \sin\beta) \leq H_{sl}(\theta, \phi) \leq \cos(\pi \sin\beta). \end{aligned} \tag{3.31}$$

3.4.3 Scaling of the Transformation Function

Linear scaling of the transformation function is only applicable to the odd case. Visible space is the region where $0 \leq \theta \leq \frac{1}{2}\pi$ and $0 \leq \phi \leq 2\pi$. From the definition of u and v in (2.14) an elliptical disc, with major axis $\mathrm{k}d_x$ and minor axis $\mathrm{k}d_y$, constitutes visible space in the uv-plane [18]. Since $|\cos x| \leq 1$, the following constraint must be imposed on $H(u, v)$:

$$|H(u,v)| \leq 1 \quad \text{for} \quad \sqrt{\left(\frac{u}{\mathrm{k}d_x}\right)^2 + \left(\frac{v}{\mathrm{k}d_y}\right)^2} \leq 1 \tag{3.32}$$

To avoid super directivity $d_x = d_y = \frac{1}{2}\lambda$ is used when applying this condition.

The transformation parameters are found using an optimisation algorithm, approximation, or some other technique, to fit the desired shape of the target contour. The

solution, however, usually does not satisfy the condition in (3.32) and scaling is therefore necessary. The following linear scaling scheme can be employed [124]

$$H'(u,v) = C_1\, H(u,v) - C_2 \tag{3.33}$$

where

$$C_1 = \frac{2}{H_{max} - H_{min}} \tag{3.34a}$$

$$C_2 = C_1\, H_{max} - 1 \tag{3.34b}$$

and H_{max} and H_{min} are the maximum and minimum values of $H(u,v)$ which usually have to be found numerically. Obviously this scaling does not change the shape of the contours defined by $H(u,v) = constant$;, only the original ψ_p value associated with a specific contour changes to

$$\psi'_p = \arccos(C_1 \cos\psi_p - C_2) \tag{3.35}$$

Since the transformation function for the even case does not have a t_{00} coefficient, the linear scaling technique cannot be applied. For the even case the transformation function must be normalised or the constraint (3.32) must be included and enforced in the determination of the transformation coefficients. Normalisation can be done by

$$H'(u,v) = C\, H(u,v) \tag{3.36}$$

where $C = |H(u,v)|_{max}$.

3.4.4 Transformation Function Synthesis by Approximation

If the desired contour can be written in an analytical form, for example an elliptical contour,

$$\frac{u^2}{a^2} + \frac{v^2}{b^2} = 1 \tag{3.37}$$

where a and b are the major and minor axes of the elliptical contour, then approximation can be used to determine the values of the transformation coefficients. The Taylor series for the trigonometric functions, sin and cos, are

$$\begin{aligned} \cos x &= 1 - \tfrac{x^2}{2!} + \tfrac{x^4}{4!} \cdots \\ \sin x &= x - \tfrac{x^3}{3!} + \tfrac{x^5}{5!} \cdots \end{aligned} \tag{3.38}$$

With small values of x the series can be truncated. These truncated or approximated series are then substituted into the transformation function, and the powers of u and v are set to the values of the corresponding powers in the function describing the contour.

An alternative approach is to select a number of cuts and ensure that the desired contour is at the correct position in these cuts. If the total number of adjustable transformation coefficients is K, one can choose $K-1$ ϕ-cuts and set up $K-1$ equations,

$$\begin{aligned} \text{Odd case:} \quad & H(\theta_k, \phi_k) = \cos(\psi_0) \\ \text{Even case:} \quad & H(\theta_k, \phi_k) = \cos(\tfrac{1}{2}\psi_0) \end{aligned} \tag{3.39}$$

using

$$H(0,0) = 1 \tag{3.40}$$

as the Kth equation, and then simple matrix inversion can be used to determine the transformation coefficients.

The approximation methods work well if only a few transformation function coefficients are used and the desired contours are relatively simple, smooth functions such as circles or ellipses. Thus they are of little use in synthesising planar arrays with arbitrarily contoured array factors. References [95, 92] contain more information on these methods.

3.4.5 Transformation Function Synthesis by Constrained Optimisation

The problem can be formulated as a linear approximation problem. The error function can be defined as

$$\begin{aligned} \text{Odd case:} \quad & \varepsilon = \cos(\psi_0) - H[u, f(u)] \\ \text{Even case:} \quad & \varepsilon = \cos(\tfrac{1}{2}\psi_0) - H[u, f(u)] \end{aligned} \tag{3.41}$$

with $v = f(u)$. Applying the constraint presented in equation (3.32), one variable can be written as a function of the others, leaving one less parameter to be optimised. Standard linear optimisation routines can be used for the optimisation. The transformation parameters obtained with these methods will usually require scaling.

Another procedure for the design of contours of any shape will next be described. The algorithm can design one or more contours simultaneously and it can be used with transformations of any I and J values. We explore the procedure for a one contour mapping. Assume the requirement is the mapping of the point $\psi = \psi_0$ to a contour $u = f_u(\theta, \phi)$ and $v = f_v(\theta, \phi)$. A set of error equations can then be formulated on some set of discrete samples, as

$$\begin{aligned} \text{Odd case:} \quad & \varepsilon(\theta_k, \phi_k) = \cos(\psi_0) - H[f_u(\theta_k, \phi_k), f_v(\theta_k, \phi_k)] \\ \text{Even case:} \quad & \varepsilon(\theta_k, \phi_k) = \cos(\tfrac{1}{2}\psi_0) - H[f_u(\theta_k, \phi_k), f_v(\theta_k, \phi_k)] \end{aligned} \tag{3.42}$$

We must then minimise

$$E_1 = \max |\varepsilon(\theta_k, \phi_k)| \tag{3.43}$$

or

$$E_2 = \sum_k \varepsilon^2(\theta_k, \phi_k) \tag{3.44}$$

subject to equality constraints of the form

$$H(\theta_k, \phi_k) = \alpha \tag{3.45}$$

and inequality constraints of the form

$$\begin{aligned} \text{Odd case:} \quad & -1 \leq H(\theta_k, \phi_k) \leq \beta \\ \text{Even case:} \quad & -\beta \leq H(\theta_k, \phi_k) \leq \beta \end{aligned} \tag{3.46}$$

The quantity E_1 can be minimised by linear programming, or if the inequality constraints (3.46) are not present E_2 can be optimised using least squares techniques. The advantage of this approach is that no analytical function for the contour shape is needed.

The transformation design problem can also be stated in the same form as the design problem for two-dimensional equi-ripple digital filters. The transformation coefficients can be obtained from the impulse response coefficients of a digital filter. Fast and efficient algorithms exist [125, 126] to determine the impulse response of such small digital filters. A more complete discussion of these methods is provided in reference [92].

3.4.6 The Transformation Function as a Planar Array

The transformation function has the same form as a planar array factor. Since the transformation function is a real function the planar array factor must also be pure real, thus the determination of the transformation coefficients is equivalent to a "field synthesis" problem. Although it may seem that we end up where we started, it must be noted that the number of transformation coefficients is only a fraction of the number of final planar array elements. Also, field synthesis is generally simpler than power synthesis [111]. The excitations of the planar array $F_H(u, v)$ formed by the transformation function are

$$\begin{aligned} \mathbf{a}_{ij} &= \tfrac{1}{4}\left[t_{ij}^{cc} - t_{ij}^{ss} - \mathrm{j}(t_{ij}^{cs} + t_{ij}^{sc})\right] \\ \mathbf{a}_{i-j} &= \tfrac{1}{4}\left[t_{ij}^{cc} + t_{ij}^{ss} + \mathrm{j}(t_{ij}^{cs} - t_{ij}^{sc})\right] \\ \mathbf{a}_{-ij} &= \tfrac{1}{4}\left[t_{ij}^{cc} + t_{ij}^{ss} - \mathrm{j}(t_{ij}^{cs} - t_{ij}^{sc})\right] \\ \mathbf{a}_{-i-j} &= \tfrac{1}{4}\left[t_{ij}^{cc} - t_{ij}^{ss} + \mathrm{j}(t_{ij}^{cs} + t_{ij}^{sc})\right] \end{aligned} \tag{3.47}$$

From expression (3.47) it is clear that $\mathbf{a}_{ij} = \mathbf{a}^*_{-i-j}$ and $\mathbf{a}_{i-j} = \mathbf{a}^*_{-ij}$. This will always result in a pure real array factor. Any of the planar array synthesis techniques discussed in Chapter 2 can be used to determine the transformation coefficients, but field synthesis

methods will work best, as the phase of the radiation pattern is known. Since the "array factor" of the transformation function "array" is pure real the generalised projection method (Section 2.8.4) is ideally suited to determine the transformation coefficients; as the sets involved in field synthesis are convex, convergence is guaranteed. In general scaling will be necessary for transformation function parameters computed in this manner.

3.5 Planar Arrays with Non-Rectangular Boundaries and/or Lattices

The transformation based synthesis technique described in Sections3.2 and 3.3 can also be used to synthesise planar arrays with non-rectangular boundaries and/or lattices if we purposefully set specific transformation coefficients equal to zero. We demonstrate this in the present section.

Firstly, the synthesis of planar arrays with rectangular grids but non-rectangular boundaries (say octagonal or near-circular boundaries) will be discussed in Section 3.5.1. Secondly, the synthesis of planar arrays with non-rectangular lattices (for instance hexagonal arrays) is addressed in Section 3.5.2.

3.5.1 Arrays with Rectangular Lattices but Non-Rectangular Boundaries

The transformation function has the same form as a small planar array factor, thus the transformation coefficients can be graphically represented in a fashion similar to planar array excitations. The transformation function must have the same "shape" as the final planar array; for an array with an elliptical boundary the transformation "array" must also have an elliptical "boundary". Two examples are shown in Figure 3.8; the circles represent the transformation coefficients that must be set to zero and the dots represent non-zero, adjustable coefficients. The first example (Figure 3.8(a)) is the transformation needed for an octagonally shaped planar array, while the second (Figure 3.8(b)) is for a planar array with an elliptical boundary.

The synthesis method follows the steps outlined in the illustrative example #1 in Section 3.2.2, except for the first step, which is expanded to take the boundary of the array into account. Not only must the number of transformation coefficients (I and J) be determined, but also which of the transformation coefficients must be set to zero to obtain the correct boundary shape.

Illustrative Example #3

Let us consider the design requirement to be a planar array with octagonal boundary. A circular footprint contour at -3dB is desired.

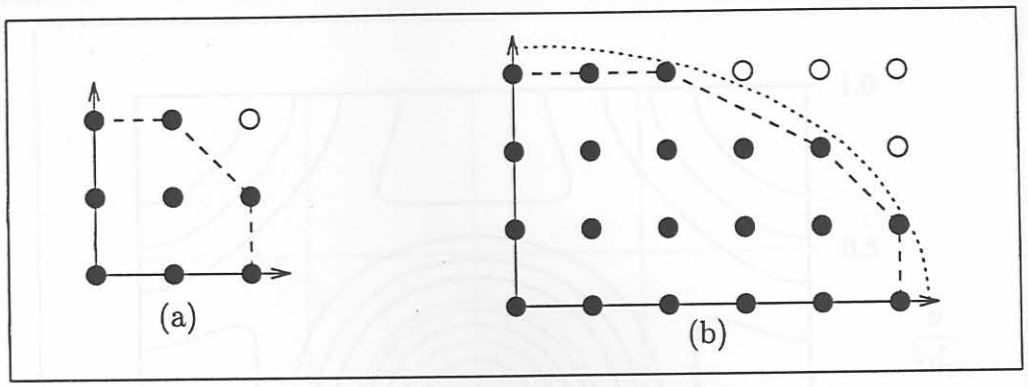

Figure 3.8: Graphical representation of the transformation coefficients for arrays with non-rectangular boundaries, the circles representing zero coefficients. (a) Rectangular grid with an octagonal boundary. (b) Rectangular grid and a near-elliptical boundary. The dashed line indicates the boundary of the final planar array.

Coefficient	Value	Coefficient	Value
t_{00}	-.549205	t_{11}	.739280
$t_{01}=t_{10}$	.129086	$t_{12}=t_{21}$	.129086
$t_{02}=t_{20}$	.146790	t_{22}	0

Table 3.3: Illustrative Example #3: Transformation coefficients.

1. An array with a rectangular grid and an octagonal boundary can be achieved by a transformation with $I = J = 2$, but $t_{22}^{xx} = 0$ in order to obtain the octagonal boundary. The transformation function is shown graphically in Figure 3.8(a), the solid line shows the array boundary shape (only one quadrant is depicted).

2. The number of elements used for the prototype linear array is 15; or $Q=7$.

3. The prototype linear array was synthesised using the method of Orchard, Elliot and Stern [54]. Six roots were placed off the unit circle. The main beam peak-to-peak ripple is 1dB and the sidelobe level is -20dB. The inter-element spacing used in this step is $d=\frac{1}{2}\lambda$. A -3dB beamwidth of 71° was obtained.

4. Due to the octagonal symmetry of the required contour shape only five unique transformation coefficients are available to control the contour shape. The transformation coefficients were computed using the approximation-by-cuts approach discussed in the latter half of Section 3.4.4. The coefficient values are listed in Table 3.3.

5. The algorithm in Section A.1.3 in Appendix A was used to compute the planar array excitation. Although $M=N=14$, suggesting an array of 729 elements, only 617 elements are excited.

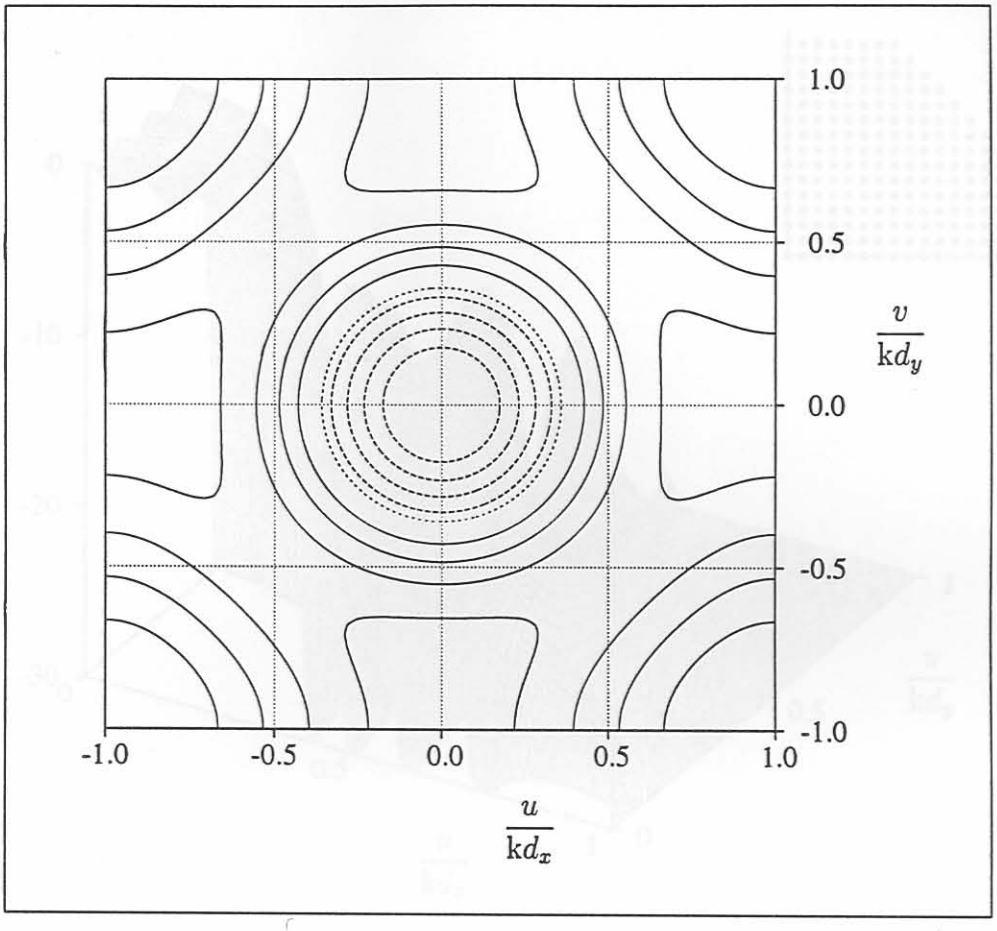

Figure 3.9: Illustrative Example #3: A contour plot of the transformation function. The dotted line represents the -3dB contour, the dashed lines contours in the main beam region and solid lines contours in the sidelobe region.

A contour plot of the transformation function is displayed in Figure 3.9. The -3dB beamwidth contour of the planar array factor, represented by the dotted line in Figure 3.9, is at $\theta = 21°$. A surface plot of the planar array factor is depicted in Figure 3.10. The array geometry is shown in the top right hand corner of Figure 3.10.

3.5.2 Arrays with Triangular Lattices and Boundaries

In general, one can view a triangular grid array as a rectangular grid array with only those elements coinciding on the triangular grid excited. If one chooses the x-axis on one of the triangular lattice axes one can construct an equivalent rectangular grid array, as shown in Figure 3.11. The intersections of the dotted lines with filled circles indicate the positions of excited elements, while the unfilled circles indicate the positions of zero elements. The filled squares represent the collapsed distributions along the principal axes.

First we consider the rows of the array. The inter-element spacing of the triangular

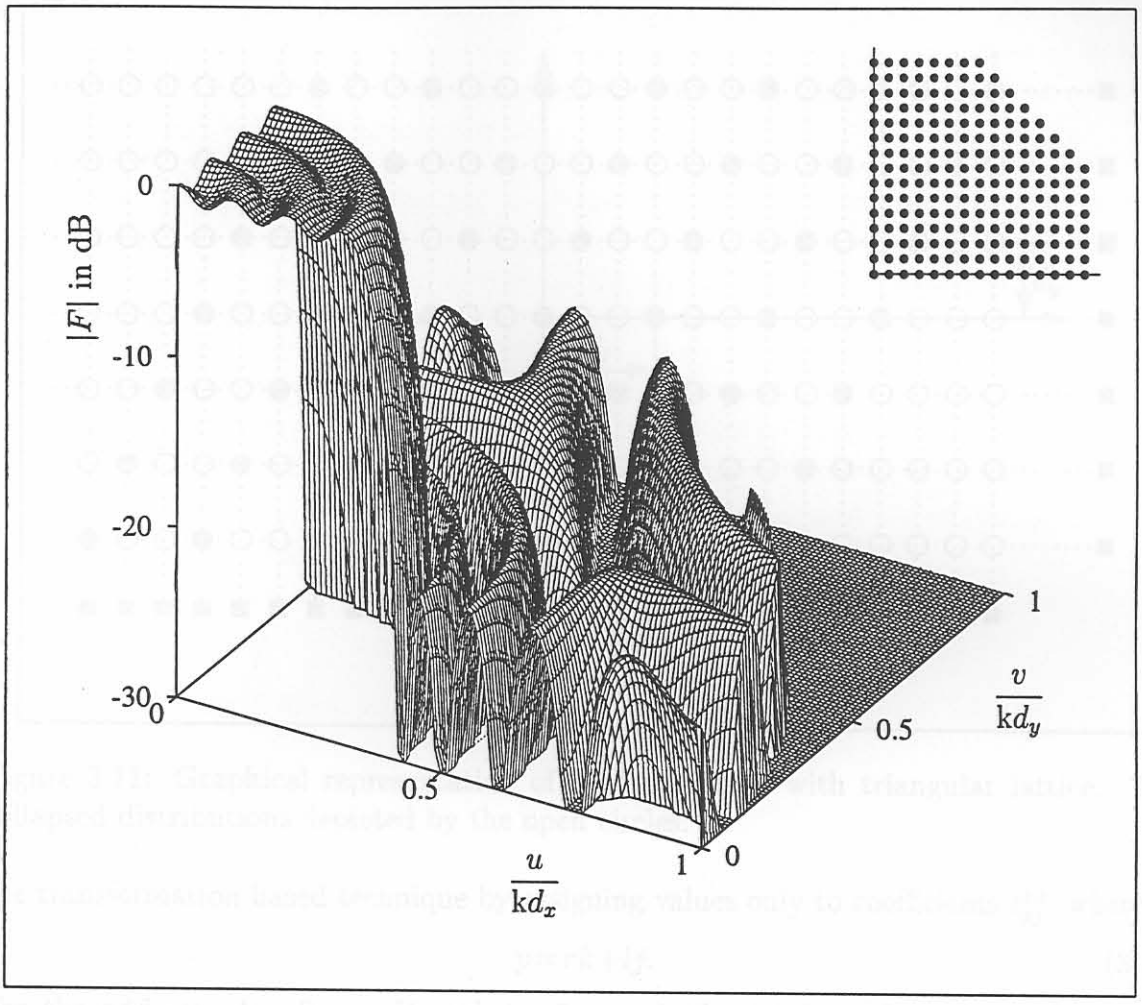

Figure 3.10: Illustrative Example #3: Surface plot of the planar array factor, with the array geometry depicted in the upper right hand corner.

grid array in the $\hat{x}$ direction is denoted by d_t, and the inter-element spacing of the collapsed distribution in the $\hat{x}$ direction by d_x. The inter-element spacings are indicated in Figure 3.11. If the ratio between d_t and d_x is an integer the triangular grid array can be synthesised with the transformation based synthesis method. Let us assume this to be the case and denote the ratio $r = d_t/d_x$. Only the r-th element in each row of the equivalent rectangular grid array will be excited. In addition, the selected elements have a horizontal shift from one row to the next. This shift will be an integer of units d_x, and denoted by k. In the case shown in Figure 3.11 every third element in each row of the rectangular grid is excited, thus $r=3$; and the horizontal shift is $l=1$. The other principal plane is less complicated; the inter-element spacing d_y of the collapsed distribution in the $\hat{y}$ direction is simply the distance between the rows of the triangular grid.

The transformation function coefficients must have the same "shape" as the unit cell of the planar array. Since only the elements at positions $((rm+ln)d_x, nd_y)$ of the equivalent rectangular lattice are excited, the triangular array can be synthesised with

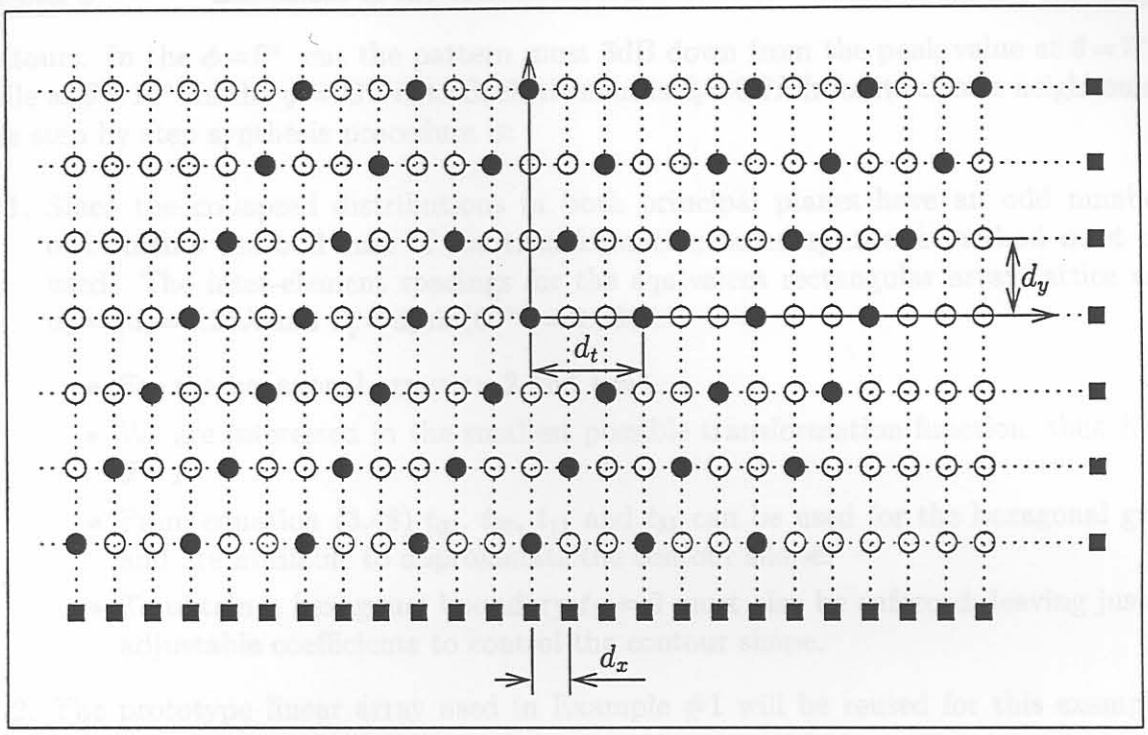

Figure 3.11: Graphical representation of a planar array with triangular lattice. The collapsed distributions depicted by the open circles.

the transformation based technique by assigning values only to coefficients t_{pj}^{xx}, where

$$p=rk+lj. \tag{3.48}$$

For the odd case $k=0,\ldots,K$ and $j=0,\ldots,J$; the total number of transformation coefficients is $(I+1)\times(J+1)$ of which $(K+1)\times(J+1)$ will be non-zero. In the even case $k=1,\ldots,K$ and $j=1,\ldots,J$; from a total of $I\times J$ transformation coefficients $K\times J$ are non-zero. For both the odd and the even case

$$I=rK+lJ \tag{3.49}$$

In order to synthesise triangular arrays yet another extension to the first step in the synthesis procedure must be made. First, r and l must be determined from the geometry of the array considered. The number of coefficients K and J are then selected. From these values the total number of transformation coefficients can be computed, as well as which coefficients are non-zero. Lastly, in order to obtain the correct array boundary some of the non-zero transformation coefficients must also be set to zero. The synthesis method is best illustrated by an example.

Illustrative Example #4

A typical example of an array with triangular lattice is a hexagonal array. Consider the design of a 10 ring hexagonal planar array with a requirement of elliptical footprint

contours. In the $\phi=0°$ cut the pattern must 3dB down from the peak value at $\theta=7°$, while at $\theta=10°$ in the $\phi=90°$ cut. Each element is $d_t=0.7\lambda$ from its closets neighbours. The step by step synthesis procedure is:

1. Since the collapsed distributions in both principal planes have an odd number of elements the odd case of the transformation based synthesis method must be used. The inter-element spacings for the equivalent rectangular array lattice are $d_x=\frac{1}{2}d_t=0.35\lambda$ and $d_y=d_t\sin(60°)=0.606\lambda$.
   - For the hexagonal array $r=2$ and $k=1$.
   - We are interested in the smallest possible transformation function, thus $K=J=1$.
   - From equation (3.48) t_{00}, t_{20}, t_{11} and t_{31} can be used for the hexagonal grid and are available to approximate the contour shape.
   - To obtain a hexagonal boundary $t_{31}=0$ must also be enforced; leaving just 3 adjustable coefficients to control the contour shape.
2. The prototype linear array used in Example #1 will be reused for this example, $Q=10$.
3. The same prototype linear array excitation as in Example #1 is used.
4. The approximation-by-cuts method described in Section 3.4.4 can be used to obtain the contour transformation coefficients. Only two cuts, $\phi=0°$ and $\phi=90°$, are needed. The coefficient values determined in this manner are $t_{00}=-0.208559$, $t_{11}=0.537601$ and $t_{20}=0.670958$. No scaling is needed, even if $d_x=\frac{1}{2}\lambda$.
5. The planar array distribution can now be obtained using the algorithms in Section A.1.2 of Appendix A

Figure 3.12 displays a contour plot of the transformation function. The transformation function coefficients for the hexagonal array are graphically presented in the upper right hand corner of the figure. The filled circles represent adjustable coefficients and the non-filled circles the "off-grid" zero coefficients. The crossed circle represents the "on-grid" transformation parameter that must be set to zero to obtain a hexagonal boundary. The solid line shows the final array boundary shape. The array factor is shown in Figure 3.13.

3.6 Representative Example: An Africa-Shaped Contour Footprint Pattern

Let the requirement for this example be a strictly controlled contour in the shape of Africa as seen from a geo-stationary position above the equator. The geometry of the array is a square lattice ($d_x=d_y=0.72\lambda$) with the corner elements lopped off to fit in a circular boundary.

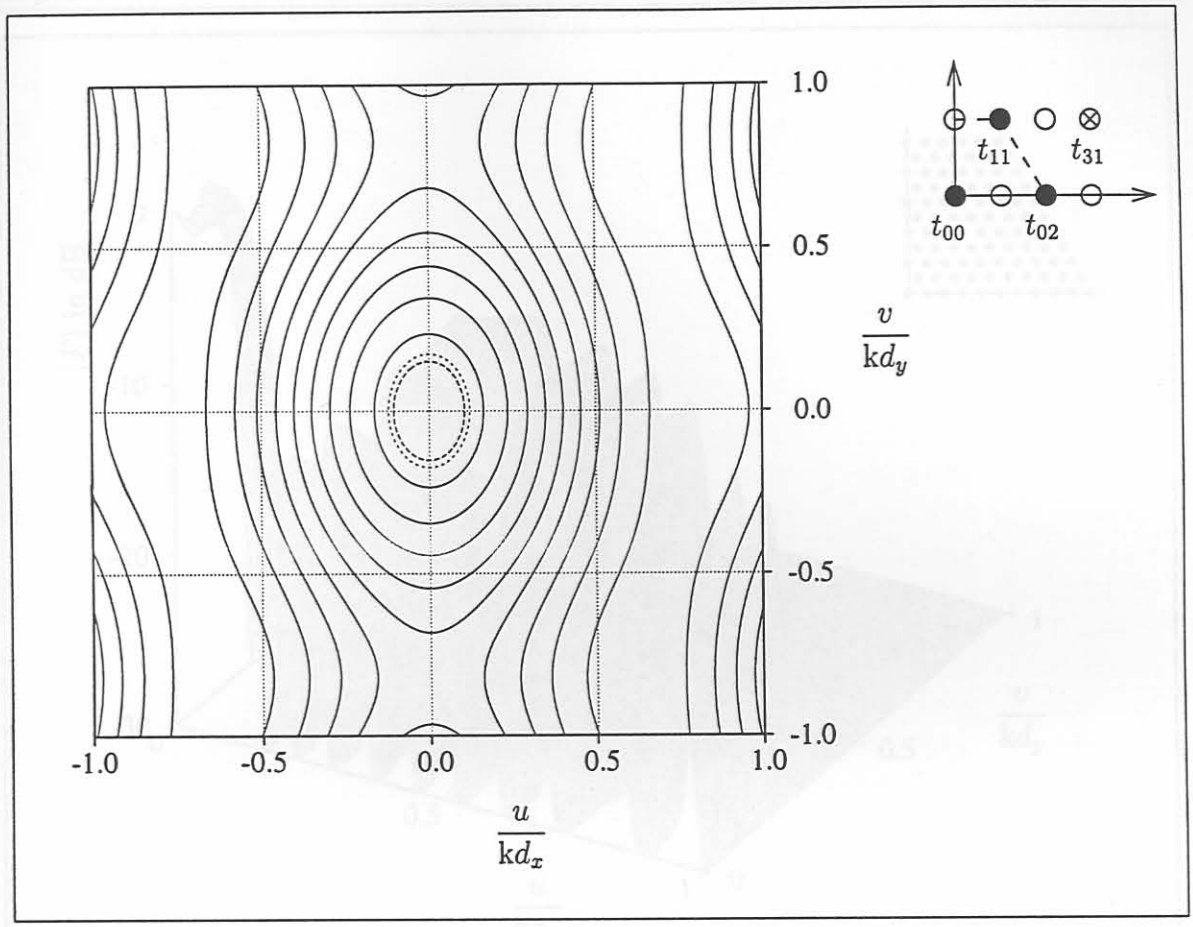

Figure 3.12: Illustrative Example #4: A contour plot of the transformation function, with the transformation function depicted on the right. The dashed line represents the -1dB contour and the dotted line the -3dB contour.

1. A transformation with $I=J=5$ gives enough flexibility to approximate the contour of the African continent adequately. To get a near circular boundary $t_{45}^{xx}=t_{54}^{xx}=t_{55}^{xx}$.

2. The prototype linear array consists of 21 ($Q=10$) elements.

3. The prototype linear array is synthesised using the method of Orchard, Elliott and Stern [53]. The sidelobe level was set at -30dB, and the main beam ripple at 1.0dB. To obtain the narrow beamwidth two zeros had to be moved from the Schelkunoff unit circle.

4. A total of 109 transformation coefficients are available to control the contour shape. The values of the transformation coefficients were obtained using the general projection planar array synthesis method with weighted least squares as the back projector (this method will be discussed in Section 5.2.3). The projection method is ideally suited for determination of the coefficients as the transformation function is pure real, and the sets involved are convex. The transformation parameters are listed in Table 3.4. A contour plot of the transformation function is shown in Figure 3.14.

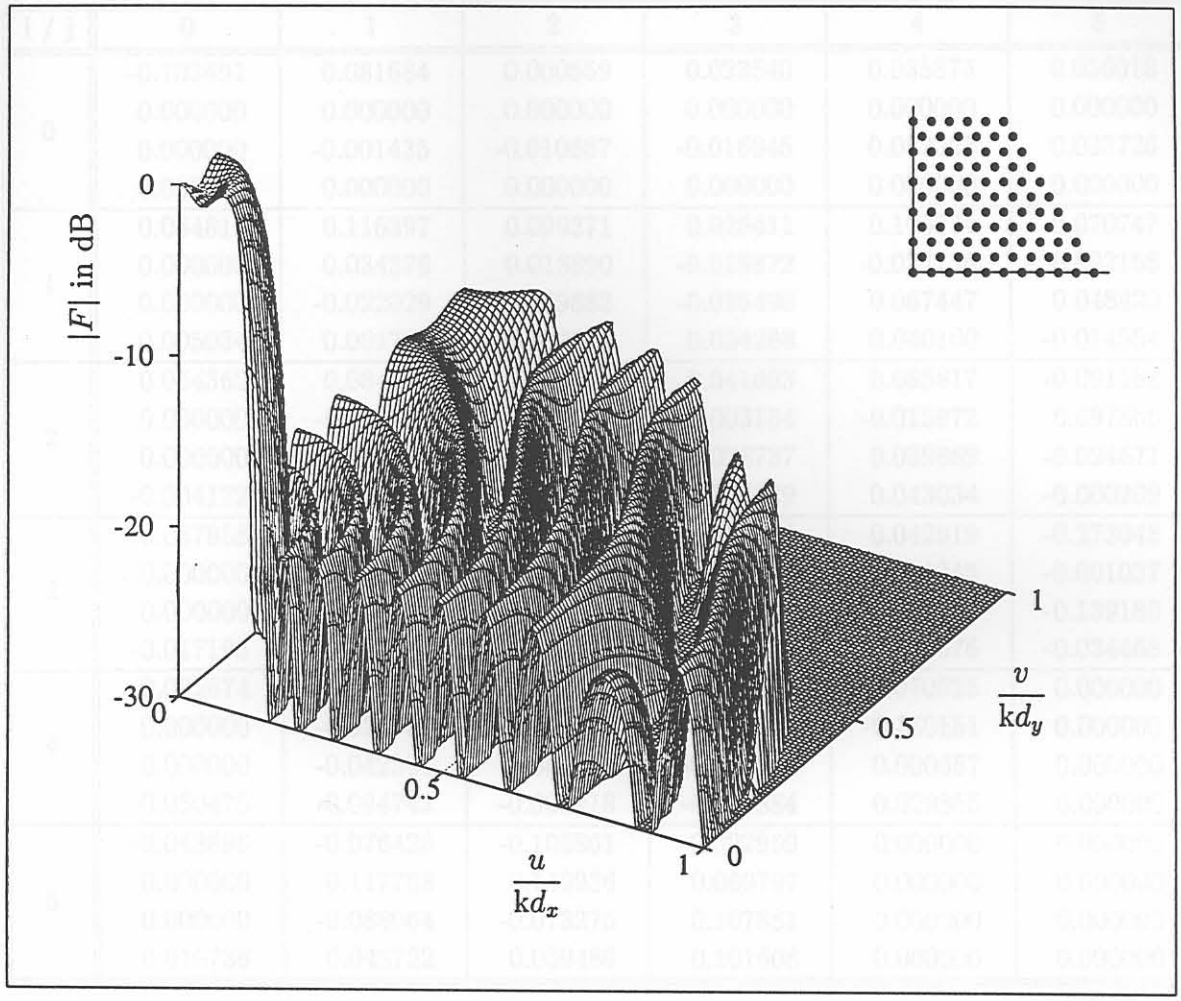

Figure 3.13: Illustrative Example #4: Surface plot of the planar array factor (with the array geometry depicted in the upper right corner).

5. The planar array excitations were then computed using the information forthcoming from the solutions of the two sub-problems.

The planar array distribution is graphically shown in Figure 3.15; one can see that the excitations decrease from the centre outward; this is inherent to the transformation based method. The excitations near the edge of the array are dependent on a few terms of $H^q(u,v)$ with q large. Since the transformation coefficients are generally smaller than one, the excitations at these far-out positions will be small. These small elements far from the origin of the array, with a magnitude of less than 1% the magnitude of the largest excitation, may be removed without seriously degrading the radiation pattern. This will result in an array with a circular boundary of diameter of 64λ and 6293 elements. With all the elements of magnitude less than 1% (or -40dB) of the largest excitation removed, only 0.13% (or -29dB) of the total power of the synthesised array will be lost. This array has 3822 non-zero elements in a circular boundary. The main beam contours are not

i / j	0	1	2	3	4	5
0	-0.103491	0.081684	0.000659	0.023540	0.035873	0.056018
	0.000000	0.000000	0.000000	0.000000	0.000000	0.000000
	0.000000	-0.001435	-0.010687	-0.016845	0.062322	0.033726
	0.000000	0.000000	0.000000	0.000000	0.000000	0.000000
1	0.084819	0.116397	0.099371	0.025411	0.106774	0.070747
	0.000000	0.034376	0.013890	-0.019872	-0.024756	0.092168
	0.000000	-0.022029	-0.009882	-0.036490	0.067447	0.048420
	0.005034	0.001793	0.002313	0.034268	0.040160	-0.014554
2	0.054362	0.084796	0.095682	0.041693	0.085817	-0.091182
	0.000000	-0.016720	-0.034881	0.003184	-0.015972	0.097866
	0.000000	-0.081815	-0.043515	0.028737	0.039869	-0.024671
	-0.004172	-0.021291	0.008764	-0.006829	0.043034	-0.000269
3	0.037958	0.038334	0.105628	0.102171	0.042919	-0.273048
	0.000000	-0.030287	-0.027655	-0.019976	-0.025345	-0.001037
	0.000000	-0.037993	-0.040805	0.014134	0.072372	-0.139180
	-0.017198	-0.034351	0.007507	0.016134	-0.008676	-0.034468
4	0.092674	0.190139	0.107466	0.005586	-0.070625	0.000000
	0.000000	-0.024303	-0.079479	-0.098116	-0.140151	0.000000
	0.000000	-0.042361	-0.060640	-0.036315	0.000667	0.000000
	-0.030475	-0.094742	-0.080918	-0.062884	0.029855	0.000000
5	-0.043896	-0.076426	-0.105861	-0.022959	0.000000	0.000000
	0.000000	0.117768	0.149936	0.069797	0.000000	0.000000
	0.000000	-0.088064	-0.073275	0.107881	0.000000	0.000000
	0.010736	0.048722	0.059486	0.101608	0.000000	0.000000

Table 3.4: Representative Example: The transformation function coefficients. The four elements in each cell of the table are t_{ij}^{cc} t_{ij}^{ss} t_{ij}^{cs} and t_{ij}^{sc} , in that order

noticeably changed and all the sidelobes are below a level of -24.5dB (all but one sidelobe is below -27.5dB). The planar array factor is depicted in Figures 3.16 and 3.17 (a surface and a contour plot of only the inner part of the array factor). The highest sidelobe peak is at $(u, v) = (0.193, 0.167)$ and can be seen in these two figures.

3.7 Comparison with Similar Methods

It is instructive to establish the relationship between transformation function and the different transformations that have been proposed to synthesise planar arrays. These transformations were briefly discussed in Section 2.7.2. It will be shown in Sections 3.7.1 to 3.7.4 that all these transformations are special cases of the transformation based synthesis method proposed in this chapter. In addition, some of the limitations suffered by these transformations can be overcome by the transformation based synthesis technique.

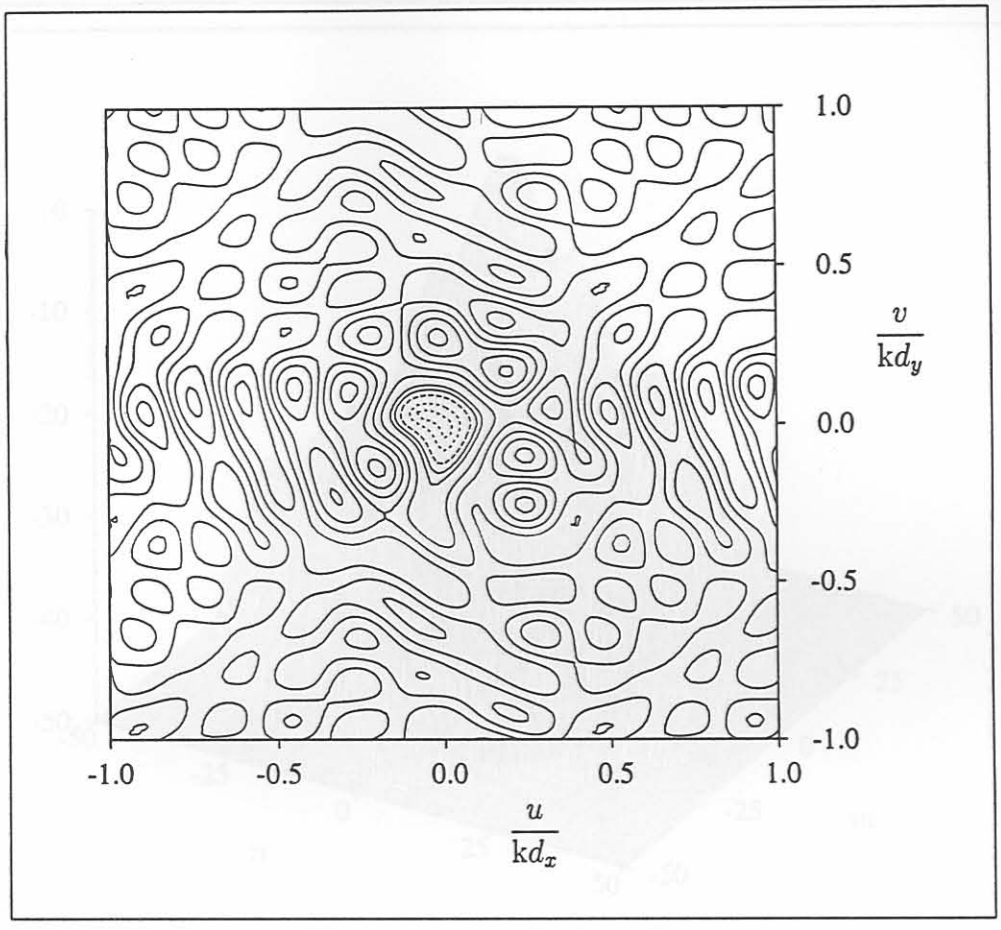

Figure 3.14: Representative Example: A contour of the transformation function. The dashed line is the strictly controled contour, solid lines are contours in the sidelobe region and the dotted lines are contours in the main beam region.

The similarities between the convolution synthesis method (which were mentioned in Section 2.7.3) and the transformation based synthesis technique will be discussed in Section 3.7.5.

3.7.1 The Baklanov Transformation

The use of a transformation to map a linear array excitation to a planar array excitation was first proposed by Baklanov [82] in 1966. Tseng and Cheng [81] substituted the Baklanov transformation into a Chebyshev polynomial to synthesise scanable square planar arrays with Chebychev patterns in every ϕ-cut. They considered arrays with an odd as well as an even number of elements.

The Baklanov transformation, here written in terms of the u and v as defined in this

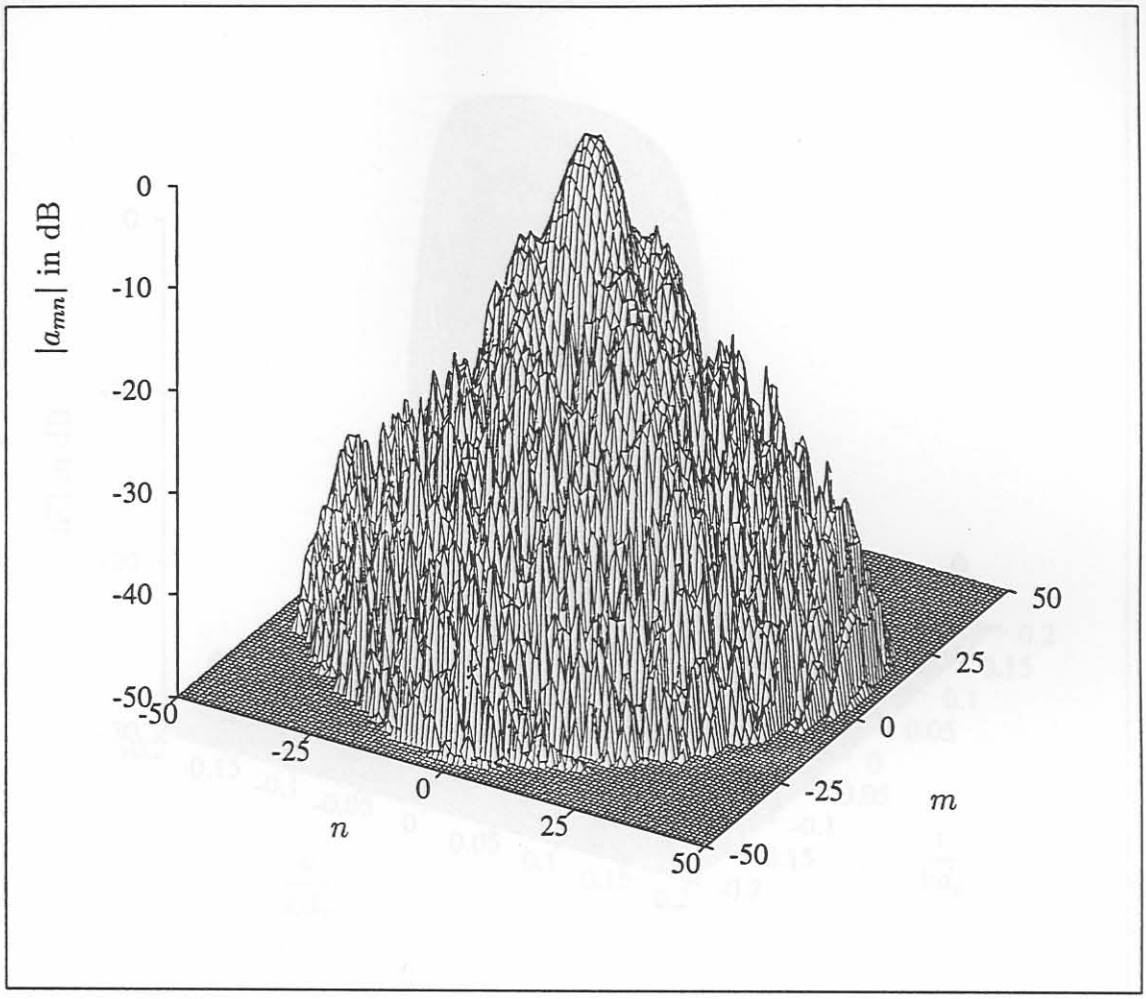

Figure 3.15: Representative Example: A plot of the planar array excitations normalised to the largest excitation.

chapter, is

$$w = w_0 \cos(\tfrac{1}{2}u)\cos(\tfrac{1}{2}v) \tag{3.50}$$

where w is the Chebychev polynomial variable. The Chebychev polynomial is related to the prototype linear array factor by

$$w = w_0 \cos(\tfrac{1}{2}\psi) \tag{3.51}$$

From the definition of the odd case transformation function in equation (3.19) the Baklanov transformation is a special case of the transformation function with $I = J = 1$ and $t_{11} = 1$. For an odd number of array elements the Baklanov transformation reduces to

$$\cos(\tfrac{1}{2}\psi) = \cos(\tfrac{1}{2}u)\cos(\tfrac{1}{2}v) \tag{3.52}$$

If both sides of equation (3.52) are squared and after some manipulation, equation (3.52) can be written as

$$\cos(\psi) = -\tfrac{1}{2} + \tfrac{1}{2}\cos(u) + \tfrac{1}{2}\cos(v) + \tfrac{1}{2}\cos(u)\cos(v) \tag{3.53}$$

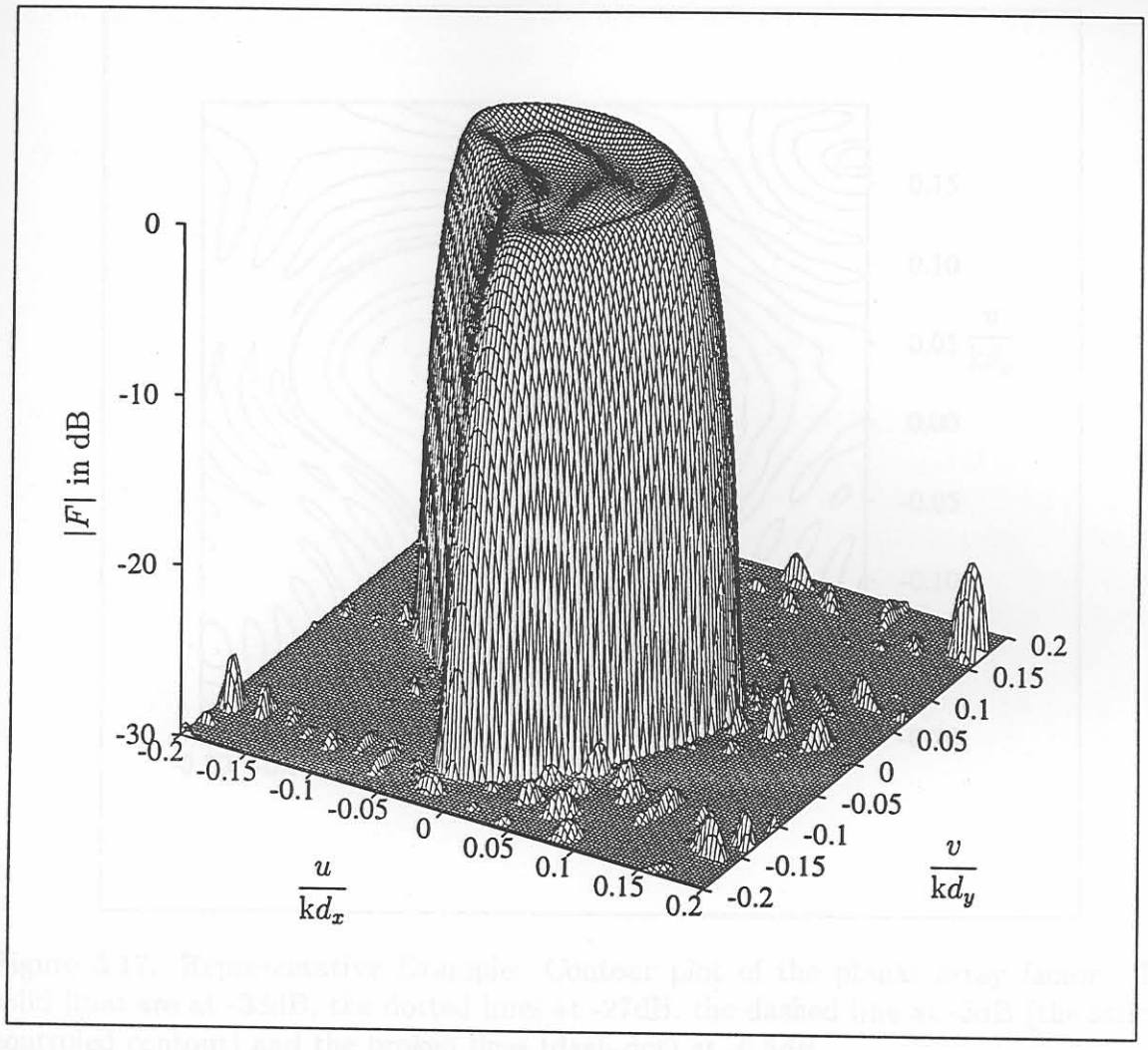

Figure 3.16: Representative Example: A surface plot of the planar array factor, only the centre part is shown.

This is equal to odd case transformation function (defined in equation (3.7)) if $I=J=1$ and $-t_{00}=t_{01}=t_1=t_{11}=1$. The Chebyshev polynomial is related to a prototype linear array with a Chebyshev pattern. Thus the Baklanov transformation synthesis method proposed by Tseng and Cheng is a special case of the transformation based synthesis technique. Tseng and Cheng mentioned that other combinations of $\cos u$ and $\cos(v)$ are possible [81], but did not pursue the possibility.

3.7.2 Extension of Baklanov Transformation by Goto

Goto [83] showed that any symmetrical linear array distribution can be written in an appropriate polynomial form to allow the use of the Baklanov transformation. This allows one to map the symmetrical linear array factor to a planar array factor. The linear array is what we call the prototype linear array.

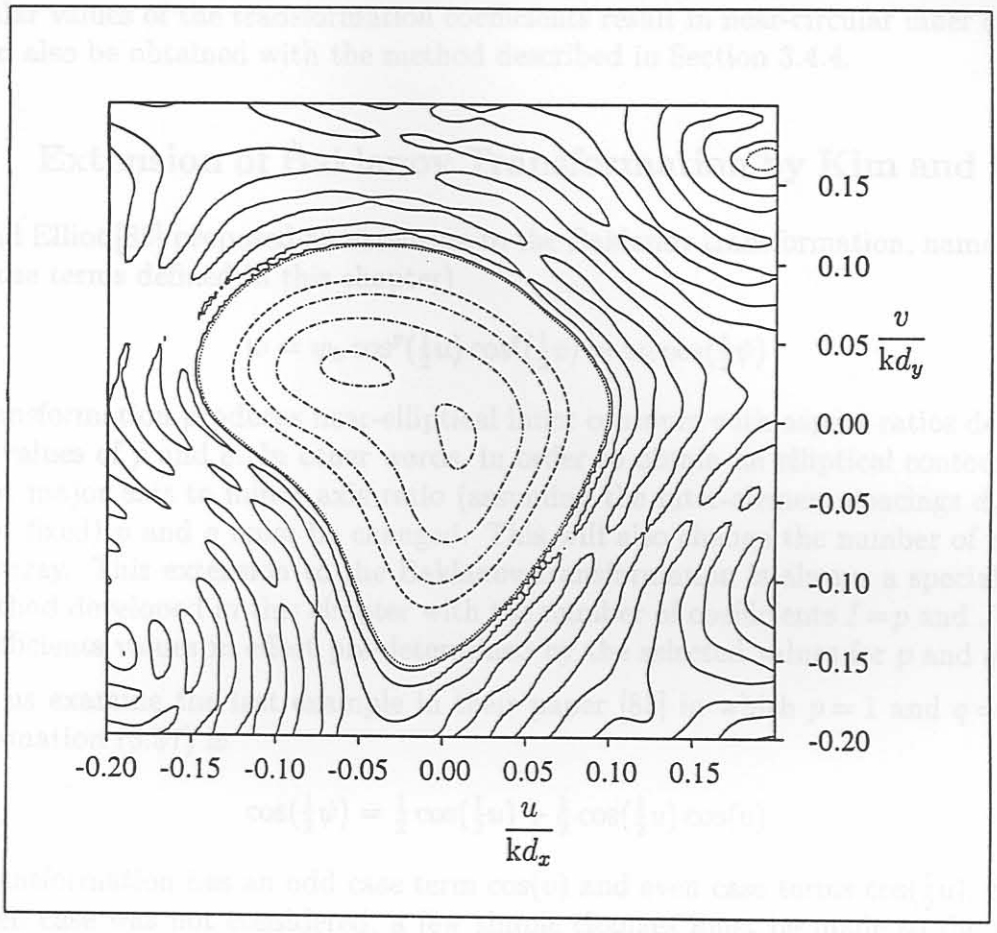

Figure 3.17: Representative Example: Contour plot of the planar array factor. The solid lines are at -33dB, the dotted lines at -27dB, the dashed line at -3dB (the strictly controled contour) and the broken lines (dash-dot) at -0.5dB

In the same paper he used the transformation (written in the terms defined in this chapter)

$$w = \cos(u)\cos(v) \tag{3.54}$$

to obtain a hexagonal lattice array. He later [84] proposed the transformation (again written in the terms defined in this chapter)

$$w = \alpha + \beta\cos(\psi) = \tfrac{1}{2}\cos(u)\left[\cos(u) + \cos(v)\right]. \tag{3.55}$$

where $\alpha = \frac{7}{16}$ and $\beta = \frac{9}{16}$ for a hexagonal array with $d_y = \sqrt{3}d_x$. After some manipulation (3.55) becomes

$$\cos(\psi) = \frac{1}{\beta}\left(\frac{1}{4} - \alpha\right) + \frac{1}{2\beta}\cos(u)\cos(v) + \frac{1}{4\beta}\cos(2u) \tag{3.56}$$

which is equal to the odd case transformation function of size $I=1, J=2$ and coefficients $t_{00} = -\frac{1}{3}, t_{11} = \frac{8}{9}, t_{20} = \frac{4}{9}1$ and $t_{10} = t_{01} = t_{02} = 0$. It is interesting to note that these

particular values of the transformation coefficients result in near-circular inner contours, and can also be obtained with the method described in Section 3.4.4.

3.7.3 Extension of Baklanov Transformation by Kim and Elliott

Kim and Elliot [85] proposed an extension to the Baklanov transformation, namely (written in the terms defined in this chapter)

$$w = w_0 \cos^p(\tfrac{1}{2}u)\cos^q(\tfrac{1}{2}v) = w_0 \cos(\tfrac{1}{2}\psi) \tag{3.57}$$

The transformation produces near-elliptical inner contours with aspect ratios dependent on the values of p and q. In other words, in order to obtain an elliptical contour with a different major axis to minor axis ratio (assuming the inter-element spacings d_x and d_y are kept fixed) p and q must be changed. This will also change the number of elements of the array. This extension to the Baklanov transformation is always a special case of the method developed in this chapter with the number of coefficients $I=p$ and $J=q$ and the coefficients values in effect pre-determined by the selected values for p and q.

Let us examine the last example in their paper [85] in which $p=1$ and $q=2$. The transformation (3.57) is

$$\cos(\tfrac{1}{2}\psi) = \tfrac{1}{2}\cos(\tfrac{1}{2}u) + \tfrac{1}{2}\cos(\tfrac{1}{2}u)\cos(v) \tag{3.58}$$

This transformation has an odd case term $\cos(v)$ and even case terms $\cos(\frac{1}{2}u)$. Since an odd/even case was not considered, a few simple changes must be made to the problem to convert it into an odd case problem. To convert the 10 element prototype linear array to an odd number of elements, a zero element is placed between all the original elements (resulting in a total of 19 elements), thus the inter-element spacing is halved but the radiation pattern stays the same. In addition the planar array inter-element spacings are halved as well. The converted transformation is

$$\cos(\psi') = \tfrac{1}{2}\cos(u') + \tfrac{1}{2}\cos(u')\cos(2v') \tag{3.59}$$

where the variables are primed to indicate the conversion. This is an odd case transformation function with $I'=1$ and $J'=2$. The transformation coefficients are $t'_{10}=\frac{1}{2}, t'_{12}=\frac{1}{2}$ and $t'_{00}=t'_{10}=t'_{11}=t'_{02}=0$. With this arrangement some of the planar array elements will be zero: $a'_{mn}=0$ for $m=$even and $n=$odd. In order to convert the planar array obtained by the synthesis procedure back, the non-zero elements must be mapped to the original array elements

$$a_{m\,n} = a'_{2m-1\,2n}. \tag{3.60}$$

Kim and Elliott remark on the fact that although the angular extent of the flat-top is less in the $\phi=90°$ cut (trace #2 in Figure 3.18) than in the $\phi=0°$ cut (trace #1

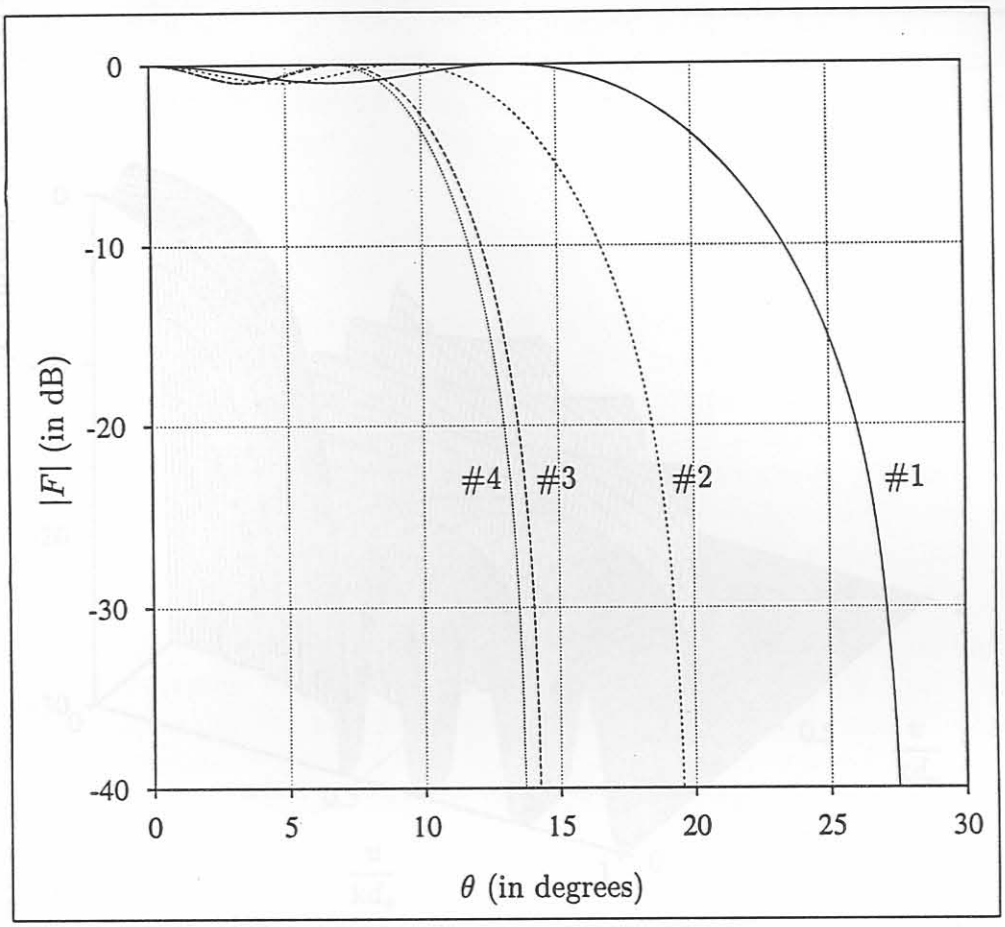

Figure 3.18: The principal cuts for the 10 by 19 element array:#1 ϕ=0° cut, #2 ϕ=90° cut of Kim and Elliot, #3 $\phi = 90°$ cut of optimal transformation function and #4 the pattern of a 19 element linear array.

in Figure 3.18), and the fall-off is steeper, the $\phi = 90°$ cut is not as narrow as it would be for a 19 element linear array with two roots off the Shelkunoff unit circle (trace #4 in Figure 3.18). The beamwidth in the $\phi = 90°$ cut is 42% wider than that of the 19 element linear array. With a better selection of transformation coefficients the beam in the $\phi = 90°$ cut can be much narrower. The optimum transformation coefficients are $t'_{10} = 0.1142$ and $t'_{12} = 0.8858$; this results in a much narrower beam in the $\phi = 90°$ cut (trace #3 in Figure 3.18). Compared to the 19 element linear array factor the optimum transformation coefficients result in an increased first-null beamwidth of only 3.6% in the ϕ=90° pattern cut. The planar array factor is displayed in Figure 3.19

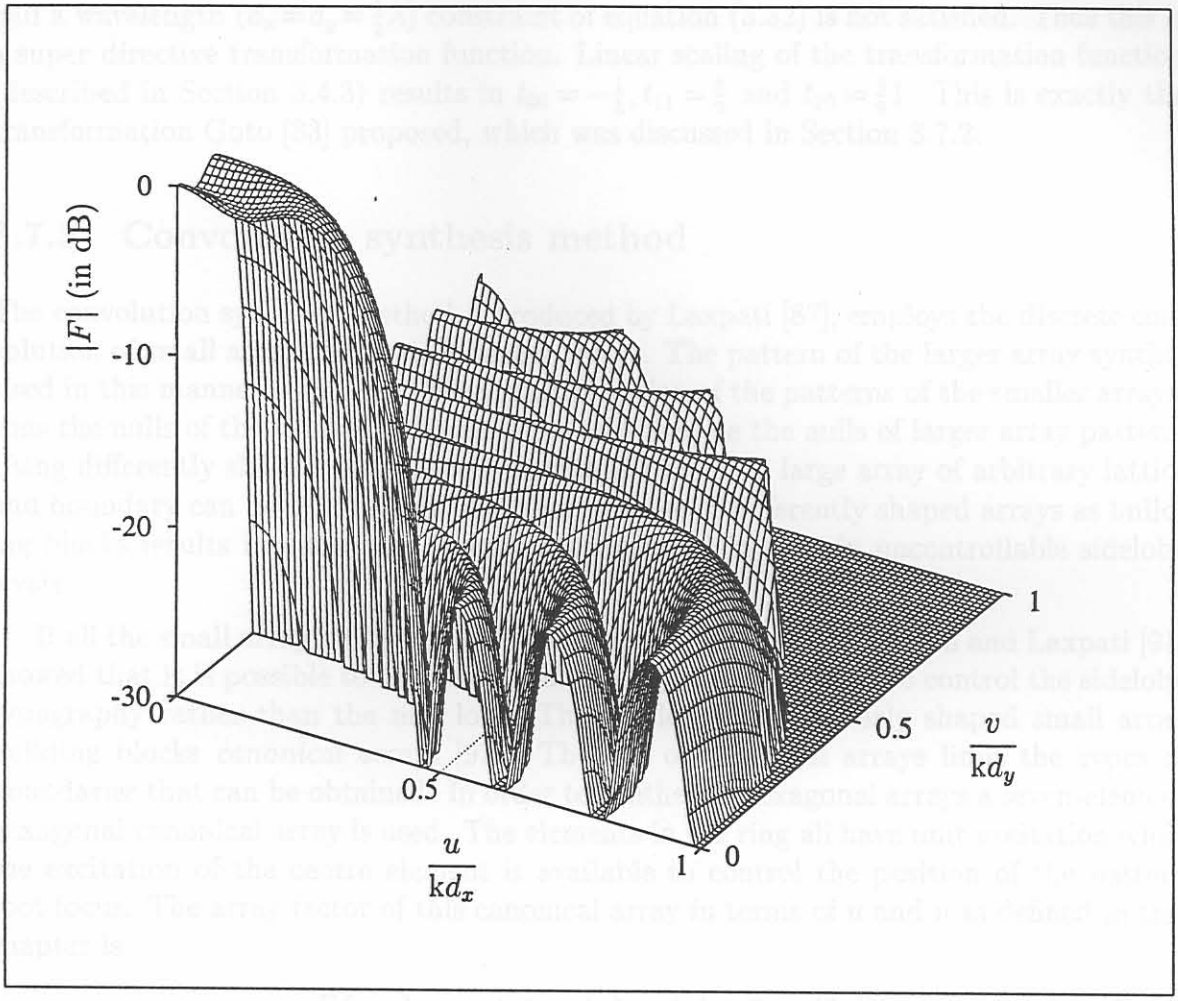

Figure 3.19: Surface plot of the 10 by 19 element planar array factor with optimum transformation coefficients (north-east quadrant only).

3.7.4 Extension of Baklanov Transformation by Kim

Kim [86] proposed an alternative transformation to Goto for the synthesis of hexagonal arrays (again using the the terms defined in this chapter):

$$w^2 = w_0^2 \cos(u) \cos\left(\tfrac{1}{2}u + \tfrac{1}{2}v\right) \cos\left(\tfrac{1}{2}u - \tfrac{1}{2}v\right) = w_0^2 cos^2(\tfrac{1}{2}\psi) \tag{3.61}$$

After some manipulation the transformation (3.61) can be written as

$$\cos(\psi) = -\tfrac{1}{2} + \cos(u)\cos(v) + \tfrac{1}{2}\cos(2u) \tag{3.62}$$

This is equal to the odd case transformation function with $I=2$ and $J=1$ and $-t_{00} = t_{20} = \frac{1}{2}$, $t_{11}=1$ and $t_{01}=t_{10}=t_{21}=0$.

In his paper Kim used $d_t = \frac{1}{2}\lambda$, thus $d_x = \frac{1}{4}\lambda$ and $d_y = \frac{\sqrt{3}}{4}\lambda$; for these values the constraint of equation (3.32) is satisfied. However, if the inter-element spacings are set to

half a wavelength ($d_x = d_y = \frac{1}{2}\lambda$) constraint of equation (3.32) is not satisfied. Thus this is a super directive transformation function. Linear scaling of the transformation function (described in Section 3.4.3) results in $t_{00} = -\frac{1}{3}, t_{11} = \frac{8}{9}$ and $t_{20} = \frac{4}{9}1$. This is exactly the transformation Goto [83] proposed, which was discussed in Section 3.7.2.

3.7.5 Convolution synthesis method

The convolution synthesis method, introduced by Laxpati [87], employs the discrete convolution of small arrays to produce larger arrays. The pattern of the larger array synthesised in this manner is obtained from multiplication of the patterns of the smaller arrays; thus the nulls of the smaller array patterns will then be the nulls of larger array pattern. Using differently shaped small arrays as building blocks a large array of arbitrary lattice and boundary can be synthesised. However, the use of differently shaped arrays as building blocks results in differently shaped root loci and in turn in uncontrollable sidelobe levels.

If all the small array building blocks have the same geometry Shelton and Laxpati [91] showed that it is possible to use the convolution synthesis method to control the sidelobe typography rather than the null loci. They called these similarly shaped small array building blocks *canonical arrays* [91]. The use of canonical arrays limit the types of boundaries that can be obtained. In order to synthesise hexagonal arrays a seven-element hexagonal canonical array is used. The elements in the ring all have unit excitation while the excitation of the centre element is available to control the position of the pattern root locus. The array factor of this canonical array in terms of u and v as defined in this chapter is

$$F_i(u,v) = a_i + 4\cos(u)\cos(v) + 2\cos(2u) \tag{3.63}$$

By using a linear mapping the authors were able to relate the value of a_i to the roots of a polynomial. In this case they selected a Chebyshev polynomial. In order to compare the transformation based method with the convolution based method the transformation function must be set equal to the canonical array factor. This transformation function will need scaling; linear scaling has the same purpose as linear mapping. Using equation (3.34) we obtain $C_1 = \frac{2}{9}$ and $C_2 = \frac{2a_i}{9} + \frac{1}{3}$; and the scaled transformation function is

$$H(u,v) = -\frac{1}{3} + \frac{8}{9}\cos(u)\cos(v) + \frac{4}{9}\cos(2u) \tag{3.64}$$

This is exactly the same transformation as that proposed by Goto [84], as mentioned in Section 3.7.2.

In order to synthesise square arrays a nine square canonical array is used. The corner elements have an excitation of α, the centre element a_i and the rest have unit excitation. Two degrees of freedom are available to control the position and shape of the pattern root locus. The array factor for a nine-element square canonical array is

$$F_i(u,v) = a_i + 4\alpha\cos(u)\cos(v) + 2\left(\cos(u) + \cos(v)\right) \tag{3.65}$$

The transformation function must be set equal to the canonical array factor. Linear scaling gives $C_1 = \frac{1}{2+4\alpha}$ and $C_2 = \frac{c_i+2}{2+4\alpha}$; and the scaled transformation function is

$$H(u,v) = -\frac{1}{1+2\alpha} + \frac{1}{1+2\alpha}\left(\cos(u)+\cos(v)\right) + \frac{2\alpha}{1+2\alpha}\cos(u)\cos(v) \tag{3.66}$$

The convolution synthesis method is again a special case of the transformation based synthesis method. For $\alpha_i = \frac{1}{2}$ the non-zero transformation function coefficients are $-t_{00} = t_{01} = t_1 = t_{11} = 1$. This is identical to the Baklanov transformation. Although α gives some control over the contour shape, the inner contours are always near circular. Shelton and Laxpati changed the value of α to optimise the dynamic range of the distribution. Although only symmetrical patterns were used it is possible to use canonical arrays with a complex excitation to obtain non-symmetrical patterns. In order to have control over the sidelobe level only the excitation of the centre element must be changed. This would be a special case of the transformation based synthesis technique for arbitrary contours. In fact the planar array formed by the transformation function (described in Section 3.4.6) is identical to the canonical array.

3.8 General Remarks and Conclusions

The transformation based synthesis technique has firstly been extended to the synthesis of planar arrays with arbitrary contoured footprint patterns, secondly to allow the synthesis of planar arrays with non-rectangular boundaries and thirdly to enable the synthesis of planar arrays with non rectangular boundaries.

The transformation based synthesis technique utilises a transformation that divides the problem into two decoupled sub-problems. One sub-problem (the contour transformation problem) involves the determination of certain coefficients in order to achieve the required footprint contours. The number of contour transformation coefficients which must be used depends on the complexity of the desired contour, but is very small in comparison to the number of planar array elements. The other sub-problem consists of a prototype linear array synthesis, for which powerful methods for determining appropriate element excitations, already exist. The size required for the prototype linear array depends on the amount of allowable ripple in the coverage area number and the detail of the beam shape through any cross-section. Simple recursive formulas then determine the final planar array excitations from the information forthcoming from the above two sub-problem solutions. The final planar array size is linked to the number of contour transformation coefficients and the prototype linear array size.

The synthesis technique can also be seen as a division of the synthesis problem into two separate problems; one pertaining to the shape of the footprint and the other involving the sidelobe level and main beam ripple. The separation of the synthesis procedure into two sub-problems not only is good from a computation point of view, but aids understanding by highlighting which considerations will finally determine the required array size (viz. contour complexity; allowed coverage ripple; final planar array directivity). The technique

in effect provides a structured procedure for spreading out the linear array excitations, thereby eliminating any guesswork that may otherwise be required.

The transformation coefficients can be seen as an inverse Fourier transformation of the desired contour shape. Thus as the complexity of the strictly controlled contour increases or its "beamwidth" decreases, more transformation function coefficients must be used to approximate the contour. If the number of transformation coefficients increase, the number of elements in the prototype linear array must decrease to keep the planar array size fixed. This in turn limits the performance (beamwidth, sidelobe ratio and main beam ripple) obtainable with the prototype linear array. Furthermore, the transformation function coefficients can be calculated such that the beamwidth is the narrowest possible in any particular pattern cut. The method works well when synthesising reconfigurable arrays where neither a change in inter-element spacing nor a change in the number of array elements is easily incorporated.

The biggest advantage of the transformation based synthesis technique is its computational efficiency. The final planar array excitations are very simply related to the prototype linear array excitation, which means that the technique can be used to rapidly synthesise even very large arrays. The computer time required to perform such a synthesis is relatively short, using very little system resources; making it feasible to conduct parametric studies of array performance and to perform design tradeoff studies even for very large arrays.

Numerical optimisation methods usually solve a set of equations (represented as a matrix in computer memory) subject to a set of constraints, where the number of equations is generally more than the number of unknowns. The memory requirements and the processing power needed for these optimisation methods increase rapidly as the number of array elements increase. In contrast, the memory requirement for the transformation based synthesis technique is small, approximately 12 times the total number of elements in real numbers and the total number of elements in complex numbers. In addition the processing time to synthesise large arrays with the transformation based synthesis technique is in the order of seconds, even on a modest personal computer.

However, the transformation based synthesis method does suffer some limitations. The foremost shortcoming is that the method can not be used to synthesise planar arrays with an arbitrary number of elements. For instance, consider the transformation for the odd case planar array. If a transformation of say $I = J = 2$ is required to obtain the desired contour shape then only planar arrays with $M = N = 2Q+1$ can be synthesised. This limitation is even worse for the even case planar arrays.

More detailed contour shapes can be achieved if all the planar array excitations are optimised by using a numerical optimisation synthesis technique. However, no phase information is known about the planar array factor; this has severe consequences on the optimisation procedures. These optimisation techniques are usually unstable and very dependent on good starting values. If the requirements on the planar array factor can not be met with the transformation based synthesis method, this method can be used to get a good set of starting values for optimisation techniques.

Chapter 4

The Synthesis of Planar Array Difference Distributions

4.1 Introduction

The Zolotarev polynomial distribution [42, 44] or its modification [45, 46] can be used for the synthesis of linear arrays with optimum difference pattern performance. The Cheng-Tseng method [81], though powerful in the synthesis of planar sum patterns, cannot be extended to planar difference patterns. While some spreading-out procedure can be used with linear array techniques for the synthesis of planar arrays [127], this spreading-out relies on a certain amount of experienced guesswork which, while relatively straightforward for sum pattern synthesis, is not at all simple for difference patterns. The synthesis method proposed here uses the transformation based technique discussed in the previous chapter as part of the method. The sum pattern forthcoming from the transformation based synthesis is multiplied by a difference pattern to add the appropriate null loci to the sum pattern; thus the proposed synthesis method relies on the convolution synthesis method as one of its steps. The convolution synthesis method is discussed in Section 2.7.3.

The planar array difference pattern is an odd function about the difference axis. The zero at the difference null can be factored out (let us call this the *factored difference pattern*) from the planar array difference pattern to leave a *factored sum pattern* (an even function). Thus the planar array difference pattern can be written as the product of the factored difference pattern f_d and the factored sum pattern f_s, while the excitation of the final planar array will be the convolution of the factored difference array excitation and the factored sum excitation. The array giving the factored sum pattern we will call the *interim sum array*, while that giving the factored difference pattern will be called the *interim difference array*.

The essential idea of the synthesis method is as follows: a set of excitations for the interim sum planar array is obtained using the transformation based synthesis method.

This is then convolved with the excitations of the interim difference array, to give the final planar array difference excitations.

4.2 The Synthesis Procedure Step by Step

For a specified planar array geometry, the procedure involves a number of steps:

1. Determine the best geometry for the interim difference array. There is no clearcut way to choose the geometry of the interim difference array, but it must be kept as small as possible while ensuring that the geometry of the interim sum array is such that it can be synthesised with the transformation based synthesis technique. It will typically be in the shape of the array unit cell. Once the geometry of the interim difference array is set, the interim sum array geometry is obtained by a de-convolution of the planar array and interim difference array geometries.

2. Determine the geometry of the interim sum array by de-convolving the interim difference array from the final planar array.

3. Decide on the number of transformation coefficients to use, and determine which of these must be set to zero to obtain the correct array lattice and boundary.

4. Synthesise the difference distribution of the archetypal linear array. The number of elements depends on the number of elements needed for the prototype linear array and the size of the interim difference array. The prototype linear array size in turn depends on the number of transformation coefficients and the size of the interim sum array.

5. Factor out the zero(s) corresponding to the zero(s) of the factored difference pattern from the archetypal linear array factor to give the prototype linear array factor and excitation.

6. Calculate the transformation coefficients. The design requirements can be minimum beamwidth in all cuts, maximum directivity or maximum bore sight slope.

7. Compute the interim sum array using the transformation based synthesis method. The prototype linear array and the transformation coefficients are obtained in the previous steps.

8. The interim difference array excitations are selected in such a way that the zeros are in the correct positions. It is easy to calculate these positions from the transformation function and the known location of the zero removed from the archetypal linear array.

9. The final planar array excitations are obtained by a convolution of the interim sum array and the interim difference array. On the pattern plane this is equivalent to multiplying the interim sum array factor and the interim difference array factor.

The method uses a linear array synthesis technique appropriate for difference patterns as one of its steps to enable the synthesis of planar arrays with difference patterns in a selected principal plane pattern cut. The sidelobes are all equal to or below those of the archetypal linear array, but not unnecessarily low, since this would cause an unwanted increase in the width of the difference pattern principal lobes. The technique in effect provides a structured procedure for spreading-out the collapsed distributions, thereby eliminating any guesswork that may be required. The method, including the choice of the interim difference array, is best demonstrated by a few examples.

4.3 Examples of Planar Array Difference Distributions

Two examples will be presented. First we will look at the synthesis of a rectangular (both lattice and boundary) array with an even number of elements in both principal planes. The second example is of a hexagonal array with 5 rings. Each step in the design procedure will be discussed.

Illustrative Example #1

We choose a rectangular grid planar array with 20 by 20 elements (that is $M=N=10$). Assume half wavelength inter-element spacing. The synthesis procedure is then step by step:

1. The interim difference array is kept as simple as possible, a four element array.
2. The interim sum array is a 19 by 19 element rectangular array.
3. The interim sum array excitations are obtained using the odd case of transformation based synthesis method with $I=J=1$, with no coefficient set to zero.
4. The archetypal linear array, consisting of 20 elements, is synthesised using the Zolotarev polynomial method with the maximum sidelobe ratio set at 20dB.
5. Since the interim difference array consists of only four elements, its collapsed distribution along the $\phi=0°$ cut will have only one zero, at $\psi=0$. With this zero removed from the archetypal linear array zeros, the prototype linear array excitations are computed. The number of elements in the prototype linear array are 19.
6. The transformation coefficients are selected for near-circular contours: $t_{00}=-\frac{1}{2}$ and $t_{01}=t_{10}=t_{11}=\frac{1}{2}$.
7. Compute the interim sum array distribution.

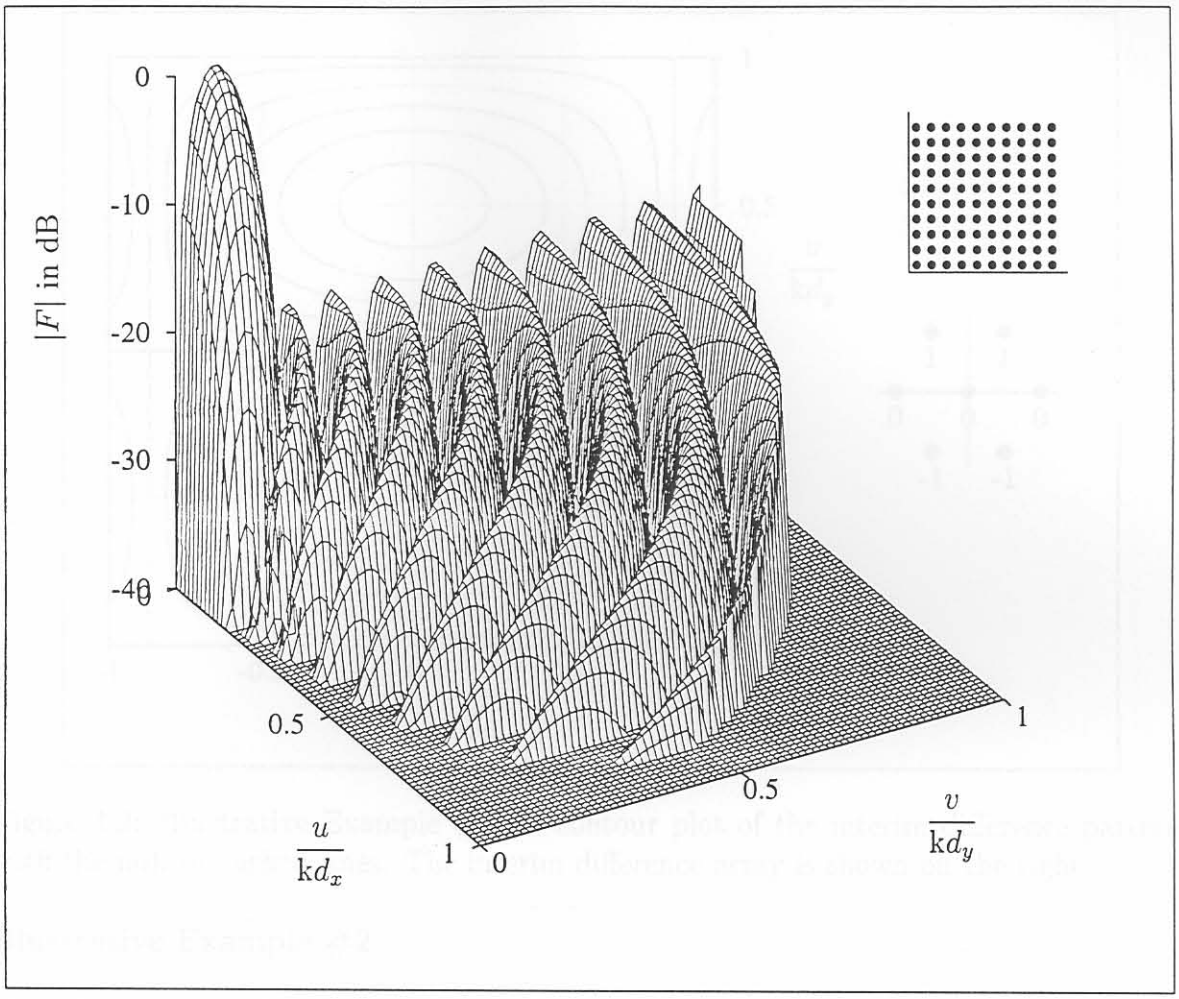

Figure 4.1: Illustrative Example #1: Surface plot of the planar array factor of the difference distribution.

8. The interim difference planar array is a four element array. Its excitations are required to be antisymmetric (180° out of phase) about the $\phi=0°$ principal plane, and in-phase about the $\phi=90°$ principal plane. The result is a factored difference pattern $f_d=\cos(\frac{1}{2}u)\sin(\frac{1}{2}v)$.

9. The final difference distribution is then computed by the convolution of the interim sum and interim difference array excitations.

The difference pattern is displayed in Figure 4.1. The sidelobe and all other pattern behaviour in the principal difference plane of the planar array are the same as that designed for the archetypal linear array. Furthermore, if the excitations of the archetypal linear array are real, then so are those of the final planar array.

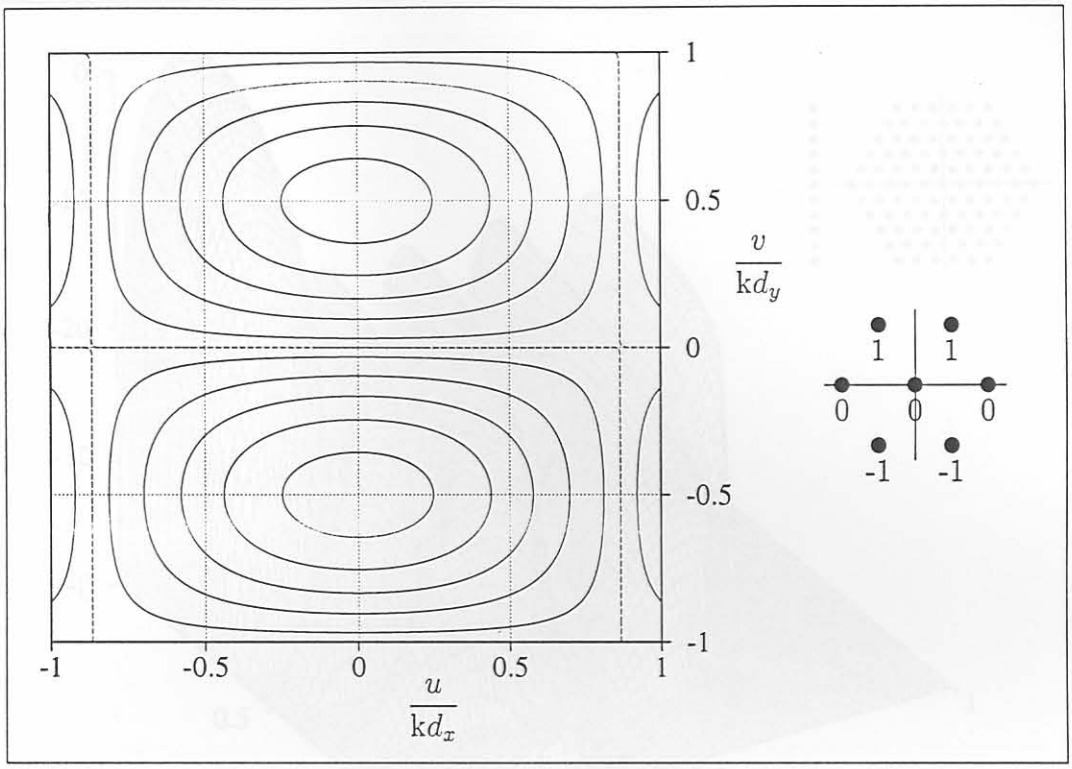

Figure 4.2: Illustrative Example #2: A contour plot of the interim difference pattern, with the null in dashed lines. The interim difference array is shown on the right.

Illustrative Example #2

Consider an example of a hexagonal planar array with five rings. Difference patterns about both principal planes are required. Assume the inter-element spacing (the distance between an element and its six closest neighbours) is $d = 0.577\lambda$. As the collapsed distributions along the principal planes differ, the synthesis procedure must be repeated for the two different cases. Let us look at the two cases separately, first with the difference null along $\phi = 0°$, and then with the difference null along $\phi = 90°$. The synthesis procedure will again be followed step by step.

1. The interim difference array for both cases is the smallest unit cell of a hexagonal array, a seven element (or one ring) hexagonal array.

2. From the first step, it is clear that the interim sum array will be a four ring hexagonal array.

3. The transformation coefficients are chosen to represent the unit cell of the interim sum array, as mentioned in Section 3.4.6), thus $I = 2$ and $J = 1$, with $t_{01} = t_{10} = t_{21} = 0$.

4. As the interim sum array consists of 4 hexagonal rings, the collapsed distribution along the x-axis will have 17 elements. Since $I = 2$, the prototype linear array will

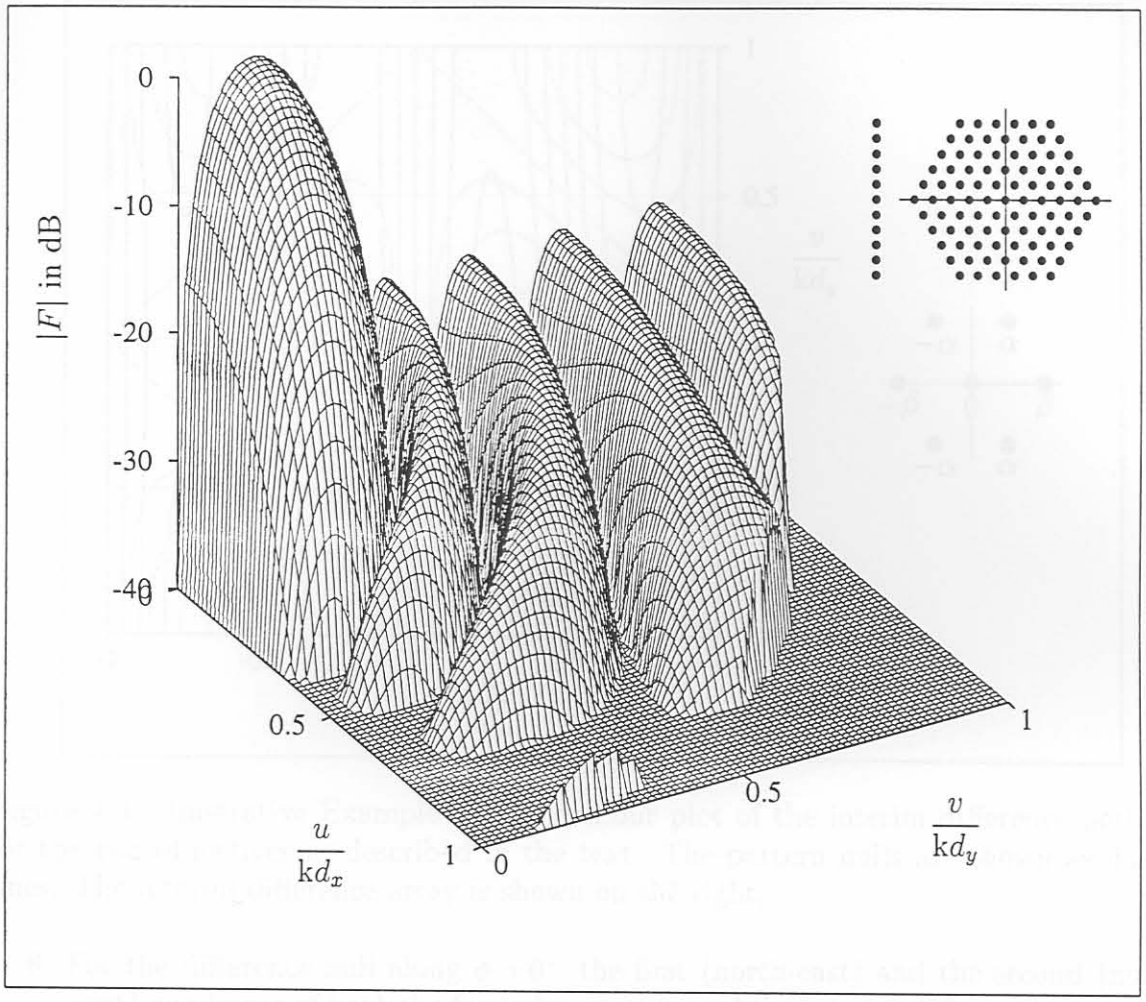

Figure 4.3: Illustrative Example #2: Surface plot of the planar array factor, with the array geometry (and the collapsed distribution) drawn on the right.

have 9 elements, or $Q=4$. Thus for this case the archetypal linear array is an 11 element array, with an inter-element spacing of a half wavelength (to avoid super directivity). The synthesis problem is solved using the Zolotarev method.

5. Since we know the interim difference array geometry, we can determine which zeros must be removed from the archetypal linear array factor, namely the zeros at $\psi=0°$ and $\psi=90°$. The remaining 8 zeros are used to compute the prototype linear array excitations.

6. The transformation function coefficients are chosen in order to obtain the minimum beamwidth in all cuts ($t_{00}=-\frac{1}{4}$, $t_{11}=1$, and $t_{20}=\frac{1}{4}$, as discussed in Section 3.5.2). This will also result in the maximum (non-super-directive) bore-sight slope for this particular geometry and case.

7. With the information obtained in steps 5 and 6, compute the interim sum array excitation.

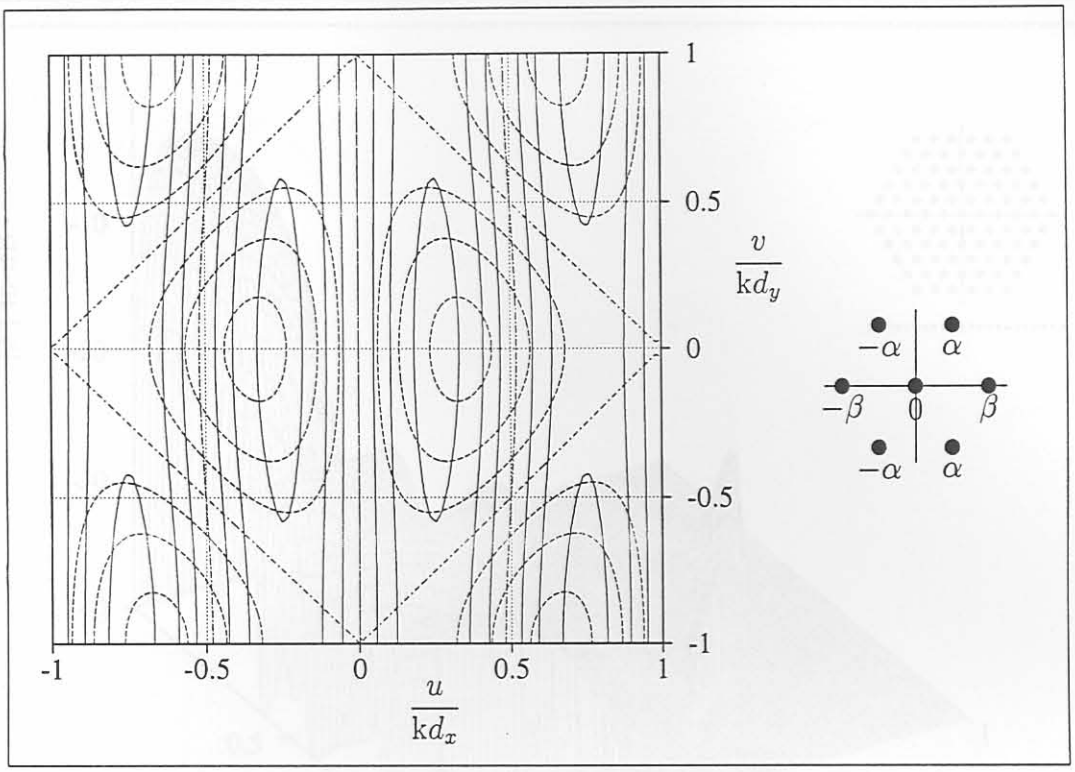

Figure 4.4: Illustrative Example #2: A contour plot of the interim difference patterns for the two objectives as described in the text. The pattern nulls are shown as dotted lines. The interim difference array is shown on the right.

8. For the difference null along $\phi = 0°$ the first (north-east) and the second (north-west) quadrants of both the final planar array and the interim difference array must be excited 180° out of phase with the third (south-west) and fourth (south-east) quadrants. All the elements at $y = 0$ must be switched off. Thus unit excitation, for the 4 non-zero elements, is the only solution for the interim difference array excitations. The factored difference pattern, drawn in Figure 4.2, is $f_d = \cos(u)\sin(v)$. The interim difference array is depicted on the right hand side of Figure 4.2.

9. The final planar array excitation is calculated from the interim sum array and the interim difference array excitations, using a two dimensional discrete convolution.

Figure 4.3 depicts the final planar array factor. The maximum sidelobe level is -20dB and the difference null is along the $\phi = 0°$ cut. In total only 80 non-zero elements are needed. The array geometry is drawn in the upper right hand corner of the figure.

Next we consider the case with the difference null along $\phi = 90°$. The first three steps are exactly the same as for the previous case, and will not be repeated. Starting from Step 4:

4. The collapsed distribution of the interim sum array in the $\phi = 90°$ plane is a 9 element linear array. The prototype linear array will have 9 elements, since $J = 1$.

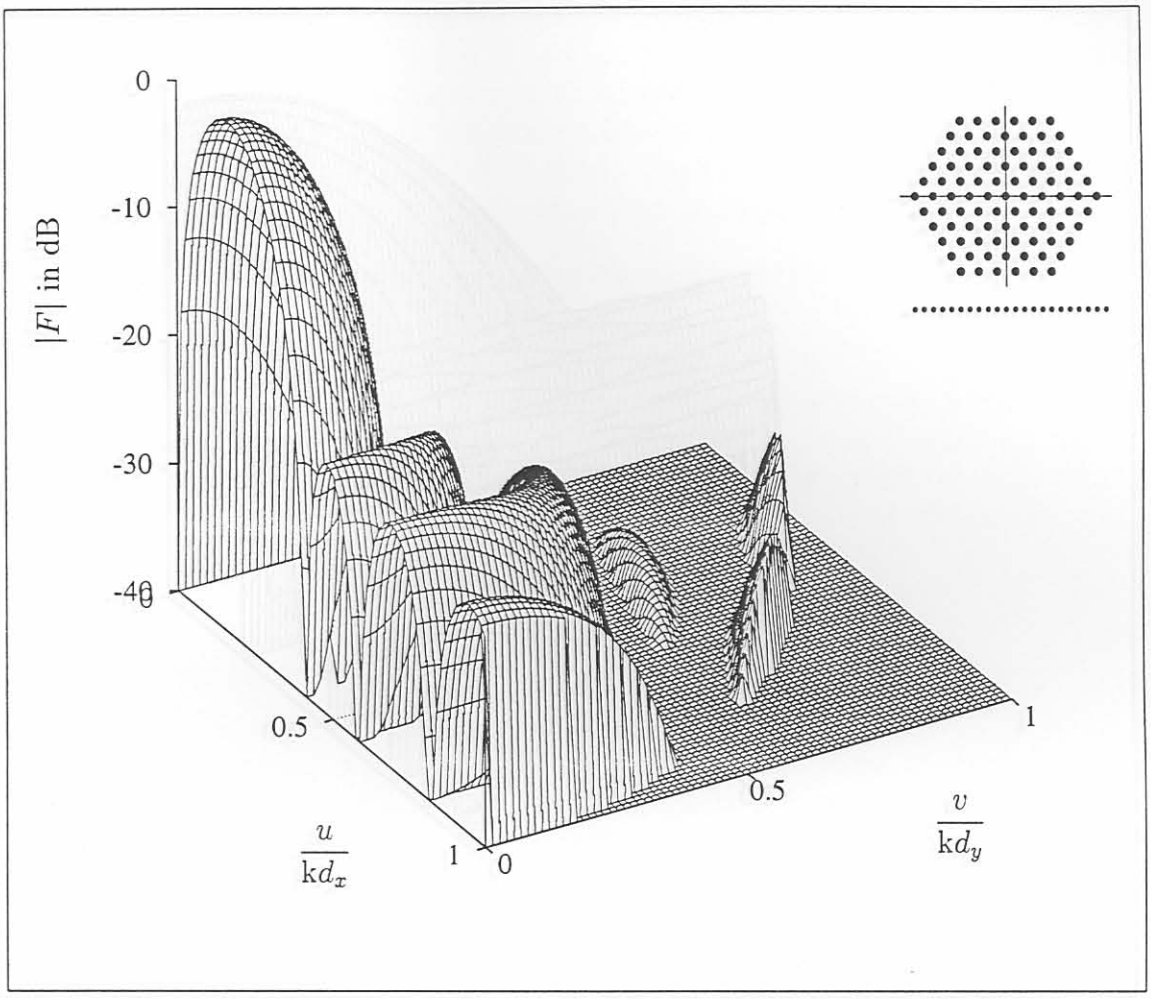

Figure 4.5: Illustrative Example #2: Surface plot of the planar array factor, with minimum beamwidths in all cuts as the design objective. The array geometry (and the collapsed distribution) is drawn on the right.

The interim difference removes two nulls from the planar pattern in the $=90°$ plane, thus the archetypal linear array must have 11 elements (with half wavelength inter-element spacing as before). The archetypal linear array and the interim arrays do not differ for this example, but in general this may not be the case.

5. The zeros at $\psi=0°$ and $\psi=90°$ are factored from the archetypal linear array factor, and the remainder are used to calculate the prototype linear array excitations.

6. As in the previous case, the transformation function coefficients are chosen to minimise the beamwidth in all cuts. However, this is not the only sensible objective, maximisation of the bore-sight slope will result in a different set of transformation coefficients for this geometry and case ($t_{00} = -0.1051$, $t_{11} = 0.2168$ and $t_{20} = 0.8883$). A number of possibilities exist between these two extreme objectives, requiring engineering judgement to obtain the best solution for the application at

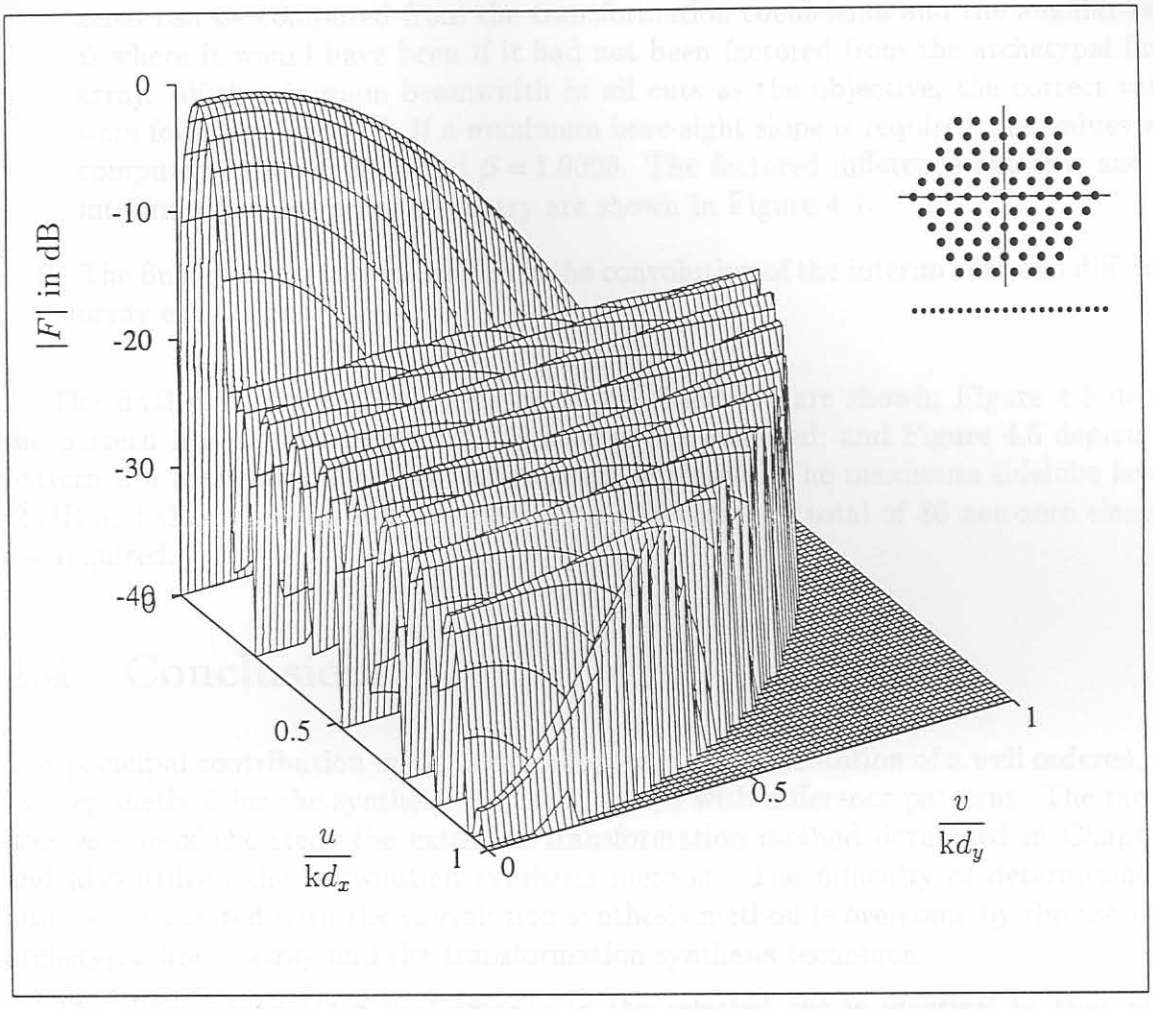

Figure 4.6: Illustrative Example #2: Surface plot of the planar array factor, designed for maximum bore-sight slope; with the array geometry (and the collapsed distribution) drawn on the right.

hand. To illustrate, the results of both these objectives will be shown.

7. The transformation based technique is used to compute the interim sum array excitation.

8. The first and fourth quadrants and the second and third quadrants of the final planar array and the interim difference array must be excited 180° out of phase to produce a difference null along $\phi = 90°$. All the elements at $y = 0$ must be switched off. This leaves 6 non-zero excitations to control the factored difference pattern

$$f_d = \alpha \sin(u)\cos(v) + \beta \sin(2u)$$

The values of α and δ must be chosen in such a manner that the zeros factored out of the archetypal linear array will be placed at the correct positions to ensure that the sidelobes will not be higher than the specification. The position of these

zeros can be computed from the transformation coefficients and the angular value ψ where it would have been if it had not been factored from the archetypal linear array. With minimum beamwidth in all cuts as the objective, the correct values were found to be $\alpha = \beta$. If a maximum bore-sight slope is required, the values were computed as $\alpha = 0.0610$ and $\beta = 1.0000$. The factored difference patterns and the interim difference array geometry are shown in Figure 4.4.

9. The final planar array excitation is the convolution of the interim sum and difference array excitations.

The final planar array factor for both the objectives are shown; Figure 4.5 depicts the pattern if minimum beamwidth in all cuts are required; and Figure 4.6 depicts the pattern if a maximum bore-sight slope is the objective. The maximum sidelobe level is -20dB and the difference null is along the $\phi = 90°$ cut. A total of 86 non-zero elements are required.

4.4 Conclusions

The principal contribution made in this chapter is the presentation of a well ordered, step by step method for the synthesis of planar arrays with difference patterns. The method uses as one of the steps the extended transformation method developed in Chapter 3, and also utilises the convolution synthesis method. The difficulty of determining the null loci associated with the convolution synthesis method is overcome by the use of the archetypal linear array and the transformation synthesis technique.

The difference pattern performance in the selected cut is identical to that of the archetypal linear array used, and will thus be optimum if the latter is optimum. In the other pattern cuts the sidelobes are below those of the archetypal linear array, but not unnecessarily low. The technique in effect provides a structured procedure for spreading out the linear array excitations, thereby eliminating any guesswork that may otherwise be required. Due to the simplicity of the method the synthesis of even very large arrays is rapid, making it feasible to conduct parametric studies of array performance and to perform design trade-off studies.

Preliminary work has been published by the author [128]

Chapter 5

Conformal Array Synthesis as the Intersection of Sets

5.1 Introductory Remarks

Conformal antenna arrays offer a number of advantages [129]. On high speed aircraft flush mounted radiators eliminate the need for radomes, and thus also the problems associated with radomes, such as radome heating, ablation, bore sight errors and side lobe degradation. Printed circuit microwave antennas are also both light weight and robust. The other advantage is improved scanning (360° if the array elements are arranged on a circular surface compared to a planar array which is limited to about 140°). However, practical implementation problems of conformal arrays are significant and include difficulty in finding optimum element positions and polarisation matching.

Conformal array synthesis is very difficult for two reasons. Firstly the array elements do not all point in the same direction, and may not have the same polarisation. Secondly, the body on which the antenna is mounted may have a marked influence on the element patterns. The element patterns may differ substantially even for identical elements placed at different locations on the host. This means that the element pattern for each element must be computed separately, and must be accounted for in the synthesis stage of the antenna development.

Very few conformal array synthesis methods exist and most of these methods involve general optimisation which do not take advantage of the peculiar array radiation pattern properties. In the linear and planar arrays synthesis problem the array elements are assumed to be identical in all respects (directivity, polarisation and orientation), and thus the element pattern could be factored from the radiation pattern. This simplification does not carry over to conformal arrays due to the nature of the conformal array, consequently the synthesis techniques for linear and planar arrays are not transferable to conformal arrays.

The array synthesis problem can be stated as the search for an array factor that

minimises the error between the desired and the synthesised patterns. We can define a set as all the excitations that produce a radiation pattern of the desired magnitude in a specified direction. If we have a number of these sets, each at different directions in the far-field, then the intersection of all these sets, if it exists, is the solution of the synthesis problem. The chapter starts with a discussion on the evolution of the array synthesis problem as a problem of searching for the intersection of sets.

The synthesis problem can also be seen as the intersection of only two sets, the one set is all the possible radiation patterns for the given array geometry (including constraints to enable practical realization of the array), and another set as all the radiation patterns that comply with the desired radiation pattern characteristics. The synthesis problem is then finding the intersection of these two sets. Alternatively one can view the synthesis problem as the intersection of the set of all the excitations within the excitation constraints and the set of all excitations with the required radiation pattern characteristics. The intersection between the sets is found by iteratively projecting between the sets. This approach, using only two sets in the excitation or radiation pattern space to synthesise arrays with an arbitrary geometry, is explored in Section 5.3. The formulation including not only constraints on the radiation pattern but also on the excitations. Relaxation is presented to increase the rate of convergence.

Section 5.4 deals with the details of the numerical implementation of the pattern and excitation constraints. The representation of the element patterns in the software is addressed.

Any non linear numerical method may converge to a local minimum. This is an often overlooked problem. In Section 5.5 some options to select a starting pattern will be discussed. A novel method to compute a starting point as close to the global minimum as possible will then be presented in Section 5.5.3. The proposed method uses genetic algorithm to optimise the phase distribution of the field pattern.

A number of case studies are conducted in Section 5.6 to gauge the performance of various options, such as the selection of backward projector, the selection of pattern angles and the particular choice of the initial values. The importance of accurate element patterns will also be shown.

A detailed comparison with other recently published synthesis methods is discussed in Section 5.7.

The proposed method is illustrated in Section 5.8 by means of a number of examples of the various array types and radiation pattern requirements. The examples are chosen to give insight into the application of the method.

Finally, some observations are made and general conclusions are drawn in Section 5.9.

The notation and nomenclature of Chapter 2 will be used, with only the most important equations repeated for clarity.

5.2 Evolution of the Array Synthesis as the Intersection of Sets

5.2.1 Alternating Orthogonal Projections

A recursive algorithm for the restoration of images from diffraction plane data was first proposed by Gerchberg and Saxton [130]. Youla showed that the technique was equivalent to what he called *alternating orthogonal projections* [131]. The application of the method of alternating orthogonal projections to array synthesis was first proposed by Prasad [106], and subsequently extended by Ng [132, 133]. They both considered an array of isotropic elements with an arbitrary geometry. The method can be used for field synthesis only, and both authors applied only null constraints.

Consider a complex Euclidean space $\mathcal{H}$ with elements $\vec{A}$, $\vec{x}$ and $\vec{y}$. The inner-product is denoted by $(\vec{x}, \vec{y})$ and the length (or norm) of $\vec{x}$ is defined as

$$\|\vec{x}\| = \sqrt{(\vec{x}, \vec{x})} = \vec{x}\vec{x}^H \geq 0 \tag{5.1}$$

where the $[\,]^H$ denotes the adjoint or complex conjugate transpose.

Let $\mathcal{R}$ be any linear subspace in $\mathcal{H}$, and $\mathcal{R}^\perp$ its orthogonal complement, thus $\mathcal{H} = \mathcal{R} \oplus \mathcal{R}^\perp$. Any element $\vec{A}$ possesses a unique decomposition

$$\vec{A} = \vec{x} + \vec{y} \tag{5.2}$$

with $\vec{x} \in \mathcal{R}$ and $\vec{y} \in \mathcal{R}^\perp$. Since $\vec{x}$ and $\vec{y}$ are elements in orthogonal spaces, they are orthogonal, thus $(\vec{x}, \vec{y}) = 0$. The two linear operators $\mathbf{P}$ and $\mathbf{Q}$, defined by $\vec{x} = \mathbf{P}\vec{A}$ and $y = \mathbf{Q}\vec{A}$, are the associated orthogonal projection operators projecting $\vec{A}$ onto $\mathcal{R}$ and $\mathcal{R}^\perp$ respectively. The properties $\mathbf{P}^2 = \mathbf{P}$, $\mathbf{Q}^2 = \mathbf{Q} = \tilde{I} - \mathbf{P}$, $\mathbf{P} = \mathbf{P}^H$ and $\mathbf{Q} = \mathbf{Q}^H$ are well known (where $\tilde{I}$ is the identity matrix).

The problem we are faced with is: if $\vec{A} \in \mathcal{H}$ belongs to a known subspace $\mathcal{R}_2$, with only its orthogonal projection $\vec{x} = \mathbf{P}_1\vec{A}$ onto the known subspace $\mathcal{R}_1$ given, can $\vec{A}$ be reconstructed from $\vec{x}$ and the projection operators?

Let $\mathbf{P}_1$, $\mathbf{Q}_1$, $\mathbf{P}_2$ and $\mathbf{Q}_2$ denote the projection operators projecting $\vec{A}$ onto $\mathcal{R}_1$ $\mathcal{R}_1^\perp$, $\mathcal{R}_2$ $\mathcal{R}_2^\perp$, respectively. Since $\vec{A} \in \mathcal{R}_2$, $\vec{A} = \mathbf{P}_2\vec{A}$ and

$$\vec{x} = \mathbf{P}_1\vec{A} = (\tilde{I} - \mathbf{Q}_1)\vec{A} = (\tilde{I} - \mathbf{Q}_1\mathbf{P}_2)\vec{A}. \tag{5.3}$$

The vector $\vec{A}$ is uniquely determined by $\vec{x}$ if, and only if, the inverse operator $\tilde{C} = (\tilde{I} - \mathbf{Q}_1\mathbf{P}_2)^{-1}$ exists. Youla [134] showed that if either

$$\mathcal{R}_2 \cap \mathcal{R}_1^\perp = \{0\}$$

or

$$\angle(\mathcal{R}_2, \mathcal{R}_1^\perp) > 0$$

where $\cap$ is the set intersection, $\{0\}$ is the zero vector and $\angle(\mathcal{R}_2, \mathcal{R}_1^{\perp})$ is the angle between the linear subspaces $\mathcal{R}_2$ and $\mathcal{R}_1^{\perp}$; then the sequence $\{\vec{A}_k\}$ generated by

$$\vec{A}_{k+1} = \vec{x} + \mathbf{Q}_1\mathbf{P}_2\vec{A}_k \quad \text{for } k = 1 \to \infty, \quad \vec{A}_1 = \vec{x} \tag{5.4}$$

converges to $\vec{A}$ in norm and is strictly monotone. The recursive formula (5.4) is called the method of alternating orthogonal projections. The name is derived from the geometrical interpretation of the iterative process of projecting between orthogonal subspaces [106].

In the array synthesis context (and notation used in this thesis), $\vec{A}$ is the excitation vector and $\vec{B}_m$ is the space vector (the mth row of the radiation matrix $\tilde{B}$ (2.6)). Let $\vec{B}_d$ be the space vector in the desired main beam direction and $\vec{B}_1, \vec{B}_2, \ldots, \vec{B}_M$ the space vector in the directions where the radiation pattern is required to exhibit nulls. The synthesis problem in this is then: can the excitation vector $\vec{A}$ be reconstructed such that

$$\vec{B}_d\vec{A} = 1 \quad \text{and} \quad \vec{B}_m\vec{A} = 0 \quad \text{for } m = 1, 2, \ldots, M. \tag{5.5}$$

Prasad [106] conjectured an iterative algorithm for the sequence $\{\vec{A}_k\}$,

$$\vec{A}_{k+1} = \vec{B}_d + \mathbf{Q}_1(\mathbf{P}_1\mathbf{P}_2 \ldots \mathbf{P}_M)\vec{A}_k \quad \text{for } k = 1 \to \infty \tag{5.6}$$

with $\vec{A}_1 = \vec{B}_d$ and the operators (in array pattern synthesis terms)

$$\mathbf{Q}_1 = \tilde{I} - \vec{B}_d^H(\vec{B}_d\vec{B}_d^H)^{-1}\vec{B}_d \tag{5.7}$$

and

$$\mathbf{P}_m = \tilde{I} - \vec{B}_m^H(\vec{B}_m\vec{B}_m^H)^{-1}\vec{B}_m \tag{5.8}$$

Ng [132] developed a similar but simpler algorithm,

$$\vec{A}_{k+1} = \vec{B}_d + \mathbf{Q}_1\mathbf{P}_2\vec{A}_k \quad \text{for } k = 1 \to \infty \tag{5.9}$$

with $\vec{A}_1 = \vec{B}_d$. The operators $\mathbf{Q}_1$ and $\mathbf{P}_2$ are

$$\mathbf{Q}_1 = \tilde{I} - \vec{B}_d^H(\vec{B}_d\vec{B}_d^H)^{-1}\vec{B}_d \tag{5.10}$$

(the same as by Prasad) and

$$\mathbf{P}_2 = \tilde{I} - \tilde{B}^H(\tilde{B}\tilde{B}^H)^{-1}\tilde{B} \tag{5.11}$$

where $\tilde{B}$ is the radiation matrix in all the directions where nulls are desired. Ng also derived a lower boundary on the rate of convergence [133],

$$\|\xi_{k+1}\| \leq \cos^k\left[\angle(\mathcal{R}_2, \mathcal{R}_1^{\perp})\right] \|\vec{A} - \vec{B}_d\|. \tag{5.12}$$

Generally the iteration will be terminated when the error ξ_k is within design specification ξ

$$\|\vec{A} - \vec{A}_k\| = \xi_k \leq \xi \tag{5.13}$$

The method of orthogonal projections was applied, by Prasad [106] and Ng [133], to phased arrays of arbitrary array geometries, with interfering sources at fixed positions in the far field (in the null directions). They both considered only isotropic elements. The excitation vector ($\vec{A}$ in the notation above) is constructed in an appropriate "excitation subspace". The recursive algorithm starts from the known projection $\vec{B}_d$ of the excitations in a linear subspace in the main beam peak direction. The number of interference sources, or directions in which the radiation pattern level may be constrainted, must be less than the total number of elements of the array. Stated differently, the number of sets (or rows of the radiation matrix) M is restricted to a maximum of the number of array elements N ($M \leq N$). Since the sets are convex convergence to the global minimum is guaranteed.

The most severe restriction of the method is that the operators must be linear, thus the method can not be used for a general pattern synthesis as the operators associated with power synthesis are not linear. In addition, no constraints on the excitations can be implemented.

5.2.2 Successive Projections

Limitations on the type of constraints that could be imposed with alternating orthogonal projections led to improvements resulting in the method of successive projections. The method was used in field synthesis of linear arrays [135] as well as in the design of two-dimensional digital FIR filters [136]. It has also been applied to power pattern synthesis by Poulton [107, 108].

The method of successive projection is to find an intersection of a system of sets. Suppose we have a system of M sets, $\mathcal{C}_m$, $m=1,2,\ldots,M$, in a real or complex Euclidean space. Associated with each set $\mathcal{C}_m$ is a projection operator $\mathbf{P}_m$. In general, for all closed sets (convex and non-convex) we call $\vec{x} \triangleq \mathbf{P}\vec{y}$ the projection of $\vec{y}$ ($\vec{y} \notin \mathcal{C}_m$) onto $\mathcal{C}_m$ if $\vec{x} \in \mathcal{C}_m$ and if

$$\|\vec{x} - \vec{y}\| = \inf_{\vec{v} \in \mathcal{C}_1} \|\vec{y} - \vec{v}\|. \tag{5.14}$$

The projections are thus defined as

$$\mathbf{P}_m(\vec{x}, \mathcal{C}_m) = \|\vec{x} - \vec{y}\| = \inf_{\vec{v} \in \mathcal{C}_m} \|\vec{x} - \vec{v}\|. \tag{5.15}$$

In other words, the projector onto the subset $\mathcal{C} \in \mathcal{H}$ is the operator mapping a point $\vec{y} \in \mathcal{H}$ into the point $\vec{x} \in \mathcal{C} \in \mathcal{H}$, which is the nearest point of $\mathcal{C}$ to $\vec{y}$. The point $\vec{x}$ is called the projection of $\vec{y}$ onto $\mathcal{C}$. We can make the following remarks:

- a projection always exists for a closed set and

- the projection as defined in (5.15) is a unique point if $\mathcal{C}_m$ is a convex set.

The problem is then to find a common point of the system of sets $\vec{A} = \mathcal{C}_1 \in \mathcal{C}_2 \in \ldots \in \mathcal{C}_M$. The method of successive projection consist in constructing a sequence $\vec{A}_0, \vec{A}_1, \ldots, \vec{A}_k$ where $\vec{A}_0$ is arbitrary. The reconstruction algorithm is

$$\vec{A}_{k+1} = \mathbf{P}_1 \mathbf{P}_2 \ldots \mathbf{P}_M \vec{A}_k \tag{5.16}$$

or the relaxed version

$$\vec{A}_{k+1} = \mathbf{T}_1 \mathbf{T}_2 \ldots \mathbf{T}_M \vec{A}_k \tag{5.17}$$

where

$$\mathbf{T}_m = \tilde{I} + \lambda_m (\mathbf{P}_m - \tilde{I}) \quad m = 1, 2, \ldots, M \tag{5.18}$$

and $\tilde{I}$ is the identity operator and λ_m is the relaxation parameter. Provided that the following two conditions hold [134]:

1. $\mathcal{C}_1, \mathcal{C}_2, \ldots, \mathcal{C}_M$ are closed convex sets with a nonempty intersection $\mathcal{C}_0 \triangleq \bigcap_{m=1}^{M} \mathcal{C}_m$

   and

2. $0 < \lambda_m < 2, \; i = 1, 2, \ldots, M$

the algorithm converges to a point in $\mathcal{C}_0$, the intersection of all the sets. The order in which the sets are selected for the successive projections is arbitrary, but in general the method of projection on to the most remote set is used, as this will increase the convergence rate.

Any number of linear inequalities of the form $(\vec{Q}, \vec{A}) \leq \alpha$ can be easily included in the method as each just forms another set $\mathcal{C}_l = \{\vec{A} : (\vec{Q}_l, \vec{A}) \leq \alpha_l\}$ (a half space) with projection of $\vec{A}$ onto the set $\mathcal{C}_l$

$$\mathbf{P}(\vec{x}, \mathcal{C}_l) = \begin{cases} \vec{A}, & \text{if } (\vec{Q}_l, \vec{A}) \leq \alpha_l \\ \vec{A} - \left[(\vec{Q}_l, \vec{A}) - \alpha_l \right] \dfrac{\vec{Q}_l}{\|\vec{Q}_l\|^2}, & \text{if } (\vec{Q}_l, \vec{A}) > \alpha_l. \end{cases} \tag{5.19}$$

When applied to antenna arrays; a set is formed by all the excitations that produce a radiation pattern of the required magnitude characteristic (a set of inequality constraints)

$$\mathcal{C}_m = \{\vec{A} : \|S_m - |\vec{B}_m \vec{A}|\| \leq \varepsilon_m\} \tag{5.20}$$

where ε_m is the toleration or the maximum allowable deviation from the desired pattern level in the (θ_m, ϕ_m)-direction, S_m is the desired pattern level in the (θ_m, ϕ_m)-direction,

$\vec{B}_m$ is the mth row of the radiation matrix in the far-field direction (θ_m, ϕ_m) and $\vec{A}$ is the excitation vector.

Any arbitrary excitation vector $\vec{A}_{m-1} \notin \mathcal{C}_m$ can be projected on $\mathcal{C}_m$, giving $\vec{A}_m \in \mathcal{C}_m$. The projections are carried out successively until the intersection is found. The order in which the sets are selected for the successive projections is arbitrary, but in generally the projection on to the most remote set (the set with largest distance between the current point and that set) is used. Elmikati and Elsohly [135] used the method of successive projection (without relaxation) to synthesise symmetrical linear arrays with real excitations. This is a field synthesis problem, thus all the sets $\mathcal{C}_m$ are convex, and converge is guaranteed.

Applying the projection definition (5.15) at any step is equivalent to finding the excitation vector that minimises [136]

$$J = \|\vec{A}_{k+1} - \vec{A}_k\|^2 + \alpha \left[(S_m - |\vec{B}_m \vec{A}_k|) - \varepsilon_m \right] \tag{5.21}$$

where α is the Lagrange multiplier, and solving for α

$$\alpha = \frac{2 \left[\|S_m - |\vec{B}_m \vec{A}_k|\| - \varepsilon_m \right]}{\|\vec{B}_m\|^2}. \tag{5.22}$$

Abo-Taleb and Fahmy [136] used these results to design two-dimensional digital filters. In the FIR filter scenario all the sets $\mathcal{C}_m$ are convex, thus the method will converge the global minimum from any arbitrary starting point.

However, in power synthesis the sets are not convex, and convergence is not guaranteed. Levi and Stark [105] showed that in many cases good convergence can be obtained with non-convex sets, but a starting point close to the intersection is prerequisite. The method of successive projections was applied to power pattern synthesis by Poulton [107, 108], using relaxation and the Lagrange multiplier, with good results.

5.2.3 Generalised Projections

As mentioned previously, the sets involved in power pattern synthesis are non-convex. More recently the generalised projections (also called alternating projections) technique has been used as the basis for a power synthesis method [110, 137, 138] which take into account the non-convexness of the sets involved. The generalised projection method allows constraints not only on the radiation pattern but also on the excitations (eg. dynamic range or smoothness), something that is most advantageous when having to deal with mutual coupling effects. The method searches for the intersection of two sets by iteratively projecting between the sets.

The two sets are, $\mathcal{C}_1$ the set of all radiation patters possible with the considered array geometry and $\mathcal{C}_2$ a set of real non-negative functions that satisfy the constraints on the radiation pattern, with projections P_1 and P_2 associated with the sets respectively. The

constraints on the radiation power pattern can be expressed as a "mask" giving the upper S_U and lower S_L values in each pattern direction. We are searching for the excitation that will minimise

$$\xi = \|S - |F|\|^2 \tag{5.23}$$

where S is the function describing the desired radiation pattern. This is done by applying the reconstruction algorithm (5.16) for two sets

$$\vec{F}_{k+1} = \mathbf{P}_1\mathbf{P}_2\vec{F}_k. \tag{5.24}$$

Franceschetti et al. [137] proposed the use of the Fast Fourier transform (FFT) of order M to facilitate efficient computation. The projections then are

$$\mathbf{P}_1 = (\text{FFT})\,\tau_A\,(\text{FFT})^{-1} \tag{5.25a}$$

$$\mathbf{P}_2 = \tau_F \tag{5.25b}$$

where

$$\tau_A : a_n = \begin{cases} a'_n & \text{if } 0 \leq n \leq N \\ 0 & \text{if } n < 0 \text{ or } n \geq N+1. \end{cases} \tag{5.26}$$

and

$$\tau_F : f'_m = \begin{cases} \frac{f_m}{|f_m|} S_{Um} & \text{if } |f_m| > S_{Um} \\ f_m & \text{if } S_{Lm} \leq |f_m| \leq S_{Um} \\ \frac{f_m}{|f_m|} S_{Lm} & \text{if } |f_m| < S_{Lm}. \end{cases} \tag{5.27}$$

The mapping of the radiation pattern into the mask is done in such a way that the phase is unchanged, only the magnitude changes. This is equivalent to the Gerchberg-Saxton [130] algorithm widely used in image reconstruction:

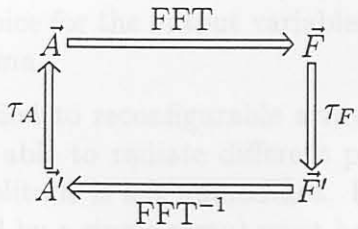

To incorporate constraints on the excitation, set $\mathcal{C}_1$ can be reduced to a set $\mathcal{C}'_1$ of all radiation patters possible with the array geometry and excitation constraints, $\mathcal{C}'_1 \subset \mathcal{C}_1$. Excitation constraints, amplitude and phase, can be imposed by adding an additional mapping τ'_C and τ''_C respectively [109],

$$\tau'_C : a_n = \begin{cases} \frac{a'_n}{|a'_n|} A_{max} & \text{if } |a'_n| > A_{max} \\ a'_n & \text{if } A_{min} \leq |a'_n| \leq A_{max} \\ \frac{a'_n}{|a'_n|} A_{min} & \text{if } |a'_n| < A_{min} \end{cases} \tag{5.28}$$

where A_{max} and A_{min} are the maximum and minimum allowable magnitude of the excitations; and

$$\tau_C'' : a_n' = \begin{cases} |a_n''| \cos\left(\angle a_n'' - \alpha_{max}\right) e^{\alpha_{max}} & \text{if } \angle a_n'' > \alpha_{max} \\ a_n'' & \text{if } \alpha_{min} \leq \angle a_n'' \leq \alpha_{max} \\ |a_n''| \cos\left(\angle a_n'' - \alpha_{min}\right) e^{\alpha_{min}} & \text{if } \angle a_n'' > \alpha_{min} \end{cases} \tag{5.29}$$

where α_{max} and α_{min} are the maximum and minimum allowable phase of the excitations. The projection onto $\mathcal{C}_1'$ is then

$$\mathbf{P}_1' = (\text{FFT})\, \tau_C' \tau_C'' \tau_A\, (\text{FFT})^{-1}. \tag{5.30}$$

The order of the operators $\tau_C' \tau_C''$ are important, exchanging them will not result in a projection onto $\mathcal{C}_1'$.

However, since the sets are non-convex, convergence (even if an intersection exists) is not guaranteed to a global minimum. One may end up in a local minima and not be able to get out, this is called a trap. Thus, a proper selection of the starting point is of the utmost importance, as a good starting point (or warm start) will be close enough to the final solution to avoid falling into a trap. Another potential problem is tunnels which lead to extremely slow convergence. Traps and tunnels are discussed in detail in Section 5.3. The choice of a good starting point should include the constraints on the excitations, for example if there is a constraint on the dynamic range of the excitations a good starting point may be obtained by a phase only synthesis where the amplitude of each element is fixed.

Use of the fast Fourier transform and the inverse fast Fourier transform (although computationally very fast) limits the application of the method to uniformly spaced linear and planar arrays. The method was extended to the synthesis of non-uniformly spaced arrays [72]. By using singular value decomposition as part of the projection onto $\mathcal{C}_1$ the method has been extended to conformal array synthesis [112]. Bucci et al. [113] also adopted a non-standard choice for the output variables in the generalised projection method and to avoid local minima.

The method was also extended to reconfigurable arrays by phase-only control [139, 140], that is an array which is able to radiate different patterns by changing only the excitation phases while the amplitude is left unmodified. For this type of reconfigurable array Q array patterns (radiated by a single array) must be synthesised at the same time in order to achieve the best common amplitude distribution. The first set $\boldsymbol{\mathcal{C}_1}$ is the set of all the Q-tuples of array factors that belong to the Cartesian product

$$\boldsymbol{\mathcal{C}_1} = \underbrace{\mathcal{C}_1^1 \times \mathcal{C}_1^2 \times \cdots \times \mathcal{C}_1^Q}_{Q\text{times}} \tag{5.31}$$

and satisfy the additional requirement

$$|a_{n,1}| = |a_{n,2}| = \cdots = |a_{n,Q}| \quad \text{for } n = 1, 2, \ldots, N. \tag{5.32}$$

The second set $\mathcal{C}_2$ is the Cartesian product of all the radiation pattern masks

$$\mathcal{C}_2 = \underbrace{\mathcal{C}_2^1 \times \mathcal{C}_2^2 \times \cdots \times \mathcal{C}_2^Q}_{Q\text{times}}. \tag{5.33}$$

The intersection $\mathcal{C}_1 \cap \mathcal{C}_2$ is the solution to this synthesis problem. Bucci et al. [140] derived the necessary projections.

5.3 The Synthesis Problem as an Intersection of Two Sets

The sets involved in the array synthesis problem are usually not convex sets. In general, very little can be said about the reconstruction algorithm when the projections are not onto convex sets. However, when only two sets are involved a number of interesting conclusions can be made. The restriction of two sets is not so serious, as two or more sets can be combined to form single more complex sets for which it is still possible to derive a projection operator [105].

In this section the synthesis of an arbitrary array will be viewed as the search for the intersection of two excitation sets. Unlike the previous formulations which all consider sets in the "pattern space" this formulation considers sets in the "excitation space" as well as sets in the "pattern space". In the "excitation space" the one set is the set of all possible excitations satisfying the excitation constraints; and the other set is the set of all excitations that produce radiation patterns that satisfy the radiation pattern requirements. In the "pattern space" the one set is the set of all radiation patterns possible with the given geometry; and the other set is the set of radiation patterns satisfying the pattern constraints. Both these formulation allow for both field and power pattern synthesis.

All the equations in this section are for the general two-dimensional case of an array of arbitrary sources at arbitrary positions. The two dimensions refer to the pattern angles (θ, ϕ). These expressions can be simplified for the less general cases (eg. linear or planar arrays). The simplification will be given at the relevant example in the Section 5.8. All the necessary equations defined or derived previously will be repeated for convenience.

5.3.1 The Transformation Operators Between the Excitation and Pattern Spaces

To transform from the excitation space to the pattern space will be referred to as the forward operator; and the transformation from the radiation pattern space to the excitation space will be referred to as the backward operator.

The radiation pattern has the form of a discrete Fourier transformation; the Fourier transformation can be used to calculate the radiation pattern from an excitation and the

inverse Fourier transformation to calculate the excitation from a radiation pattern. The use of the Fourier and inverse Fourier transformation pair is proposed in references [137, 110]. Implementing the Fourier transformation by using the fast Fourier transformation (FFT) is computationally very fast. However, Fourier transformations can only be applied to equi-spaced linear and planar arrays and can not take element patterns into account. This limitation makes Fourier transformation useless for conformal array synthesis.

The Forward Operator

The radiation pattern of an arbitrary array in the direction (θ, ϕ) is (as already defined in equation (2.2)),

$$F(\theta,\phi) = \sum_{n=1}^{N} a_n \, E_n(\theta,\phi) \, e^{\mathrm{j}k(x_n \sin\theta\cos\phi + y_n \sin\theta\sin\phi + z_n\cos\theta)} \tag{5.34}$$

where (x_n, y_n, z_n) is the position; $E_n(\theta,\phi)$ is the element pattern and a_n is the relative constrainted complex excitation of the nth array element; and N is the total number of elements in the array.

The radiation pattern in M different far-field directions can be written in vector notation

$$\vec{F} = \tilde{B}\,\vec{A} \tag{5.35}$$

where $\vec{A} = [a_1, a_2, \ldots, a_N]^T$ is the excitation vector, $\vec{F} = [F_1, F_2, \ldots, F_M]^T$ is the pattern vector and $\tilde{B}$ is the radiation matrix with matrix elements

$$b_{mn} = E_n(\theta_m,\phi_m) \, e^{\mathrm{j}k(x_n \sin\theta_m\cos\phi_m + y_n \sin\theta_m\sin\phi_m + z_n\cos\theta_m)}.$$

The mth row vector of the radiation matrix $\tilde{B}$ is $\vec{B}_m$, thus $F_m = \vec{B}_m\vec{A}$ is the value of the two dimensional radiation pattern in direction (θ_m, ϕ_m). The elements of $\tilde{B}$ are a function of the array geometry (which is fixed for a particular synthesis problem) and the selected far-field directions.

The columns of the rectangular matrix $\tilde{B}$ are linearly independent. The vector $\vec{F} = \tilde{B}\vec{A}$ is a vector in the space spanned by the columns of $\tilde{B}$.

The Backward Operator

The backward operator is needed to calculate an excitation from a function in the pattern space and is the inverse of the radiation matrix. There are two problems in determining the inverse of the radiation matrix:

1. The perturbed or constrainted radiation pattern is not in the space spanned by the columns of $\tilde{B}$; thus there will not be an excitation that can produce the perturbed radiation pattern exactly.

2. The radiation matrix $\tilde{B}$ is generally over determined (more equations than unknowns).

A number of possibilities for the pseudo-inverse of the radiation pattern exist. The pseudo-inverse of matrix $\tilde{B}$ can be determined using least squares:

$$\tilde{C} = \left(\tilde{B}^H \tilde{B}\right)^{-1} \tilde{B}^H. \tag{5.36}$$

The method of least squares, also referred to as maximum likelihood, minimises $\|\vec{F} - \tilde{B}\vec{A}\|$. Matrix $\tilde{C}$ is also called the *general inverse* or the *general reciprocal* of matrix $\tilde{B}$. The maximum likelihood inverse can be used for arbitrary arrays of arbitrary radiators in a three-dimensional space. One drawback of least squares is that all the equations (the far-field in a particular direction) have equal importance. This means that a point outside the radiation pattern mask that must move to fit in the mask is just as important as a point that is already in the radiation pattern mask (and for which some movement can be allowed as long as it stays in the mask). Singular value decomposition, proposed by Mazzarella and Panariello [112], will yield the same result as least squares, as it minimises the same function.

Weighted least squares will overcome the shortcomings of least squares. The pseudo-inverse of the radiation matrix using weighted least squares is:

$$\tilde{C} = \left(\tilde{B}^H \tilde{W} \tilde{B}\right)^{-1} \tilde{B}^H \tilde{W} \tag{5.37}$$

where $\tilde{W}$ is a diagonal weighting matrix. The inverse minimises $\|\tilde{W}(\vec{F} - \tilde{B}\vec{A})\|$; and is unique. Weighted least squares allows certain directions (constraints) to be emphasised more than others, and can be used to synthesise arbitrary arrays of arbitrary radiators in a three-dimensional space. The advantage and disadvantage of the weighted least squares pseudo-inverse is investigated in Section 5.6.1

5.3.2 The Sets Associated with the Synthesis Problem

In the synthesis problem we can identify four different sets, two sets in the "pattern space" and two sets in the "excitation space":

1. The set of radiation patterns satisfying the pattern constraints.
2. The set of excitations satisfying the excitation constraints.
3. The set of all radiation patterns possible with the given array geometry and possible excitations.
4. The set of excitations that produce radiation patterns within the pattern requirements.

Let us first define the sets and associated projectors.

Radiation pattern sets:

Pattern space $\mathcal{P}$ is a complex Euclidean space with subsets $\mathcal{C}_f$ and $\mathcal{C}_{f'}$. The set of all radiation patterns possible with the array geometry and any allowable excitation is

$$\mathcal{C}_f = \left\{ \mathcal{F} : F(\theta,\phi) = \sum_{n=1}^{N} a_n \, E_n(\theta,\phi) \, e^{\mathrm{j}k(x_n \sin\theta\cos\phi + y_n \sin\theta\sin\phi + z_n\cos\theta)} \right\} \tag{5.38}$$

with $a_n \in \mathcal{C}_a$ that will be defined in equation (5.43). In the matrix notation defined in Section 5.3.1 the set is

$$\mathcal{C}_f = \left\{ \mathcal{F} : \vec{F} = \tilde{B}\vec{A} \right\}. \tag{5.39}$$

$\mathcal{C}_{f'}$ is the set square integratable functions (real, non-negative for power pattern synthesis) that fulfil the constraints on the radiation pattern, which is generally defined by a power pattern mask with $S_L(\theta,\phi)$ the lower limit and $S_U(\theta,\phi)$ the upper limit,

$$\mathcal{C}_{f'} = \left\{ \mathcal{F}' : S_L(\theta,\phi) \leq |F'(\theta,\phi)|^2 \leq S_U(\theta,\phi) \right\} \tag{5.40}$$

or for a discrete far-field

$$\mathcal{C}_{f'} = \left\{ \mathcal{F}' : S_{Lm} \leq |f'_m|^2 \leq S_{Um} \right\}. \tag{5.41}$$

It is important to note that $\mathcal{C}_{f'}$ is a non-convex set.

Excitation sets:

Excitation space $\mathcal{E}$ is a complex Euclidean space with subsets $\mathcal{C}_a$ and $\mathcal{C}_{a'}$. Let $\mathcal{C}_{a'}$ be the set of all possible excitations that will produce an acceptable radiation pattern

$$\mathcal{C}_{a'} = \left\{ \mathcal{A}' \leftrightarrow \mathcal{F}' : S_L \leq |F'|^2 \leq S_U \right\} \tag{5.42}$$

with S_U and S_L the upper and lower limits of the required radiation pattern.

The second set in the excitation space is the set of all the excitations satisfying the excitation constraints. These constraints can be on the magnitude as well as the phase of the excitations

$$\mathcal{C}_a = \{ \mathcal{A} : A_{Ln} \leq |a_n| \leq A_{Un};\ \alpha_{Ln} \leq \angle a_n \leq \alpha_{Un} \} \tag{5.43}$$

where $\angle$ denotes the argument of a complex number. A_{Un} denotes the upper limit and A_{Ln} the lower limit of the excitation amplitude of the nth element excitation; and α_{Un} and α_{Ln} the upper and lower limits of the phase of the nth element excitation. Depending on the excitation constraints $\mathcal{C}_a$ may or may not be convex.

5.3.3 The Projections between Related Sets

A projection is defined as the mapping of a point outside a set to the point just inside the set nearest to the original point (5.15). However, the sets involved in power pattern synthesis are not convex; the following remarks can be made regarding non-convex sets [105]:

- There may be a set of points that satisfy the definition of the projection (5.15);
- The closeness of a set is a sufficient condition for the existence of a projection onto the set.

Since some of the sets, as defined in the previous section are non-convex, a procedure for uniquely choosing one of the possible points is needed, and is usually achieved through satisfying another condition. This eliminates the ambiguity that would otherwise result from non-singleton projection points.

The Projector from $\mathcal{C}_f$ to $\mathcal{C}_{f'}$

A number of radiation field pattern have the same power pattern; apart from the trivial associations $|F| = |-F| = |F^*|$, for every complex zero z_0 of F

$$|F(u)| = \left| [F(u)] \left[\frac{z_0^* e^{ju} - 1}{e^{ju - z_0}} \right] \right|.$$

As the set is non-convex the most appropriate projection must be selected; for power pattern synthesis the phase of the radiated field must be preserved. The mapping of the radiation pattern to fit in the prescribed magnitude while preserving its phase distribution is

$$\tau_F : f'_m = \begin{cases} \frac{f_m}{|f_m|}\sqrt{S_{Um}} & \text{if } |f_m|^2 > S_{Um} \\ f_m & \text{if } S_{Lm} \leq |f_m|^2 \leq S_{Um} \\ \frac{f_m}{|f_m|}\sqrt{S_{Lm}} & \text{if } |f_m|^2 < S_{Lm}. \end{cases} \tag{5.44}$$

The projector is

$$\mathrm{P}_F = \tau_F \tag{5.45}$$

and the unique projection from any point $\vec{F}$ in pattern space $\mathcal{P}$ onto the set of accepable radiation patterns $\mathcal{C}_{f'}$ is

$$\vec{F}' \in \mathcal{C}_{f'} : \vec{F}' = \tau_F \vec{F} = \mathrm{P}_F \vec{F} \tag{5.46}$$

Note that constraining the radiation pattern to have a prescribed magnitude is not equivalent to projecting onto a convex set.

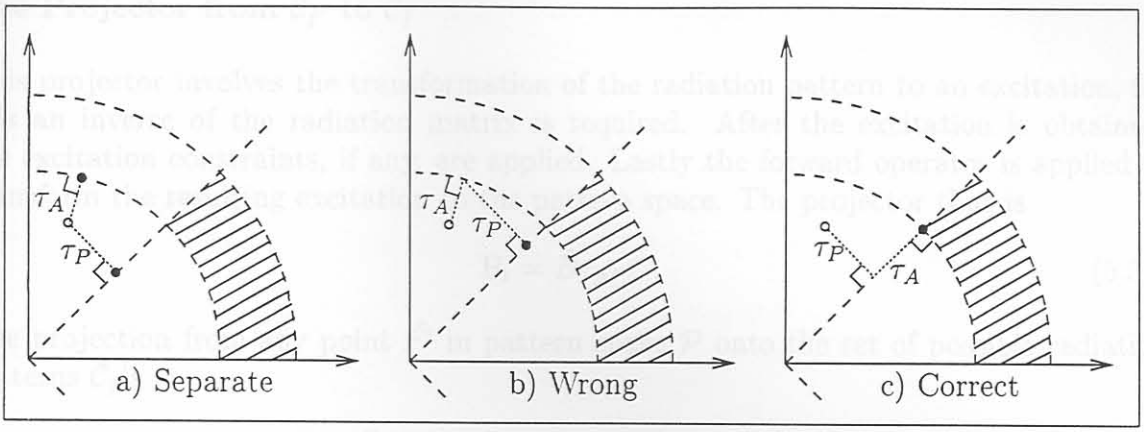

Figure 5.1: Application of the excitation projection: a) amplitude and phase separately, b) combined but wrong as the result is not in the defined set (the shaded region) and c) correct as the result is just inside the set.

The Projector from $\mathcal{C}_{a'}$ to $\mathcal{C}_a$

This projection operator is in essence the application of the excitation constraints. Excitation constraints can be imposed by mapping the excitation phase angle while keeping the excitation amplitude fixed

$$\tau_P : a_n = \begin{cases} |a'_n| \cos\left(\angle a'_n - \alpha_{Un}\right) e^{\alpha_{Un}} & \text{if } \angle a'_n > \alpha_{Un} \\ a'_n & \text{if } \alpha_{Ln} \leq \angle a'_n \leq \alpha_{Un} \\ |a'_n| \cos\left(\angle a'_n - \alpha_{Ln}\right) e^{\alpha_{Ln}} & \text{if } \angle a'_n > \alpha_{Ln} \end{cases} \tag{5.47}$$

and mapping the excitation amplitude while keeping the excitation phase angle fixed,

$$\tau_A : a_n = \begin{cases} \frac{a'_n}{|a'_n|} R_{Un} & \text{if } |a'_n| > R_{Un} \\ a'_n & \text{if } R_{Ln} \leq |a'_n| \leq R_{Un} \\ \frac{a'_n}{|a'_n|} R_{Ln} & \text{if } |a'_n| < R_{Ln}. \end{cases} \tag{5.48}$$

for each excitation. The projector is the combined phase and magnitude mapping

$$\mathbf{P}_A = \tau_{AP} = \tau_A \tau_P. \tag{5.49}$$

It is important to note that the order of the projections can not be interchanged otherwise the resulting projection will not be on $\mathcal{C}_a$. This is illustrated in Figure 5.1. Both the amplitude and phase are constrainted; the shaded region in each of the figures is the set defined by the constraints. The open circle indicate the position of a'_n and the filled circle the position of a_n. Figure 5.1a) show the mapping separately. If the mapping are combined in the wrong order the "projection" is not on to set $\mathcal{C}_a$, as shown in Figure 5.1b). The correct order of the mappings to form the projection is displayed in Figure 5.1b), a_n is in $\mathcal{C}_a$. The correct projection, projecting any point $\vec{A}'$ in excitation space $\mathcal{E}$ onto the set of acceptable excitations $\mathcal{C}_a$, is

$$\vec{A} \in \mathcal{C}_a : \vec{A} = \tau_A \tau_P \vec{A}' = \mathbf{P}_A \vec{A}'. \tag{5.50}$$

The Projector from $\mathcal{C}_{f'}$ to $\mathcal{C}_f$

This projector involves the transformation of the radiation pattern to an excitation; for this an inverse of the radiation matrix is required. After the excitation is obtained, the excitation constraints, if any, are applied. Lastly the forward operator is applied to transform the resulting excitation to the pattern space. The projector thus is

$$\mathrm{P}_1 = \tilde{B}\tau_{AP}\tilde{C}. \tag{5.51}$$

The projection from any point $\vec{F}'$ in pattern space $\mathcal{P}$ onto the set of possible radiation patterns $\mathcal{C}_f$is

$$\vec{F} \in \mathcal{C}_f : \vec{F} = \tilde{B}\tau_{AP}\tilde{C}\vec{F}' = \mathrm{P}_1\vec{F}'. \tag{5.52}$$

Depending on the excitation constraints, this may not be a projection onto a convex set.

The Projector from $\mathcal{C}_a$ to $\mathcal{C}_{a'}$

Using the forward operator the excitation is transformed to the pattern space, where the radiation pattern constraints are applied. The constrainted radiation pattern is the transformed back the the excitation space by means of the back operator.

$$\mathrm{P}_2 = \tilde{C}\tau_F\tilde{B}. \tag{5.53}$$

The projection, projecting any point $\vec{A}$ in excitation space $\mathcal{E}$ onto the set of possible excitations $\mathcal{C}_a$, is

$$\vec{A}' \in \mathcal{C}_{a'} : \vec{A}' = \tilde{C}\tau_F\tilde{B}\vec{A} = \mathrm{P}_2\vec{A}. \tag{5.54}$$

This is not a projection onto a convex set.

If the radiation pattern obtained with the forward operator satisfy the radiation constraints (if τ_F in a unit operator) then $\vec{A}' = \vec{A}$.

5.3.4 Synthesis Algorithm

The synthesis problem is solved when the simultaneous intersection of the sets in both the excitation and pattern spaces is found. The synthesis problem may be presented as a modified Gerchberg-Saxton algorithm:

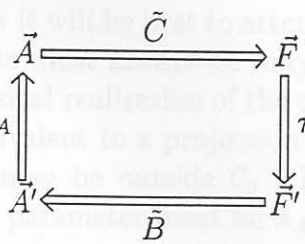

The synthesis problem may be attempted in the excitation space or the pattern space:

$$\begin{aligned} \text{Excitation Space:} \quad & \vec{A}_{k+1} = \mathbf{P}_A \mathbf{P}_2 \vec{A}_k \\ \text{Pattern Space:} \quad & \vec{F}_{k+1} = \mathbf{P}_1 \mathbf{P}_F \vec{F}_k \end{aligned} \tag{5.55}$$

where $\vec{A}_k$ is the estimate of $\vec{A}$ at the kth iteration of the synthesis; and $\vec{F}'_k$ is the estimate of $\vec{F}'$ at the kth iteration of the synthesis. The reconstruction algorithms then are:

Excitation space: Pattern space:

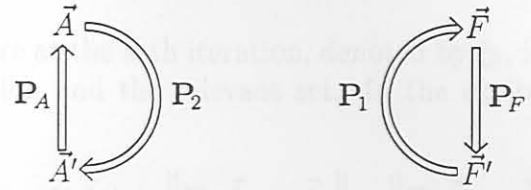

The columns of the rectangular radiation matrix $\tilde{B}$ are linearly independent. The vector $\vec{F} = \tilde{B}\vec{A}$ is a vector in the space spanned by the columns of $\tilde{B}$. However, the perturbed vector $\vec{F}' = \tau_F \vec{F}$ is not in the space spanned by the columns of $\tilde{B}$. As a result the excitations obtained with $\vec{A}' = \tilde{C}\vec{F}'$ will not yield $\vec{F}'$ exactly. This is due to the fact that $\tilde{B}\tilde{C} \neq \tilde{C}\tilde{B}$. Since the projectors are in general not unitary, the projectors $\mathbf{P}_1$ and $\mathbf{P}_2$ are in general not metric projectors.

5.3.5 Relaxation

Relaxation can be used as a convergence accelerator. The relaxed version of (5.55) is

$$\begin{aligned} \text{Excitation Space:} \quad & \vec{A}_{k+1} = \mathbf{T}_A \mathbf{T}_2 \vec{A}_k \\ \text{Pattern Space:} \quad & \vec{F}_{k+1} = \mathbf{T}_1 \mathbf{T}_F \vec{F}_k \end{aligned} \tag{5.56}$$

where

$$\mathbf{T}_i = 1 + \lambda_i(\mathbf{P}_i - 1) \quad i = 1, 2, A, F \tag{5.57}$$

with λ_i the relaxation parameters.

The synthesis can be executed on either the radiation pattern space or the excitation space. If relaxation is applied in the pattern space a pattern may be obtained that does not have an excitation due to the non-convex sets involved. On the other hand if relaxation is applied in the excitation space a physical realizable excitation will always be obtained. From this point of view it will be best to attempt the synthesis in the excitation space. The excitation constraints must always be fully applied as these constraints are generally used to ensure the physical realisation of the array. Since the application of the excitation constraints is not equivalent to a projection onto a convex set, the excitation $\vec{A}_{k+1}$ obtained with relaxation may be outside $\mathcal{C}_a$ (thus not satisfying the excitation constraints); thus the relaxation parameter msut be $\lambda_A = 1$.

Thus the synthesis algorithm used in this thesis is

$$\vec{A}_{k+1} = \mathrm{P}_A \mathrm{T}_2 \vec{A}_k \quad \text{with } \mathrm{T}_2 = 1 + \lambda_2(\mathrm{P}_2 - 1). \tag{5.58}$$

Since the excitation constraints are enforced (projection on a non-convex set), $\lambda_A = 1$, the current excitation will be realizable.

5.3.6 Performance Evaluation

The performance measure at the k-th iteration, denoted by ξ_k, is the sum of the distances between the k-th iteration and the relevant set. In the excitation space the summed-distance error is

$$\xi_k = \xi(\vec{A}_k) = \left\|\mathrm{P}_A \vec{A}_k - \vec{A}_k\right\| + \left\|\mathrm{P}_2 \vec{A}_k - \vec{A}_k\right\| \tag{5.59}$$

and in the pattern space

$$\xi_k = \xi(\vec{F}_k) = \left\|\mathrm{P}_1 \vec{F}_k - \vec{F}_k\right\| + \left\|\mathrm{P}_F \vec{F}_k - \vec{F}_k\right\|. \tag{5.60}$$

Although the projectors P_1 and P_2 are both idempotent ($P^2 = P$), they are in general not unitary; and thus not metric projectors. The error reduction property

$$\xi_{k+1} \leq \xi_k. \tag{5.61}$$

is not ensured for the recursion given in equation (5.55) or its relaxed version (5.56). This does not destroy the possibility of using the proposed algorithm.

The synthesis problem is solved when the simultaneous intersection of the sets in both the excitation and pattern spaces is found. Let us then define the performance measure as the summed-distance in both spaces

$$\xi_k = \left\|\mathrm{P}_F \vec{F}_k - \vec{F}_k\right\| + \left\|\mathrm{P}_1 \vec{F}_k - \vec{F}_k\right\| + \left\|\mathrm{P}_A \vec{A}_k - \vec{A}_k\right\| + \left\|\mathrm{P}_2 \vec{A}_k - \vec{A}_k\right\| \tag{5.62}$$

In the previous section we argued that it would be best to attempt synthesis in the excitation space. Substituting the projector and keeping in mind that in the k-th iteration $\vec{F}_k = \tilde{B}\tau_A \vec{A}_k$

$$\xi_k = \left\|\tau_F \tilde{B}\tau_A \vec{A}_k - \tilde{B}\tau_A \vec{A}_k\right\| + \left\|\tau_A \vec{A}_k - \vec{A}_k\right\| + \left\|\tilde{C}\tau_F \tilde{B}\vec{A}_k - \vec{A}_k\right\|. \tag{5.63}$$

The second term in (5.62) is zero since $\tilde{C}\tilde{B} = \tilde{I}$. If $\lambda_A = 1$, as previously motivated, then the performance measure reduce to

$$\begin{aligned} \xi_k &= \left\|\tau_F \tilde{B}\vec{A}_k - \tilde{B}\vec{A}_k\right\| + \left\|\tilde{C}\tau_F \tilde{B}\vec{A}_k - \vec{A}_k\right\| \\ &= \|\vec{F}'_k - \vec{F}_k\| + \|\vec{A}'_k - \vec{A}_k\| \end{aligned} \tag{5.64}$$

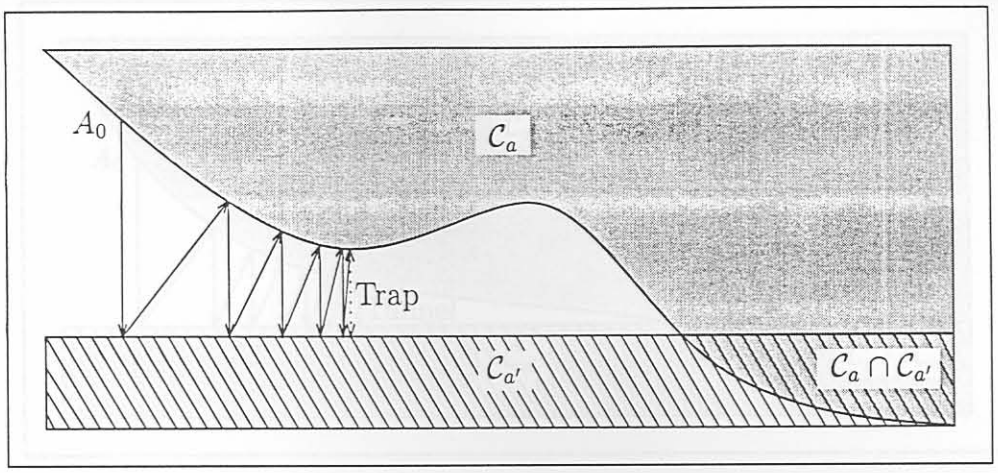

Figure 5.2: Illustrating traps, starting from $\vec{A}_0$ the sequence $\{\vec{A}_k\}$ converges to the trap, instead of the true solution belonging to $\mathcal{C}_a \cap \mathcal{C}_{a'}$

since $\tau_A \vec{A}_k = \vec{A}_k$. If the first term in equation (5.64) is zero the second term will also be zero since $\vec{A}'_k = \tilde{C}\vec{F}'_k = \tilde{C}\vec{F}_k = \tilde{C}\tilde{B}\vec{A}_k = \vec{A}_k$. This can also be deduced from the definitions of the sets, $\mathcal{C}_f$ is the set of all radiation patterns obtainable with all the allowable excitations. Thus, from an engineering point of view it is only important to know how well the current excitation's radiation pattern meets the pattern requirements.

$$\xi_k = \xi(\vec{A}_k) = \left\| \mathbf{P}_F \tilde{B}\vec{A}_k - \tilde{B}\vec{A}_k \right\| = \left\| \mathbf{P}_F \vec{F}_{k+1} - \vec{F}_{k+1} \right\|. \tag{5.65}$$

5.3.7 Traps and Tunnels

The synthesis problem is finding the intersection of the specified sets. However, since the sets are non-convex, convergence to a global maximum, even if an intersection between the relevant sets exists, can not be guaranteed. The reconstruction may end up in a local minima and not be able to proceed to the global minimum, this is called a trap. Mathematically the condition for a trap is when the error does not decrease from iteration to iteration and is larger than zero,

$$\xi_{k+1} = \xi_k > 0 \tag{5.66}$$

The condition can also be stated as

$$\begin{aligned} \text{Excitation Space:} \quad & \mathbf{P}_A \mathbf{P}_2 \vec{A}_k = \vec{A}_k, \quad \vec{A}_k \neq \vec{A} \\ \text{Pattern Space:} \quad & \mathbf{P}_1 \mathbf{F}_F \vec{F}_k = \vec{F}_k, \quad \vec{F}_k \neq \vec{F}. \end{aligned} \tag{5.67}$$

A trap is graphically presented in Fig. 5.2.

Another potential problem is tunnels which lead to extremely slow convergence. A tunnel is when the reduction in error from iteration to iteration is very small,

$$\xi_{k+1} \leq \xi_k, \quad \text{but} \quad \xi_{k+1} \approx \xi_k. \tag{5.68}$$

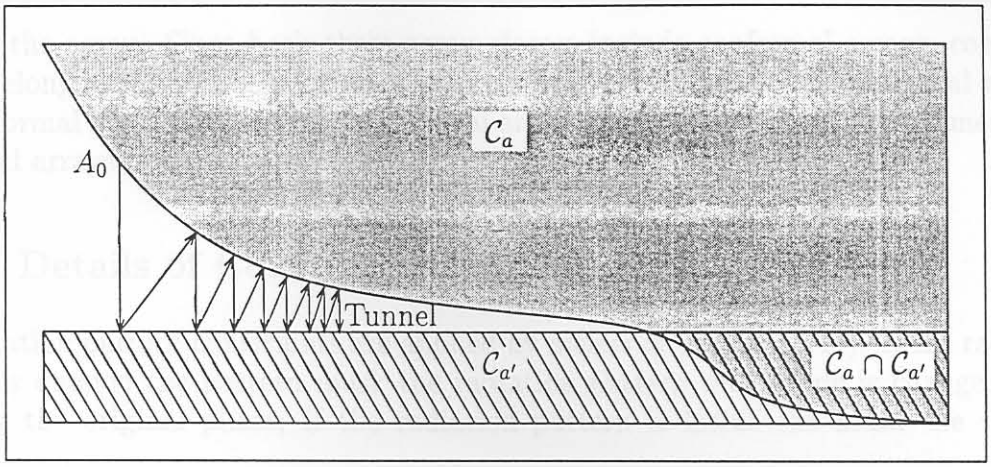

Figure 5.3: Illustrating tunnels, starting from $\vec{A}_0$ the sequence $\{\vec{A}_k\}$ converges to the true solution belonging to $C_a \cap C_{a'}$ through a long tunnel.

The effect of a tunnel is illustrated in Fig. 5.3. Relaxation, discussed in the previous section, can be used to alleviate this problem.

As stated earlier, a proper selection of the starting point is of the utmost importance, as a good starting point will be close enough to the final solution to avoid falling into a trap. Selecting a good starting point is not simple, the selection should take into account all the constraints. Various methods have been investigated, as discussed in Section 5.5.

5.4 Implementation Detail

In this section the computer program implementation of the intersection of sets synthesis technique will be discussed in some detail. However, before we embark on this discussion we need to define some terms.

Arrays with an array pattern of only one angular variable (say ϕ) will be referred to as one dimensional pattern arrays, or simply "one dimensional arrays". This class of arrays includes all linear arrays as well as conformal arrays where we are only interested in the pattern in the plane of the array.

Two dimensional pattern arrays, or simply "two dimensional arrays", are arrays with radiation patterns with two angular variables, (θ, ϕ). This class of arrays will include planar arrays where we are interested in a pattern in half-space; and conformal arrays where the radiation patterns are functions of both (θ, ϕ).

Although some arrays may seem to be a two dimensional array at first glance due to the array geometry, one has to consider the radiation pattern in order to classify the array. If the radiation pattern is of interest only in one plane, or dependent on only one angular variable, the array should be classified as a one dimensional array. An example of such an one dimensional array is an circular array which is used to scan 360° in the

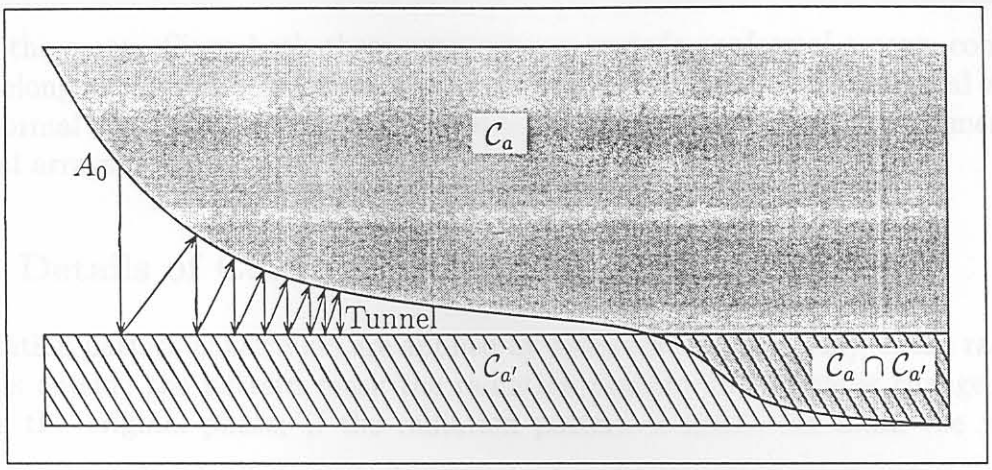

Figure 5.3: Illustrating tunnels, starting from $\vec{A}_0$ the sequence $\{\vec{A}_k\}$ converges to the true solution belonging to $C_a \cap C_{a'}$ through a long tunnel.

The effect of a tunnel is illustrated in Fig. 5.3. Relaxation, discussed in the previous section, can be used to alleviate this problem.

As stated earlier, a proper selection of the starting point is of the utmost importance, as a good starting point will be close enough to the final solution to avoid falling into a trap. Selecting a good starting point is not simple, the selection should take into account all the constraints. Various methods have been investigated, as discussed in Section 5.5.

5.4 Implementation Detail

In this section the computer program implementation of the intersection of sets synthesis technique will be discussed in some detail. However, before we embark on this discussion we need to define some terms.

Arrays with an array pattern of only one angular variable (say ϕ) will be referred to as one dimensional pattern arrays, or simply "one dimensional arrays". This class of arrays includes all linear arrays as well as conformal arrays where we are only interested in the pattern in the plane of the array.

Two dimensional pattern arrays, or simply "two dimensional arrays", are arrays with radiation patterns with two angular variables, (θ, ϕ). This class of arrays will include planar arrays where we are interested in a pattern in half-space; and conformal arrays where the radiation patterns are functions of both (θ, ϕ).

Although some arrays may seem to be a two dimensional array at first glance due to the array geometry, one has to consider the radiation pattern in order to classify the array. If the radiation pattern is of interest only in one plane, or dependent on only one angular variable, the array should be classified as a one dimensional array. An example of such an one dimensional array is an circular array which is used to scan 360° in the

plane of the array. Since both these array classes include conformal arrays, conformal arrays belonging to the first group will be called "one dimensional conformal arrays" and conformal arrays in the two dimensional array group will be called "two dimensional conformal arrays".

5.4.1 Details of Constraints on Radiation Pattern

The radiation pattern constraints are applied by means of a mask (5.44). If the radiation pattern is outside the pattern mask the radiation pattern magnitude is changed while retaining the original phase; if the radiation pattern is inside the mask the value is retained.

In the case of one dimensional arrays pencil beams as well as shaped beams can be synthesised. For shaped beams, the radiation pattern mask is described by a polynomial of the pattern angle $S(\theta)$ in the main or shaped beam region. This is often referred to as the shaping function. A zero to maximum ripple R specifies the acceptable level above and below the shaping function. The pattern mask in the shaped beam region is

$$S_U(\theta) = S(\theta) + R \quad \text{and} \quad S_L(\theta) = S(\theta) - R. \tag{5.69}$$

To set the main beam peak at 0dB the absolute level of the shaping function must be allowed to move up or down slightly. Since the shaping function is in polynomial form, the constant term can be used to control the shaping function level. On each side of the main beam, between the main beam region and the sidelobe regions is a transition region. The width of the transition regions control the roll-off from the main beam to the sidelobe level.

In the case of two dimensional arrays shaped beam patterns as well as contoured footprint patterns can be synthesised. Contoured patterns are described by a set of θ-values for a number of ϕ-cuts; the first θ-value indicates the end of the main beam region and the second indicates the start of the sidelobe region. The ripple inside the main beam must also be specified.

Shaped beams are specified in one ϕ in the same manner as for the one dimensional arrays. Similar to the contoured beam specification, θ-values in a number of ϕ-cuts are used to control the main beam roll-off. The software is written such that the shaped beam can only be specified in the $\phi = 0°$ -cut and the direction $(0, 0)$ must be in the main beam region.

The side lobe region, for all the different pattern types have a default sidelobe level. In addition to the default sidelobe level the sidelobe region can by divided into a number of piece wise linear subsections. Fixed nulls can also be specified anywhere in the sidelobe region, with a target suppression at each nulls.

In pattern synthesis we are interested in the radiated power, expressed in decibels. Thus both the pattern and the mask is in decibels. The error distance of the m-th pattern point of the k-th iteration is the distance between the pattern of the k-th iteration before

and after the application of the pattern mask:

$$\xi_{km} = 10\left|\log(|f'_m|^2) - \log(|f_m|^2)\right| \tag{5.70}$$

The total radiation pattern error at the k-th iteration is the average of the error distances at all pattern angles

$$\xi_k = \frac{1}{M}\sum_{m=1}^{M}\xi_{km} = \frac{10}{M}\sum_{m=1}^{M}\left|\log(|f'_m|^2) - \log(|f_m|^2)\right|. \tag{5.71}$$

If the weighted least squares inverse is used in the back projector relative weights must be assigned for each row of the radiation matrix. Aside from the default weight of one, the main lobe region and each sidelobe subregion are assigned a nominal weight according to its particular importance. Each of the fixed nulls are also assigned an individual weight. The relative weight of each pattern point is dependent on the error distance of that pattern point. The weight function consists of three linear sections:

$$w_m = w_0\begin{cases}1 & \text{if } \xi_{km} \le \xi_0\\ w_{slope}(\xi_{km} - \xi_0) & \text{if } \xi_0 \le \xi_{km} \le \xi_p\\ w_{peak} & \text{if } \xi_{km} \ge \xi_p\end{cases} \tag{5.72}$$

where ξ_0, w_{slope} and w_{peak} are specified by the user, w_0 is the default or nominal weight of the particular region and ξ_p is calculated from

$$\xi_p = \xi_0 + (w_{peak} - 1)/w_{slope}. \tag{5.73}$$

5.4.2 Detail of Constraints on Excitation

Four different excitation constraints have been implemented: symmetric, pure real and dynamic range and smoothness.

The excitation can be constrainted to be symmetric in both magnitude and phase

$$a_n = a_{N+1-n} = \tfrac{1}{2}(a'_n + a'_{N+1-n}) \tag{5.74}$$

or symmetry in just the magnitude only

$$\begin{aligned}|a_n| = |a_{N+1-n}| &= \tfrac{1}{2}\left(|a'_n| + |a'_{N+1-n}|\right)\\ \angle a_n &= \angle a'_n\\ \angle a_{N+1-n} &= \angle a'_{N+1-n}\end{aligned} \tag{5.75}$$

The pure real excitation constraint is applied by keeping the magnitude of excitation constant and changing the phase to 0° or 180° depending on the sign of the real part of the original excitation

$$a_n = \text{sign}(\mathcal{R}\{a'_n\})|a'_n|. \tag{5.76}$$

The dynamic range is defined as the ratio of the maximum excitation to the minimum excitation (2.25). Since a change in the largest excitation will influence the radiation pattern the most changes are made only to the smaller excitations. The phase of the excitation is preserved. If the magnitude of an excitation is below a_{off} that element is switched off.

$$a_n = \begin{cases} a'_n & \text{if } |a'_n| \geq a_{min} \\ a_{min}\dfrac{a'_n}{|a'_n|} & \text{if } a_{off} \leq |a'_n| < a_{min} \\ 0 & \text{if } |a'_n| < a_{off} \end{cases} \tag{5.77}$$

where a_{min} is the minimum allowable excitation to obtain the specified dynamic range.

The smoothness constraint is implemented by fractionally increasing the element a_n with the maximum $\frac{|a_{n\pm1}|}{|a_n|}$ until the required smoothness is obtained.

After applying the excitation constraints the power of the excitation is normalised to the total power of the original excitation:

$$\sum_{n=1}^{N} |a_n|^2 = \sum_{n=1}^{N} |a'_n|^2. \tag{5.78}$$

5.4.3 Element Patterns

Before any synthesis can be attempted the field pattern of each element, including the effects of the host vehicle on the element pattern, must be determined. Geometrical Theory of Diffraction (GTD) is an effective numerical technique for analysing the radiation of an element, taking into account the effect of the vehicle it is mounted on. Recent publications [120, 121, 113] used analytical functions for element patterns. The power patterns of the elements showed good correlation. The main difference between the analytical and GTD element patterns can be summarised as follows: Analytical element patterns do not have any phase variation (the functions are pure real), while the element patterns generated with GTD showed large phase variation off the broadside direction. The radiation pattern summation includes the field pattern and not the power pattern of the array elements. Although the power patterns of the two approaches are similar the lack of phase information in the analytical functions may cause serious inaccuracies, as will be shown later in Section 5.6.4.

Even if the radiation element used in the conformal array may have good cross polar characteristics, a slanted edge of the host vehicle will cause a cross polar component in the radiated field pattern. Thus, for the general conformal array case not only must the co-polarisation pattern be obtained, but also the cross polarisation pattern. This can also be computed using GTD. The projection method is adaptable to take both the co- and cross polarisation into account during the synthesis of conformal arrays. Geometrical Theory of Diffraction was implemented for only elliptical cylinders (of which circular arc arrays are a special case) and spherical arrays.

Cubic splines interpolation (an interpolation scheme which is continuous up to the second derivative) of the GTD element patterns of the one dimensional conformal array cases is implemented. This gives a very accurate radiation pattern even between the GTD pattern sample points. Due to a lack of computer power (CPU speed as well as memory) the two-dimensional case was programmed to use linear interpolation for both the co- and cross polarisation.

A number of analytical element patterns have also been implemented. Results of an investigation into the importance of accurate element patterns (versus analytical element patterns) are presented in Section 5.6.4.

5.5 Starting Point Selection

The choice of a particular starting point (or set of initial values) may cause any non-linear numerical optimisation algorithm to fall in a local minima, thus the initial values of the optimisation parameters (excitations in the array synthesis case) are crucial to the success of any optimisation process. A proper selection of the starting point will be close enough to the final solution to avoid falling into a trap. The choice of a good starting point should include the constraints on the excitations, for example if there is a constraint on the dynamic range of the excitations a good starting point may be obtained by a phase only synthesis where the amplitude of each element is fixed.

For uniformly spaced linear arrays the method of Orchard, Elliot and Stern [54] can be used. The method is root-based and gives a number of patterns that satisfy the pattern requirements. The one that best approximates the other constraints (eg. excitation smoothness) can be chosen. This starting point will be close to the point of convergence. For uniformly spaced planar arrays the methods of Chapter 3 or Chapter 4 will give a good initial point. However, there is no clear way to select a starting point for conformal arrays.

Finding a good starting point is not simple because of the non-linear nature of the synthesis problem. A number of different methods to obtain a good starting point is investigated in this section.

5.5.1 Radiation Pattern Mask

One obvious solution may be the excitation obtained by the back projector from the centre of the mask ($\frac{1}{2}(S_U+S_L)$) with a zero phase. The disadvantage of this approach is that a non-optimal phase distribution is forced onto the radiation pattern from the onset of the iterations; which may lead to a local minima. A possible way to overcome this difficulty is to assign some phase function or even a random phase to the mask.

5.5.2 Component Beam Technique

A number of pattern angles are chosen in the shaped beam region. For every pattern angle a pencil beam with its peak at that pattern angle is computed. We will refer to these pencil beams as *component beams*. To obtain a component beam the radiation pattern at angles in the sidelobe region is set to zero. This removes the phase ambiguity in the power synthesis problem. Maximum likelihood or weighted least squares can be used to compute the excitation of each component beam in a single step. Weighted least squares will give better sidelobe level performance as the weight of the main beam can be increased relative to the sidelobe weights. The starting radiation pattern is then the summation of each component beam, weighted with the desired value of the radiation pattern. An additional phase shift can also be applied to each of the component beams.

This is reminiscent of Woodward synthesis, except that the component beams are not orthogonal beams in general and the number of component beams used is higher than the number of orthogonal beams used in Woodward synthesis.

5.5.3 Genetic Algorithm to Obtain a Phase Function

Genetic algorithm is a powerful tool in the optimisation of non-linear functions, especially for functions of few variables. Unfortunately the large number of variables in array synthesis makes genetic algorithm unsuitable for array synthesis problems. However, by drasticly reducing the number of variables, genetic algorithm can be used to find good initial values, or warm start, for the general synthesis problem

The phase variation in the shaped beam region of an array pattern is smooth, making possible the definition of a phase function with few variables. Let us first consider shaped beams in one principal cut of the antenna pattern. The variables are a number of coordinates, each consisting of a pattern angle θ_i in the principal pattern cut and the phase α_i at that pattern angle. The pattern angle of the last coordinate is anchored at the end of the shaped beam region. The phase function $P(\theta)$ is the cubic splines interpolation between these coordinates. If I coordinates are chosen, the phase function consist of $(2I-1)$ variables.

A number of pattern angles (M) are chosen in the shaped beam region and the component beams in those directions $C_m(\theta)$ are determined as discussed in the previous section. The radiation pattern is then the summation of each component beam, weighted with the desired value of the radiation pattern as well as shifted in phase with the values of the phase function at that pattern angle θ,

$$F(\theta) = \sum_{m=1}^{M} S(\theta_m) e^{P(\theta_m)} C_m(\theta). \tag{5.79}$$

The excitation for this radiation pattern can easily be computed

$$a_n = \sum_{m=1}^{M} S(\theta_m) e^{P(\theta_m)} c_{nm} \tag{5.80}$$

where a_n is the n-th excitation and c_{nm} the n-th excitation of the of the m-th component beam.

Genetic algorithm is used to find the best values for the phase function variables. After calculating the excitation by using (5.80), the excitation constraints are applied. The cost function optimised by genetic algorithm is the total pattern error (5.71) of the radiation pattern produced by the constrainted excitation.

This calls to mind the well known Woodward synthesis method. The major differences are that the component beams are not orthogonal as well as the additional phase shift of each of the component beams.

The proposed method is as follows:

- Select a number of directions in the shaped beam region (θ_m).
- For each of these pattern directions compute a corresponding component beam $C_m(\theta)$.
- Use genetic algorithm to find the optimum phase function $P(\theta_i, \alpha_i)$.

In the case of flat-top or fan beams for both one dimensional and two dimensional arrays between 5 $(I = 3)$ and 11 $(I = 6)$ variables are needed to describe the phase function adequately.

In the case of contoured footprint patterns each phase function coordinate consists of both pattern angles (θ_i, ϕ_i) and the phase values α_i. The pattern angles are selected in a small number of rings around the direction $(0, 0)$, which is also the phase reference point. The phase function is a linear interpolation of these coordinates. Genetic algorithm optimises only the phase values α_i.

5.6 Application and Convergence

In order to get a better grasp of the convergence phenomena it is imperative to look into the algorithmic detail of the specific implementation. Two systems for selection of the pattern angles are available. The first is a fixed number of pattern angles uniformly spaced in the main beam and sidelobe regions. The second system finds all the extrema of difference between the radiation pattern and the shaping function in the main beam region; and the sidelobe peaks in the sidelobe region. All these extrema angles are incorporated into the set of pattern angles.

The algorithm is divided into an outer and an inner loop. In the outer loop the optimum absolute value for the shaping function is set (see Section 5.4.1). If the second pattern angle selection scheme is chosen a new set of pattern angles is determined as described above in each outer loop; and the radiation matrix must be recomputed. A change in either the shaping function level or the pattern angles result in a "new" synthesis problem. The inner loop uses the information forthcoming from the outer loop to perform the projection with or without relaxation. The outer loop in effect creates a new synthesis problem for the inner loop using the excitation of the previous outer loop iteration as new starting point. Convergence in the outer loop can not be guaranteed; $\xi_{k+1} \leq \xi_k$ does not hold.

If weighted least squares is used as the backward projector the inverse of the radiation matrix must be computed in each inner loop iteration; because the relative weighting (depending on the radiation pattern) changes with each iteration. This will cause a slight increase in execution time for each iteration.

Since the optimum value for the relaxation parameter (if relaxation is selected) is calculated numerically in each of the inner loops, the application of relaxation will result in a significant increase in execution time per iteration. However, relaxation should reduce the total number of iterations.

Convergence and the rate of convergence depend on a number of factors:

1. The type of backward operator: maximum likelihood method (abbreviated as "MLM") or weighted least squares (abbreviated as "WLS").
2. Whether or not relaxation is used.
3. The number and directions of far-field angles.
4. The initial or starting values.
5. Radiation pattern constraints.
6. Excitation constraints.

There exist a lot of interaction between these factors. A number of case studies have been used to gauge the performance of various options available. The first two factors will be discussed and also illustrated by case study #1; and the next two in case studies #2 and #3, respectively. The radiation pattern constraints and the excitation constraints do not influence the convergence directly, but determine some of the sets involved. Too strict constraints will result in sets with no intersection. The influence of the constraints is implicit in all case studies and examples, and will thus not be investigated on its own.

An equi-spaced linear array is used in the first three case studies because various optimal (or near optimal) synthesis methods exist for this kind of array. The first three case studies are based on a sixteen element ($N=16$), uniformly spaced linear array, with inter element spacing $d_x = 0.5\lambda$. The pattern requirement is a $\csc^2(\phi)$ main beam from

$\phi=100°$ to $\phi=140°$, with a maximum peak-to-peak ripple of 1.0dB. A sidelobe level of -20dB is required, except from 70° to the main beam where the sidelobes must be below -30dB. This is the pattern synthesised by Orchard, Elliott and Stern [54], and is often used in literature as a benchmark. The pattern obtained in [54] has a main lobe below -30dB at 90.6° and below -20dB at 142.0° ; and the dynamic range of the excitation is $DR=5.15$.

Although the choice of element patterns may not have a marked effect on the convergence, the last case study shows the importance of accurate element patterns in the analysis and synthesis of conformal arrays.

5.6.1 Case Study #1: Backward Operators and Relaxation

Two starting points will be investigated. The first set of initial values is the excitation obtained by Orchard et al. [54], with the smaller excitations increased to obtain a dynamic range of $DR=3.33$. This set of initial values is known to be close to a global minimum. The other starting point is obtained by the component beams with a genetic algorithm optimised phase distribution. The starting excitation selection will be discussed in more detail in case study #3. Both pattern angle selection systems will be used. For the selection system that include all the extrema angles, the minimum number of angles is twice the number of array elements. The number of pattern angles used in the fixed angle system is ten times the number of array elements. The trials are:

1. Orchard excitation start excitation and extrema pattern angles selection with the number of pattern angles $M \geq 32$.
2. Genetic Algorithm initial excitation and extrema pattern angles selection with the number of pattern angles $M \geq 32$.
3. Orchard excitation start excitation and fixed pattern angles with the number of pattern angles $M=161$.

In addition to the radiation pattern specifications described, the excitation is optimised to give the smallest possible dynamic range $DR=3.75$. For all the cases the inner iterations are terminated after a maximum of 50 iterations or when the error ξ_k decreased with a factor of 5.

The convergence rates for the three different trial runs are drawn in Figure 5.4. The legend used is "NM" for maximum likelihood as backward projector without relaxation; "NW" for weighted least square as backward projector without relaxation; "RM" maximum likelihood as backward projector with relaxation and "RW" for weighted least squares as backward projector with relaxation. Table 5.1 lists the execution or CPU time and number of iteration for each trial. The computer is a DEC Alpha 266 running the OFS1 Unix operating system. When comparing the convergence rates and execution times a number of conclusions can be drawn:

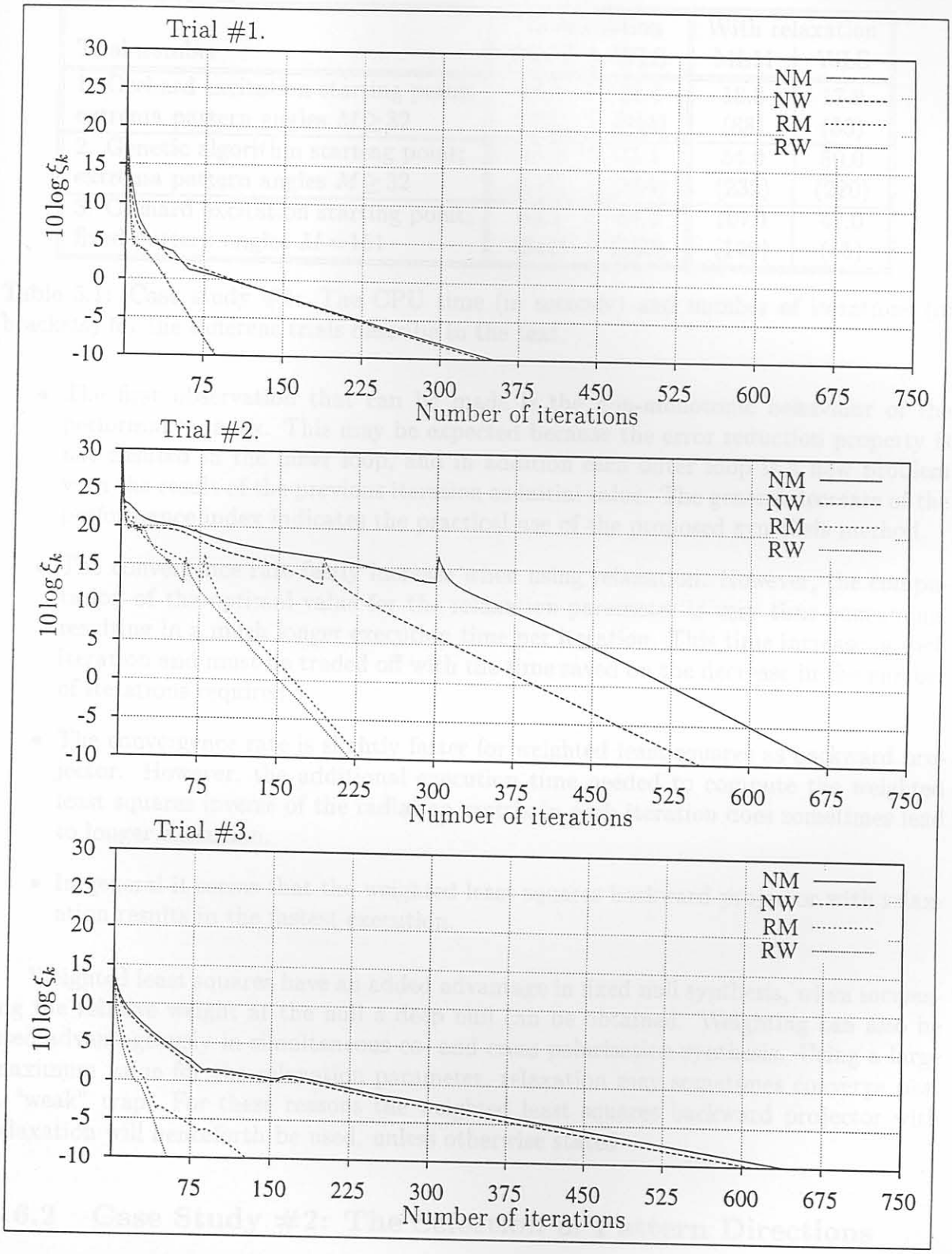

Figure 5.4: Case study #1: Convergence for the different applications. "NM" ≡ MLM without relaxation; "NW" ≡ WLS without relaxation; "RM" ≡ MLM with relaxation and "NW" ≡ WLS with relaxation.

Trial number	No relaxation MLM	No relaxation WLS	With relaxation MLM	With relaxation WLS
1. Orchard excitation starting point; extrema pattern angles $M \geq 32$	25.3 (353)	24.4 (344)	18.8 (88)	17.9 (86)
2. Genetic algorithm starting point; extrema pattern angles $M \geq 32$	50.8 (675)	41.1 (555)	54.0 (232)	50.0 (220)
3. Orchard excitation starting point; fixed pattern angles $M = 161$	63.1 (642)	63.1 (550)	107.1 (129)	47.0 (55)

Table 5.1: Case study #1: The CPU time (in seconds) and number of iterations (in brackets) for the different trials describe in the text.

- The first observation that can be made is the non-monotonic behaviour of the performance index. This may be expected because the error reduction property is not ensured in the inner loop, and in addition each outer loop is a new problem with the result of the previous iteration as initial value. The general decrease of the performance index indicates the practical use of the proposed syntehsis method.

- The convergence rate fastly increase when using relaxation. However, the computation of the optimal value for the relaxation parameter is very time consuming, resulting in a much longer execution time per iteration. This time increase in each iteration and must be traded off with the time saved on the decrease in the number of iterations required.

- The convergence rate is slightly faster for weighted least squares as backward projector. However, the additional execution time needed to compute the weighted least squares inverse of the radiation matrix in each iteration does sometimes lead to longer execution.

- In general it seems that the weighted least squares backward projector with relaxation results in the fastest execution.

Weighted least squares have an added advantage in fixed null synthesis, when increasing the relative weight at the null a deep null can be obtained. Weighting can also be used advantageously in simultaneous co- and cross polarisation synthesis. Using a large maximum value for the relaxation parameter, relaxation may sometimes converge past a "weak" trap. For these reasons the weighted least squares backward projector with relaxation will henceforth be used, unless otherwise stated.

5.6.2 Case Study #2: The Selection of Pattern Directions

The software is written such that for both pattern angles selection schemes have a higher density in the shaped beam region than the sidelobe region. No pattern angle is selected in transition regions. A number of angles are always included:

Description	M	DR	No relaxation Time	Iterations	Error	With relaxation Time	Iterations	Error
Trial 1:	*81*	*3.50*	*7.0*	*828*	*81.7*	*6.3*	*37*	*79.2*
Orchard,	161	3.50	67.9	831	25.5	31.2	58	23.7
Fixed M	241	3.50	161.3	831	8.7	132.3	58	8.1
	321	3.75	106.0	469	10.5	47.6	48	8.5

Table 5.2: Case study #2: The dynamic range, CPU time (in seconds), number of iterations and radiation pattern error for different numbers of pattern angles for the first trial.

- the start and end angles of the shaped beam region,
- the start of the sidelobe regions and
- all fixed null angles.

Four trials will be investigated using weighted least squares as backward operator with and without relaxation. The two starting points used in the previous case study will be used again. The excitation is constrainted to obtain the lowest possible dynamic range. The trials are:

1. Orchard excitation start excitation and fixed pattern angles.
2. Genetic algorithm initial excitation and fixed pattern angles.
3. Orchard excitation start excitation and extrema pattern angle selection.
4. Genetic algorithm initial excitation and extrema pattern angle selection.

Determining the fixed pattern angles is straight forward and not CPU intensive. The number of pattern angles must be large enough to ensure that all extrema angles are included in the set of angles. This would require large matrixes, resulting in long computation of the radiation matrix and its inverse. If the pattern sampling is too coarse not every peak outside pattern mask will be included in numerical error function, and thus may not be representative of the true error. With the extrema angle selection scheme the numerical search algorithm is used to obtain the pattern extrema in the outer loop. This operation is very CPU intensive. Since the number of extrema is in the same order as the number of array elements, the matrixes are smaller and less time is spent on their computation.

The results from the different trials are tabulated in Table 5.2 and Table 5.3. The different trials have very similar results in the radiation pattern as well as the excitation, as can be seen in Figure 5.5. In this figure the radiation pattern and excitation of the emphasised rows in Tables 5.2 and 5.3 are shown.

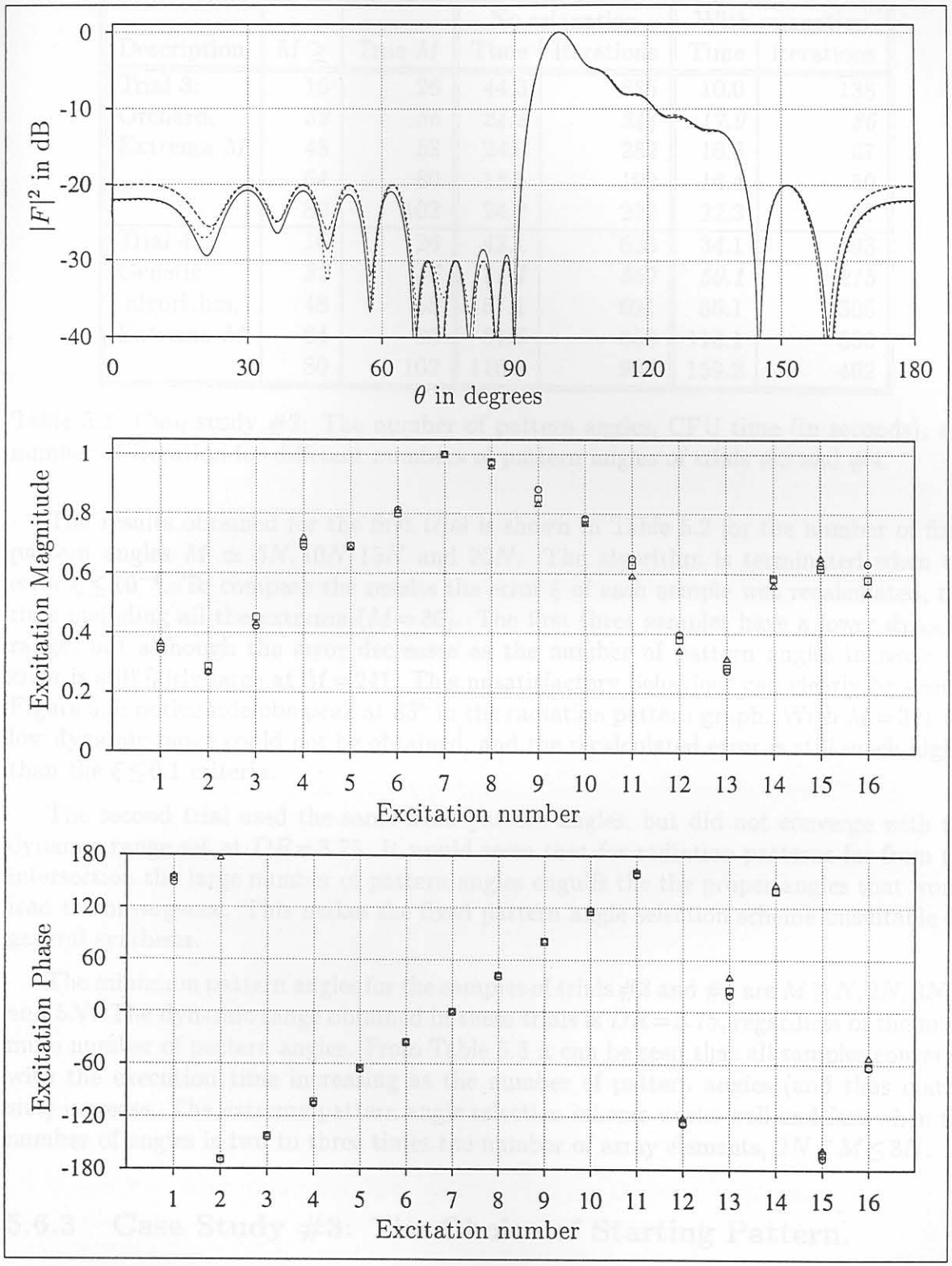

Figure 5.5: Case Study #2: The radiation pattern (top) and excitation amplitude (middle) and phase (bottom) for some trials (see text). (Legend: $\square \equiv$ first trial, $\odot \equiv$ third trial and $\triangle \equiv$ fourth trial.)

Description	$M \geq$	True M	No relaxation Time	No relaxation Iterations	With relaxation Time	With relaxation Iterations
Trial 3:	16	26	44.3	885	10.0	138
Orchard,	*32*	*36*	*24.2*	*344*	*17.9*	*86*
Extrema M	48	58	24.0	282	18.3	67
	64	80	18.5	192	16.4	50
	80	102	24.2	222	22.3	57
Trial 4:	16	26	42.1	633	34.1	193
Genetic	*32*	*36*	*41.1*	*557*	*50.1*	*215*
algorithm,	48	58	57.1	691	86.1	306
Extrema M	64	80	81.6	856	118.1	350
	80	102	116.1	998	159.2	402

Table 5.3: Case study #2: The number of pattern angles, CPU time (in seconds), and number of iteration for different numbers of pattern angles of trials #3 and #4.

The results obtained for the first trial is shown in Table 5.2 for the number of fixed pattern angles $M \simeq 5N, 10N, 15N$ and $20N$. The algorithm is terminated when the error $\xi \leq 10^{-4}$. To compare the results the error ξ of each sample was recalculated, this time including all the extrema ($M = 36$). The first three samples have a lower dynamic range, but although the error decreases as the number of pattern angles increase the error is still fairly large at $M = 241$. This unsatisfactory behaviour can clearly be seen in Figure 5.5; notice sidelobe peak at 83° in the radiation pattern graph. With $M = 321$ the low dynamic range could not be obtained, and the recalculated error is still much higher than the $\xi \leq 0.1$ criteria.

The second trial used the same fixed pattern angles, but did not converge with the dynamic range set at $DR = 3.75$. It would seem that for radiation patterns far from the intersection the large number of pattern angles engulfs the the proper angles that would lead to convergence. This makes the fixed pattern angle selection scheme unsuitable for general synthesis.

The minimum pattern angles for the samples of trials #3 and #4 are $M \geq N, 2N, 3N, 4N$ and $5N$. The dynamic range obtained in these trials is $DR = 3.75$, regardless of the minimum number of pattern angles. From Table 5.3 it can be seen that all samples converge, with the execution time increasing as the number of pattern angles (and thus matrix size) increase. The extrema pattern angle selection scheme works well and fast when the number of angles is two to three times the number of array elements, $2N \leq M \leq 3N$.

5.6.3 Case Study #3: The Choice of Starting Pattern.

The purpose of this case study is to illustrate the importance of a good starting point, as well as to show the relative performance of the different starting pattern selection algorithms. For each starting values the dynamic range of the excitation is interactively

Starting pattern selection	Dynamic Range
Orchard, Elliot and Stern's synthesis method	3.75
Unit excitation distribution	4.15
Pattern mask with zero phase distribution	4.90
Pattern mask with random phase distribution	4.55
Component beams with zero phase distribution	3.90
Component beams with linear phase distribution	3.90
Component beams with random phase distribution	4.95
Component beams with Genetic algorithm, 7 parameters	4.00
Component beams with Genetic algorithm, 9 parameters	3.75
Component beams with Genetic algorithm, 11 parameters	3.90

Table 5.4: Case study #3: The dynamic range obtained by the various starting pattern selection schemes

lowered to obtain a suitable radiation pattern with the excitation with the lowest dynamic range. Weighted least squares is selected as the backward projector and relaxation is used.

In the case of pencil beams a single component beam will be a good starting pattern. However, in the case of shaped or contoured beams a good representation of the phase in the shaped region is very important as the phase distribution tends to carry over from iteration to iteration. This phenomenon has also been noted by others [141].

To illustrate the component beam approach, the top graph in Figure 5.6 shows some possible component beams for this case. The bottom graph displays the component beam starting pattern with the phase function optimised by genetic algorithm with nine parameters, as well as the final pattern obtained with the synthesis method. The radiation pattern obtained with Orchard's synthesis method is also drawn as a reference.

The best dynamic range obtained for each initial values selection method is tabulated in Table 5.4. From the different dynamic range values it is clear that a multitude of traps do exist. As expected starting points that do not consider the phase distribution in the shaped beam region do fall into traps. The genetic algorithm must optimise few enough variables to obtain an answer in a reasonable time. However, too few parameters will result in a function that does not adequately describe the phase distribution. With this in mind, the table shows that nine parameters are a good choice for the shaped beam synthesis problem in the case study. An increase in the shaped beam beamwidth or, to a lesser extent, an increase in the number of elements will require more variables. A "simpler" beam shape, like a flat-top beam, less variables will be adequate.

It does not seem unreasonable to assume that the Orchard synthesis method result in an excitation very close to the optimum. Since the excitation obtained with the nine parameter component beam starting pattern result in almost exactly the same excitation (less than 0.3% difference in magnitude and less than 0.2° difference in phase) one may assume that the component beam approach with genetic algorithm to optimise the phase distribution will result in near optimum patterns. This, of course, cannot be guaranteed.

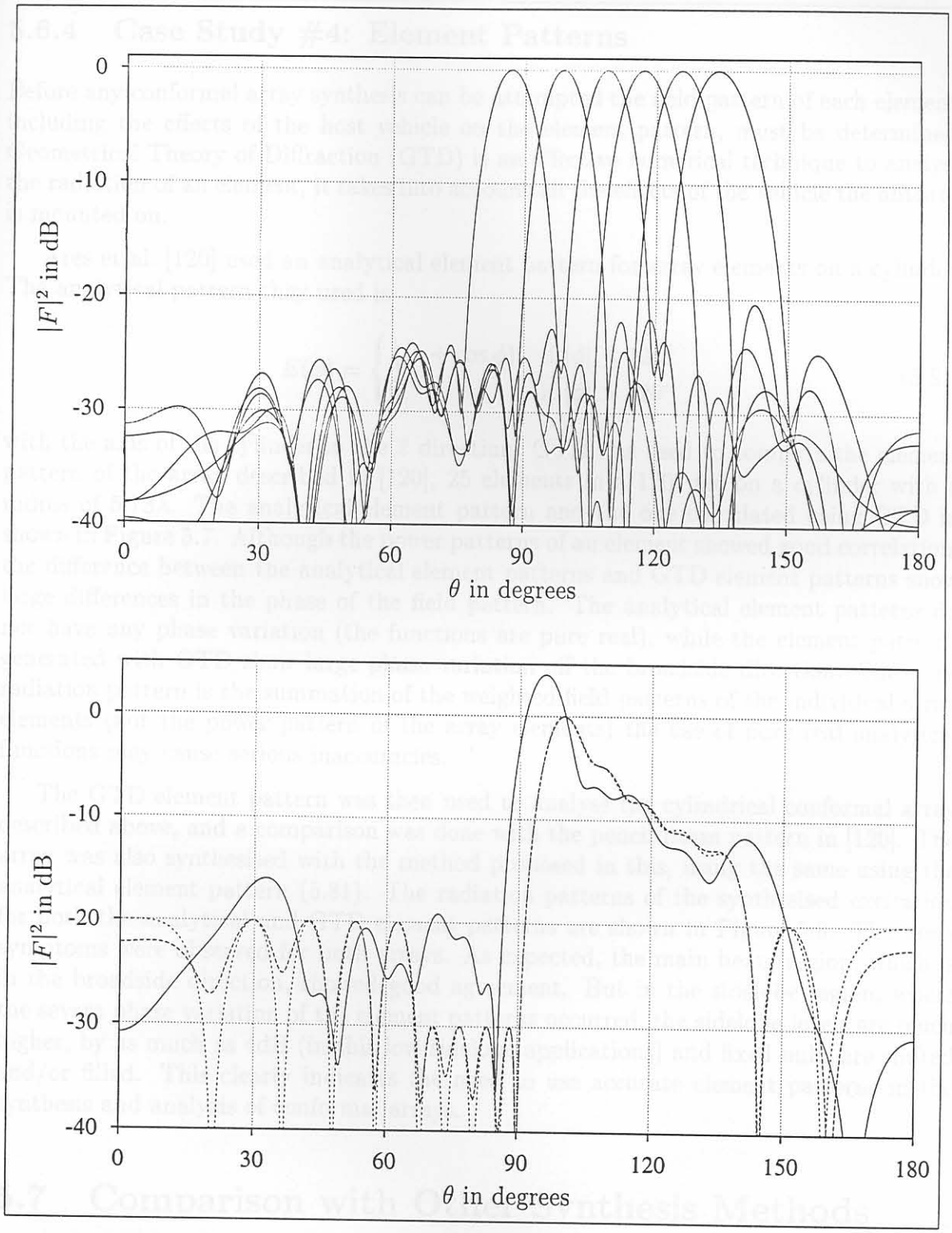

Figure 5.6: Case study #3: The top graph display the component beams used to obtain the starting pattern. The starting pattern shown as the solid trace in the bottom graph. The dashed line in the bottom graph represent the final optimised pattern and the dotted line pattern obtained by Orchard's method (as a reference pattern).

5.6.4 Case Study #4: Element Patterns

Before any conformal array synthesis can be attempted the field pattern of each element, including the effects of the host vehicle on the element pattern, must be determined. Geometrical Theory of Diffraction (GTD) is an effective numerical technique to analyse the radiation of an element, it takes into account all the effects of the vehicle the antenna is mounted on.

Ares et al. [120] used an analytical element pattern for array elements on a cylinder. The analytical pattern they used is

$$E(\phi) = \begin{cases} \frac{1}{3}(1+\cos\phi) & \text{if } |\phi| \leq 120^\circ \\ 0 & \text{if } |\phi| > 120^\circ \end{cases} \tag{5.81}$$

with the axis of the cylinder in the $\hat{z}$ direction. GTD was used to compute the element pattern of the array described in [120]; 25 elements in a 120° arc on a cylinder with a radius of 5.73λ. The analytical element pattern and the one calculated using GTD in shown in Figure 5.7. Although the power patterns of an element showed good correlation, the difference between the analytical element patterns and GTD element patterns show large differences in the phase of the field pattern. The analytical element patterns do not have any phase variation (the functions are pure real), while the element patterns generated with GTD show large phase variation off the broadside direction. Since the radiation pattern is the summation of the weighted field patterns of the individual array elements (not the power pattern of the array elements) the use of pure real analytical functions may cause serious inaccuracies.

The GTD element pattern was then used to analyse the cylindrical conformal array described above, and a comparison was done with the pencil beam pattern in [120]. The array was also synthesised with the method proposed in this, using the same using the analytical element pattern (5.81). The radiation patterns of the synthesised excitation for both the analytical and GTD element patterns are shown in Figure 5.8. The same symptoms were observed for both arrays. As expected, the main beam region, which is in the broadside direction, showed good agreement. But in the sidelobe region, where the severe phase variation of the element patterns occurred, the sidelobe levels are much higher, by as much as 4dB (in this low sidelobe applications) and fixed nulls are shifted and/or filled. This clearly indicates the need to use accurate element patterns in the synthesis and analysis of conformal arrays.

5.7 Comparison with Other Synthesis Methods

5.7.1 Iterative Least Squares Methods

Carlson and Willner [141] first suggested using weighted least squares in the synthesis of arrays. The weighted least squares is analytical and yields an optimal pattern, for the

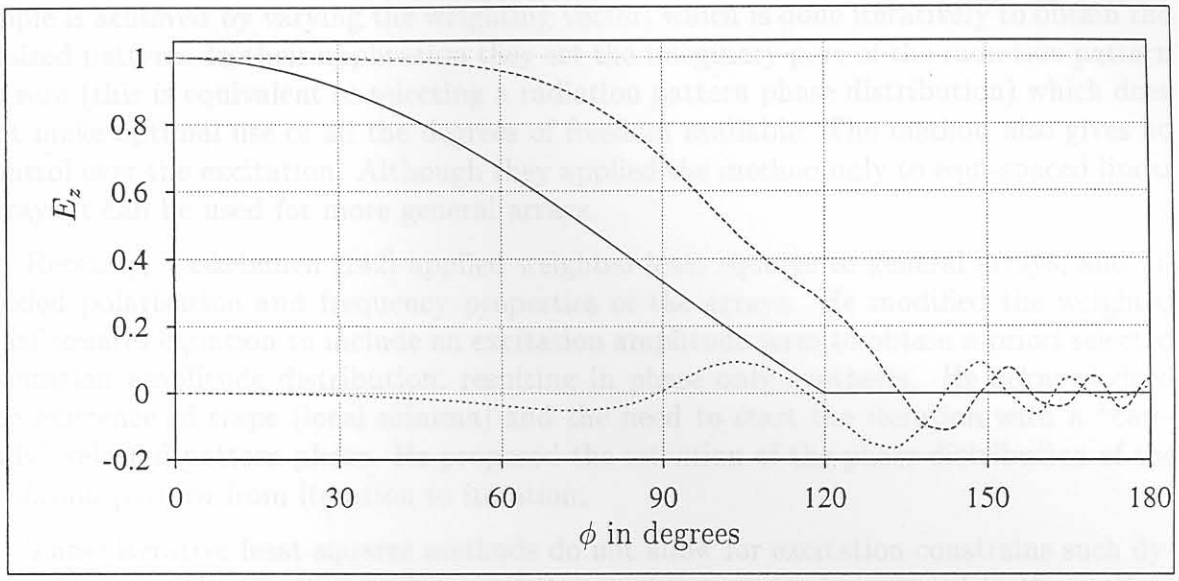

Figure 5.7: Case study #4: The analytical element pattern (the solid line) and the real (dashed line) and imaginary (dotted line) parts of the GTD element pattern.

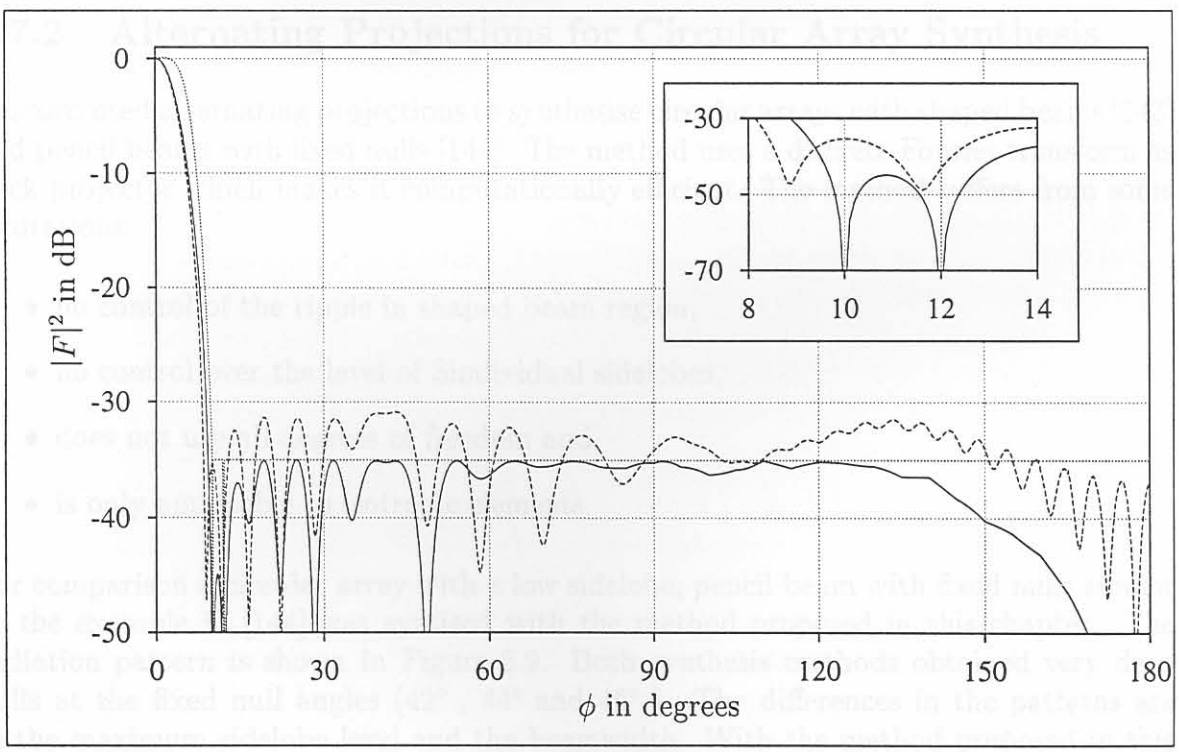

Figure 5.8: Case study #4: The solid curve is synthesised radiation pattern with analytical element patterns; the dashed curve is same excitation but with GTD element patterns. The magnification shows the region of the radiation pattern at the fixed null positions.

specific set of values, in a single computation. Control of the sidelobe level or main beam ripple is achieved by varying the weighting vector; which is done iteratively to obtain the desired pattern. In their application they set the imaginary part of the radiation pattern to zero (this is equivalent to selecting a radiation pattern phase distribution) which does not make optimal use of all the degrees of freedom available. The method also gives no control over the excitation. Although they applied the method only to equi-spaced linear arrays it can be used for more general arrays.

Recently, Vaskelainen [142] applied weighted least squares to general arrays, and included polarisation and frequency properties of the arrays. He modified the weighted least squares equation to include an excitation amplitude term to obtain a priori selected excitation amplitude distribution, resulting in phase only synthesis. He acknowledged the existence of traps (local minima) and the need to start the iteration with a "carefully" selected pattern phase. He proposed the retention of the phase distribution of the radiation pattern from iteration to iteration.

These iterative least squares methods do not allow for excitation constrains such dynamic range. The iterative variation of the weighting vector is included in the method proposed in the thesis when the weighed least squares is used as the backward operator (5.72).

5.7.2 Alternating Projections for Circular Array Synthesis

Vescovo used alternating projections to synthesise circular arrays with shaped beams [143] and pencil beams with fixed nulls [144]. The method uses a discrete Fourier transform as back projector which makes it computationally efficient. The method suffers from some limitations:

- no control of the ripple in shaped beam region,
- no control over the level of Sindividual sidelobes,
- does not use all degrees of freedom and
- is only applicable to isotropic elements.

For comparison a circular array with a low sidelobe, pencil beam with fixed nulls similar to the example in [144] was syntised with the method proposed in this chapter. The radiation pattern is shown in Figure 5.9. Both synthesis methods obtained very deep nulls at the fixed null angles (42° , 44° and 46°). The differences in the patterns are in the maximum sidelobe level and the beamwidth. With the method proposed in this chapter a uniform sidelobe level of -52dB was obtained (compared to a maximum sidelobe level of -37dB) with an additional null between the main lobe and the fixed nulls.

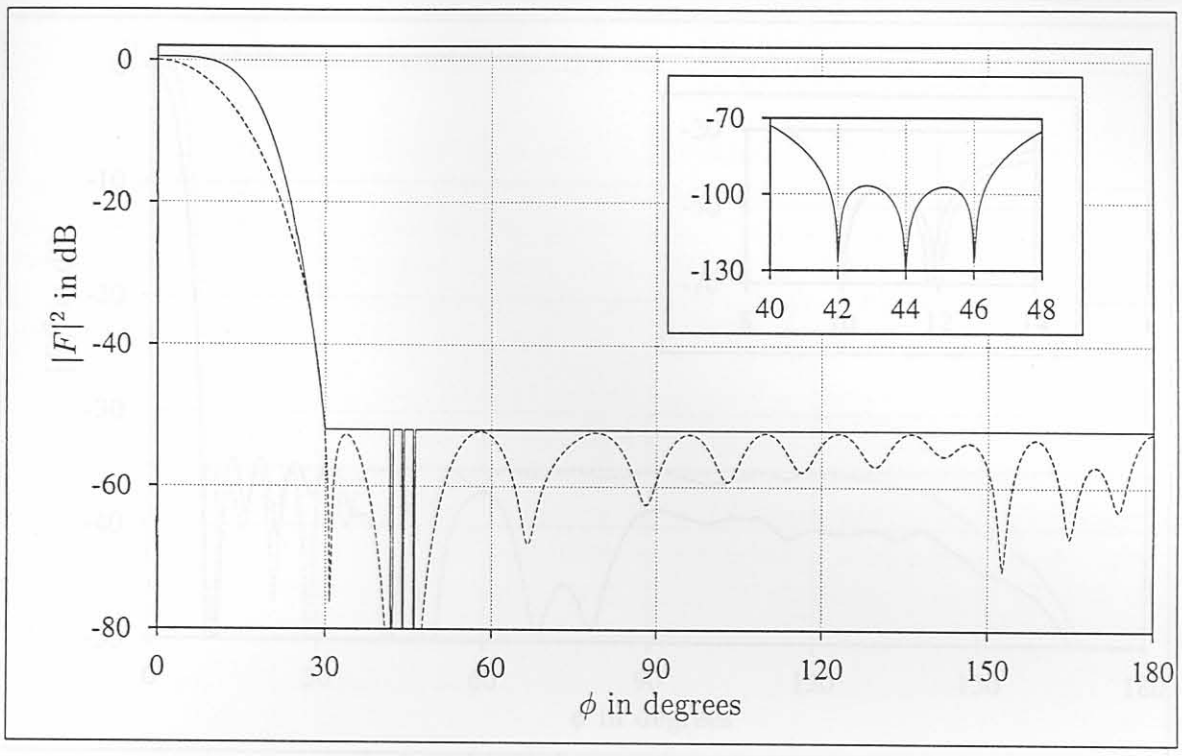

Figure 5.9: Radiation pattern for circular array, the magnification shows the radiation pattern at the fixed nulls

5.7.3 Generalised Projection Method

Recently Bucci, D'Elia and Romito extended the generalised projection method to power synthesis for conformal arrays [113]. They mention the problem of traps, and in order to avoid being trapped in local minima they adopted a non-standard choice of output variables; the power pattern instead of the field values. The backward operator can be performed by any minimisation algorithm. They used a self-scaled version of the BFGS (Broyden-Fleatcher-Golfarb-Shanno) method which takes into account the quadratic nature of the radiation pattern to be optimised.

They applied the method to synthesise contoured footprint and fan beam patterns for both a rectangular planar array and cylindrical array. The radiation patterns they published in [113] have high sidelobes in the principal planes, with very low sidelobes in the off principal plane cuts. This indicates a non-optimal solution to the synthesis problem. Sidelobes in rings around the main beam, as those in example 5.8.4 (rectangular array, see Figure 5.15) and example 5.8.5 (conformal array, see Figure 5.17), indicate a better solution.

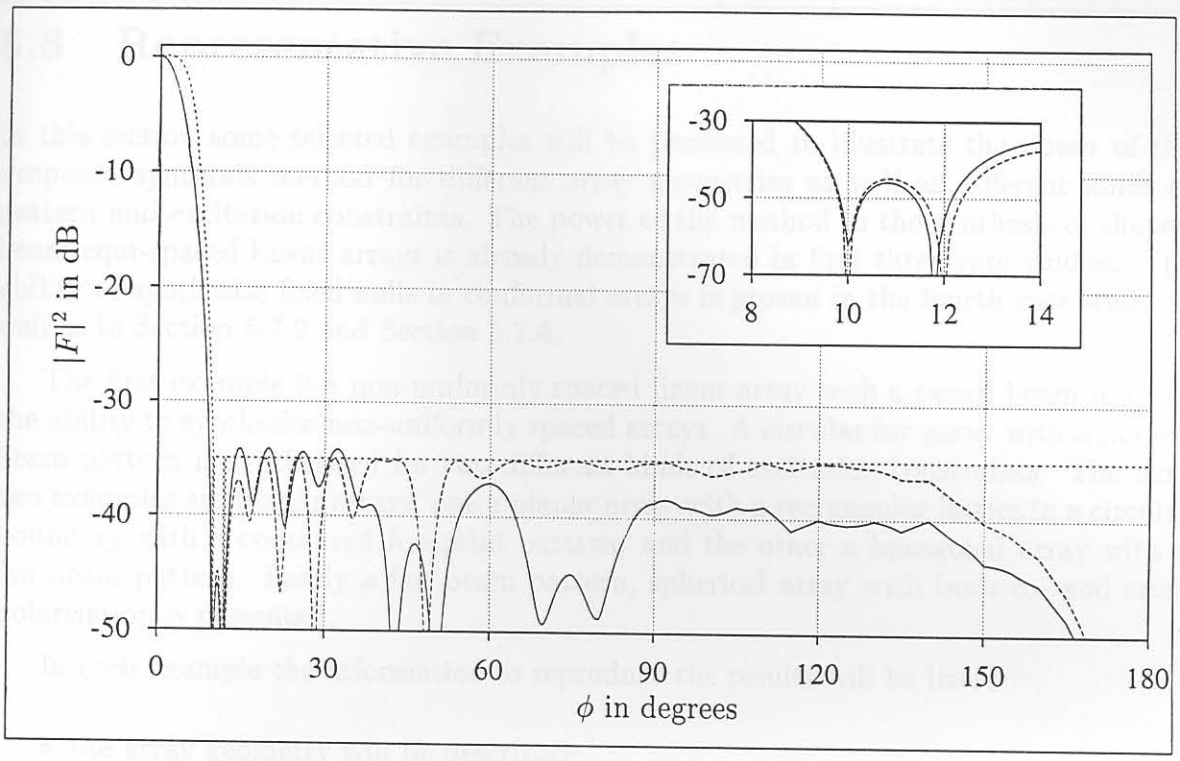

Figure 5.10: The radiation patterns obtained with simulated annealing (solid curve) and from the intersection of sets method (dashed curve). The magnification shows the region of the radiation pattern at the fixed nulls.

5.7.4 Simulated Annealing

Ares et al. [120, 121] used simulated annealing to synthesise conformal arrays. The cost function, the function to be minimised, can include terms to control the radiation pattern as well as terms placing constraints on the excitation. The authors claim that simulated annealing avoids local minima and converges to the global minimum of the cost function. To refute this claim one only has to obtain better results in one case.

Ares et al. [120] investigated a 25 element, 120° circular arc array on a cylinder with a radius of 5.73λ. The object of their first example is to synthesise a pencil beam with their fixed nulls at $\pm 10°$ and $\pm 12°$, while minimising the dynamic range. The authors did not meet the sidelobe level specification of -35dB they set, four sidelobe peaks are above this level with the highest peak at -34.2dB. The dynamic range they achieved is $DR=6.17$. For comparison, the dynamic range was iteratively minimised with the intersection of sets approach, while maintaining the same pattern requirements The same analytical element patterns were used. The dynamic range improved from $DR=6.17$ to $DR=4.85$, in addition the sidelobe level specification of -35dB was achieved. Thus a minima closer to global minimum was obtained with the method proposed in this chapter compared to the results obtained with simulated annealing. Both radiation pattern are shown in Figure 5.10, due to the symmetrical pattern only one half is shown.

5.8 Representative Examples

In this section some selected examples will be presented to illustrate the power of the proposed synthesis method for different array geometries as well as different kinds of pattern and excitation constraints. The power of the method in the synthesis of shaped beam equi-spaced linear arrays is already demonstrated in first three case studies. The ability to synthesise fixed nulls in conformal arrays is proven in the fourth case study as well as in Section 5.7.2 and Section 5.7.4.

The first example is a non-uniformly spaced linear array with a pencil beam to show the ability to synthesise non-uniformly spaced arrays. A circular arc array with a shaped beam pattern is synthesised for two different kinds of excitation constraints. The next two examples are planar arrays, one a planar array with a rectangular lattice in a circular boundary with a contoured footprint pattern; and the other a hexagonal array with a fan beam pattern. Lastly a fan beam pattern, spherical array with both co- and cross polarisation is presented.

In each example the information to reproduce the results will be listed:

- the array geometry will be described;
- followed by the specification of the radiation pattern requirements;
- next the excitation constraints, if any will be specified
- and the starting point selection will described

Additional notes and a short discussion will conclude each example.

5.8.1 Example #1: Linear non equi-spaced array with a pencil beam

This example is the synthesis of a thinned or non-uniformly spaced linear array. This is a one dimensional array. The specification are:

- Geometry: Sixteen elements are removed from a 32 isotropic element equi-spaced linear array, with the inter element spacing of the original array $d = \frac{1}{2}\lambda$.
- Pattern specification: A pencil beam radiation pattern with the narrowest possible beam width for a required sidelobe level of -13dB.
- Excitation constraints: No excitation constraints imposed.
- Starting point: A single component beam in the broad side direction.

Since the array consist of isotropic elements the radiation pattern and the array factor is the same. The radiation pattern and excitation for this array in shown in Figure 5.11. For comparison two uniformly spaced arrays, one with the same number of elements ($N = 16$) and original array $N = 32$, with Dolph-Chebychev distributions are also shown. The beamwidth of the thinned array is slightly less than the mean of the beamwidths of the reference Dolph-Chebychev arrays. On the excitation plot one can see that the thinned array does not have any edge brightening, while both reference arrays do exhibit edge brightening.

The proposed synthesis method does not have any provision to select which elements must be removed, for that [145] was used as a guide.

5.8.2 Example #2: Circular arc array with a shaped beam and tapered sidelobe levels

The circular arc array is an one dimensional conformal array. With the array in the xy-plane, the pattern is of interest in the xy-plane and is a function of ϕ only. For this example a shaped beam pattern with non uniform sidelobe level topography is required.

- Geometry: 45 elements are positioned at equal angular increments in a 120° arc on an infinite cylinder with a radius of $R = 15,34\lambda$. This radius and spacing produce an element on an arc spacing of 0.73λ. The elements are axial slots with length 0.48λ and width 0.01λ, the element patterns are calculated using GTD.
- Pattern specification:
  - a $\csc^2(\phi)$ shaped main beam from $\phi = -10°$ to $\phi = 30°$ with a peak-to-peak ripple of 1dB,
  - an inner sidelobe level from the main beam to $\phi = \pm 60°$ of -25dB,
  - sloping sidelobe envelope from -25dB at $\phi = \pm 60°$ to -30dB at $\phi = \pm 150°$,
  - and an outer sidelobe level from $\phi = \pm 150°$ to $\phi = \pm 180°$ of -30dB.
- Excitation constraints: Two different excitation constraints are imposed. Firstly the dynamic range (2.25) was interactively optimised and secondly the smoothness (2.26) was optimised.
- Starting point: Component beams with a nine variable phase function optimised with Genetic Algorithm was used for both cases.

The radiation patterns and excitation (amplitude only) for the two different sets of excitation constraints are displayed in Figure 5.12.

For the case where the dynamic range was optimised, the optimum dynamic range of $DR = 9.0$ was obtained; while the smoothness of this excitation is $S_m = 2.61$. On the

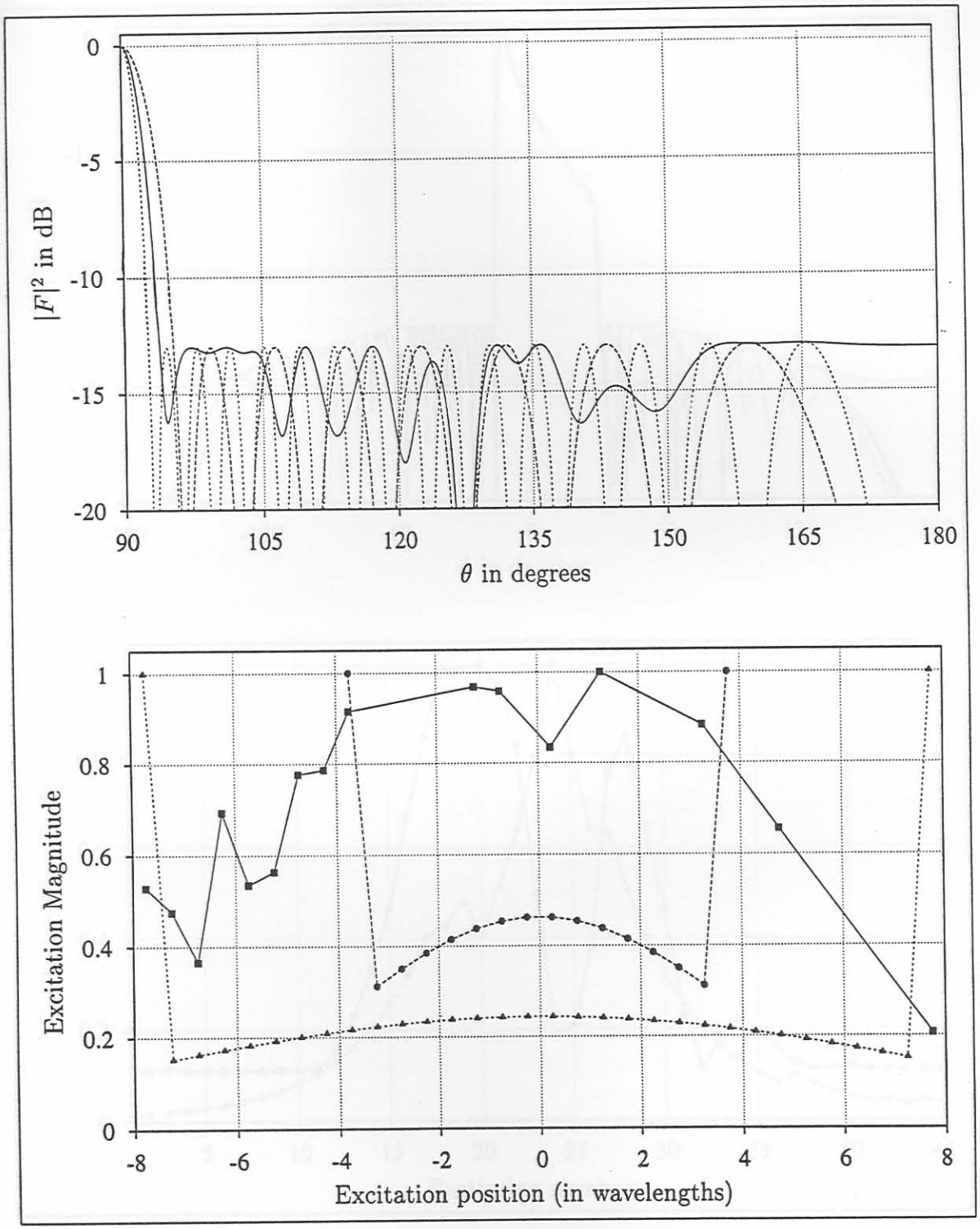

Figure 5.11: Example #1: The top graph show the radiation patterns of the thinned array (solid line) and the Dolph-Chebychev distributions. The excitations of these arrays are displayed on the bottom graph using the same line types.

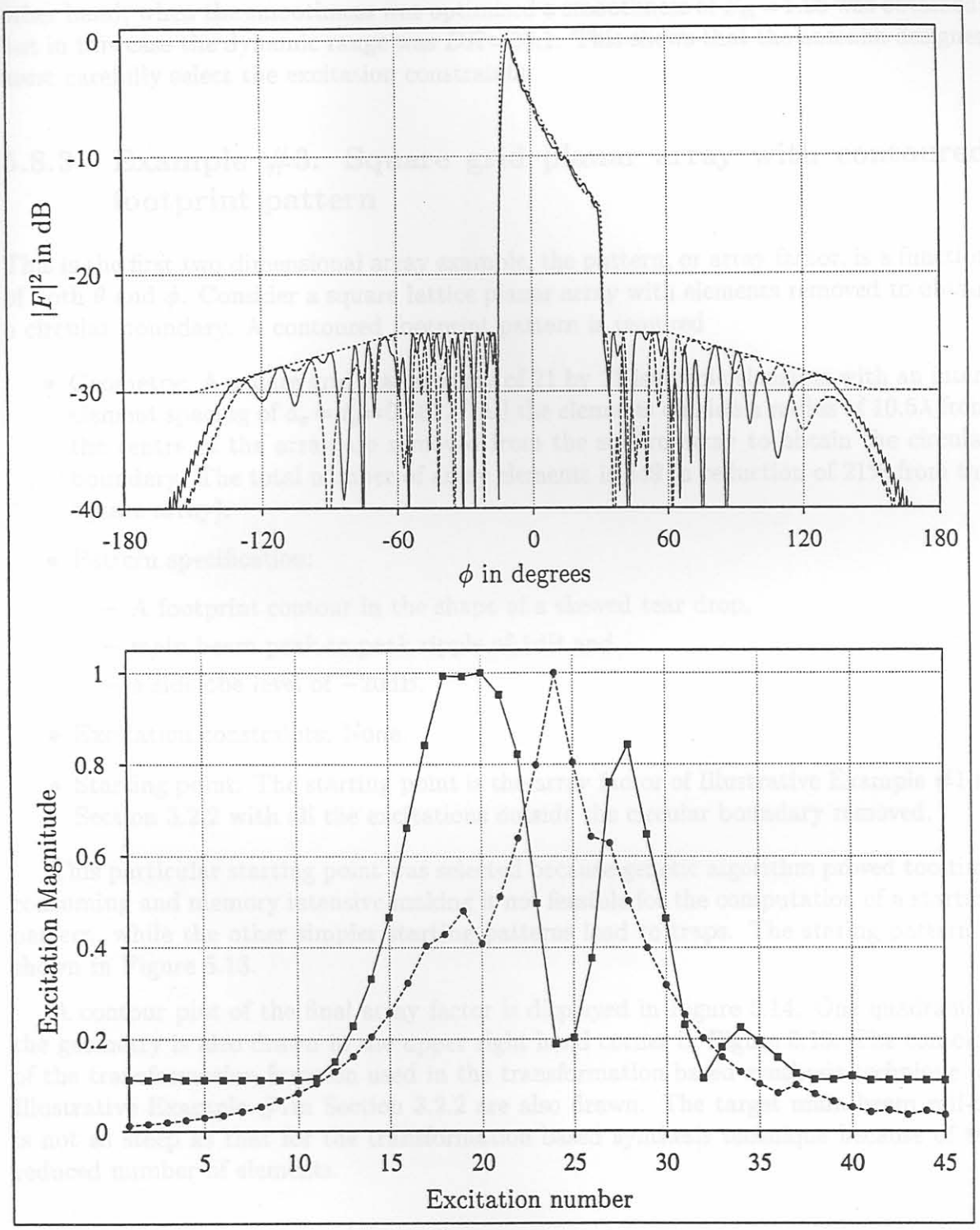

Figure 5.12: Example #2: The radiation patterns and excitations of the cylindrical arc arrays for the two different excitation constraints. The result with the dynamic range optimised is drawn by the solid traces and the result for the optimum smoothness is the dashed traces. The dotted curve represents the pattern mask.

other hand, when the smoothness was optimised a smoothness of $S_m = 1.26$ was obtained; but in this case the dynamic range was $DR = 83.1$. This shows that the antenna designer must carefully select the excitation constraints.

5.8.3 Example #3: Square grid planar array with contoured footprint pattern

This is the first two dimensional array example, the pattern, or array factor, is a function of both θ and ϕ. Consider a square lattice planar array with elements removed to obtain a circular boundary. A contoured footprint pattern is required

- Geometry: A square grid planar array of 21 by 21 isotropic elements with an inter-element spacing of $d_x = d_y = 0.662\lambda$. All the elements outside a radius of 10.5λ from the centre of the array are removed from the square array to obtain the circular boundary. The total number of array elements is 349 (a reduction of 21% from the square array).
- Pattern specification:
  - A footprint contour in the shape of a skewed tear drop,
  - main beam peak-to-peak ripple of 1dB and
  - a sidelobe level of -20dB.
- Excitation constraints: None.
- Starting point: The starting point is the array factor of Illustrative Example #1 in Section 3.2.2 with all the excitations outside the circular boundary removed.

This particular starting point was selected because genetic algorithm proved too time consuming and memory intensive making it not feasible for the computation of a starting pattern, while the other simpler starting patterns lead to traps. The staring pattern is shown in Figure 5.13.

A contour plot of the final array factor is displayed in Figure 5.14. One quadrant of the geometry is also drawn in the upper right hand corner in Figure 5.13. The contours of the transformation function used in the transformation based synthesis technique for Illustrative Example #1in Section 3.2.2 are also drawn. The target main beam roll-off is not as steep as that for the transformation based synthesis technique because of the reduced number of elements.

5.8.4 Example #4: Hexagonal planar array with a fan beam pattern

This example shows the performance of the intersection of sets synthesis method in shaped beam synthesis of a shaped beam hexagonal array.

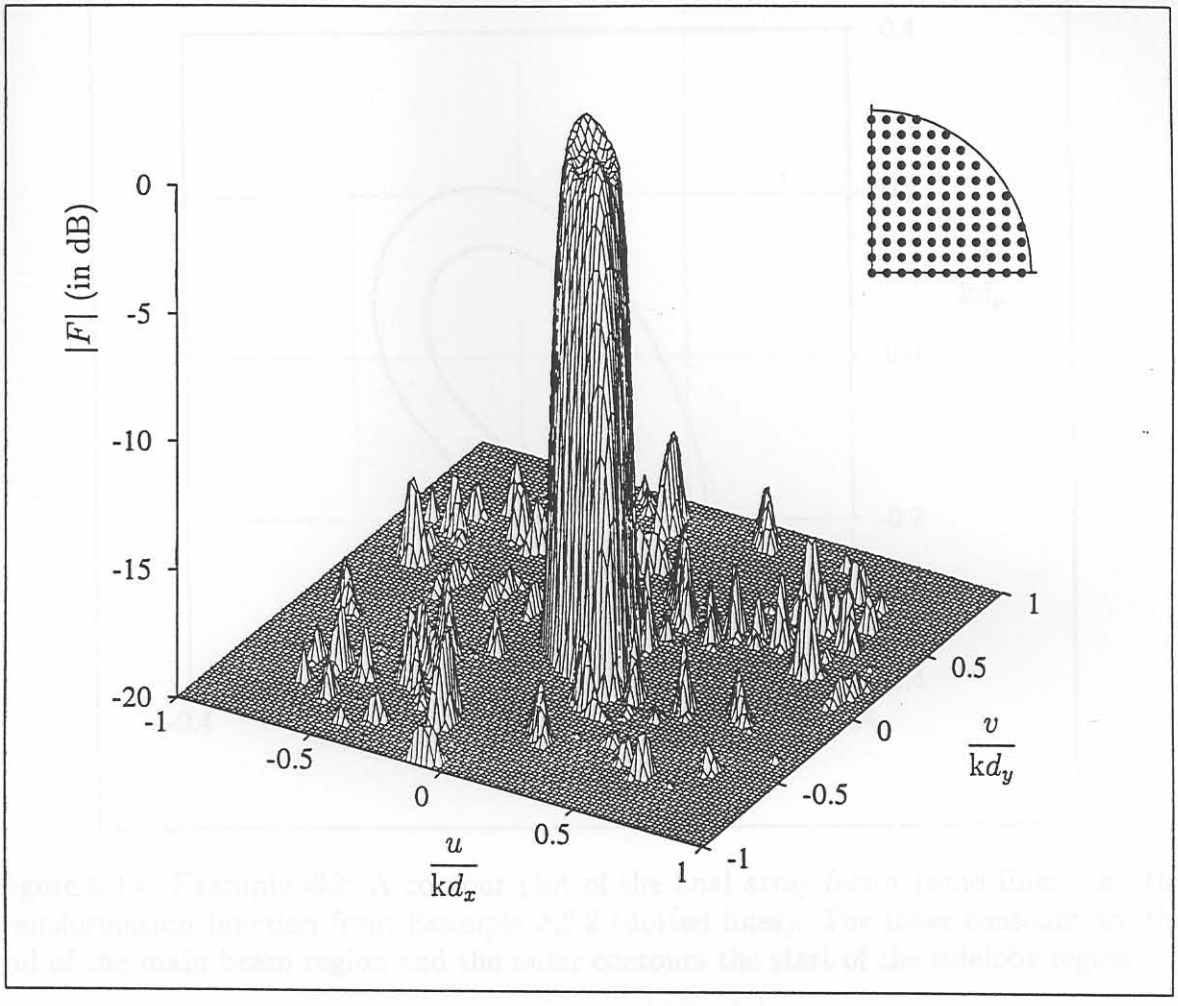

Figure 5.13: Example #3: A surface plot of the starting pattern, the planar array factor synthesised with the transformation based technique, with the corner elements removed.

- Geometry: A six ring hexagonal array with a total of 127 isotropic elements. The element spacing in the hexagonal lattice (shortest distance between any two elements) is $d_t = 0.577\lambda$. Thus the inter element spacing of collapsed distribution along the $\hat{x}$-axis is $d_x = \frac{1}{2}d_t = 0.288\lambda$ and that along the $\hat{y}$-axis is $d_y = d_t \sin(60^\circ) = \frac{1}{2}\lambda$.
- Pattern specification:
  - a $\csc^2(\theta)$ shaped main beam from $\theta = -10^\circ$ to $\theta = 30^\circ \pm 1^\circ$ in the $\phi = 0^\circ$ -cut (along the $\hat{x}$-axis),
  - the narrowest pencil beam possible in the $\phi = 90^\circ$ -cut (along the $\hat{y}$-axis),
  - a peak-to-peak ripple of 2dB and
  - a sidelobe level of -20dB.
- Excitation constraints: None.

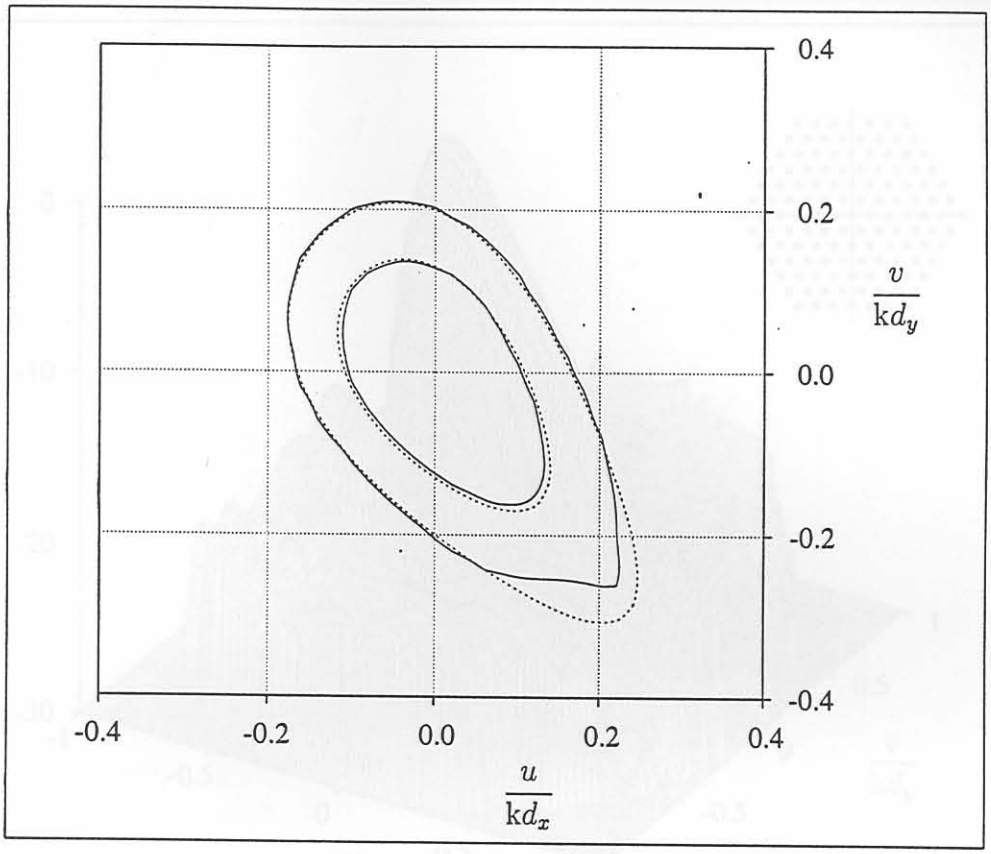

Figure 5.14: Example #3: A contour plot of the final array factor (solid lines) and the transformation function from Example 3.2.2 (dotted lines). The inner contours are the end of the main beam region and the outer contours the start of the sidelobe region.

- Starting point: Component beams with a seven parameter (one dimensional) phase function optimised with Genetic Algorithm.

The radiation pattern of the synthesised array is shown in Figure 5.15. Notice the circular sidelobe topography, this is indicative of a high excitation efficiency.

5.8.5 Example #5: Spherical array with simultaneous co- and cross polarisation pattern synthesis

In this example a full two dimensional conformal array (two pattern angles), on a spheroid with simultaneous co- and cross polarisation patterns is synthesised.

- Geometry:
  - Five rings of radiating elements on a spherical surface, a total of 91 elements.
  - The spherical surface has a radius of 10λ.

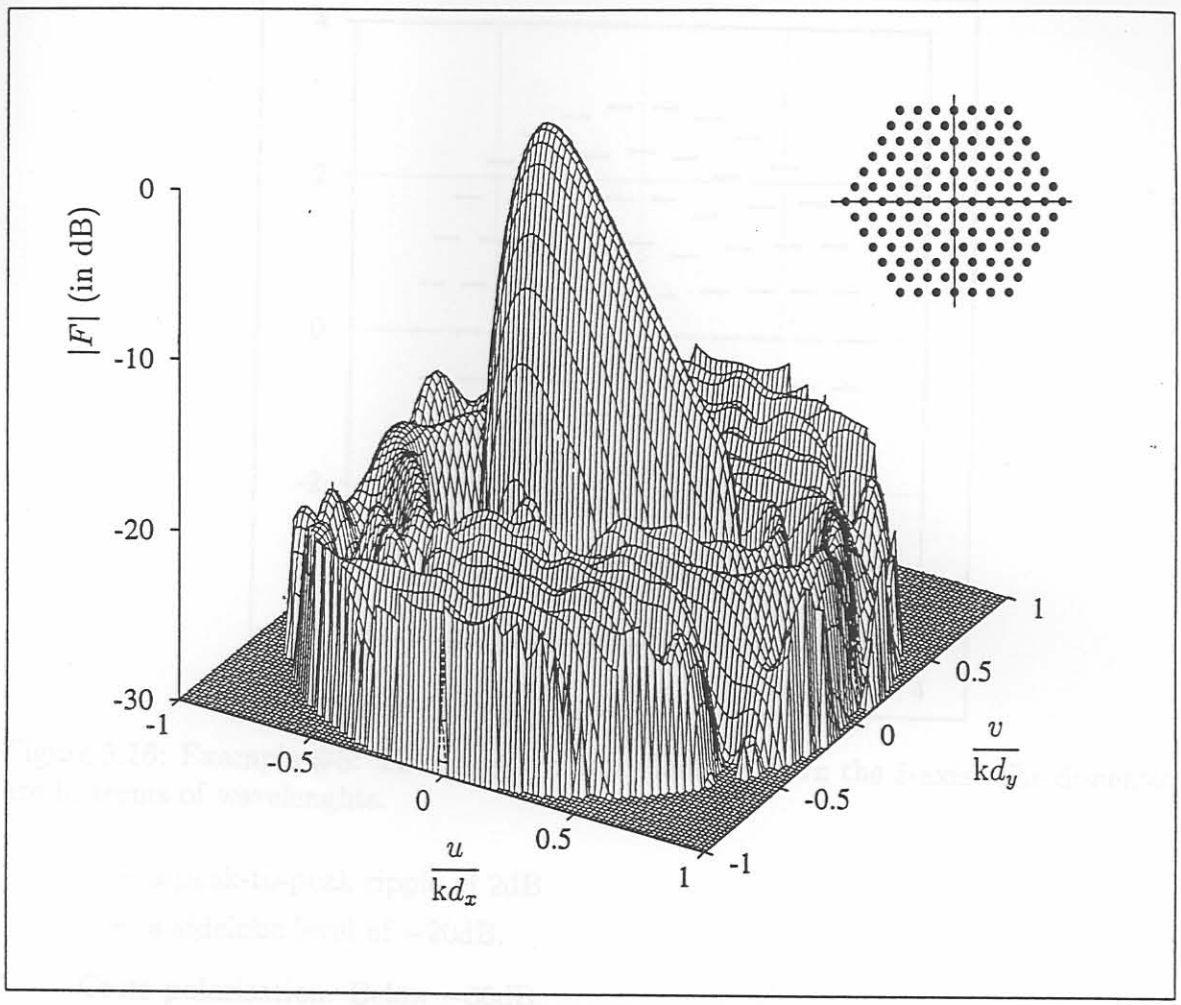

Figure 5.15: Example #4: A surface plot of the planar array factor of the hexagonal arrays with the array geometry in the upper right hand corner.

  - Each of the concentric rings of elements is at a constant θ-angle. The θ angle increased with 3.44° for each new ring, thus the arc-radius of each ring increased by 0.6λ.
  - The radiators are slots with length 0.48λ and width 0.01λ. Due to symmetry all the element patterns will be identical. The element pattern, both co- and cross polarisation, was calculated with GTD. The elements are oriented to obtain maximum co-polarisation in the broadside ($\hat{z}$) direction.

- Pattern specification:
  Co-polarisation:
  - a $\csc^2(\theta)$ shaped main beam from $\theta = -10°$ to $\theta = 30° \pm 2°$ in the $\phi = 0°$ principal cut,
  - the narrowest beamwidth possible in the $\phi = 0°$ principal cut,

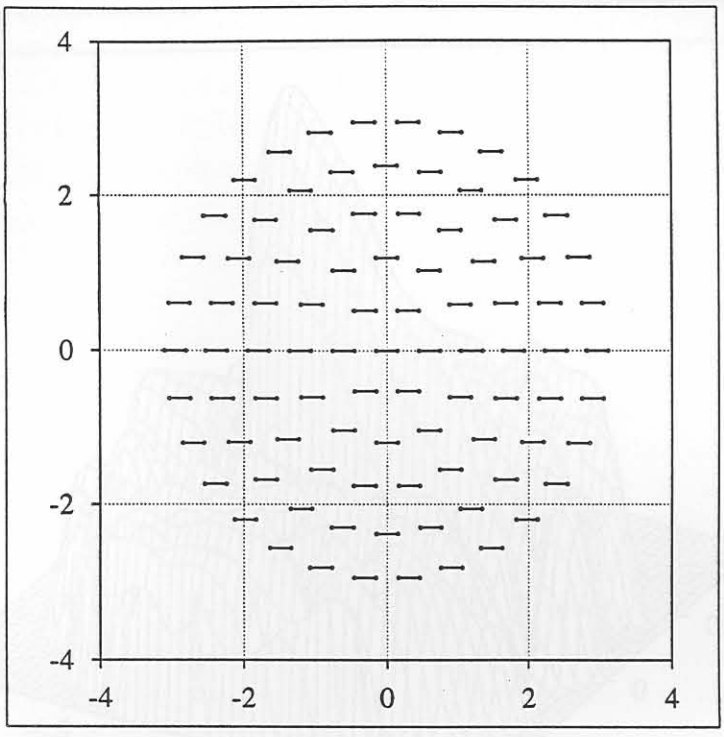

Figure 5.16: Example #5: The array geometry looking down the $\hat{z}$-axis. The dimensions are in terms of wavelenghts.

- a peak-to-peak ripple of 2dB
- a sidelobe level of -20dB.

Cross polarisation: Below -30dB.

- Excitation constraints: None.
- Starting point: Component beams with a seven parameter (one dimensional) phase function optimised with Genetic Algorithm.

The geometry of the array, as seen looking down the $\hat{z}$-axis is drawn in Figure 5.16. The elements are oriented to get the best possible cross polarisation suppression in the bore sight ($\theta = 0°$) direction. A surface plot of the final co-polarised radiation pattern is displayed in Figure 5.17. Again, notice the circular sidelobe topography, indicating a high excitation efficiency. Figure 5.18 show the radiation pattern in the $\phi = 0$ principal cut.

5.9 General Remarks and Conclusions

The synthesis of arrays of arbitrary geometry and elements can be stated as the search for the intersection of properly defined sets. Proper sets were defined in both the radiation

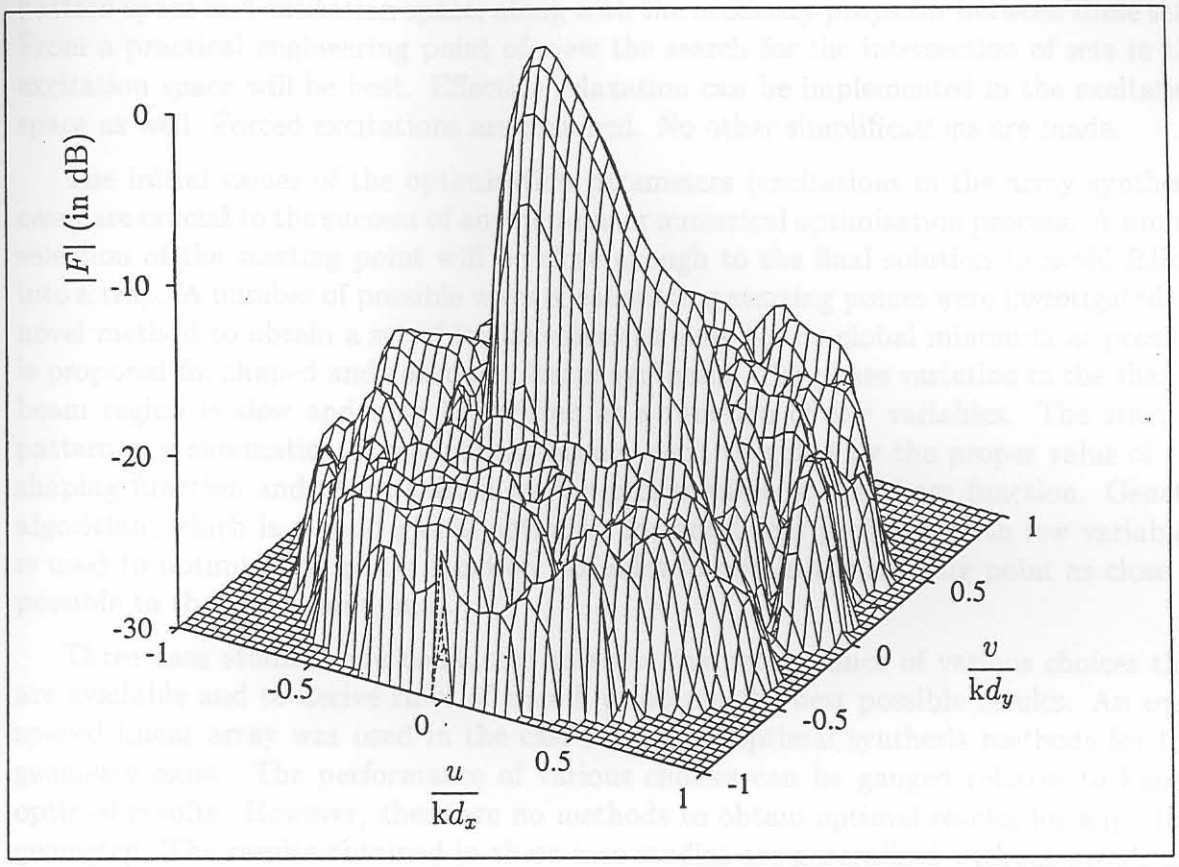

Figure 5.17: Example #5: A surface plot of the co-polarisation radiation pattern in the upper half space.

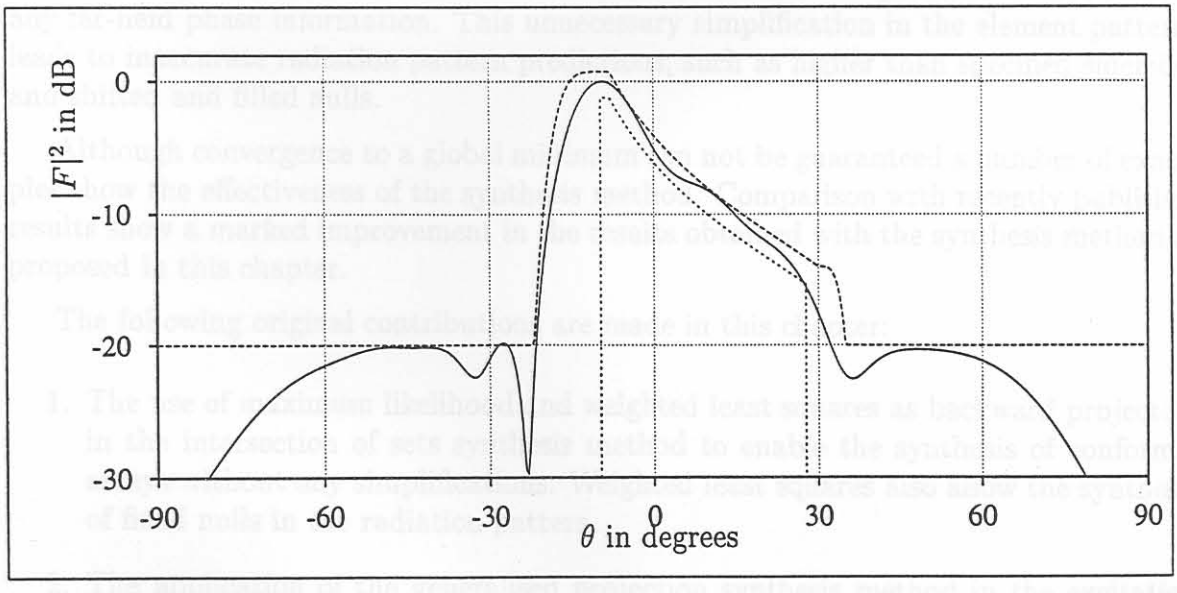

Figure 5.18: Example #5: The $\phi = 0$ principal cut through the radiation pattern in the solid line trace, with the radiation pattern mask in dashed lines.

pattern space and excitation space; along with the necessary projector between these sets. From a practical engineering point of view the search for the intersection of sets in the excitation space will be best. Effective relaxation can be implemented in the excitation space as well. Forced excitations are assumed. No other simplifications are made.

The initial values of the optimisation parameters (excitations in the array synthesis case) are crucial to the success of any non-linear numerical optimisation process. A proper selection of the starting point will be close enough to the final solution to avoid falling into a trap. A number of possible ways of calculating starting points were investigated. A novel method to obtain a set of initial values as close to the global minimum as possible is proposed for shaped and contoured beam synthesis. The phase variation in the shaped beam region is slow and may be written as a function of few variables. The starting pattern is a summation of component beams, each weighted by the proper value of the shaping function and phase shifted by the proper value of the phase function. Genetic algorithm, which is a good global optimiser for non-linear problems with few variables, is used to optimise the phase function variables to obtain the starting point as close as possible to the global minimum.

Three case studies were conducted to show the performance of various choices that are available and to derive rules of thumb to obtain the best possible results. An equi-spaced linear array was used in the case studies as optimal synthesis methods for this geometry exist. The performance of various choices can be gauged relative to known optimal results. However, there are no methods to obtain optimal results for any other geometry. The results obtained in these case studies are generalised without proof, and should not be considered as more than rules of thumb.

The importance of practical element patterns in the analysis and synthesis of conformal arrays is shown. The analytical functions used for element patterns do not contain any far-field phase information. This unnecessary simplification in the element patterns leads to inaccurate radiation pattern predictions, such as higher than specified sidelobes and shifted and filled nulls.

Although convergence to a global minimum can not be guaranteed a number of examples show the effectiveness of the synthesis method. Comparison with recently published results show a marked improvement in the results obtained with the synthesis method as proposed in this chapter.

The following original contributions are made in this chapter:

1. The use of maximum likelihood and weighted least squares as backward projectors in the intersection of sets synthesis method to enable the synthesis of conformal arrays without any simplifications. Weighted least squares also allow the synthesis of fixed nulls in the radiation pattern.

2. The application of the generalised projection synthesis method in the excitation space. This ensures that all the excitation constraints necessary to implement the array are always satisfied. It also allows for the application of relaxation.

3. Effective relaxation in the excitation space as a convergence accelerator for slowly converging problems.

4. The importance of practical element patterns in the analysis and synthesis of conformal arrays is shown.

5. The component beam and radiation pattern phase function approach to obtain a starting point as close as possible to the global minimum to avoid traps.

The author published preliminary work on the proposed method [146].

Chapter 6

Conclusions

A number of inadequacies in conventional array synthesis methods have been identified and addressed.

The transformation based synthesis method, prior to this thesis, could be used for the synthesis of rectangular planar arrays with quadrantal or centro symmetrical footprint patterns only. The transformation technique is extended to enable the synthesis of planar arrays with arbitrary contoured footprint patterns; planar arrays with non rectangular boundaries and planar arrays with triangular lattices. The transformation based synthesis technique utilises a transformation that divides the problem into two decoupled sub-problems. One sub-problem (the contour transformation problem) involves the determination of certain coefficients in order to achieve the required footprint contours. The number of contour transformation coefficients which must be used depends on the complexity of the desired contour, but is very small in comparison to the number of planar array elements. The other sub-problem consists of a prototype linear array synthesis, for which powerful methods for determining appropriate element excitations, already exist. The separation of the synthesis procedure into two sub-problems is not only good from a computational point of view, but aids understanding by highlighting which considerations will finally determine the required array size (viz. contour complexity; allowed coverage ripple; final planar array directivity). Simple recursive formulas then determine the final planar array excitations from the information forthcoming from the above two sub-problem solutions. The final planar array size is linked to the number of contour transformation coefficients and the prototype linear array size. The biggest advantage of the transformation based synthesis technique is its computational efficiency, making it feasible to conduct parametric studies of array performance design tradeoff studies even for very large arrays. However, the transformation based synthesis method does suffer some limitations, it can not be used to synthesise planar arrays with an arbitrary number of elements and it does not use all the degrees of freedom due to the very nature of the technique. Existing transformations were all shown to be special cases of the extended transformation based synthesis technique methods presented in the thesis.

No useful difference pattern synthesis method exists for planar arrays. A well ordered,

step by step procedure for the synthesis of planar arrays with difference patterns is presented. The method utilises the convolution synthesis method and uses the extended transformation method as one of the steps. The technique in effect provides a structured procedure for spreading out the linear array excitations, thereby eliminating any guesswork that may otherwise be required. The result is near-optimum difference patterns for planar arrays with rectangular or hexagonal lattices. The difference pattern performance in the selected cut is identical to that of the archetypal linear array used, and will thus be optimum if the latter is optimum. In the other pattern cuts the sidelobes are below those of the archetypal linear array, but not unnecessarily low. The synthesis procedure is very rapid for even very large arrays, making it feasible to conduct design trade-off and parametric studies.

Synthesis of conformal arrays is an ill conditioned inverse problem with a multitude of local minima. Unlike linear and planar arrays, where the element pattern can be factored from the radiation pattern, no such simplification can be made to ease the conformal array synthesis problem. Due to the non linear nature of conformal array synthesis an effective conformal array synthesis method must have a rapid rate of convergence and some measure of confidence that the result will be close to the optimal solution. Previously no effective conformal array synthesis technique existed. The synthesis of arrays of arbitrary geometry and elements can be stated as the search for the intersection of properly defined sets. Proper sets were defined in both the radiation pattern space and excitation space; along with the necessary projector between these sets. From a practical engineering point of view the search for the intersection of sets in the excitation space will be best. Effective relaxation can be implemented in the excitation space as well. A proper selection of the starting point is needed to avoid falling into a trap. A number of possible ways of calculating starting points were investigated, and a novel method to obtain a set of initial values as close to the global minimum as possible is proposed for shaped and contoured beam synthesis. The phase variation in the shaped beam region is slow and may be written as a function of a few variables. The starting pattern is a summation of component beams, each weighted by the proper value of the shaping function and phase shifted by the proper value of the phase function. Genetic algorithm is used to optimise these phase function variables. Case studies were used to derive rules of thumb for obtaining the selection of various options available in the implementation of the method to obtain the best possible results. The importance of practical element patterns in the analysis and synthesis of conformal arrays was also shown. The intersection of sets method obtained better results than other existing methods.

A large number of representative examples were presented in each chapter to show the advantages of the proposed synthesis methods.

References

[1] A. D. Olver, "Basic properties of antennas," in *The Handbook of Antenna Design* (A. W. Rudge, K. Milne, A. D. Olver, and P. Knight, eds.), vol. 1 and 2, ch. 1, London, UK: Peter Peregrinus Ltd., 2 ed., 1986.

[2] H. J. Kuno and T. A. Midford, "The evolution of MMIC packaging," in *IEEE AP-S Int. Symp. Digest*, vol. 2, (Ann Arbor, MI, USA), pp. 1005–1008, June 1993.

[3] N. J. Parsons, "Optical interconnection and packaging for active array antenna," in *IEEE AP-S Int. Symp. Digest*, vol. 2, (Ann Arbor, MI, USA), pp. 1001–1004, June 1993.

[4] H. R. Fetterman, S. R. Forrest, and D. V. Plant, "Optical controlled phased array radar receivers," in *IEEE AP-S Int. Symp. Digest*, vol. 3, (Ann Arbor, MI, USA), pp. 1523–1525, June 1993.

[5] R. R. Kunath, "Applications of optics in arrays," in *IEEE AP-S Int. Symp. Digest*, vol. 3, (Ann Arbor, MI, USA), pp. 1526–1529, June 1993.

[6] J. F. Rose, B. A. Worley, and M. M. Lee, "Antenna patterns for prototype two-dimensional digital beamforming array," in *IEEE AP-S Int. Symp. Digest*, vol. 3, (Ann Arbor, MI, USA), pp. 1544–1547, June 1993.

[7] G. V. Borgiotti, "Conformal arrays," in *The Handbook of Antenna Design* (A. W. Rudge, K. Milne, A. D. Olver, and P.Knight, eds.), vol. 1 and 2, ch. 11, London, UK: Peter Peregrinus Ltd., 2 ed., 1986.

[8] R. C. Hansen, ed., *Microwave Scanning Antennas.* Los Altos, CA, USA: Peninsula Publishing, 1985.

[9] W. L. Stutzman and G. A. Thiele, *Antenna Theory and Design.* New York, N.Y., USA: John Wiley & Sons, 1981.

[10] R. S. Elliott, *Antenna Theory and Design.* Englewood Cliffs, N.Y., USA: Prentice-Hall, 1981.

[11] A. W. Rudge, K. Milne, A. D. Olver, and P. Knight, eds., *The Handbook of Antenna Design*, vol. 1 and 2. London, UK: Peter Peregrinus Ltd., 2 ed., 1986.

[12] M. T. Ma, *Theory and Application of Antenna Arrays.* New York, N.Y., USA: John Wiley & Sons, 1974.

[13] Y. T. Lo and S. W. Lee, eds., *Antenna Handbook.* New York, N.Y., USA: Van Nostrand Reinhold Com., 1988.

[14] D. A. McNamara, C. W. I. Pistorius, and J. A. G. Malherbe, *Introduction to the Uniform Geometrical Theory of Diffraction.* Boston, MA, USA: Artech House, 1990.

[15] R. F. Harrington, *Field Computation by Moment Methods.* New York, N.Y., USA: MacMillan, 1968.

[16] E. A. Wolff, *Antenna Analysis*, ch. 2, pp. 22–23. Boston, MA, USA: Artech House, 1988.

[17] R. C. Hansen, "Planar arrays," in *The Handbook of Antenna Design* (A. W. Rudge, A. D. O. K. Milne, and P. Knight, eds.), vol. 1 and 2, ch. 10, London, UK: Peter Peregrinus Ltd., 2 ed., 1986.

[18] D. R. Rhodes, *Synthesis of Planar Antenna Sources.* London, UK: Clarendon Press, 1974.

[19] R. S. Elliott, "Array pattern synthesis - Part II: Planar arrays," *IEEE Antennas Propagat. Soc. Newsletter*, pp. 5–10, April 1986.

[20] IEEE Std 145-1983, "IEEE standard definitions of terms for antennas," *IEEE Trans. Antennas and Propagat.*, vol. AP-31, pp. 5–29, June 1983.

[21] D. K. Cheng, "Optimisation techniques for antenna arrays," *Proc. IEEE*, vol. 59, pp. 1664–1674, Dec 1971.

[22] D. A. McNamara, "Quadratic forms for the performance indices of symmetrical and anti-symmetrical linear arrays," *Electron. Lett.*, vol. 23, pp. 148–149, Feb 1987.

[23] M. J. Buckley, "Synthesis of shaped beam antenna patterns using implicitly constrainted current elements," *IEEE Trans. Antennas Propagat.*, vol. AP-44, pp. 192–197, Feb 1996.

[24] O. M. Bucci, G. Mazzarella, and G. Panariello, "Array synthesis with smooth excitation," in *IEEE AP-S Int. Symp. Digest*, vol. II, (Dallas, Texas, USA), pp. 856–859, May 1990.

[25] R. C. Hansen, "Linear arrays," in *The Handbook of Antenna Design* (A. W. Rudge, K. Milne, A. D. Olver, and P. Knight, eds.), vol. 1 and 2, ch. 9, London, UK: Peter Peregrinus Ltd., 2 ed., 1986.

[26] S. A. Schelkunoff, "A mathematical theory of linear arrays," *Bell Syst. Tech. J.*, vol. 22, pp. 80–107, 1943.

[27] R. C. Hansen, "Measurement distance effects on low sidelobe patterns," *IEEE Trans. Antennas and Propagat.*, vol. AP-32, pp. 591–594, June 1984.

[28] R. L. Pritchard, "Optimum directivity patterns for linear point arrays," *J. Acoust. Soc. Amer.*, vol. 25, pp. 879–891, Sept 1953.

[29] Y. T. Lo, S. W. Lee, and Q. H. Lee, "Optimisation of directivity and signal-to-noise ratio of an arbitrary antenna array," *Proc. IEEE*, vol. 54, pp. 1033–1045, Aug 1966.

[30] C. L. Dolph, "A current distribution for broadside arrays which optimises the relationship between beam width and side-lobe level," *Proc. IRE*, vol. 34, pp. 335–348, June 1946.

[31] D. Barbiere, "A method of calculating the current distribution of Tschebyscheff arrays," *Proc. IRE*, vol. 40, pp. 78–82, Jan 1952.

[32] R. J. Stegen, "Excitation coefficients and beamwidths of Tschebyscheff arrays," *Proc. IRE*, vol. 41, pp. 1671–1674, Nov 1953.

[33] R. J. Stegen, "Gain of Tchebycheff arrays," *IRE Trans. Antennas Propagat.*, vol. AP-8, pp. 629–631, Nov 1960.

[34] G. J. van der Maas, "A simplified calculation for Dolph-Tchebycheff arrays," *J. Appl. Phys.*, vol. 25, pp. 121–124, Jan 1954.

[35] A. D. Bresler, "A new algorithm for calculating the current distributions of Dolph-Chebyshev arrays," *IEEE Trans. Antennas Propagat.*, vol. AP-28, pp. 951–952, Nov 1980.

[36] R. C. Hansen, "The theory of antenna arrays," in *Microwave Scanning Antennas* (R. C. Hansen, ed.), vol. I, ch. 1, Los Altos, CA, USA: Peninsula Publishing, 1985.

[37] A. T. Villeneuve, "Taylor patterns for discrete arrays," *IEEE Trans. Antennas Propagat.*, vol. AP-32, pp. 1089–1093, Oct 1984.

[38] R. C. Hansen, "Aperture efficiency of Villeneuve-$\bar{n}$ arrays," *IEEE Trans. Antennas Propagat.*, vol. AP-33, pp. 668–669, June 1985.

[39] D. A. McNamara, "Generalised Villeneuve $\bar{n}$-distribution," *IEE Proc., Pt. H*, vol. 136, pp. 245–249, June 1989.

[40] D. A. McNamara and E. Botha, "Generalised villeneuve distributions and various definitions of root-mean-square sidelobe levels," *Electron. Lett.*, vol. 29, pp. 989–990, May 1993.

[41] O. R. Price and R. F. Hyneman, "Distribution function for monopulse antenna difference patterns," *IRE Trans. Antennas Propagat.*, vol. AP-8, pp. 567–576, Nov 1960.

[42] D. A. McNamara, "Optimum monopulse linear array excitations using Zolotarev polynomials," *Electron. Lett.*, vol. 21, pp. 681–682, Aug 1985.

[43] D. A. McNamara, "Tables of Zolotarev polynomial difference distributions for linear transducer arrays," *J. Acoust. Soc. Am.*, vol. 87, pp. 1336–1339, March 1990.

[44] D. A. McNamara, "The direct synthesis of optimum difference patterns for discrete linear arrays using Zolotarev distributions," *IEE Proc., Pt. H*, vol. 140, pp. 495–500, Dec 1993.

[45] D. A. McNamara, "Discrete $\bar{n}$-distribution for difference patterns," *Electron. Lett.*, vol. 22, pp. 303–304, March 1986.

[46] D. A. McNamara, "The performance of Zolotarev and modified-Zolotarev difference pattern array distributions," *IEE Proc., Pt. H*, vol. 140, pp. 495–500, Dec 1993.

[47] D. A. McNamara, "Excitation providing maximum directivity for difference arrays of discrete elements," *Electron. Lett.*, vol. 23, pp. 780–781, July 1987.

[48] D. A. McNamara, "Maximisation of the normilised boresight slope of a difference arrays of discrete elements," *Electron. Lett.*, vol. 23, pp. 1158–1160, Oct 1987.

[49] D. A. McNamara, "Synthesis of sum and difference patterns for two-section monopulse arrays," *IEE Proc., Pt. H*, vol. 135, pp. 371–374, Dec 1988.

[50] P. M. Woodward, "Method of calculating the field over a plane aperture required to produce a given polar diagram," *J. IEE, Pt. IIIA*, vol. 93, pp. 1554–1558, 1947.

[51] K. Milne, "Synthesis of power radiation pattern for linear array antennas," *IEE Proc., Pt. H*, vol. 134, pp. 285–296, June 1987.

[52] R. S. Elliott, "Improved pattern synthesis for equispaced linear arrays," *Alta Frequenza*, vol. 51, pp. 296–300, Nov/Dec 1983.

[53] R. S. Elliott and G. J. Stern, "A new technique for shaped beam synthesis of equispaced arrays," *IEEE Trans. Antennas Propagat.*, vol. AP-32, pp. 1129–1133, Oct 1984.

[54] H. J. Orchard, R. S. Elliott, and G. J. Stern, "Optimising the synthesis of shaped beam antenna patterns," *IEE Proc., Pt. H*, vol. 132, pp. 63–68, Feb 1985.

[55] Y. U. Kim and R. S. Elliott, "Shaped-pattern synthesis using pure real distributions," *IEEE Trans. Antennas and Propagat.*, vol. AP-36, pp. 1645–1649, Nov 1988.

[56] J. A. Rodriguez, E. Botha, and F. Ares, "Extension of the orchard-elliot synthesis method to pure-real nonsymmetrical-shaped patterns," *IEEE Trans. Antennas Propagat.*, vol. AP-45, pp. 1317–1318, Aug 1997.

[57] F. Ares, A. Vieriro, E. Moreno, and S. R. Rengarajan, "Extension of orchard's pattern syntehsis technique for overdetermined systems," *Electromagnetics*, vol. 17, pp. 15–23, Jan/Feb 1997.

[58] C. J. Bouwkamp and N. G. de Bruyn, "The problem of optimum current distribution," *Philips Res. Rep.*, vol. 1, pp. 135–158, 1945-1946.

[59] T. T. Taylor, "Design of line-source antennas for narrow beamwidth and low sidelobes," *IRE Trans. Antennas Propagat.*, vol. AP-3, pp. 16–28, Jan 1955.

[60] R. S. Elliott, "Design of line source antennas for sum patterns with sidelobes of individually arbitrary heights," *IEEE Trans. Antennas Propagat.*, vol. AP-24, pp. 76–83, Jan 1976.

[61] F. Ares, R. S. Elliott, and E. Moreno, "Optimised synthesis of shaped line-source antenna beams," *Electron. Lett.*, vol. 29, pp. 1136–1137, June 1993.

[62] E. T. Bayliss, "Design of monopulse antennas for difference patterns with side lobes," *Bell Syst. Tech. J.*, vol. 47, pp. 623–640, 1968.

[63] R. S. Elliott, "Design of line source antennas for difference patterns with side lobes of individually arbitrary heights," *IEEE Trans. Antennas Propagat.*, vol. AP-24, pp. 310–316, May 1976.

[64] R. S. Elliott, "On discretizing continuous aperture distributions," *IEEE Trans. Antennas Propagat.*, vol. AP-25, pp. 617–621, Sept 1977.

[65] S. W. Autrey, "Approximate synthesis of nonseparable design responses for rectangular arrays," *IEEE Trans. Antennas Propagat.*, vol. AP-35, pp. 907–912, Aug 1987.

[66] C. F. Winter, "Using continuous aperture illuminations discretely," *IEEE Trans. Antennas Propagat.*, vol. AP-25, pp. 695–700, Sept 1977.

[67] C. F. Winter, "Further discrete optimizations for continuous aperture illumination," *IEEE Trans. Antennas Propagat.*, vol. AP-28, pp. 125–128, Jan 1980.

[68] W. V. T. Rusch, "The current state of the reflector antenna art," *IEEE Trans. Antennas Propagat.*, vol. AP-32, pp. 313–329, March 1984.

[69] P. D. Patel and K. K. Chan, "Optimisation of contoured beams for satelitte antennas," *IEE Proc., Pt. H*, vol. 132, pp. 400–406, Oct 1985.

[70] A. R. Cherrette, S. W. Lee, and R. J. Acosta, "A method for producing a shaped contour radiation pattern using a single shaped reflector and a single feed," *IEEE Trans. Antennas Propagat.*, vol. AP-37, pp. 698–706, June 1989.

[71] W. Bornemann, P. Balling, and W. J. English, "Synthesis of spacecraft array antennas for Intelsat frequency reuse multiple contoured beams," *IEEE Trans. Antennas Propagat.*, vol. AP-33, pp. 1186–1193, Nov 1985.

[72] G. Mazzarella and G. Panariello, "A projection-based synthesis of non-uniform arrays," in *IEEE AP-S Int. Symp. Digest*, vol. 2, (London, Ontario, Canada), pp. 1164–1167, June 1991.

[73] A. R. Cherette and D. C. D. Chang, "Phased array contour beam shaping by phase optimisation," in *IEEE AP-S Int. Symp. Digest*, vol. II, (Vancouver, Canada), pp. 475–478, June 1985.

[74] J. E. Richie and H. N. Kritikos, "Linear program synthesis for direct broadcast satellite phased arrays," *IEEE Trans. Antennas Propagat.*, vol. AP-36, pp. 345–348, March 1988.

[75] P. Balling, W. Bornemann, and H. H. Viskum, "Reconfigurable contoured beam antenna using fixed sub-beam forming networks," in *IEEE AP-S Int. Symp. Digest*, vol. II, (Syracuse, NY, USA), pp. 510–513, June 1988.

[76] C. Mangenot, T. Judasz, and P. F. Combes, "Power synthesis of shaped beam antenna patterns," in *IEEE AP-S Int. Symp. Digest*, vol. II, (San Jose, CA, USA), pp. 420–423, June 1989.

[77] J. E. Richie and H. N. Kritikos, "Preliminary shaped beam synthesis using product function," *IEEE Trans. Antennas Propagat.*, vol. AP-38, pp. 1504–1507, Sept 1990.

[78] R. S. Elliott and G. J. Stern, "Footprint patterns obtained by planar arrays," *IEE Proc., Pt. H*, vol. 137, pp. 108–112, April 1990.

[79] R. S. Elliott and G. J. Stern, "Shaped patterns from a continuous planar aperture distribution," *IEE Proc., Pt. H*, vol. 135, pp. 366–370, Dec 1988.

[80] F. Ares, R. S. Elliott, and E. Moreno, "Design of planar arrays to obtain efficient footprint patterns with an arbitrary footprint boundary," *IEEE Trans. Antennas Propagat.*, vol. AP-42, pp. 1509–1514, Nov 1994.

[81] F. I. Tseng and D. K. Cheng, "Optimum scannable planar arrays with an invariant side lobe level," *Proc. IEEE*, vol. 56, pp. 1771–1778, Nov 1968.

[82] Y. V. Baklanov, "Chebyshev distribution of current for a planar array of radiators," *Radio Eng. Electron. Phys. (USSR)*, vol. 11, pp. 640–642, 1966.

[83] N. Goto, "Nonseparable pattern of planar arrays," *IEEE Trans. Antennas Propagat.*, vol. AP-20, pp. 104–106, Jan 1972.

[84] N. Goto, "Pattern synthesis of hexagonal planar arrays," *IEEE Trans. Antennas and Propagat.*, vol. AP-20, pp. 479–481, July 1972.

[85] Y. U. Kim and R. S. Elliott, "Extensions of the Tseng-Cheng pattern synthesis technique," *J. Electromagn. Waves Applic.*, vol. 2, pp. 255–268, March/April 1988.

[86] Y. U. Kim, "A transformation technique to produce almost rotationally symetrical hexagonal array patterns," *J. Electromagn. Waves Applic.*, vol. 4, pp. 359–369, April 1990.

[87] S. R. Laxpati, "Synthesis of planar arrays based on convolution technique," *Electron. Lett.*, vol. 16, pp. 918–919, Nov 1980.

[88] S. R. Laxpati and J. P. Shelton, "Theory of null synthesis of planar arrays," in *IEEE AP-S Int. Symp. Digest*, vol. I, (Las Angeles, CA, USA), pp. 40–43, June 1981.

[89] J. P. Shelton and S. R. Laxpati, "Applications of null synthesis to hexagonal arrays," in *IEEE AP-S Int. Symp. Digest*, vol. I, (Las Angeles, CA, USA), pp. 44–47, June 1981.

[90] S. R. Laxpati, "Planar array synthesis with prescribed pattern nulls," *IEEE Trans. Antennas Propagat.*, vol. AP-30, pp. 1176–1183, Nov 1982.

[91] J. P. Shelton and S. R. Laxpati, "Synthesis of hexagonal and square arrays using discrete convolution," *Radio Science*, vol. 19, pp. 1229–1237, Sept/Oct 1984.

[92] R. M. Mersereau, W. F. G. Mecklenbrauker, and T. F. Quatieri, "McClellan transformations for two-dimensional digital filtering : I - design," *IEEE Trans. Circuits Syst.*, vol. CAS-23, pp. 405–414, July 1976.

[93] D. A. McNamara and E. Botha, "Transformation-based synthesis technique for planar arrays with contoured beams," *Electron. Lett.*, vol. 27, pp. 1502–1504, Aug. 1991.

[94] E. Botha and D. A. McNamara, "A contoured beam synthesis technique for planar arrays with quadrantal and centro-symmetry," *IEEE Trans. Antennas Propagat.*, vol. AP-41, pp. 1222–1231, Sept. 1993.

[95] E. Botha, "Improved synthesis techniques for uniformly-spaced planar arrays," MEng., University of Pretoria, Pretoria, RSA, March 1991.

[96] T. T. Taylor, "Design of circular apertures for narrow beamwidth and low sidelobes," *IRE Trans. Antennas Propagat.*, vol. AP-8, pp. 17–22, Jan 1960.

[97] R. C. Hansen, "Circular aperture distribution with one parameter," *Electron. Lett.*, vol. 11, p. 184, April 1975.

[98] R. C. Hansen, "A one-parameter circular aperture distribution with narrow beamwidth and low sidelobes," *IEEE Trans. Antennas Propagat.*, vol. AP-24, pp. 477–480, July 1976.

[99] R. S. Elliott, "Design of circular apertures for narrow beamwidth and asymmetric side lobes," *IEEE Trans. Antennas Propagat.*, vol. AP-23, pp. 523–527, July 1975.

[100] W. D. White, "Circular aperture distribution functions," *IEEE Trans. Antennas Propagat.*, vol. AP-25, pp. 714–716, Sept 1977.

[101] O. Graham, R. M. Johnson, and R. S. Elliott, "Design of circular apertures for sum patterns with ring side lobes of individually arbitrary heights," *Alta Frequenza*, vol. 47, pp. 21–25, 1978.

[102] R. F. E. Guy, "General radiation-pattern synthesis technique for array antennas of arbitrary configuration and element type," *IEE Proc. , Pt. H.*, vol. 135, pp. 241–248, Aug 1988.

[103] A. Ksienski, "Equivalence between continuous and discrete radiating arrays," *Can. J. of Phys.*, vol. 39, pp. 335–349, 1961.

[104] W. L. Stutzman and E. L. Coffey, "Radiation pattern synthesis of planar antennas using the iterative soampling method," *IEEE Trans. Antennas Propagat.*, vol. AP-23, pp. 764–769, Nov 1975.

[105] A. Levi and H. Stark, "Image restoration by the method of generalised projections with application to restoration from magnitude," *J. Opt. Soc. Am., Pt. A.*, vol. 1, pp. 932–943, Sept 1984.

[106] S. Prasad, "Generalized array pattern synthesis by the method of alternating orthogonal projections," *IEEE Trans. Antennas Propagat.*, vol. AP-28, pp. 328–332, May 1980.

[107] G. T. Poulton, "Power pattern synthesis using the method of successive projections," in *IEEE AP-S Int. Symp. Digest*, vol. 2, (Philadelphia, PA, USA), pp. 667–670, June 1986.

[108] G. T. Poulton, "Antenna power pattern synthesis using the method of successive projections," *Electron. Lett.*, vol. 22, pp. 1042–1043, Sept 1986.

[109] O. M. Bucci, G. Franceschetti, G. Mazzarella, and G. Panariello, "A general projection approach to array synthesis," in *IEEE AP-S Int. Symp. Digest*, vol. I, (San Jose, CA, USA), pp. 146–149, June 1989.

[110] O. M. Bucci, G. Franceschetti, G. Mazzarella, and G. Panariello, "Intersection approach to array pattern synthesis," *IEE Proc., Pt. H*, vol. 137, pp. 349–357, Dec 1990.

[111] O. M. Bucci, G. D'Elia, G. Mazzarella, and G. Panariello, "Antenna pattern synthesis: a new general approach," *Proc. IEEE*, vol. 82, pp. 358–371, March 1994.

[112] G. Mazzarella and G. Panariello, "Pattern synthesis of conformal arrays," in *IEEE AP-S Int. Symp. Digest*, vol. 2, (Ann Arbor, DT, USA), pp. 1054–1057, June/July 1993.

[113] O. M. Bucci, G. D'Elia, and G. Romito, "Power synthesis of conformal arrays by a generalised projection method," *IEE Proc., Pt. H*, vol. 142, pp. 467–471, Dec 1995.

[114] D. S. Luenberger, *Linear and nonlinear programming.* Addison-Wesley, 1984.

[115] S. M. Sanzgiri and J. K. Butler, "Constrained optimization of the performance indices of arbitrary array antennas," *IEEE Trans. Antenna Propagat.*, vol. AP-19, pp. 493–498, July 1971.

[116] G. L. Wilson, "Computer optimization of transducer array patterns," *J. Acoust. Soc. Am.*, vol. 59, pp. 195–203, Jan 1976.

[117] O. Einarsson, "Optimisation of planar arrays," *IEEE Trans. Antennas Propagat.*, vol. AP-27, pp. 86–92, Jan 1979.

[118] J. F. DeFord and O. P. Gandhi, "Phase-only synthesis of minimum peak sidelobe patterns for linear and planar arrays," *IEEE Trans. Antennas Propagat.*, vol. AP-36, pp. 191–201, Feb 1988.

[119] N. H. Farhat and B. Bai, "Phased-array antenna pattern synthesis by simulated annealing," *Proc. IEEE*, vol. 75, pp. 842–844, June 1987.

[120] F. Ares, S. R. Rengarajan, J. A. F. Lence, A.Trastoy, and E. Moreno, "Synthesis of antenna patterns of circular arc arrays," *Electron. Lett.*, vol. 32, pp. 1845–1846, 26 Sept 1996.

[121] J. A. Ferreira and F. Ares, "Pattern synthesis of conformal arrays by the simulated annealing technique," *Electron. Lett.*, vol. 33, pp. 1187–1189, 3 July 1997.

[122] J. H. McClellan, "The design of two-dimensional digital filters by transformations," in *Proc. 7th Annual Princeton Conf. Information Sciences and Systems*, pp. 247–251, 1973.

[123] M. R. Spiegel, *Mathematical Handbook of Formulas and Tables.* New York, N.Y., USA: McGraw-Hill, 1968.

[124] D. T. Nguyen and M. N. S. Swamy, "Formulas for parameter scaling in the McClellan tranform," *IEEE Trans. Circuits Syst.*, vol. CAS-33, pp. 108–109, Jan 1986.

[125] Y. Kamp and J. P. Thiran, "Chebyshev approximation for two-dimensional nonrecursive digital filters," *IEEE Trans. Circuits Syst.*, vol. CAS-22, pp. 208–218, March 1975.

[126] R. M. Mersereau, D. B. Harris, and H. S. Hersey, "An efficient algorithm for the design of equiripple two-dimensional FIR digital filters," in *Proc. IEEE Int. Symp. on Circuits and Systems*, pp. 405–414, April 1975.

[127] R. S. Elliott, "Synthesis of rectangular planar arrays for sum patterns with ring side lobes of arbitrary topography," *Radio Sci.*, vol. 12, pp. 653–657, 1977.

[128] E. Botha and D. A. McNamara, "Direct synthesis of near-optimum difference patterns for planar arrays," *Electron. Lett.*, vol. 28, pp. 753–754, April 1992.

[129] W. H. Kummer, "Basic array theory," *Proc. IEEE*, vol. 80, pp. 127–139, Jan 1992.

[130] R. W. Gerchberg and W. O. Saxton, "A practical algorithm for the determination of phase from image and diffraction plane pictures," *Optik*, vol. 35, pp. 237–246, 1972.

[131] D. C. Youla, "Generalized image restoration by the method of alternating orthogonal projections," *IEEE Trans. Circuits Syst.*, vol. CAS-25, pp. 694–702, Sept 1978.

[132] T. S. Ng, "Generalised array pattern sythesis using the projection matrix," *IEE Proc., Pt. H*, vol. 132, pp. 44–46, Feb 1985.

[133] T. S. Ng, "Array pattern synthesis by the method of alternating orthogonal projections: the general case," *IEE Proc., Pt. H*, vol. 132, pp. 451–454, Dec 1985.

[134] D. C. Youla and H. Webb, "Image restoration by the method of projections onto convex sets. part i," *IEEE Trans. Med. Imaging.*, vol. TMI-1, pp. 81–94, 1982.

[135] H. Elmikati and A. A. Elsohly, "Externsion of projection method to nonuniformly linear antenna arrays," *IEEE Trans. Circuits Syst.*, vol. CAS-31, pp. 801–805, Sept 1984.

[136] A. Abo-Taleb and M. M. Fahmy, "Design of FIR two-dimensional digital filters by successive projections," *IEEE Trans. Circuits Syst.*, vol. CAS-31, pp. 801–805, Sept 1984.

[137] G. Franceschetti, G. Mazzarella, and G. Panariello, "Array synthesis with excitation constraints," *IEE Proc., Pt. H*, vol. 135, pp. 400–407, Dec 1988.

[138] O. M. Bucci, G. D'Elia, G. Mazzarella, and G. Panariello, "Antenna pattern synthesis: a new general approach," *Proc. IEEE*, vol. 82, pp. 358–371, March 1994.

[139] O. M. Bucci, G. Mazzarella, and G. Panariello, "Reconfigurable array by phase-only control," in *IEEE AP-S Int. Symp. Digest*, vol. I, (San Jose, CA, USA), pp. 142–145, June 1989.

[140] O. M. Bucci, G. Mazzarella, and G. Panariello, "Reconfigurable arrays by phase-only control," *IEEE Trans. Antennas Propagat.*, vol. AP-39, pp. 919–925, July 1991.

[141] B. D. Carlson and D. Willner, "Antenna pattern synthesis using weighted least squares," *IEE Proc., Pt. H*, vol. 139, pp. 11–16, Feb 1992.

[142] L. I. Vaskelainen, "Iterative least-squares synthesis methods for conformal arrays antennas with optimized polarization and frequency properties," *IEEE Trans. Antennas Propagat.*, vol. AP-45, pp. 1179–1185, July 1997.

[143] R. Vescovo, "Array factor synthesis for circular antenna arrays," in *IEEE AP-S Int. Symp. Digest*, vol. 3, (Ann Arbor, DT, USA), pp. 1574–1577, June/July 1993.

[144] R. Vescovo, "Pattern synthesis with null constraints for circular arrays of equally spaced isotropic elements," *IEEE Trans. Antennas Propagat.*, vol. AP-43, pp. 1405–1410, Dec 1995.

[145] M. J. Rossouw, J. Joubert, and D. A. McNamara, "Thinned arrays using a modified minimum redundancy synthesis technique," *Electron. Lett.*, vol. 33, pp. 826–827, 8 May 1997.

[146] E. Botha and D. A. McNamara, "Conformal array synthesis using alternating projections, with maximum likelihood estimation used in one of the projection operators," *Electron. Lett.*, vol. 29, pp. 1733–1734, Sept. 1993.

Appendix A

Recursive Formulas and Algorithms for the Transformation Based Planar Array Synthesis Technique

The notationally complex derivations and algorithmic details of the transformation based synthesis technique, discussed in Chapter 3, are given in this Appendix. As in Chapter 3, the two planar array categories will be treated separately. The odd case (an odd number of elements along each principal plane) will be discussed in Section A.1 and even case (an even number of elements along each principal plane) in Section A.2. The derivation of the formulas, as well as, "ready to implement" algorithms for b_q, c_{mn} and c_{mn}^{xx} for both cases are supplied. Although it may be possible to write these in what may be considered a more mathematically elegant fashion, such recursion relations are ideally suited to computation.

A.1 Formulas and Algorithms : The Odd Case

A.1.1 Computation of b_q

The prototype linear array factor, a summation of cosines weighted by the relative excitations a_q, can be expressed in a polynomial form, with b_q the coefficients and $\cos\psi_p$ the variable of the polynomial.

The prototype linear array is a $2Q+1$ element, uniformly spaced linear array with symmetrical excitation and with inter-element spacing d. The prototype linear array factor can be in the usual form (3.4) or in a polynomial form (3.6)

$$F_p(\psi_p) = \sum_{q=0}^{Q} \zeta_q \, a_q \, \cos(q\psi_p) = \sum_{q=0}^{Q} b_q \, \cos^q \psi_p \qquad \text{(A.1)}$$

The recurrence relations (3.5) can be written in one equation

$$\cos^n x = \frac{1}{2^n} \sum_{i=0}^{n}{}^{2} \zeta_i \binom{n}{\frac{1}{2}(n-i)} \cos(ix) \tag{A.2}$$

where $\sum^2$ indicates a step size of two (i.e. $i=i+2$). Using the recurrence relation (A.2) the prototype linear array factor in a polynomial form (A.1) can be expressed as

$$F_p(\psi_p) = \sum_{q=0}^{Q} \sum_{i=0}^{q}{}^{2} \frac{\zeta_q\, b_i}{2^q} \binom{i}{\frac{1}{2}(q-i)} \cos(i\psi_p) \tag{A.3}$$

but for any function of two indices $f(m,n)$,

$$\sum_{m=0}^{M} \sum_{n=0}^{m} f(m,n) = \sum_{n=0}^{M} \sum_{m=n}^{M} f(m,n) \tag{A.4}$$

hence, the summations on the right side of (A.3) can be changed,

$$F_p(\psi_p) = \sum_{q=0}^{Q} \left\{ \sum_{i=q}^{Q}{}^{2} \frac{\zeta_q\, b_i}{2^i} \binom{i}{\frac{1}{2}(i-q)} \right\} \cos(q\psi_p) \tag{A.5}$$

The equation is matched with the prototype linear array factor (A.1) to obtain b_q. The b_q values are computed from the prototype linear array excitations, a_q, with the recursive formula

$$b_q = 2^q \left[a_q - \sum_{i=q+2}^{Q}{}^{2} \frac{b_i}{2^i} \binom{i}{\frac{1}{2}(i-q)} \right] \tag{A.6}$$

in the order $q=Q, Q-1, \ldots, 0$.

A.1.2 Computation of c_{mn} for Quadrantal Symmetric Contours

Derivation of the Formulas

This section deals with the formulas necessary for the computation of c_{mn} of Section 3.2.1. Although these formulas appeared in[95, 94] they are included here for completeness. The only information needed to compute these coefficients are the b_q values forthcoming from the prototype linear array excitations, and the transformation parameters, t_{ij}.

In order to structure the computation let h_{kl} denominate the coefficient of the general term $\cos ku \cos lv$, h_{kl}^q the of $[H(u,v)]^q$. $[H(u,v)]^q$ can then be written as

$$\begin{aligned} [H(u,v)]^q &= [H(u,v)]^{q-1} \times H(u,v) \\ &= \sum_{k=0}^{(q-1)I} \sum_{l=0}^{(q-1)J} h_{kl}^{q-1} \cos(ku)\cos(lv) \times \sum_{i=0}^{I} \sum_{j=0}^{J} t_{ij} \cos(iu)\cos(jv) \end{aligned} \tag{A.7}$$

The use of the recurrence relations (3.5) enable $[H(u,v)]^q$ to be written in the subsequent form

$$[H(u,v)]^q = \sum_{k=0}^{Iq}\sum_{l=0}^{Jq} h_{kl}^q \cos(ku)\cos(lv) \tag{A.8}$$

Algorithm for the computation of c_{mn}

- Step #1: Initiate

$$c_{mn} = 0 \text{ for } \begin{cases} m = 0,1,2,\ldots,QI \\ n = 0,1,2,\ldots,QJ \end{cases}$$

$$h_{kl}^q = 0 \text{ for } \begin{cases} k = 0,1,2,\ldots,QI \\ l = 0,1,2,\ldots,QJ \\ q = 0,1,2,\ldots,Q \end{cases}$$

$$c_{00} = b_0$$

- Step #2: $q = 1$

$$h_{ij}^q = t_{ij} \text{ for } \begin{cases} i = 0,1,2,\ldots,I \\ j = 0,1,2,\ldots,J \end{cases}$$

$$c_{mn} = c_{mn} + b_q h_{mn}^q \text{ for } \begin{cases} m = 0,1,2,\ldots,qI \\ n = 0,1,2,\ldots,qJ \end{cases}$$

- Step #3: $q = q + 1$

$$h_{mn}^q = h_{mn}^q + \frac{1}{\zeta_{|i|}\zeta_{|j|}} t_{|i||j|} h_{kl}^{q-1} \text{ for } \begin{cases} i = -I,-(I-1),\ldots,-1,0,1,\ldots,I \\ j = -I,-(I-1),\ldots,-1,0,1,\ldots,J \\ k = 0,1,2,\ldots,(q-1)I \\ l = 0,1,2,\ldots,(q-1)J \\ m = |k+i| \\ n = |l+j| \end{cases}$$

$$c_{mn} = c_{mn} + b_q h_{mn}^q \text{ for } \begin{cases} m = 0,1,2,\ldots,qI \\ n = 0,1,2,\ldots,qJ \end{cases}$$

Repeat Step #3 up to, and including, the case $q = Q$. As only the information of the previous iteration is needed to compute the values of the current iteration, only two matrices for h_{kl} are needed. The first matrix contains the values of the previous iteration and the second matrix the updated values of the current iteration.

A.1.3 Computation of c_{mn}^{xx} for Arbitrary Contours

Derivation of the Formulas

The algorithms and formulas necessary to compute c_{mn}^{cc}, c_{mn}^{ss}, c_{mn}^{cs} and c_{mn}^{sc} of Section 3.2.2 are provided in this section. The only data used in these formulas are are the b_q values (forthcoming from the prototype linear array excitations) and the transformation parameters, t_{ij}^{cc}, t_{ij}^{ss}, t_{ij}^{cs} and t_{ij}^{sc}.

To structure the computation of these coefficients let g_{kl}^{q} denominate the coefficient of the general term $\cos ku \cos lv$, h_{kl}^{q} the coefficient of the the general term $\sin ku \sin lv$, r_{kl}^{q} the coefficient of the the general term $\cos ku \sin lv$ and s_{kl}^{q} the coefficient of the the general term $\sin ku \cos lv$ in $[H(u,v)]^q$. $[H(u,v)]^q$ is then formulated as

$$\begin{aligned}
[H(u,v)]^q &= [H(u,v)]^{q-1} \times H(u,v) \qquad \text{(A.9)}\\
&= \sum_{k=0}^{(q-1)I} \sum_{l=0}^{(q-1)J} \left[g_{kl}^{q-1} \cos(ku)\cos(lv) + h_{kl}^{q-1} \sin(ku)\sin(lv) + \right.\\
&\qquad \left. r_{kl}^{q-1} \cos(ku)\sin(lv) + s_{kl}^{q-1} \sin(ku)\cos(lv) \right]\\
&\quad \times \sum_{i=0}^{I} \sum_{j=0}^{J} \left[t_{ij}^{cc} \cos(iu)\cos(jv) + t_{ij}^{ss} \sin(iu)\sin(jv) + \right.\\
&\qquad \left. t_{ij}^{cs} \cos(iu)\sin(jv) + t_{ij}^{sc} \sin(iu)\cos(jv) \right]
\end{aligned}$$

With the use of the following relations

$$\begin{aligned}
\cos A \cos B &= \tfrac{1}{2}\left[\cos(A-B) + \cos(A+B)\right]\\
\sin A \cos B &= \tfrac{1}{2}\left[\sin(A-B) + \sin(A+B)\right] \qquad \text{(A.10)}\\
\sin A \sin B &= \tfrac{1}{2}\left[\sin(A-B) + \sin(A+B)\right]
\end{aligned}$$

$[H(u,v)]^q$ can then be written in the subsequent form

$$\begin{aligned}
[H(u,v)]^q = \sum_{k=0}^{Iq} \sum_{l=0}^{Jq} &\left[g_{kl}^{q} \cos(ku)\cos(lv) + h_{kl}^{q} \sin(ku)\sin(lv) + \right. \qquad \text{(A.11)}\\
&\left. r_{kl}^{q} \cos(ku)\sin(lv) + s_{kl}^{q} \sin(ku)\cos(lv) \right]
\end{aligned}$$

Algorithm for the computation of c_{mn}^{xx}

- Step #1: Initiate

$$\left.\begin{aligned} c_{mn}^{cc} &= 0 \\ c_{mn}^{ss} &= 0 \\ c_{mn}^{cs} &= 0 \\ c_{mn}^{sc} &= 0 \end{aligned}\right\} \text{ for } \left\{\begin{aligned} m &= 0,1,2,\ldots,QI \\ n &= 0,1,2,\ldots,QJ \end{aligned}\right.$$

$$\left.\begin{aligned} g_{kl}^{q} &= 0 \\ h_{kl}^{q} &= 0 \\ r_{kl}^{q} &= 0 \\ s_{kl}^{q} &= 0 \end{aligned}\right\} \text{ for } \left\{\begin{aligned} k &= 0,1,2,\ldots,QI \\ l &= 0,1,2,\ldots,QJ \\ q &= 0,1,2,\ldots,Q \end{aligned}\right.$$

$$c_{00} = b_0$$

- Step #2: $q = 1$

$$\left.\begin{aligned} g_{ij}^{q} &= t_{ij}^{cc} \\ h_{ij}^{q} &= t_{ij}^{ss} \\ r_{ij}^{q} &= t_{ij}^{cs} \\ s_{ij}^{q} &= t_{ij}^{sc} \end{aligned}\right\} \text{ for } \left\{\begin{aligned} i &= 0,1,2,\ldots,I \\ j &= 0,1,2,\ldots,J \end{aligned}\right.$$

$$\left.\begin{aligned} c_{mn}^{cc} &= c_{mn}^{cc} + b_q g_{mn}^{q} \\ c_{mn}^{ss} &= c_{mn}^{ss} + b_q h_{mn}^{q} \\ c_{mn}^{cs} &= c_{mn}^{cs} + b_q r_{mn}^{q} \\ c_{mn}^{sc} &= c_{mn}^{sc} + b_q s_{mn}^{q} \end{aligned}\right\} \text{ for } \left\{\begin{aligned} m &= 0,1,2,\ldots,qI \\ n &= 0,1,2,\ldots,qJ \end{aligned}\right.$$

- Step #3: $q = q + 1$

$$g_{mn}^{q} = g_{mn}^{q} + \frac{1}{\zeta_{|i|}\zeta_{|j|}}\left[\, t_{|i||j|}^{cc}\, g_{kl}^{q-1} + \Upsilon_i\Upsilon_j\, t_{|i||j|}^{ss}\, h_{kl}^{q-1} - \Upsilon_j\, t_{|i||j|}^{cs}\, r_{kl}^{q-1} - \Upsilon_i\, t_{|i||j|}^{sc}\, s_{kl}^{q-1}\right]$$

$$h_{mn}^{q} = h_{mn}^{q} + \frac{\Upsilon_{k+i}\Upsilon_{l+j}}{\zeta_{|i|}\zeta_{|j|}}\left[t_{|i||j|}^{cc}\, h_{kl}^{q-1} + \Upsilon_i\Upsilon_j\, t_{|i||j|}^{ss}\, g_{kl}^{q-1} + \Upsilon_j\, t_{|i||j|}^{cs}\, s_{kl}^{q-1} + \Upsilon_i\, t_{|i||j|}^{sc}\, r_{kl}^{q-1}\right]$$

$$r_{mn}^{q} = r_{mn}^{q} + \frac{\Upsilon_{l+j}}{\zeta_{|i|}\zeta_{|j|}}\left[\, t_{|i||j|}^{cc}\, r_{kl}^{q-1} - \Upsilon_i\Upsilon_j\, t_{|i||j|}^{ss}\, s_{kl}^{q-1} + \Upsilon_j\, t_{|i||j|}^{cs}\, g_{kl}^{q-1} - \Upsilon_i\, t_{|i||j|}^{sc}\, h_{kl}^{q-1}\right]$$

$$s_{mn}^{q} = s_{mn}^{q} + \frac{\Upsilon_{k+i}}{\zeta_{|i|}\zeta_{|j|}}\left[\, t_{|i||j|}^{cc}\, s_{kl}^{q-1} - \Upsilon_i\Upsilon_j\, t_{|i||j|}^{ss}\, r_{kl}^{q-1} - \Upsilon_j\, t_{|i||j|}^{cs}\, h_{kl}^{q-1} + \Upsilon_i\, t_{|i||j|}^{sc}\, g_{kl}^{q-1}\right]$$

$$\text{for} \begin{cases} i = -I, -(I-1), \ldots, -1, 0, 1, \ldots, I \\ j = -J, -(J-1), \ldots, -1, 0, 1, \ldots, J \\ k = 0, 1, 2, \ldots, (q-1)I \\ l = 0, 1, 2, \ldots, (q-1)J \end{cases} \quad \text{with} \begin{cases} m = |k+i| \\ n = |l+j| \\ \Upsilon_i = \text{sign}(i) \end{cases}$$

$$\left.\begin{aligned} c^{cc}_{mn} &= c^{cc}_{mn} + b_q g^q_{mn} \\ c^{ss}_{mn} &= c^{ss}_{mn} + b_q h^q_{mn} \\ c^{cs}_{mn} &= c^{cs}_{mn} + b_q r^q_{mn} \\ c^{sc}_{mn} &= c^{sc}_{mn} + b_q s^q_{mn} \end{aligned}\right\} \text{for} \begin{cases} m = 0, 1, 2, \ldots, qI \\ n = 0, 1, 2, \ldots, qJ \end{cases}$$

Repeat Step #3 up to, and including, $q = Q$. Note that only two matrices for each of h_{kl}, g_{kl} rkl and s_{kl} are needed. The first matrix of each holds the values of the previous iteration and the second matrix holds the revised values of the current iteration. Although this algorithm seems formidable, it is easy to program and execution is extremely rapid.

A.2 Formulas and Algorithms : The Even Case

A.2.1 Computation of b_q

In this case, the prototype linear array is a $2Q$ element, uniformly spaced, symmetrical excited linear array. The prototype linear array factor can be expressed in two forms, the usual form (3.17) or the polynomial form (3.18)

$$F_p(\psi_p) = 2 \sum_{q=1}^{Q} a_q \cos\left[\tfrac{1}{2}(2q-1)\psi_p\right] = \sum_{q=1}^{Q} b_q \cos^{2q-1}\left(\tfrac{1}{2}\psi_p\right) \tag{A.12}$$

Using the same procedure (only latter of the recurrence relations (3.5b) is needed) the recursive formula for computing the b_q values from the prototype linear array excitations is,

$$b_q = 2^{2q-1}\left[a_q - \sum_{i=q+1}^{Q} \frac{b_i}{2^{2i-1}} \binom{2i-1}{i-q}\right] \tag{A.13}$$

in the order $q = Q, Q-1, \ldots, 0$.

A.2.2 Computation of c_{mn} for Quadrantal Symmetric Contours

Derivation of the Formulas

The formulas required for the computation of c_{mn} coefficients of Section 3.2.1 are presented this section. The information forthcoming from the solution of the two sub-

problems, are all that are needed to calculate these coefficients.

To structure the computation, let h_{kl} denominate the coefficient of the general term $\cos[\frac{1}{2}(2k-1)u]\cos[\frac{1}{2}(2l-1)v]$ of $[H(u,v)]^{2q-1}$. $[H(u,v)]^{2q-1}$ is then expressed as

$$\begin{aligned}[H(u,v)]^{2q-1} &= [H(u,v)]^{2q-3} \times [H(u,v)]^2 \\ &= \sum_{k=1}^{(2q-3)I} \sum_{l=1}^{(2q-3)J} h_{kl}^{2q-3} \cos\left[\tfrac{1}{2}(2k-1)u\right] \cos\left[\tfrac{1}{2}(2l-1)v\right] \\ &\quad \times \left\{ \sum_{i=1}^{I} \sum_{j=1}^{J} t_{ij} \cos\left[\tfrac{1}{2}(2i-1)u\right] \cos\left[\tfrac{1}{2}(2j-1)v\right] \right\}^2 \end{aligned} \tag{A.14}$$

Using the recurrence relations (3.5b) enable $[H(u,v)]^{2q-1}$ to be written in the subsequent form

$$[H(u,v)]^{2q-1} = \sum_{k=1}^{(2I-1)q} \sum_{l=1}^{(2J-1)q} h_{kl}^{2q-1} \cos\left[\tfrac{1}{2}(2k-1)u\right] \cos\left[\tfrac{1}{2}(2l-1)v\right] \tag{A.15}$$

It will be easier, and computationally faster, to compute $[H(u,v)]^2$ and use its coefficients, $\mathbf{t}_{ij}$, where $\mathbf{t}_{ij}$ is the coefficient of the general term $\cos(iu)\cos(jv)$, in the algorithm.

$$[H(u,v)]^2 = \sum_{i=0}^{2I-1} \sum_{j=0}^{2J-1} \mathbf{t}_{ij} \cos(iu) \cos(jv) \tag{A.16}$$

Algorithm for the computation of c_{mn}

- Step #1: Initiate

$$c_{mn} = 0 \text{ for } \begin{cases} m = 1, 2, 3, \ldots, QI \\ n = 1, 2, 3, \ldots, QJ \end{cases}$$

$$h_{kl}^{q} = 0 \text{ for } \begin{cases} k = 1, 2, 3, \ldots, QI \\ l = 1, 2, 3, \ldots, QJ \\ q = 1, 2, 3, \ldots, Q \end{cases}$$

$$\mathbf{t}_i j =$$

- Step #2: $q = 1$

$$h_{ij}^{q} = t_{ij} \text{ for } \begin{cases} i = 1, 2, 3, \ldots, I \\ j = 1, 2, 3, \ldots, J \end{cases}$$

$$c_{mn} = c_{mn} + b_q h_{mn}^{q} \text{ for } \begin{cases} m = 1, 2, 3, \ldots, qI \\ n = 1, 2, 3, \ldots, qJ \end{cases}$$

- Step #3: $q = q + 1$

$$h_{mn}^{q} = h_{mn}^{q} + \frac{1}{4} t_{ij} h_{kl}^{q-1} \text{ for } \begin{cases} i = -I, -(I-1), \ldots, -1, 1, \ldots, I \\ j = -I, -(I-1), \ldots, -1, 1, \ldots, J \\ k = 1, 2, 3, \ldots, (q-1)I \\ l = 1, 2, 3, \ldots, (q-1)J \\ m = |k + i| \\ n = |l + j| \end{cases}$$

$$c_{mn} = c_{mn} + b_q h_{mn}^{q} \text{ for } \begin{cases} m = 1, 2, 3, \ldots, qI \\ n = 1, 2, 3, \ldots, qJ \end{cases}$$

Repeat Step #3 until $q = Q$. Only two matrices for h_{kl} are needed, one with present values and the other with the previous iteration's values.

A.2.3 Computation of c_{mn}^{xx} for Arbitrary Contours

No details of the derivation of the formulas will be presented as they are analogous to that of Section A.1.3. The algorithm for the computation of c_{mn}^{xx} is:

- Step #1: Initiate

$$\left.\begin{aligned} c_{mn}^{cc} &= 0 \\ c_{mn}^{ss} &= 0 \\ c_{mn}^{cs} &= 0 \\ c_{mn}^{sc} &= 0 \end{aligned}\right\} \text{ for } \begin{cases} m = 1, 2, 3, \ldots, QI \\ n = 1, 2, 3, \ldots, QJ \end{cases}$$

$$\left.\begin{aligned} g_{kl}^{q} &= 0 \\ h_{kl}^{q} &= 0 \\ r_{kl}^{q} &= 0 \\ s_{kl}^{q} &= 0 \end{aligned}\right\} \text{ for } \begin{cases} k = 1, 2, 3, \ldots, QI \\ l = 1, 2, 3, \ldots, QJ \\ q = 1, 2, 3, \ldots, Q \end{cases}$$

$$c_{00} = b_0$$

- Step #2: $q = 1$

$$\left.\begin{aligned} g_{ij}^{q} &= t_{ij}^{cc} \\ h_{ij}^{q} &= t_{ij}^{ss} \\ r_{ij}^{q} &= t_{ij}^{cs} \\ s_{ij}^{q} &= t_{ij}^{sc} \end{aligned}\right\} \text{ for } \left\{\begin{aligned} i &= 0, 1, 2, \ldots, I \\ j &= 0, 1, 2, \ldots, J \end{aligned}\right.$$

$$\left.\begin{aligned} c_{mn}^{cc} &= c_{mn}^{cc} + b_q g_{mn}^{q} \\ c_{mn}^{ss} &= c_{mn}^{ss} + b_q h_{mn}^{q} \\ c_{mn}^{cs} &= c_{mn}^{cs} + b_q r_{mn}^{q} \\ c_{mn}^{sc} &= c_{mn}^{sc} + b_q s_{mn}^{q} \end{aligned}\right\} \text{ for } \left\{\begin{aligned} m &= 1, 2, 3, \ldots, qI \\ n &= 1, 2, 3, \ldots, qJ \end{aligned}\right.$$

- Step #3: $q = q + 1$

$$g_{mn}^{q} = g_{mn}^{q} + \frac{1}{\zeta_{|i|}\zeta_{|j|}}\left[\, t_{|i||j|}^{cc}\, g_{kl}^{q-1} + \Upsilon_i \Upsilon_j\, t_{|i||j|}^{ss}\, h_{kl}^{q-1} - \Upsilon_j\, t_{|i||j|}^{cs}\, r_{kl}^{q-1} - \Upsilon_i\, t_{|i||j|}^{sc}\, s_{kl}^{q-1}\right]$$

$$h_{mn}^{q} = h_{mn}^{q} + \frac{\Upsilon_{k+i}\Upsilon_{l+j}}{\zeta_{|i|}\zeta_{|j|}}\left[t_{|i||j|}^{cc}\, h_{kl}^{q-1} + \Upsilon_i \Upsilon_j\, t_{|i||j|}^{ss}\, g_{kl}^{q-1} + \Upsilon_j\, t_{|i||j|}^{cs}\, s_{kl}^{q-1} + \Upsilon_i\, t_{|i||j|}^{sc}\, r_{kl}^{q-1}\right]$$

$$r_{mn}^{q} = r_{mn}^{q} + \frac{\Upsilon_{l+j}}{\zeta_{|i|}\zeta_{|j|}}\left[\, t_{|i||j|}^{cc}\, r_{kl}^{q-1} - \Upsilon_i \Upsilon_j\, t_{|i||j|}^{ss}\, s_{kl}^{q-1} + \Upsilon_j\, t_{|i||j|}^{cs}\, g_{kl}^{q-1} - \Upsilon_i\, t_{|i||j|}^{sc}\, h_{kl}^{q-1}\right]$$

$$s_{mn}^{q} = s_{mn}^{q} + \frac{\Upsilon_{k+i}}{\zeta_{|i|}\zeta_{|j|}}\left[\, t_{|i||j|}^{cc}\, s_{kl}^{q-1} - \Upsilon_i \Upsilon_j\, t_{|i||j|}^{ss}\, r_{kl}^{q-1} - \Upsilon_j\, t_{|i||j|}^{cs}\, h_{kl}^{q-1} + \Upsilon_i\, t_{|i||j|}^{sc}\, g_{kl}^{q-1}\right]$$

$$\text{for } \left\{\begin{aligned} i &= -I, -(I-1), \ldots, -1, 1, \ldots, I \\ j &= -I, -(I-1), \ldots, -1, 1, \ldots, J \\ k &= 1, 2, 3, \ldots, (q-1)I \\ l &= 1, 2, 3, \ldots, (q-1)J \end{aligned}\right. \quad \text{with } \left\{\begin{aligned} m &= |k+i| \\ n &= |l+j| \\ \Upsilon_i &= \text{sign}(i) \end{aligned}\right.$$

$$\left.\begin{aligned} c_{mn}^{cc} &= c_{mn}^{cc} + b_q g_{mn}^{q} \\ c_{mn}^{ss} &= c_{mn}^{ss} + b_q h_{mn}^{q} \\ c_{mn}^{cs} &= c_{mn}^{cs} + b_q r_{mn}^{q} \\ c_{mn}^{sc} &= c_{mn}^{sc} + b_q s_{mn}^{q} \end{aligned}\right\} \text{ for } \left\{\begin{aligned} m &= 1, 2, 3, \ldots, qI \\ n &= 1, 2, 3, \ldots, qJ \end{aligned}\right.$$

Repeat Step #3 up to, and including, the case $q = Q$. Again, just two matrices for each of h_{kl}, $g_{kl}\, rkl$ and s_{kl} are needed. The algorithm is easy to program, though it may looks imposing.